AN INVESTIGATION OF GALACTIC STRUCTURE FROM THE STUDY OF NORTHERN-HEMISPHERE EARLY TYPE STARS AT INTERMEDIATE GALACTIC LATITUDES

A. E. Lynas-Gray

A Thesis Submitted for the Degree of PhD
at the
University of St Andrews

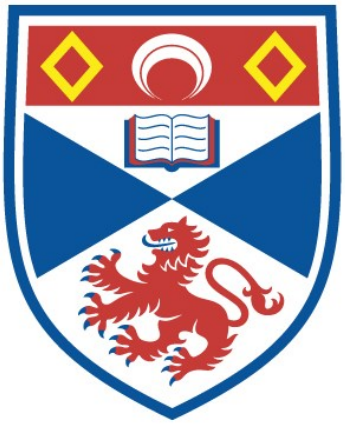

1976

An Investigation of Galactic Structure from the Study of Northern Hemisphere Early Type Stars at Intermediate Galactic Latitudes

by

A.E. Lynas-Gray

A dissertation submitted for the degree of Doctor of Philosophy at the University of St. Andrews.

Dublin

June 1976.

Certificate

I certify that Anthony Eugene Lynas - Gray has spent nine terms in research work at the University Observatory, St. Andrews, that he has fulfilled the conditions of Ordinance General No. 12 and Senate Regulations under Resolution of the University Court, 1967, No. 1, and that he is qualified to submit the accompanying dissertation in application for the degree of Ph.D.

Declaration

Except where reference is made to the work of others, the research described in this thesis and the composition of the thesis are my own work. No part of this work has been submitted for another degree at this or any other University. Under Ordinance General No. 12, I was admitted to the Faculty of Science of the University of St. Andrews as a research student on the 1st October 1971, to carry out photometric and spectroscopic observations of early type stars at intermediate galactic latitudes, with the general aim of investigating the comparison of stellar spatial and velocity distributions with those of the interstellar medium. I was accepted as a candidate for the degree of Ph.D. on the 1st October 1972, under Resolution of the University Court, 1967, No. 1.

CONTENTS

Acknowledgements

I acknowledge the kindness and assistance freely given to me, at all stages of this work, by my supervisor, Dr.P.W.Hill, and my colleague, Dr. D. Kilkenny. I am grateful to the Directors and staffs of the St. Andrews University Observatory, the St. Andrews University Computing Laboratory, Dunsink Observatory, l'Observatoire de Haute Provence, and the Royal Greenwich Observatory for their kind assistance at various stages in this work.

I am indebted to the "Commission des Programmes" and the "Large Telescope Users Panel" for generous allocations of observing time. Finally, my thanks are due to Professor P.A.Wayman for proof reading the manuscript, to Mr. W. Dumpleton for his painstaking efforts with the diagrams, and to Miss Mary Callanan for typing the thesis.

This work was supported by the University of St. Andrews, the Dublin Institute for Advanced Studies, the Science Research Council and the French Government.

ABSTRACT

Photometric and spectroscopic observations have been made of northern hemisphere early type stars at intermediate galactic latitudes. Stellar distances, the corresponding distances from the galactic plane and the interstellar reddening along the lines of sight have been derived. The available published data was used to support the observational results. The HI spiral features seem to have corresponding optical counterparts, and the agreement between the two patterns is remarkably good. The neutral hydrogen kinematic distances depart from the stellar distances. This can be explained in terms of the density wave theory, with a small modification which may be the result of a non-zero distance from the galactic plane. The Local Arm extends to about 500pc above the galactic plane and the Perseus Arm to 1 kpc. Thus it seems that the interpretation of intermediate latitude high and intermediate velocity features, as vertical extensions to the spiral arms in the galactic plane, may be correct.

Stellar and interstellar calcium radial velocities suggest that these intermediate latitude spiral features adhere closely to differential galactic rotation, and that the small departures from this motion exhibit a significant correlation with the predictions of the density wave theory. Published proper motions are used together with the stellar radial velocities to derive the components of the stellar space motions with respect to their local standards of rest. In cases where the component normal to the galactic plane was significantly different from zero, the dynamical lifetime was calculated on the assumption that the star was formed in the galactic plane. These were found to be compatible with the evolutionary lifetimes for only half of the stars considered, suggesting that about 50% of intermediate latitude OB stars were formed in or near the galactic plane and subsequently ejected from it. The remainder seem to have been formed at considerable distances

from the galactic plane, and a scheme for explaining this is proposed. This scheme also explains the apparent assymetry between the northern and southern galactic hemispheres. A few interesting high velocity stars and OB star associations are also considered.

A List of Tables

A List of Illustrations

List of Plates

CHAPTER ONE

Introduction

1.1 Historical Development of Galactic Astronomy

1.2 Recent Studies of Galactic Structure at Intermediate and High Galactic Latitudes, and the Aims of this Present Investigation.

1.1 The Historical Development of Galactic Astronomy

A comprehensive review of the development of galactic astronomy has been given by Kienle (1969). Consequently only a brief summary will be attempted in order to present the research reported here in its historical context.

Proper motion determinations by Halley were the first scientific studies of stellar motions. These proper motion studies were continued into the eighteenth century, and in 1760 Mayer published the first catalogue of proper motions. By this time it had become generally accepted that a " stellar system " existed, and Kant adopted the view that the Andromeda Nebula was an external " stellar system " similar to our own.

Major advances were made by Herschel in the early years of the nineteenth century. By basing his distance determinations on the assumption that all stars have the same luminosity as the Sun, he established that the Galaxy consisted of a disk, in which most of the stars were concentrated. Little progress was made after this until the distribution of globular clusters was studied by Shapley (1918). Unlike other celestial objects, the globular clusters show no concentration towards the galactic plane. In fact they appear to describe a sphere with the galactic plane as a diametrical plane, which enabled the distance from the Sun to the galactic centre to be determined. This model of the Galaxy became firmly established with the discovery of differential galactic rotation by Lindblad (1926) and Oort (1927), because the apparent solar motion, star streaming and the assymetry in stellar velocities could now be explained.

The accurate determination of stellar distances became feasible after the discovery of interstellar reddening by Trumpler (1930a) and the establishment of the UBV photometric and MK spectral classification systems by Johnson and Morgan (1953). The existence of spiral

structure, suggested earlier by Morgan et al. (1952, 1953), was established by Hiltner (1956) using accurate stellar distances determined in this way.

The possibility that the hyperfine emission line of hydrogen, at a wavelength of 21cm, would be observable was first suggested by van de Hulst (1945). It was first observed by Ewen & Purcell (1951). More extensive 21cm observations were made by van de Hulst, Muller & Oort (1954), and these were interpreted as being indicative of spiral structure already reported (Morgan et al., 1952, 1953). Similar observations in the direction of the galactic centre, by Kwee et al. (1954), enabled a rotation curve, giving the neutral hydrogen angular velocity as a function of galactocentric distance, to be derived for the inner regions of the galaxy.

Schmidt (1956) used a mass distribution model for the galaxy and was able to verify this rotation curve theoretically, and extend it to the outer regions of the galaxy. However, this theory quickly ran into difficulties, because the kinematic distances predicted from radial velocities for neutral hydrogen did not agree with the photometrically determined distances for the optical spiral tracers. The same problem was encountered with regard to HII regions and their exciting stars.

A further difficulty arose with regard to explaining the permanence of spiral structure. It became obvious that the galactic magnetic field was far too weak to prevent the spiral arms from "winding-up". Consequently a new approach to the theory of galactic structure was needed. This led to the development of the density wave theory. The principle aspects of this are reviewed by Lin et al. (1969).

This theory successfully explains the permanence of spiral structure in the galactic plane. It does not, however, attempt to discuss the spiral structure at intermediate galactic latitudes,

if it does in fact exist at all. Neither is any attempt made to account for the origin of spiral structure in a galaxy. A successful theory to account for these aspects of galactic structure has yet to be presented.

1.2 Recent Studies of Galactic Structure at Intermediate and High Galactic Latitudes, and the Aims of this Investigation

Any future developments of a theory to successfully account for the existence and evolution of galactic spiral structure, will probably take the form of some minor modifications to the existing density wave theory (§1.1). Before any such theoretical advance can be contemplated, however, the full extent of the spiral arms, in distance from the galactic plane as well as in distance from the galactic centre, must be known. For this reason, extensive 21cm surveys have been carried out, at intermediate galactic latitudes, those by Kepner (1970), Davies (1972) and Verschuur (1973a) being the most notable.

Extensive intermediate and high velocity features were found, which on the basis of kinematic distances, appeared to be extensions to the well known spiral arms in the direction away from the galactic plane. In fact there was evidence to suggest that the further the spiral arm from the galactic centre, the further it extended from the galactic plane. Furthermore, it can be seen from star catalogues that early type stars appear to exist in considerable numbers at intermediate galactic latitudes. Thus, certain questions arise for which answers have to be sought.

In the first instance, are these stars really normal early type stars? If so, are they associated with the neutral hydrogen features, and if they are, do they participate in differential galactic rotation. Intermediate latitude stars can be considered as stars in the galactic plane if their positions and motions are projected onto the galactic plane. Thus, if it turns out that these intermediate latitude OB stars approximately follow differential galactic rotation, then any departures from this could usefully be compared with the predictions of the density

wave theory.

Furthermore, the existance of early type stars at intermediate latitudes has to be explained. Traditionally, early type stars are thought to have been formed in dense regions close to the galactic plane. If this is the case, then any distant stars observed at intermediate galactic latitudes must have been ejected from the galactic plane, in which case the ejection itself has to be explained. In the event of there being no evidence for the ejection of stars from the galactic plane, then a scheme for explaining the formation of stars away from the galactic plane has to be devised.

In any attempt to resolve some of these uncertainties, a survey of intermediate latitude OB stars in the Southern Hemisphere has just been completed by Kilkenny et al. (1975), and Kilkenny & Hill (1975). They have shown that stars of type B2 and earlier, at distances of up to 1 kpc. from the galactic plane, appear to follow spiral structure in the plane. Furthermore, these stars appear to participate in differential galactic rotation.

A similar survey conducted in the Northern Hemisphere is reported in this thesis. This survey was begun in 1971 at which time, only Kepner's paper had been published. Consequently it was decided to restrict the observations to include only those stars which lay in the area of the sky surveyed by Kepner (1970). Kilkenny (1973) has pointed out that the advantage of observing at intermediate latitudes, if the OB stars are found to reflect the spiral structure in the galactic plane, is that it should be possible to trace distant spiral arms without the handicap of dense interstellar absorption found in the galactic plane. Kilkenny was able to trace the Arm-II in the direction of the galactic centre, and similarly it was hoped to trace the Arm II, in the anticentre direction, in this survey.

CHAPTER TWO

THE THEORETICAL ASPECTS OF THE OBSERVATIONS UNDERTAKEN

2.1 Introduction

The complete description of our galactic stellar system can be expressed by a frequency function F (Trumpler and Weaver, 1953, page 234) given by

$$F = F\,(l,b,r,M,S,U,V,W\,) \text{ - - - - - - - - - - - - - } (2.1.1),$$

where

l = galactic longitude of a star,
b = galactic latitude of the star,
r = distance from the observer to the star,
M = absolute magnitude of the star,
S = spectral type of the star

and U,V and W are three rectangular velocity coordinates.

In practice the function F is generally rewritten as

$$F = D(l,b,r)\ \phi(M,S,U,V,W \,/\, l,b,r) \text{ - - - - - - - -} (2.1.2)$$

In this case D(l,b,r) is the total star density at the point having coordinates l,b,r and ϕ defines the relative distribution of stars of differing values of M,S,U,V and W in the vicinity of the point defined by (l,b,r). An explicit form for the functions D and ϕ cannot be determined because insufficient observational data are available. In fact the problem is so complex, that F can only be determined for a few stars of a particular spectral type. It can be hoped that this gives some indication of galactic structure.

By analogy, a complete description of the intrinsically non-luminous interstellar medium is given by a density distribution and state of motion of each class, i, of interstellar particle, molecule or atom, of the form

$$G_i = G_i(l,b,r,U,V,W) \text{ - - - - - - - - - - - - - } (2.1.3)$$

In this case, there is the additional complication of being unable to measure the motions of the interstellar medium in a direction perpendicular to the line of sight directly. Consequently, the most that can be hoped for is to determine a function

$$G_i' = G_i' (l,b,r,V_i) \text{ - - - - - - - - - - - - - - - (2.1.4)},$$

where V_i is the velocity along the line of sight of each class, i, of interstellar particle, molecule or atom. As with the function F, only a crude determination of G_i' can be made, for only a few classes of interstellar particle, at a few differing values of l,b and r.

A further difficulty encountered in the determination of G_i' is that only a mean distance along the line of sight to a star can be determined. A method for doing this has been suggested by Stibbs (1975), and is as follows. Let r be the distance of the star, and suppose that x is a variable giving distance along the line of sight. Then the corresponding variable giving the height above the galactic plane is $z = x \sin(b)$. Suppose that $\rho(z)$ is the density of the interstellar medium given by

$$\rho(z) = \rho_o \exp(-(z/h)^n) \text{ - - - - - - - - - - - - (2.1.5)},$$

where ρ_o is the density of the interstellar medium in the galactic plane,

h = a constant, depending upon the medium, and

n = 0,1,2 - - - - - etc., to be determined.

The mean distance of the particles making up a constituent of the interstellar medium, along the line of sight to a star, can be defined by

$$\bar{r} = \int_o^r \rho(z)\, x\,dx \Big/ \int_o^r \rho(z)\, dx \text{ - - - - - - - (2.1.6)}$$

From equations (2.1.5) and (2.1.6) considering the case of n = 0 gives

$$\bar{r}_o = \int_o^r x\,dx \Big/ \int_o^r dx \ ,$$

$$\therefore \ \bar{r}_o = \frac{r}{2} \qquad \text{- (2.1.7)}$$

From equations (2.1.5) and (2.1.6), considering the case of n = 1 gives

$$\bar{r}_1 = \int_o^r \exp\,(-z/h)\ x\,dx \Big/ \int_o^r \exp\,(-z/h)\ dx$$

Substituting for z in terms of x and evaluating the integrals gives

$$\bar{r}_1 = \frac{h\ \mathrm{cosec}\ (b)}{(1 - \exp(-\alpha))}\ [\ 1-(1 + \alpha)\exp(-\alpha)\ ] \text{ - - - - - - - -(2.1.8),}$$

where $\alpha = r \sin b/h$.

Similarly, equation (2.1.6) can be evaluated for higher values of n. The case chosen, to which an attempt is made to fit the observed data, depends on the value of n chosen for equation (2.1.5).

Thus it can be seen that only a very crude picture of galactic structure can be obtained by observing a few stars and the interstellar medium in the directions of these stars. It can then be hoped that a model, developed as a result of such observations, will successfully predict the results of subsequent observations.

All the parameters which describe the functions F and G_i' can be determined for a given star by direct or indirect means. The galactic longitude and latitude can be calculated from the measured position of a star on the celestial sphere (Blaauw et al., 1958). The stellar distances, aboslute magnitudes and space motion components are determined using the methods indicated in the remaining sections of this chapter. The radial velocities and spectral types are discussed later (§5.1). The selection of stars for observation is discussed in Chapter 3.

2.2 The Theory of Intrinsic Colour and Absolute Magnitude Determination

In an attempt to develop an understanding of galactic structure, the difficulty of determining the interstellar reddening along the lines of sight of stars has to be overcome. This was done by means of wide band photoelectric photometry of the programme stars, using the UBV system, as defined by Johnson & Morgan (1953). The principles involved in carrying out and reducing UBV observations are discussed later (Chapter 6).

One fairly obvious method of measuring interstellar reddening is in terms of the colour excesses E_{B-V} and E_{U-B}. This was proposed by Johnson & Morgan (1953) and has been in use ever since. The colour excesses are defined by

$$E_{B-V} = (B-V) - (B-V)_o \quad - - - - - - - - - - - - \quad (2.2.1),$$

and

$$E_{U-B} = (U-B) - (U-B)_o \quad - - - - - - - - - - - - \quad (2.2.2),$$

where (B-V) and (U-B) are the observed colour indices outside the earth's atmosphere, and $(B-V)_o$ and $(U-B)_o$ are the colour indices that would be observed outside the earth's atmosphere if there were no interstellar reddening. That is, they are the intrinsic colour indices.

In establishing the UBV system, Johnson & Morgan made some important contributions to the understanding of interstellar reddening. These were later confirmed by Hiltner & Johnson (1956). A large number of MK spectral type standard stars (Morgan et al., 1943) were observed on the UBV system and the resulting (U-B) was plotted as a function of the resulting (B-V). They noticed that all unreddened stars lay along a unique curve characteristic of their MK spectral type. Reddened stars of a given spectral type on the other hand lay along a straight line of a certain slope (Fig. 10 in Johnson & Morgan, 1953).

The reddening lines for the stars of different colour classes of OB stars are very nearly parallel, and so Johnson and Morgan deduced that there existed a reddening-free parameter, Q, for OB stars, defined as

$$Q = (U-B) - \frac{E_{U-B}}{E_{B-V}} . \quad (B-V) \quad - - - - - - - - - - - \quad (2.2.3),$$

This can be effectively demonstrated by substitution in equation (2.2.3) from equations (2.2.1) and (2.2.2) which gives

$$Q = (U-B)_o - \frac{E_{U-B}}{E_{B-V}} . \quad (B-V)_o \quad - - - - - - - - - - - \quad (2.2.4).$$

From a consideration of observational data on OB stars, Johnson & Morgan were able to show that the relation

$$\frac{E_{U-B}}{E_{B-V}} = 0.72 + 0.05\ E_{B-V} \quad - - - - - - - - - - - - \quad (2.2.5),$$

was valid to a good approximation. Substitution for E_{U-B} / E_{B-V} in equation (2.2.3) gives

$$Q = (U-B) - 0.72\ (B-V) - 0.05(B-V)^2 \quad - - - - - - \quad (2.2.6),$$

Thus Q is a reddening-free parameter for OB stars, which is solely a function of the colour of the star, or alternatively, the effective temperature. A more accurate determination of the reddening trajectory was made by Serkowski (1963), who used published UBV photometry of early type stars, and took the effects of polarization into consideration. Klinkmann (1973) has used the results of Serkowski's reddening trajectories to derive an improved expression for Q as

$$Q = (U-B) - 0.58(B-V) + 0.45(B-V)(B-V)_o - 0.06(B-V)^2 + 0.06(B-V)_o^2$$

$$- - - - - - - - - - - - \quad (2.2.7),$$

It will be noticed that $(B-V)_o$ appears in this equation. As both $(B-V)_o$ and $(B-V)$ tend to be small for OB stars, $(B-V)_o^2$ and $(B-V)(B-V)_o$ will be small enough to prevent a small error in $(B-V)_o$ from having a very significant effect on Q. Thus, if a MK spectral type has been published or can be found by spectroscopic observations (§5.1.2 & §5.7), a value of $(B-V)_o$ can be obtained from Serkowski (1963) which is of adequate accuracy.

Values for (B-V) and (U-B) are obtained from the literature or by UBV photometry (see Chapter 6). Substitution in equation (2.2.7) gives a value for Q. Further substitution in equation (2.2.3) will give E_{U-B} / E_{B-V}, which can be used in equation (2.2.5) to give E_{B-V}. Then E_{U-B}, $(B-V)_o$ and $(U-B)_o$ can be derived from equations (2.2.1), (2.2.2) and (2.2.3). The parameter traditionally used to describe the interstellar reddening is E_{B-V}, although Crawford (1973) prefers E_{U-B}. The arguments will not be pursued here, and the traditional use of E_{B-V} will be adhered to.

It has been shown by Moffat et al. (1973), that β(§4.1) and $(B-V)_o$ are functions of the absolute magnitude (M_V) and the effective temperature. As already explained, Q is purely a function of the effective temperature for OB stars. Consequently it should be possible to derive M_V and $(B-V)_o$ from β and Q, and a graphical method for doing this has been developed by Klinkmann (1973). The diagram used is that given in Fig. (2.2.1), which has been reproduced from Klinkmann's thesis.

The value of $(B-V)_o$ thus obtained can be used to check that obtained from the MK spectral type and, if necessary, Q can be re-determined. The interstellar reddening, E_{B-V}, was obtained from equation (2.2.1). This method of intrinsic colour determination was used in preference to that based on equation (2.2.5), if Hβ photometry of the star in question was available.

The β - Q Diagram for Early Type Stars

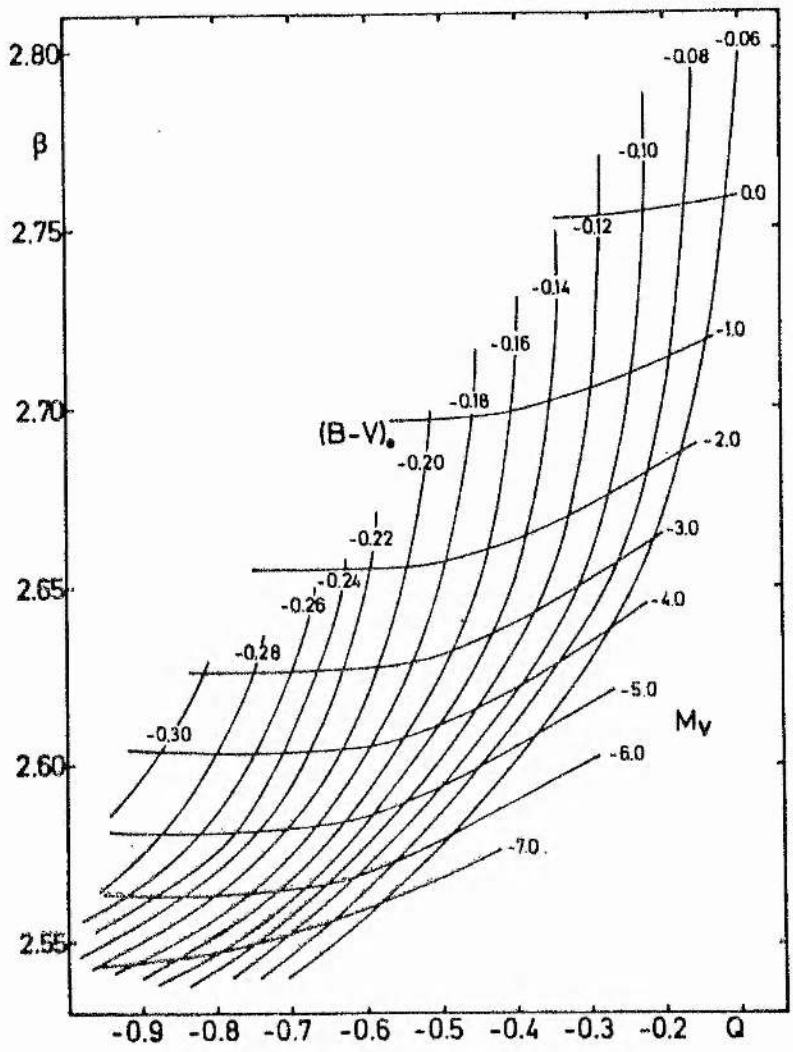

Fig 2.2.1

2.3 Distance and Galactocentric Distance Determination

The intrinsic visual magnitude of a star, which is the visual magnitude that would be observed if there were no interstellar reddening, is given by

$$V_o = V - A_V \quad \text{- - - - - - - - - - - - - - - -} \quad (2.3.1),$$

where V = the observed visual magnitude of the star on the Johnson and Morgan (1953), UBV system,

and A_V = the total absorption in the visual part of the spectrum, due to interstellar dust, measured in magnitudes.

It is apparent that there is some correlation between A_V and E_{B-V}. The relation between them is dependant upon the nature of the interstellar dust itself. If the nature and composition of the interstellar dust varies in the Milky Way, the relation between A_V and E_{B-V} will also vary. The first determination of this relation was made by Morgan et al. (1953), who obtained a value $R = (A_V/E_{B-V}) = 3.0 \pm 0.2$.

An investigation of interstellar reddening in the "Cygnus Rift" by Johnson & Morgan (1955) led them to the conclusion that R = 6 for O stars in this region, although a value R = 3 was found elsewhere. It was recognized that there were large amounts of obscuring interstellar dust in Cygnus, which is consistent with the findings of the intermediate latitude survey discussed in this analysis (§8.1). Accordingly, Johnson & Morgan (1955), proposed that this anomaly was due to relatively high concentrations of dust close to the O stars. The intense radiation from an O star, would modify the physical and chemical structure of the dust, and this would change its obscuration properties giving the anomalous value for R. This has been subsequently confirmed by Hiltner and Johnson (1956). A further study of this effect has been made by Reddish (1967) who concluded that the more luminous the star, the larger the obscuring cloud around it.

The value of R has been discussed in some detail by Schmidt-Kaler (1967), who has shown that R = 3.2 is probably better than R = 3.0. Wiemar (1974) has shown, by means of colour-magnitude diagrams, that within our galaxy there is only one mean law of interstellar extinction, a view supported by Sherwood (1975). The anomalous cases have been explained in terms of the peculiar properties in the stars themselves. The value $R = 3.2 \pm 0.2$ seems to have become widely accepted, and has been adopted here.

Thus equation (2.3.1) becomes

$$V_o = V - 3.2.E_{B-V} \quad \text{- - - - - - - - - - - - - - - -} \quad (2.3.2),$$

and the distance of each star in kiloparsecs can be calculated by substitution in the relation

$$r = \text{Antilog}_{10}[\, 0.2(V_o - M_V + 5)] \,/\, 1000 \quad \text{- - - - -} \quad (2.3.3),$$

derived by Pogson (1856).

Let z be the height of a star of galactic coordinates (l,b) above the galactic plane. Thus z is given by

$$z = r \sin b \quad \text{- - - - - - - - - - - - - - - - - - - -} \quad (2.3.4).$$

If RQ is the galactocentric distance (R_c) projected on to the galactic plane, then it can be seen from Fig. (2.3.1) that the application of the cosine formula gives

$$RQ^2 = R_o^2 + r^2\cos^2 b - 2R_o r \cos b.\cos l,$$

$$\therefore \quad RQ = (R_o^2 + r^2\cos^2 b - 2R_o r\cos b.\cos l)^{\frac{1}{2}} \quad \text{- - -} \quad (2.3.5).$$

The galactocentric distance R_c is given by

$$R_c = (RQ^2 + z^2)^{\frac{1}{2}},$$

The Determination of an Expression for Galactocentric Distance in Terms of the Heliocentric Distance and Galactic Coordinates

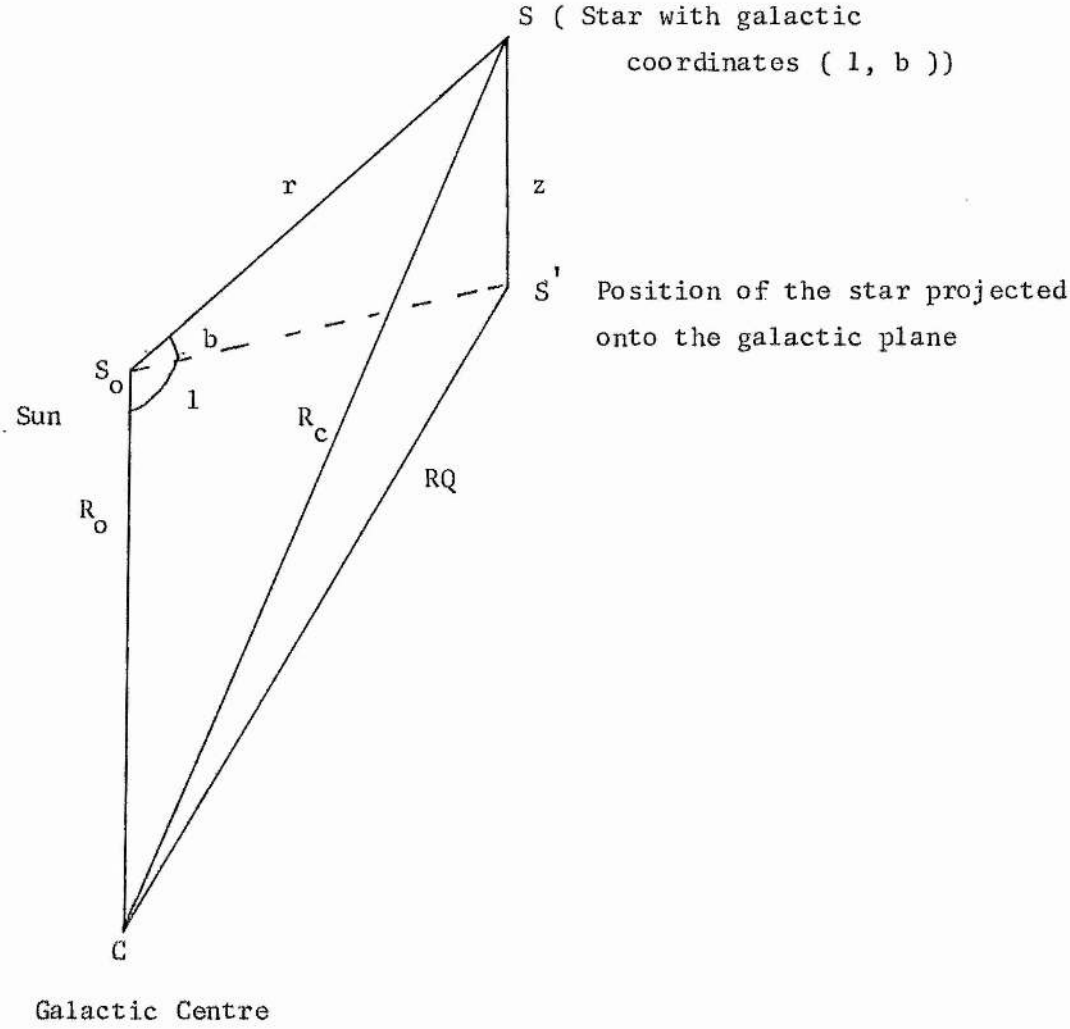

Fig 2.3.1

and substituting for RQ and z gives

$$R_c = (R_o^2 + r^2 - 2R_o r\cos b \cos l)^{\frac{1}{2}} \quad - - - - - - - - \quad (2.3.6),$$

Thus by application of equations (2.3.2), (2.3.3) and (2.3.6) the distance and galactocentric distance can be calculated for each programme star. To be strictly correct, the distances should be corrected statistically, using the method indicated by Feast and Shuttleworth (1965) and Feast (1972). However, this will not be undertaken at present, because it is not certain that the sample of programme stars (see Chapter 3), does not include subluminous stars. Furthermore, it turns out that most of the programme stars lie within 2kpc (§7.2). Balona & Feast (1974) have found that the statistical corrections are insignificant for stars within this distance, and only become large for stars beyond about 4.5 kpc. Thus it would appear that the conclusions drawn from the results (see Chapters 7, 8 and 9) are unaffected by neglecting this correction.

2.4 Space Velocity Determination

2.4.1. The Correction of Radial Velocities for Differential Galactic Rotation.

The correction of radial velocities for differential galactic rotation has been considered in detail by Kilkenny (1973), who has essentially followed the method proposed by Trumpler & Weaver (1953, page 562). For the sake of completeness, the argument will be re-discussed here. Consider the Sun S_o and a star S at respective distances of R_o and R_c from the galactic centre C, as indicated in Fig (2.4.1.1). Suppose that both have circular orbits about C, their respective orbital speeds are θ_o and θ. Assume that the solar orbit lies in the galactic plane, and that the orbit of S, galactic coordinates (l,b), is inclined at an angle α to the line of sight SS_o. In the case of $b = o$, the radial velocity of S as observed from S_o is

$$V' = \theta \cos \alpha - \theta_o \sin l \quad - - - - - - - - \quad (2.4.1.1).$$

By application of the sine formula

$$\frac{\sin (90 + \alpha)}{R_o} = \frac{\sin l}{R_c} ,$$

$$\therefore \cos \alpha = \frac{R_o}{R_c} \sin l,$$

and substitution in equation (2.4.1.1) gives

$$V' = \theta . \frac{R_o}{R_c} \sin l - \theta_o \sin l,$$

$$\therefore V' = R_o \left[\frac{\theta}{R_c} - \frac{\theta_o}{R_o} \right] \sin l .$$

The Derivation of an Expression for the Contributions to the Observed Radial Velocity and Proper Motions due to Differential Galactic Rotation

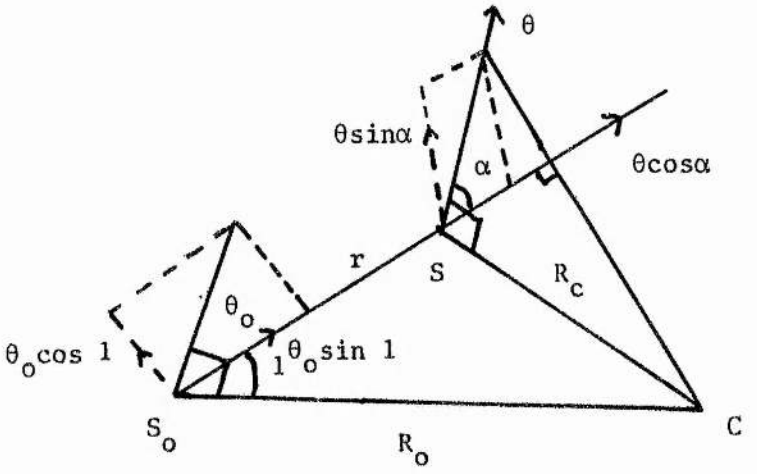

Fig 2.4.1.1

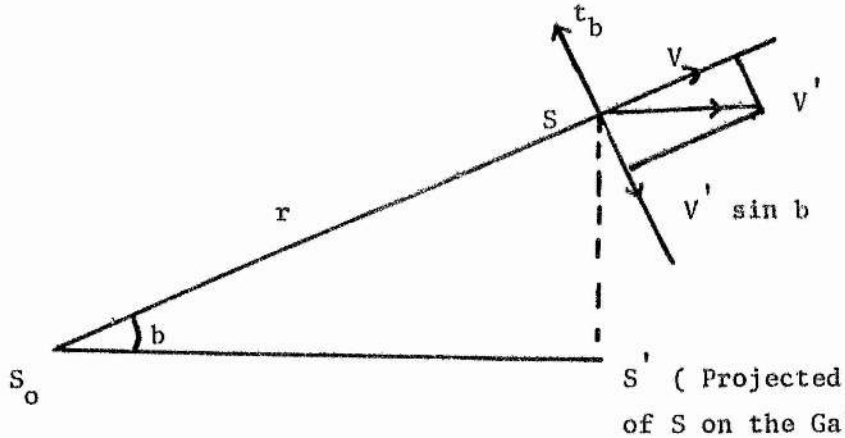

Fig 2.4.1.2

$$V' = R_o(\omega(R_c) - \omega(R_o)) \sin l,$$

where $\omega(R_c)$ and $\omega(R_o)$ are the respective angular velocities of S and S_o about C. If $b \neq 0$ then the contribution to the radial velocity of S, as observed from S_o, due to differential galactic rotation is

$$V_1 = R_o(\omega(R_c) - \omega(R_o)) \sin l \cos b \quad - - - \quad (2.4.1.2)$$

The expression for the radial velocity due to differential galactic rotation derived by Oort (1927) depends on the assumption that $r \ll R_o$ although no assumption was made about the nature of the orbits. For stars with distances of 1kpc. or more, the assumption made by Oort is hardly valid. On the other hand, the orbits of these stars are not likely to be very different from circles, except in the cases of high velocity runaway stars, and the number of these is probably very few. Hence the assumption of circular orbits is reasonable in this case.

For stars away from the galactic plane, the angular velocity should be represented by $\omega = \omega(R_c, z)$. However, observations of our own galaxy and external galaxies suggest that spiral structure persists over several revolutions. This would hardly be possible if there were a large difference in the angular velocity of rotation at different heights above the galactic plane, for a given galactocentric distance projected onto the galactic plane. Thus the assumption that ω is independant of z is justified.

To implement equation (2.4.1.2), the function $[\omega(R_c) - \omega(R_o)]$ has to be determined. This has been done by Feast & Shuttleworth (1965), and amended by Schmidt-Kaler (1967). An approximate numerical fit to Schmidt-Kaler's graphical representation of this function, derived by Kilkenny (1973), involves fitting five straight lines to the curve, which are

(1) for $R_c < 5$ kpc. $\omega = -6.45\ R_c + 52.45$,

(2) for $5 \leqslant R_c < 7$ kpc. $\omega = -4.88\ R_c + 44.40$,

(3) for $7 \leqslant R_c < 10$ kpc. $\omega = -3.33\ R_c + 33.33$,

(4) for $10 \leqslant R_c < 12$ kpc. $\omega = -2.50\ R_c + 25.00$,

and (5) for $12 \leqslant R_c$ $\omega = -1.16\ R_c + 8.93$,

where $\omega = \omega(R_c) - \omega(R_o)$. The function given by Schmidt-Kaler (1967) has not been determined outside the limits $4 \leqslant R_c \leqslant 15$ kpc, and consequently ω cannot be calculated outside this range.

The error in V_1 calculated from equation (2.4.1.2), using this approximate derivation for ω, is of the order of 0.5 km/sec. This is small in comparison with the usual errors in B star radial velocities, and when distance errors are taken into account as well, this becomes negligibly small. The variation of V_1 as a function of galactic longitude, for different values of r, is illustrated in Fig (9.3.1).

Balona & Feast (1974) have derived the relation

$$\omega = 55.056 - 9.919\ R_c + 0.310\ R_c^2 \quad \text{- - - - - - - - - - - - (2.4.1.3),}$$

from their stellar and interstellar Ca II radial velocities, taking the distance of the Sun from the galactic centre to be 9 kpc. Some estimates suggest a value of $R_o = 10$ kpc. For this reason, and because of the intention to compare the results of Kilkenny (1973) with those presented here in the future, it was decided to adopt the linear-fit method for calculating ω for each of the programme stars. In this way the correction to the radial velocities for differential galactic rotation were determined.

2.4.2 The Correction of Proper Motions for Differential Galactic Rotation.

Following the arguments given by Trumpler and Weaver (1953, page 562), and Kilkenny (1973), it can be seen from Fig (2.4.1.1) that the component of the proper motion in the direction of increasing galactic longitude, due to differential galactic rotation, is given by

$$t_l = \Theta \sin \alpha - \Theta_o \cos l \quad - - - - - - - - - - - - - \quad (2.4.2.1),$$

if it is assumed in the first instance, that $b = 0$. Furthermore,

$$R_o \cos l = r + R_c \cos(90 - \alpha),$$

and so $$\sin \alpha = \frac{R_o \cos l - r}{R_c} .$$

Substituting in equation (2.4.2.1) gives

$$t_l = \frac{\Theta}{R_c}(R_o \cos l - r) - \frac{\Theta_o}{R_o} R_o \cos l,$$

and so from the definitions of $\omega(R_c)$ and $\omega(R_o)$ (§2.4.1.1),

$$t_l = R_o[\omega(R_c) - \omega(R_o)] \cos l - \omega(R_c) r \quad - - - - - \quad (2.4.2.2).$$

From Fig (2.4.1.2), it can be seen that in the case where $b \neq 0$, the term r in equation (2.4.2.2) must be replaced by $r \cos b$, giving

$$t_l = R_o[\omega(R_c) - \omega(R_o)] [\cos l - r \cos b / R_o] - \omega(R_o) r \cos b$$

$$- - - - - \quad (2.4.2.3).$$

The Determination of the Equatorial Components of the Proper Motion

Correction due to Differential Galactic Rotation

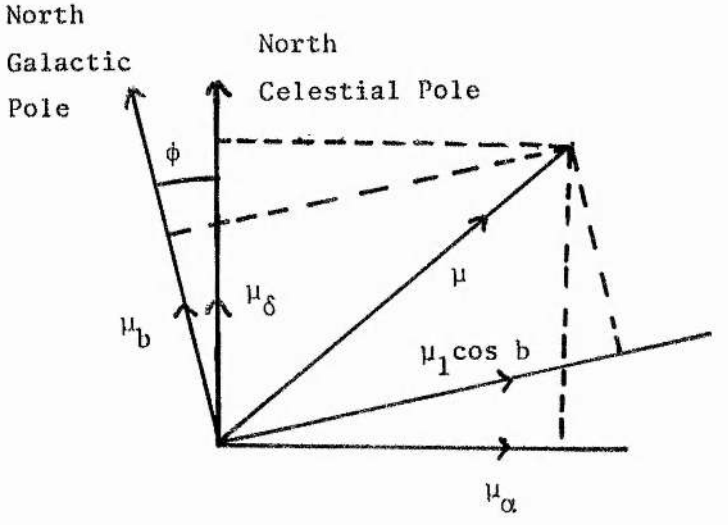

Fig 2.4.2.1

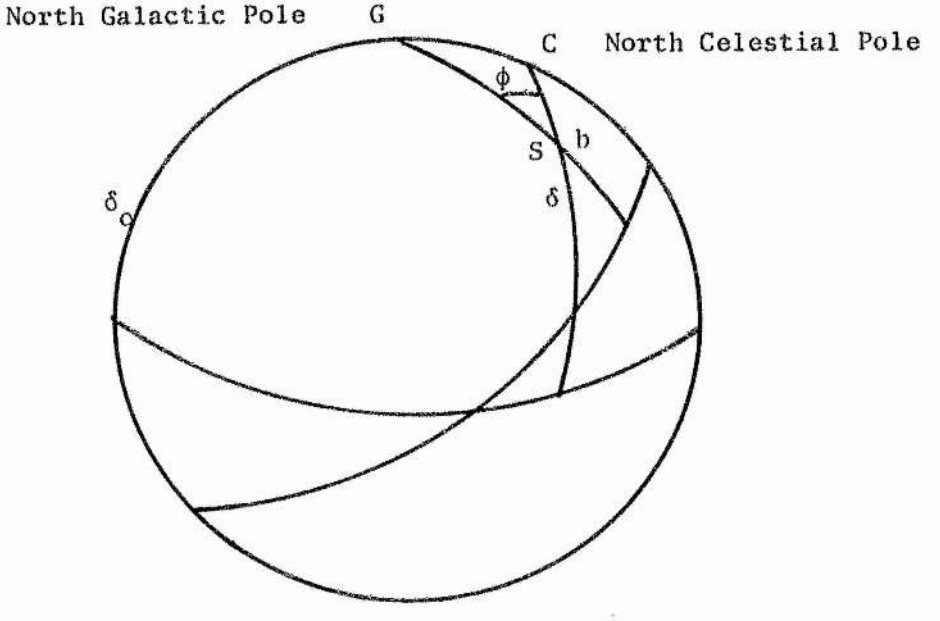

Fig 2.4.2.2

The component of proper motion in the direction of increasing galactic latitude, due to differential galactic rotation, is given by

$$t_b = -V' \sin b,$$

$$\therefore \quad t_b = -V_1 \tan b \quad - - - - - - - - - - - - - - - - \quad (2.4.2.4).$$

Now let $t_l = K\mu_l \, r \cos b \quad - - - - - - - - - - - - - - - - \quad (2.4.2.5),$

and $t_b = K\mu_b \, r \quad - - - - - - - - - - - - - - - - - - \quad (2.4.2.6),$

where μ_l and μ_b are the proper motions due to differential galactic rotation in seconds of arc per year, and K is the appropriate conversion factor. Thus equations (2.4.2.3) and (2.4.2.5) give

$$K\mu_l \, r \cos b = (\omega(R_c) - \omega(R_o)) \, [R_o \cos l - r \cos b] - \omega(R_o) r \cos b$$

$$- - - - - - - - - - \quad (2.4.2.7),$$

and equations (2.4.1.2), (2.4.2.4) and (2.4.2.6) give

$$K\mu_b r = -R_o [\omega(R_c) - \omega(R_o)] \sin l \sin b \quad - - - - - \quad (2.4.2.8).$$

Assuming that R_o = 10kpc. and Θ_o = 250 km/s (Allen, 1973, p.283), $\omega(R_o)$ = 25 km/s/kpc. This can be substituted into equation (2.4.2.7) and then using the value of $[\omega(R_c) - \omega(R_o)]$ derived in the manner already described (§2.4.1), equations (2.4.2.7) and (2.4.2.8) give the values of μ_l and μ_b for each star. By resolution into components, see (Fig. 2.4.2.1), the corresponding corrections to the equatorial proper motions, μ'_α and μ'_δ can be derived as

$$\mu'_\alpha = \mu_l \cos b \cos \phi - \mu_b \sin \phi \quad - - - - - \quad (2.4.2.9),$$

and $\mu'_\delta = \mu_l \cos b \sin \phi - \mu_b \cos \phi \quad - - - - - \quad (2.4.2.10).$

The angle ϕ is sometimes referred to as the galactic parallactic angle, and is the angle between the galactic and celestial north poles at the star under consideration. In the spherical triangle GCS (Fig. 2.4.2.2), ϕ is given by the cosine formula as

$$\cos \phi = \frac{\sin \delta_o - \sin \delta \sin b}{\cos \delta \cos b} \quad \text{- - - - - - - - -} \quad (2.4.2.11),$$

where $\delta_o = 27.4$, is the declination of the north galactic pole (Blaauw et al., 1959). In this way, the observed radial velocities and proper motions can be corrected for the effects of differential galactic rotation.

2.4.3 The Derivation of Galactic Velocity Components from the Observed Velocity Components.

Suppose that the solar motion relative to the local standard of rest is represented by $U_\odot$, $V_\odot$ and $W_\odot$, the component towards the galactic centre, in the direction of galactic rotation and normal to the galactic plane respectively. Then considering a spherical polar coordinate system (r,l,b), the radial velocity (V_2) and the proper motion components (t_l' and t_b') that are observed as a result of the solar motion are

$$V_2 = U_\odot \cos l \cos b + V_\odot \sin l \cos b + W_\odot \sin b \text{ - - - } (2.4.3.1),$$

$$rt_b' = -U_\odot \cos l \sin b - V_\odot \sin l \sin b + W_\odot \sin b \text{ - - - } (2.4.3.2),$$

and $$rt_l' \cos b = -U_\odot \sin l + V_\odot \cos l \quad \text{- - - - - - - - - - - - } (2.4.3.3)$$

The weighted mean results of Feast & Shuttleworth (1965) were assumed as

$U_\odot = 10 \pm 0.5$ km/sec. and $V_\odot = 13 \pm 0.5$ km/sec.,

and following Kilkenny (1973) the value

$$W_\odot = 6 \pm 0.5 \text{ km/sec}$$

was adopted. These have the advantage of having been determined from OB stars, although they differ somewhat from the results of Balona & Feast (1974), which is to be expected from the fact that they derive a distance from the Sun to the Galactic Centre of 9kpc.

Any systematic errors introduced by assuming one determination instead of the other, or by taking a weighted mean of the two, will be small in comparison with the errors introduced into the space motions from other sources, such as proper motion errors. Therefore, in order to be consistent with the work of Kilkenny (1973), with whose results a comparison is to be made, the determination of the solar motion by Feast & Shuttleworth (1965) was adopted.

A substitution into equations (2.4.3.2) and (2.4.3.3) shows that t_b' and t_l' are negligible for the stars considered in this analysis. Thus the solar motion corrections to the proper motions are neglected. The radial velocities and proper motions are corrected for differential galactic rotation in the manner described previously (§2.4.1 and §2.4.2) and the residual radial velocity corrected for the solar motion as prescribed by equation (2.4.3.1). The residual radial velocity and proper motions, are those that would be observed in the local standard of rest of the star in question.

The calculation of heliocentric galactic velocity components, from these corrected radial velocities and proper motions, has been reviewed by Hill (1969). The proper motion μ_α is defined as

$$\mu_\alpha = 15\mu_\alpha' \cos \delta$$

where μ_α' is the proper motion in right ascension in seconds of

time per annum. The proper motions μ_α and μ_δ are in the directions of right ascension and declination respectively, in seconds of arc per annum. The corresponding proper motions in kms/sec. are given by

$$t_\alpha = Kr\mu_\alpha \quad - - - - - - - - - - - - - - - - - \quad (2.4.3.4),$$

and $$t_\delta = Kr\mu_\delta \quad - - - - - - - - - - - - - - - - - \quad (2.4.3.5),$$

where r and K are as defined in (§2.4.1) and (§2.4.2) respectively. The orientation in space of the initial V_r, t_α and t_δ coordinate system is dependant upon the position of the star. If μ_α and μ_δ are referred to the epoch 1950, then the V_r, t_α and t_δ system is transformed to the equatorial system for the epoch 1950. The x-axis is the direction of $\alpha = 0°$, $\delta = 0°$, the y-axis is towards $\alpha = 90°$ and $\delta = 0°$, and the z-axis is towards $\delta = +90°$.

This transformation is carried out by making two successive rotations to the coordinate system. It follows that

$$\begin{bmatrix} \dot{x} \\ \dot{y} \\ \dot{z} \end{bmatrix} = \begin{bmatrix} -\sin\alpha & \cos\alpha & 0 \\ \cos\alpha & \sin\alpha & 0 \\ 0 & 0 & 1 \end{bmatrix} \begin{bmatrix} 1 & 0 & 0 \\ 0 & -\sin\delta & \cos\delta \\ 0 & \cos\delta & \sin\delta \end{bmatrix} \begin{bmatrix} t_\alpha \\ t_\delta \\ V_r \end{bmatrix}$$

$$- - - - - - - - - \quad (2.4.3.6).$$

In general, three rotations are now required to transform the $\dot{x},\dot{y},\dot{z}$ velocity system into the heliocentric galactic U,V,W system. Here U, V and W are the velocities towards the galactic centre, in the direction of galactic rotation and normal to the galactic plane respectively, being referred to the local standard of rest of the star in question. If α_o and δ_o are the equatorial coordinates of the north galactic pole for the epoch 1950, and l_o

is the galactic longitude of the ascending node of the galactic plane on the celestial equator, then the space motion components are given by

$$\begin{bmatrix} U \\ V \\ W \end{bmatrix} = \begin{bmatrix} \cos l_o & \sin l_o & 0 \\ \sin l_o & -\cos l_o & 0 \\ 0 & 0 & 1 \end{bmatrix} \begin{bmatrix} 1 & 0 & 0 \\ 0 & \sin \delta_o & -\cos \delta_o \\ 0 & \cos \delta_o & \sin \delta_o \end{bmatrix} \begin{bmatrix} -\sin\alpha_o & \cos\alpha_o & 0 \\ \cos\alpha_o & \sin\alpha_o & 0 \\ 0 & 0 & 1 \end{bmatrix} \begin{bmatrix} \dot{x} \\ \dot{y} \\ \dot{z} \end{bmatrix}$$

- - - - - - - - (2.4.3.7).

The space velocity S is then given by

$$S = (U^2 + V^2 + W^2)^{\frac{1}{2}} \qquad - - - - - - - - - (2.4.3.8).$$

2.5 The Theory of Standard Deviation Determinations

The relation between the standard deviation of a quantity and the standard deviations in the parameters from which the quantity is determined, are in all cases derived from the relation between the quantity and the parameters, following the method given by Barford (1967, page 29). As already discussed (§2.3), the ratio of the total absorption to the selective absorption is given by

$$A_V = R.E_{B-V} ,$$

and so

$$\sigma(A_V) = A_V \left[\frac{\sigma^2(R)}{R^2} + \frac{\sigma^2(E_{B-V})}{(E_{B-V})} \right]^{\frac{1}{2}} \quad - - - - \quad (2.5.1),$$

where $\sigma(X)$ denotes, throughout, the standard deviation in a general quantity X.

Similarly, from equation (2.3.1), the standard deviation in the intrinsic visual magnitude is

$$\sigma(V_0) = (\sigma^2(V) + \sigma^2(A_V))^{\frac{1}{2}} \quad - - - - - - - - - - - \quad (2.5.2),$$

where $\sigma(A_V)$ is obtained from equation (2.5.1). The standard deviation in the distance is given, in kiloparsecs, as

$$\sigma(r) = 0.2r[\ \sigma^2(V_0) + \sigma^2(M_V)\ ]^{\frac{1}{2}} \quad - - - - - - - - \quad (2.5.3),$$

where $\sigma(V_0)$ is given by equation (2.5.2), and the standard deviation in the absolute magnitude, $\sigma(M_V)$, is assumed to be as described later (§7.2). From equation (2.3.4), it follows that

$$\sigma(z) = \sigma(r)\sin b \quad - - - - - - - - - - - - \quad (2.5.4),$$

and the standard deviation in the galactocentric distance, which follows from equation (2.3.6), is

$$\sigma(R_c) = \frac{1}{R_c}\left[R_o^2\sigma^2(R_o) + r^2\sigma^2(r) + \cos^2 l \cos^2 b\left(\frac{\sigma^2(R_o)}{R_o^2} + \frac{\sigma^2(r)}{r^2}\right)\right]^{\frac{1}{2}}$$

- - - - - - - - (2.5.5).

To obtain $\sigma(R_c)$ from the above relation, it is necessary to have an estimate of $\sigma(R_o)$, the standard deviation in the estimate of the distance of the Sun from the galactic centre. The other quantities have been discussed above or previously (§2.3). To derive the standard deviations in the space motion components, $\sigma(U)$, $\sigma(V)$ and $\sigma(W)$, it is necessary to estimate a value for $\sigma[\omega(R_o)]$, the standard deviation of the angular velocity of the Sun about the centre of the galaxy. This can be calculated from values of Oort's Constants, A and B, and a value for R_o, given by Allen (1973, page 283) as

$$R_o = 10.0 \pm 0.8 \text{ kpc.},$$

$$A = 15.0 \pm 0.8 \text{ km.sec}^{-1} \text{ kpc}^{-1}$$

and $$B = -10.0 \pm 0.8 \text{ km.sec}^{-1} \text{ kpc}^{-1}.$$

Thus the value

$$\sigma(R_o) = \pm 0.8 \text{ kpc},$$

was adopted and the relation

$$\omega(R_o) = A - B ,$$

derived by Oort (1927), gives the expression

$$\sigma[\,\omega(R_o)\,] = [\,\sigma^2(A) + \sigma^2(B)\,]^{\frac{1}{2}}$$

from which $\sigma[\ \omega(R_o)\ ]$ was calculated, using the values for $\sigma(A)$ and $\sigma(B)$ listed above.

As explained already (§2.4), the observed radial velocity of a star, V_{obs}, is thought to be made up of three parts, which are due to the solar motion with respect to the solar local standard of rest, differential galactic rotation, and the motion of the star with respect to its own local standard of rest, V_r. Thus the standard deviation in V_r, $\sigma(V_r)$ is

$$\sigma(V_r) = [\ \sigma^2(V_{obs}) + \sigma^2(V_1) + \sigma^2(V_2)\ ]^{\frac{1}{2}} \quad - - - \quad (2.5.6),$$

where $\sigma(V_1)$ is the standard deviation in the radial velocity component of differential galactic rotation. This can be derived from

$$\sigma(V_1) = V_1 \left[\frac{\sigma^2(R_o)}{R_o^2} + \frac{\sigma^2[\omega(R_c) - \omega(R_o)]}{[\omega(R_c) - \omega(R_o)]^2} \right]^{\frac{1}{2}} \quad - - - - \quad (2.5.7)$$

which follows from equation (2.4.1.2). Here $\sigma\ [\omega(R_c) - \omega(R_o)]$ is the standard deviation in the value of the function $\omega = [\omega(R_c) - \omega(R_o)]$. This is not easy to determine precisely, as it depends on how well ω represents galactic rotation, and also on the accuracy of the linear fitting technique. However, both of these errors are small in comparison with the error that arises due to an error in R_c, and so they are neglected. Since only approximate standard deviations in the space motions are required, this simplification is justified. Since $\omega = \omega(R_c)$, $\sigma(\omega)$ is given by

$$\sigma(\omega) = \frac{d\omega}{dR_c} \cdot \sigma(R_c) \quad - - - - - - - - - \quad (2.5.8),$$

where $d\omega/dR_c$ is evaluated at the appropriate value of R_c, and $\sigma(R_c)$ is given by equation (2.5.5). Following the "linear fit" technique $\sigma(\omega)$ is evaluated as indicated below :

For $R_c < 5$kpc. $\sigma(\omega) = 6.45\ \sigma(R_c)$,

for $5 \leqslant R_c < 7$kpc. $\sigma(\omega) = 4.88\ \sigma(R_c)$,

for $7 \leqslant R_c < 10$kpc. $\sigma(\omega) = 3.33\ \sigma(R_c)$,

for $10 \leqslant R_c < 12$kpc $\sigma(\omega) = 2.5\ \sigma(R_c)$,

and for $12 \leqslant R_c$ $\sigma(\omega) = 1.2\ \sigma(R_c)$.

Substitution in equation (2.5.7) yields $\sigma(V_1)$. From equation (2.4.3.1), it follows that

$$\sigma(V_2) = [\sigma^2(U_\odot)\cos^2 l \cos^2 b + \sigma^2(V_\odot)\sin^2 l \cos^2 b + \sigma^2(W_\odot)\sin^2 b]^{\frac{1}{2}} \quad \text{- - - - - - - - (2.5.9),}$$

where $\sigma(U_\odot)$, $\sigma(V_\odot)$ and $\sigma(W_\odot)$ are the standard deviations in $U_\odot$, $V_\odot$ and $W_\odot$ respectively; the adopted values for these are already given (§2.4.3). In order to obtain $\sigma(V_r)$ from equation(2.5.6), the standard deviation in the observed radial velocity, $\sigma(V_{obs})$, has to be derived. This is discussed later (§5.6).

It follows from equations (2.4.2.3) and (2.4.2.4), that the standard deviations in the corrections to the proper motions, t_l and t_b, are

$$\sigma(t_l) = [\sigma^2(\omega R_o)\cos^2 l + \sigma^2(\omega r)\cos^2 b + \sigma^2[\omega(R_o)r]\cos^2 b\ ]^{\frac{1}{2}} \quad \text{- - - - - - - - - - - - (2.5.10)}$$

and $\sigma(t_b) = \sigma(V_1) \tan b$ - - - - - - - - - - - - - - - - - - (2.5.11),

where $\sigma(R_o\omega) = R_o\omega \left[\frac{\sigma^2(R_o)}{R_o^2} + \frac{\sigma^2(\omega)}{\omega^2}\right]^{\frac{1}{2}}$,

$$\sigma[\omega(R_o)r] = r\omega(R_o)\left[\frac{\sigma^2[\omega(R_o)]}{\omega^2(R_o)} + \frac{\sigma^2(R_o)}{R_o^2}\right]^{\frac{1}{2}},$$

and $$\sigma(r\omega) = r\omega\left[\frac{\sigma^2(r)}{r^2} + \frac{\sigma^2(\omega)}{\omega^2}\right]^{\frac{1}{2}}.$$

Thus by making the appropriate substitutions, derived in the manner described above, in equations (2.5.10) and (2.5.11), $\sigma(t_l)$ and $\sigma(t_b)$ can be evaluated. From equations (2.4.2.5) and (2.4.2.6) it follows that

$$\sigma(\mu_l) = \mu_l\left[\frac{\sigma^2(r)}{r^2} + \frac{\sigma^2(t_l)}{t_l^2}\right]^{\frac{1}{2}} \text{ - - - - - - - (2.5.12)},$$

and $$\sigma(\mu_b) = \mu_b\left[\frac{\sigma^2(r)}{r^2} + \frac{\sigma^2(t_b)}{t_b^2}\right]^{\frac{1}{2}} \text{ - - - - - - - - (2.5.13)}.$$

These results are then used to determine the standard deviations in the estimated corrections to the proper motions, which are

$$\sigma(\mu'_\alpha) = [\,\sigma^2(\mu_l)\cos^2 b\,\cos^2\phi + \sigma^2(\mu_b)\sin^2\phi\,]^{\frac{1}{2}} \text{ - - - (2.5.14)},$$

and $$\sigma(\mu'_\delta) = [\sigma^2(\mu_l)\cos^2 b\,\sin^2\phi + \sigma^2(\mu_b)\cos^2\phi\,]^{\frac{1}{2}} \text{ - -(2.5.15)}.$$

These relations follow from equations (2.4.2.9) and (2.4.2.10), and can be used to derive the standard deviations of the corrected proper motions which are given by

$$\sigma(\mu''_\alpha) = [\ \sigma^2(\mu_\alpha) + \sigma^2(\mu'_\alpha)\ ]^{\frac{1}{2}} \quad \text{- - - - - - - - - - - (2.5.16),}$$

$$\text{and} \quad \sigma(\mu''_\delta) = [\ \sigma^2(\mu_\delta) + \sigma^2(\mu'_\delta)\ ]^{\frac{1}{2}} \quad \text{- - - - - - - - - - - (2.5.17),}$$

where $\sigma(\mu_\alpha)$ and $\sigma(\mu_\delta)$ are the standard deviations in the catalogued proper motions μ_α and μ_δ respectively. These are discussed later (§7.2).

As already indicated (§2.4.3) the proper motions in km/sec., t_α and t_δ, are derived from equations (2.4.3.4) and (2.4.3.5) respectively. Thus it follows that the standard deviations in these quantities are

$$\sigma(t_\alpha) = t_\alpha\ [\ \sigma^2(r)/r^2 + \sigma^2(\mu_\alpha)/\mu_\alpha^2\ ]^{\frac{1}{2}} \quad \text{- - - - - - - - - (2.5.18),}$$

$$\text{and} \quad \sigma(t_\delta) = t_\delta\ [\ \sigma^2(r)/r^2 + \sigma^2(\mu_\delta)/\mu_\delta^2\ ]^{\frac{1}{2}} \quad \text{- - - - - - - - - (2.5.19).}$$

These results are used to derive the standard deviations $\sigma(\dot{x})$, $\sigma(\dot{y})$ and $\sigma(\dot{z})$, and ultimately the standard deviations in the space velocity components U, V and W. The matrix equations below are derived from equations (2.4.3.6) and (2.4.3.7). These give the squares of the standard deviations as

$$\begin{bmatrix} \sigma^2(\dot{x}) \\ \sigma^2(\dot{y}) \\ \sigma^2(\dot{z}) \end{bmatrix} = \begin{bmatrix} \sin^2\alpha & \cos^2\alpha.\sin^2\delta & \cos^2\alpha.\cos^2\delta \\ \cos^2\alpha & \sin^2\alpha.\sin^2\delta & \sin^2\alpha.\cos^2\delta \\ 0 & \cos^2\delta & \sin^2\delta \end{bmatrix} \begin{bmatrix} \sigma^2(t_\alpha) \\ \sigma^2(t_\delta) \\ \sigma^2(V_r) \end{bmatrix}$$

$$\text{- - - - - - - - (2.5.20),}$$

$$\text{and} \quad \begin{bmatrix} \sigma^2(U) \\ \sigma^2(V) \\ \sigma^2(W) \end{bmatrix} = \begin{bmatrix} 0.005 & 0.762 & 0.234 \\ 0.243 & 0.203 & 0.554 \\ 0.753 & 0.035 & 0.212 \end{bmatrix} \begin{bmatrix} \sigma^2(\dot{x}) \\ \sigma^2(\dot{y}) \\ \sigma^2(\dot{z}) \end{bmatrix} \text{- - (2.5.21),}$$

$\sigma(U)$, $\sigma(V)$ and $\sigma(W)$ are derived by taking the appropriate square roots. The standard deviation in the space velocity of a star with respect to its local standard of rest is then given by

$$\sigma(S) = (1/S) \left[U^2\sigma^2(U) + V^2\sigma^2(V) + W^2\sigma^2(W) \right]^{\frac{1}{2}} \text{ - - - - - } (2.5.22),$$

which follows from equation (2.4.3.8). In the derivation of the above expressions, it has been assumed throughout that the errors in the equatorial, and hence galactic, coordinates of each star are negligible, as compared with the other errors considered.

2.6. The Mean Distances and Galactocentric Distances of Inter-Stellar CaII Absorption

For reasons explained later (§9.1), $\bar{r}_1$ was adopted for the mean distance of the interstellar CaII absorption. This is given by equation (2.1.8). Substitution of $\bar{r}_1$ for r in equation (2.3.6) gives the mean galactocentric distance of the interstellar CaII absorption. Considering equation (2.1.8),

$$\text{let } y = (1 - (1 + \alpha)\exp(-\alpha))(1 - \exp(-\alpha)) \quad - - - - \quad (2.6.1)$$

where $\alpha = z/h$, as defined previously (§2.1).

Thus the standard deviation in α, $\sigma(\alpha)$, is given by

$$\sigma(\alpha) = \alpha \left[\frac{\sigma^2(z)}{z^2} + \frac{\sigma^2(h)}{h^2} \right]^{\frac{1}{2}} \quad - - - - - - - - - - - - \quad (2.6.2)$$

Since y is a function of α, the standard deviation in y is

$$\sigma(y) = \frac{dy}{d\alpha} \cdot \sigma(\alpha) ,$$

$$\therefore \quad \sigma(y) = (\exp(\alpha) - 1)^{-1} (\alpha - y) \quad \sigma(\alpha) \quad - - - - - - - - - - - - (2.6.3),$$

which is derived by differentiating equation (2.6.1). Thus since

$$\bar{r}_1 = h \operatorname{cosec} b \; y ,$$

which is in effect equation (2.1.8), the standard deviation in $\bar{r}_1$ is given by

$$\sigma(\bar{r}_1) = \bar{r}_1 \left[\frac{\sigma^2(h)}{h^2} + \frac{\sigma^2(y)}{y^2} \right]^{\frac{1}{2}} \quad - - - - - - \quad (2.6.4)$$

The values of y and $\sigma(y)$ are derived in the above manner, and values of h and $\sigma(h)$ are discussed later (§8.3). By substituting $\bar{r}_1$ for r and $\sigma(\bar{r}_1)$ for $\sigma(r)$ in equation (2.5.5), the standard deviation in the mean galactocentric distance of the interstellar CaII absorption can be evaluated.

CHAPTER THREE

The Selection of Stars for the Observing Programme

3.1 Introduction

Observations of neutral hydrogen by Kepner (1970) and Davies (1972) have shown that spiral structure is still apparent at distances of one to two kiloparsecs from the galactic plane. Any attempt to confirm these observations by optical means requires that spiral arm tracers, in the appropriate part of the sky, be selected for observation. For this analysis, it was decided to restrict the observations to the area surveyed by Kepner. This area is defined by the new revised galactic coordinates (Blaauw et al., 1959) as $48° \leqslant l \leqslant 228°$ and $6° \leqslant b \leqslant 20°$.

A statistical investigation of galactic spiral structure was made by Rohlfs (1967). This showed that OB aggregates, early type clusters containing O to B2 stars, HII regions and early type Be stars are the best spiral tracers. Wolf-Rayet stars were excluded, but Schmidt-Kaler (1971) has shown that Wolf-Rayet stars are better spiral arm tracers than was suggested by Rohlfs' analysis.

Modern theories of stellar formation and evolution suggest that stars are formed in regions of relatively high concentration of neutral hydrogen, from which they then migrate. Thus it is hardly surprising that the best spiral arm tracers are OB stars and objects associated with them such as HII regions. There are other reasons for using OB stars as spiral arm tracers. For stars earlier than B5, the stellar CaIIK line is absent and so any CaIIK line present in the spectrum is interstellar in origin. This can, in theory, give information about the interstellar medium along the line of sight, as discussed in §5.1. Furthermore, by the application of a technique discussed previously (§2.2), the interstellar reddening can be determined.

Consequently, a list of the known OB stars in the area surveyed by Kepner (1970) was compiled from the "Henry Draper Catalogue" (Cannon and Pickering, 1918-1924), the "Henry Draper Extension" (Cannon, 1924-1936), and from the "Luminous Stars in the Northern Milky Way" (Hardorp et al., 1959, Stock et al., 1960, Hardorp et al., 1964, 1965, Nassau and Stephenson, 1963, and Nassau et al., 1965).

3.2 Selection of Stars from the HD Catalogue

3.2.1. Description of the Computer Programme Used.

A catalogue containing the OB stars in the HD Catalogue (Cannon and Pickering, 1918-1924) had been made on punched cards and copied onto magnetic tape. The University of St. Andrews IBM 360/44 was used to select stars in a particular part of the sky, reading the necessary data from the magnetic tape. For this purpose, a programme had been written in Fortran by Dr. P.W. Hill.

The data is read for each star in turn. The right ascension and declination are examined, to see if they lie within the limits specified by the programmer. If not then the star is rejected and the processing of information for the next star is begun. If the star is accepted, the galactic coordinates are calculated and similarly tested to ensure that they lie within the specified limits. If they do then the magnitude and spectral type are checked before the star is accepted. The data for accepted stars are listed on the line printer. These consist of the HD number (No. of star in the Henry Draper Catalogue), the BD number (Argelander, 1859-1862), the right ascension and declination processed to the required epoch, the photometric and photographic magnitudes, and the HD spectral type which is discussed later (§5.1.2).

In this way a list of stars of spectral types O to B5 was prepared. A supplementary list of B8 and B9 stars was also obtained. The reason for this was that at the time of the compilation of the HD catalogue, nothing was known of the interstellar medium. Consequently, when the interstellar CaIIK line was present, it was thought to be stellar. The appearance of this was recognised as an indication that the star was of spectral type B8 or later. Thus many early B type stars were misclassified. These are very often denoted by a "R" in the HD Catalogue. All of these stars were included in the observing list, and the remaining B8 stars formed an observing list of stars to which a lower priority was given.

3.2.2 The Removal of Emission Line, Variable and Double Stars

By modifying the job control language, the output of the programme described previously (§3.2.1) can be redirected to magnetic tape. This can then be copied onto disc giving a disc file of programme stars. A Fortran programme was written for the University of St. Andrews IBM 360/44, to list the contents of the file, but excluding stars whose HD numbers are input as data.

The catalogue of emission line stars by Wackerling (1970) was compared with the list of programme stars. Then a revised observing list was prepared using the above programme, the emission line stars being excluded. The necessity for removing emission line stars arises from the fact that narrow band photometry is to be used for absolute magnitude determination (§4.1). If published absolute magnitudes were found for these stars, then they were re-included in the list of programme stars (§7.2).

According to Petrie (1963), 51% of all B stars are double stars, and thus may exhibit variability. Thus the double and variable star catalogues were compared with the list of programme stars, including a supplementary list of programme stars prepared as described below (§3.3). A list of programme stars which are known to be binaries is given in Table (3.2.2.1) and a list of those which are known to be variable is given in Table (3.2.2.2). The catalogue by Blanco et al. (1968) was also searched, but no additional double or variable stars could be found.

In most cases the companions are very much fainter than the primaries, and consequently the magnitude variations are small even if the plane of the orbit lies along the line of sight. If the secondary is fainter than the primary, then its mass is probably much less than that of the primary, and so variations in radial velocity will probably be small. If all non-visual binaries in which the secondary is less than two magnitudes fainter than the primary are excluded, then at the very worst the observed magnitude is that of the primary to within 15%. In practice if the average is taken

Table 3.2.2.1

A List of Programme Stars in the Double Star Catalogue (Jeffers et al., 1963).

No (HD/BD)	ADS No.	Magnitudes	Notes
HD 3366	516	7.1, 10.9, 12.2	
HD 25638	2984	7.1, 12	
HD 25639		7.1, 10	
HD 41161	4655	6.5, 10.9	
HD 58383	6068	7.7, 8.8, 12.1	
HD 173087	11593	6.1, 7.5	
HD 174585	11732	5.8, 10.3	
HD 175426		5.5, 9.2	
HD 177109	11965	6.2, 13.3	
HD 177593	12003	7.1, 13.3	
HD 180163	12197	4.5, 11.1	
HD 180844	12263	7.1, 10.1, 11.4	
HD 186618	12849	8.5, 10.2	
HD 202214	14749	5.6, 8.7	
BD 58°2237		8.1, 9.3	1
HD 203025	14832	6.4, 12.6	
HD 208185	15417	8.4, 8.5	2
BD 67°1546	16879	9.8, 10.1	

Notes

1. - The fainter companion is BD 58°2236. The system constitutes a visual binary and so both stars were retained in the programme.

2. - This star was retained since the published radial velocity (Table 5.6.1) suggests that the binary nature of this star is questionable.

TABLE 3.2.2.2

A List of Programme Stars found in the General Catalogue of Variable Stars (Kukarkin et al. 1969, 1970, 1971).

No.	Name	Comments
HD 25638	SZ Cam	Variations in magnitude are small (Wesselink, 1941) and so the star is retained in the programme
HD 192035	RX Cyg	Apparently non-variable (Guetter, 1974) and so the star was retained
HD 187879	V380 Cyg	The variability of this star was not confirmed by Crawford et al. (1971) and so it was retained in the programme.
HD 188439	V819 Cyg	The variability of this star was not confirmed by Crawford et al. (1971) and so it was retained in the programme.
HD 60848	BN Gem	Magnitude variations from 6.0 → 6.6. See notes to Table (7.2.1).

over 3 or 4 nights on which the star is observed, then a better estimate of the magnitude of the primary is obtained. Similarly the mean radial velocity obtained on several different nights will give a reasonable estimate of the mean radial velocity of the system, provided that the period is not too long or equal to the interval at which the observations are made.

On the basis of these criteria, HD 186618 should be excluded from the observing list, but since it is a luminous star which is probably very distant, it was retained. Larger than average errors were to be expected in the radial velocity and photometric results for this star.

3.3 The Selection of Stars from the Henry Draper Extension and Luminous Stars in the Northern Milky Way Catalogues

Since the available observing time was limited, priority would have to be given to observing the brighter luminous stars, so as to obtain as large a sample of stars as possible. On the other hand, if galactic structure is to be investigated at distances of more than a few kiloparsecs, then the observations would have to be extended to fainter stars.

Consequently, all the OB stars listed in the "Luminous Stars in the Northern Milky Way" (Hardorp et al. 1959, Stock et al. 1960, Hardorp et al. 1964, 1965, Nassau and Stephenson 1963, and Nassau et al. 1965) were selected if they were in the area surveyed by Kepner (1970). The scheme of spectral classification used in this catalogue has been described by Slettebak and Stock (1957). Stars with a designation 'r' or '(r)', which indicates that the star is reddened or may be reddened respectively, were included. Furthermore, priority was given to observing these stars. The designations 'p' or '(p)', implying that the objective prism spectra are peculiar were also included. Stars with the designations given in Table 3.3.1 were not included in the observing list, but were used in the subsequent analysis if the relevant data had been published (§7.2).

It has been suggested by Herr (1969), that only 46% of OB^+ stars are non-emission line objects. Consequently, care was taken in selecting them for observation. The only OB^+ star in the area surveyed by Kepner (1970) is BD 35°1332. This was retained and subsequent Hβ photometry (§4.5) confirmed the absence of emission in Hβ. All the OB, OB^- and OB1 stars were retained unless they were rejected on the criterion outlined above.

The first section of the Henry Draper Extension was searched for stars of spectral type B5 or earlier, that lay in the area of the sky surveyed by Kepner (1970). Since this only produced three

TABLE 3.3.1

Reasons for Rejecting Stars with Some Designations after their Spectral Type (i.e. OB, OB^-, OB1)

Designation given to the spectral type	Reasons for Rejecting the Star
1e	Line emission, usually in one or more members of the Balmer Series. Rejected for the same reasons as HD emission line stars.
h	Hα observed in emission. This implies that other lines may be in emission as well.
ce	Continuous emission near the Balmer limit. This means that the star may be subluminous.

Note - The designation is sometimes enclosed in parentheses, which implies that the use of the classification is questionable. In these cases the star is also rejected.

additional programme stars, it was decided not search the remaining sections, in view of the labour involved. As there were sufficient stars for the available observing time, it was hardly necessary.

Those Henry Draper Extension stars for which published information was available before May 1975, were included in the subsequent analysis of galactic structure. In addition some stars, for which published data had been obtained by Chuadze (1974) were used.

3.4 The Selection of Programme Stars Requiring Hβ Observations

The list of programme stars, prepared in the manner described previously (§3.2 and §3.3), was used as a basis for preparing a list of stars requiring Hβ photometry. The literature was searched for published Hβ photometry, so as to exclude programme stars that had been observed previously. Some of these previously observed stars were retained, so that a comparison could be made with the results of other observers.

The relevant papers which had been published by the end of 1971 were, Crawford et al. (1971), Sinnerstad et al. (1968) and Haug (1970a). Of these three papers, only the first contained published Hβ photometry of the programme stars. The detailed account of the Hβ photometry is presented in Chapter 4.

After the observations had been completed a paper by Feinstein (1974) was published. This was also searched for Hβ photometry of the programme stars but none were found.

3.5 The Selection of Programme Stars Requiring Radial Velocity Determinations

A list of stars requiring spectroscopic observations was prepared in a manner similar to that discussed previously in connection with Hβ photometry (§3.4). The sources of published radial velocities at the end of July 1972 are listed at the end of Table (5.6.1). The exception is reference (2) which did not appear until later in the year.

In the first instance the catalogue by Wilson (1963) was searched, and from this a revised list of programme stars requiring radial velocity observations was prepared. Each paper was searched in turn, and at each stage a revised observing list was prepared using the computer programme described previously (§3.2.2). The papers by Plaskett and Pearce (1931), were not searched in this way, as the published velocities in these papers are given by Wilson (1963). With the publication of the catalogue by Abt and Biggs (1972), a useful check on the observing list was available.

A list of stars for which MK spectral types (§5.1.2) were required was prepared in a similar way. A search was made through references (1), (2), (4) and (6) in the list at the end of Table (5.8.1). Those stars which required MK spectral types, but did not require radial velocities, were then reincluded in the list of stars requiring spectroscopic observations. Observing these stars will not only give a spectral type, but also a check on the published radial velocities. All stars for which there were only Lick Observatory velocities available were also reincluded in the observing list, as other observers have obtained large discrepancies between their velocities and those obtained at Lick Observatory (Petrie and Pearce, 1962). The spectroscopic observations are discussed in detail in Chapter 5.

3.6 The Selection of Programme Stars Requiring UBV Observations

The sources of published UBV photometry at the end of July 1972 can be seen from the list of references given at the end of Table (6.4.1). A list of stars requiring UBV photometry was prepared in a manner similar to that used for preparing the list of stars requiring spectroscopic observations (§3.5). References (1), (3), (7), (9) and (11) were searched, and the programme stars with published UBV photometry were deleted from the observing list, although a few were retained for a comparison with the results of other observers. The details of the UBV observations carried out by Dr. P.W. Hill at K.P.N.O. are given in Chapter 6. The subsequent publication of references (2), (4), (5), (6), and (10), listed at the end of Table (6.4.1) also proved useful for comparison with the results of other observers.

CHAPTER FOUR

Hβ Photometry

4.1 Introduction

4.2 Two channel Hα and Hβ Photometry using the University of St. Andrews James Gregory Telescope.

4.2.1 Description of the Photometer

4.2.2 The Semi Automatic System used in 1971 and 1972

4.2.3 The Observations made with the Semi-Automatic System, and their Reduction

4.2.4 Final Reduction of the Semi-Automatic System Data.

4.2.5 Modifications to the Photometer made for use with the Camac System in Autumn of 1973

4.2.6 The Camac System

4.2.7 The Observations made with the Camac System and their reduction

4.3 Two channel Hβ Photometry using the Kitt Peak 36" Telescope

4.4 Single Channel Hβ Photometry using the Kitt Peak 16" Telescope

4.5 A comparison of the Different sources of Hβ Photometry

4.1 Introduction

It has been thought for some time that the width of the Hydrogen Balmer Absorption lines in stellar spectra, is correlated with the absolute magnitude of the star. This is because we expect a dwarf star to have a much higher surface gravity than a giant star. So the stellar atmospheric pressure, at the points in the atmosphere where the absorption lines are formed, will be higher in the dwarf stars. Now as well as having a natural line width, as a consequence of the Heisenberg Uncertainty Principle, and a much larger line width due to the Maxwellian Velocity Distribution of the atoms of the gaseous stellar atmosphere as a result of the atmospheric temperature, there is a pressure broadening effect. That is, the width of spectral lines tends to increase with pressure, and so we would expect dwarf stars to have much broader lines than giant stars of the same temperature.

The value of measuring the strengths of the Balmer lines of hydrogen, as a luminosity criterion for early type stars, was first illustrated by Lindblad (1922). He measured the intensity of relatively strong features in low dispersion objective prism spectra of stars of known parallax, by spectrophotometric methods, and found that there was a good correlation with absolute magnitudes, so verifying the above hypothesis. Strömgren (1951, 1952, 1956a, 1956b) found that the strengths of these strong spectral features could be measured photometrically to a very high accuracy, and hence yield fairly accurate absolute magnitudes. For OB stars, the Hβ line of hydrogen was found to be a very useful strong spectral feature for this purpose. Crawford (1958, 1960) improved the Strömgren System by using two interference filters instead of three. These were both Hβ filters, that is the maximum transmission occurred for a wavelength of 4861Å. One filter had a half width of 90Å and the other filter a half width of 15Å. The 15Å filter had the effect of excluding most of the contribution of the continuum around the Hβ line, to the light passing through this

filter. Consequently, Crawford defined the β index as

$$\beta = 2.5[\text{Log}_{10} I \text{ (90Å filter)} - \text{Log } I \text{ (15Å filter)}] + C \quad \ldots\ldots\ldots (4.1.1)$$

where I stands for the transmitted intensity, and C, for a constant.

This is thus a measure of the strength of the Hβ line, and consequently of the absolute magnitude of the star. It can be seen from equation (4.1.1) that the value of β is filter dependent. Thus it became necessary to develop a standard β system, and this has been done by Crawford and Mander (1966). As a result of this we can use filters of bandwidths different from those mentioned above, the only requisite being that the narrow filter should exclude the continuum on either side of the Hβ line and that the wide filter should not include any other interfering lines. If as many of the standard stars as possible from the list of Crawford and Mander are observed in each night of observing, as well as the programme stars, the instrumental β′ system can be transformed to the standard β system. In practice, the instrumental β index is calculated by

$$\beta' = 2.5 \ (\text{Log}_{10} I_{\omega} - \text{Log}_{10} I_{n}) \quad \text{---------- (4.1.2)}$$

where I_{ω} = Intensity through the wide filter (Star-Sky)

and I_{n} = Intensity through the narrow filter (Star-Sky).

The transformation from the instrumental β system to the standard β system is found to be linear, to a good approximation. However, Kilkenny (1975) has shown that this linear transformation is not necessarily the best. In fact, Kilkenny has found a small curvature effect in his transformations, for Hβ photometry of Southern Hemisphere Early Type Stars (Kilkenny, Hill and Schmidt-Kaler, 1975). This could be accounted for by calculating a theoretical value of the instrumental β index, for stars of different standard β index, from the transmission curves for the filters.

In practice, then, one fits a linear transformation and then looks at the residuals for the standard stars. These are obtained by taking the difference between the computed β index from the linear transformation, and the published standard β index. If these residuals exhibit any systematic variation with β, that is there is curvature in the transformation, then a polynomial can be fitted to replace the original transformation.

In a similar way, we can look at the residuals as a function of time, and also as a function of hour angle, declination and right ascension. Again if any systematic variation is found, the appropriate corrections can be deduced for the computed β indices. Having removed all such sources of systematic error, one can then use the calculated values of the β indices of the programme stars to deduce their absolute magnitude, using the calibration derived by Crawford (1973).

In practice, however, it is not quite as simple as this. The β index depends on the surface temperature of a star, as well as its surface gravity. This is because the radiation pressure will oppose the surface gravity and thereby reduce the pressure broadening effect described earlier, and this effect has been discussed in detail by Zinn (1970). It appears that this may well explain difficulties that have hitherto been experienced in deriving a calibration for absolute magnitude as a function of the β index. Absolute magnitudes have been derived, using the calibration of Graham (1967) and compared with absolute magnitudes derived from Spectral Types (Schmidt Kaler, 1965c). by Haug (1970a). Haug also noted the same discrepancy as that which was found in the above comparison, in the case of the absolute magnitude calibration as a function of β derived by Fernie (1965) as well as in the case of the calibration that he derived for his own data. He concludes therefore, that the calibration must be dependent on the spectral type of the star.

Crawford (1973) has derived a preliminary calibration for Hβ photometry, valid for zero age main sequence stars, and a method is suggested whereby evolutionary effects might be accounted for. However, the need to determine luminosities of high luminosity supergiants is also present. Accordingly, a calibration, from which the

absolute magnitude and the intrinsic colour index, $(B-V)_o$, may be derived from the β-Q diagram, was deduced by Klinkmann (1973). The parameter Q is identical with that defined by Johnson and Morgan (1953). The β-Q diagram is illustrated in Fig. 2.2.1. The theory behind this calibration has already been discussed in detail in §2.2. This method has been used with some success by Klinkmann and is used here.

The Hβ line in stellar spectra is also subject to rotational broadening. It has been pointed out by Abt and Osmer (1965) that this has no appreciable effect on the β index, provided that the narrow filter used is not appreciably less than 30Å in bandwidth. Consequently if filters used for obtaining the narrow deflection are of approximately this bandwidth, then there is no need for the effects of rotational broadening to be considered further at this stage.

4.2 Two-Channel Hα and Hβ Photometry using the University of St. Andrews James Gregory Telescope

4.2.1. Description of the Photometer

The University of St. Andrews James Gregory Telescope, hereafter referred to as the J.G.T., is a 37" Cassegrain-Schmidt Telescope. It was designed primarily for direct photography of the sky, having a focal ratio of f/2.6. The primary mirror is spherical, and at the other end of the telescope tube, there is a glass correcting plate, which is figured in such a way that it has the effect of bringing all the rays to a common focus. That is, the spherical primary mirror, when used in conjunction with this glass correcting plate, is equivalent to a parabolic mirror alone.

Mounted within the telescope tube is a 19" convex secondary mirror. When the telescope is used in the photographic mode, a photographic plate is placed at the cassegrain focus. The exact focussing is achieved through the telescope focussing knob, which has the effect of moving the plate-holder with respect to the primary mirror. In a system devised by Dr. P.W. Hill, the telescope is adapted for photometric work by placing a concave lens, known as a Barlow lens, in the place of the plate holder. When correctly adjusted, again by means of the telescope focussing knob, this has the effect of moving the cassegrain focus of the telescope into the plane of the diaphragm within the photometer.

The two-channel photometer which was used, known as the "People's Photometer", was supplied to the University of St. Andrews by courtesy of the Royal Greenwich Observatory, Herstmonceux. It is shown, attached to the telescope, in Plates 4.1 and 4.2. The interface between the photometer and the telescope, with the attached "wide field" eyepiece, which is prominent in Plate 4.1, was designed by Dr. P.W. Hill and Dr. I.G. van Breda.

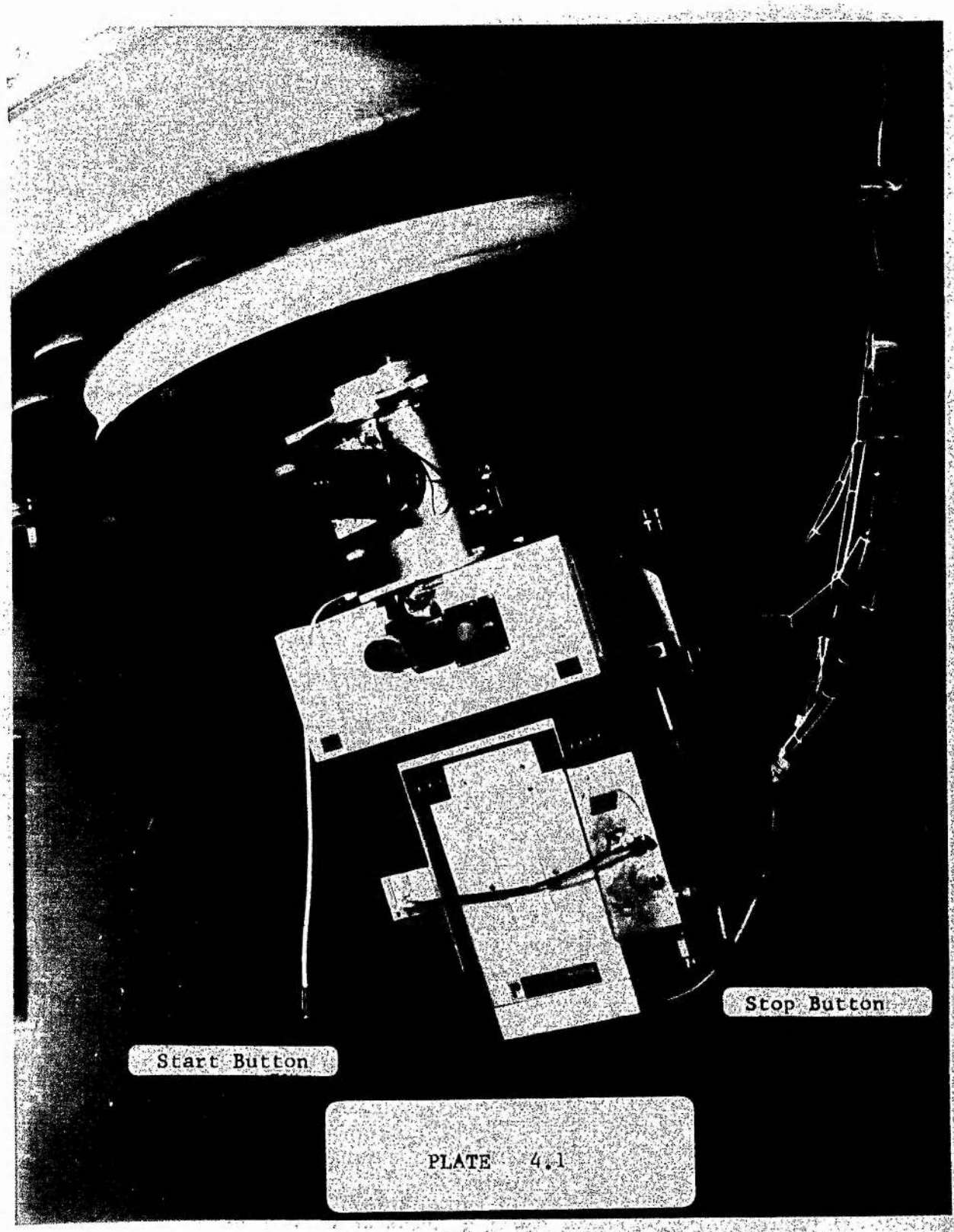

PLATE 4.1

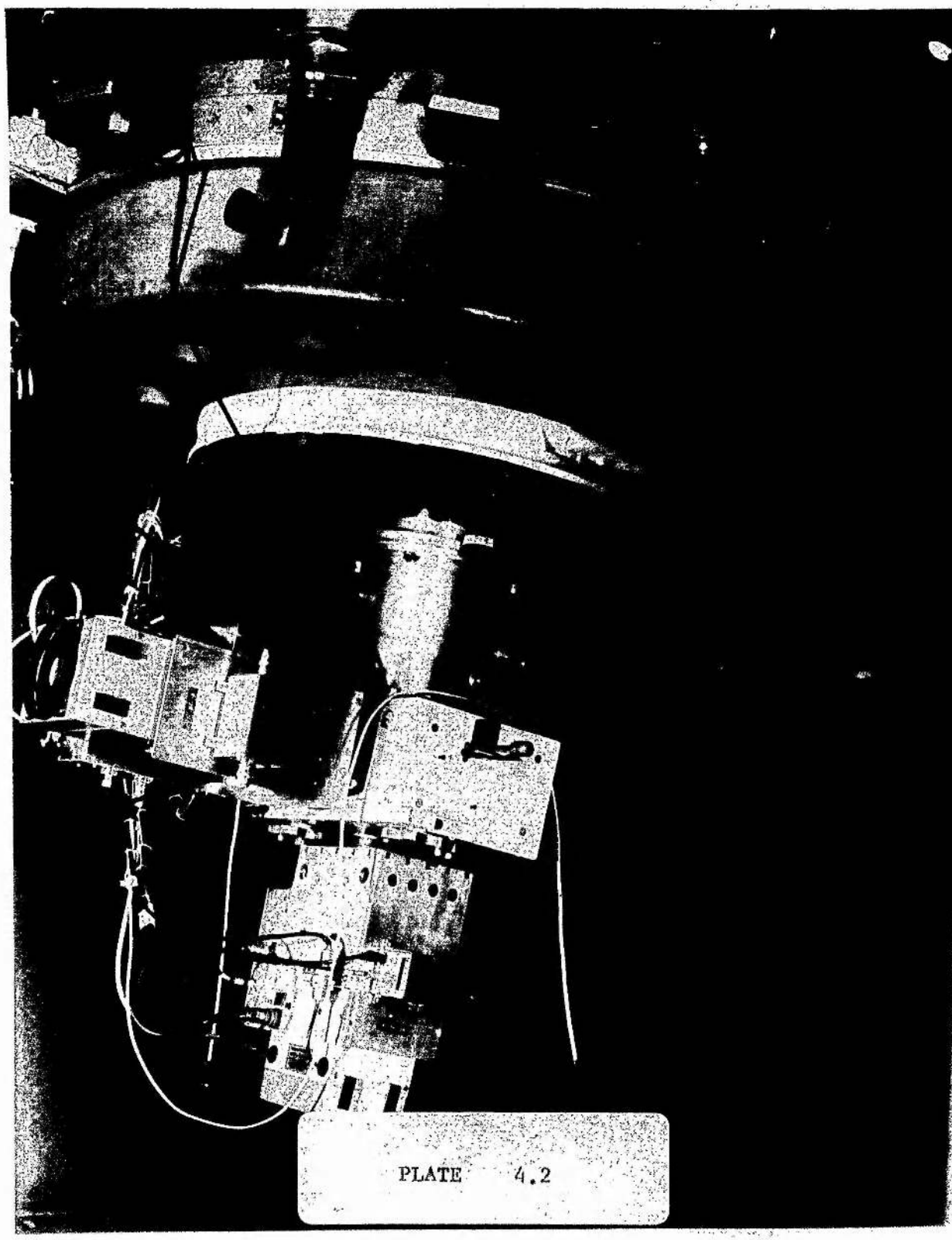

PLATE 4.2

A moveable plane mirror is mounted within the interface. In one position, the mirror directs the light from the telescope into the wide field eyepiece. In the other position, the mirror is moved out of the way, so that light from the telescope can pass into the photometer. The interface is also arranged in such a way, that on loosening the mounting bolts, the orientation of the photometer and interface with respect to the telescope can be adjusted at will. Initially the photometer was orientated so that the eyepieces were on the eastern side of the telescope whilst observing to the west of the meridian. Conversely, for observing to the east of the meridian, the photometer was rotated so that the eyepieces were on the western side of the telescope. This was done purely for reasons of convenient access. All stars to the west of the meridian were observed before any stars to the east of the meridian. Thus the change in orientation had to be made only once a night. However, it was eventually decided that this was not worthwhile, and the photometer was left in the orientation used for observing in the east, as this gave easiest access to the 2" viewfinder and 8" guider.

The light from the telescope enters the photometer and encounters a diaphragm, mounted on a diaphragm slide, with three positions in which diaphragms can be mounted. The diaphragm slide is positioned by means of a "push-pull" rod, which can be seen on the left hand side of the photometer when it is viewed in Plate 4.1. Initially, 5mm and 3mm diaphragms were used with the third position remaining empty, giving an open field view. The 3mm diaphragm was selected for observing purposes.

There is a knob mounted immediately to the right of the narrow field eyepiece. This controls the position of a slide in the photometer, which carries a beam splitter and two 45° plane mirrors. One of these plane mirrors directs the light emerging from the diaphragm into the photometer eyepiece, enabling visual inspection of the star image in the diaphragm. The other plane mirror is for use with double diaphragm photometry. In this case, light from one diaphragm is

reflected off the mirror so that it eventually enters one channel, whereas light from the other diaphragm is allowed to pass unimpeded into the second channel. This facility is not used for Hβ photometry.

For Hβ photometry, the beam splitter is placed in the beam of light from the diaphragm . This splits the light into two beams, the ratio of the intensities of the two beams being dependent on the choice of beam splitter. Initially a 50-50 beam splitter was used, but this was eventually replaced by an 80-20 beam splitter. Each of the beams encounters a filter, held in a filter slide, before passing through a fabry lens, which images the diaphragm onto the photocathode of a photomultiplier tube. The photomultiplier tubes are each housed in a "Products for Research" thermoelectrically refrigerated chamber (*Model No. TE-102TS)*. As can be seen from plate 4.2, one of these chambers is attached directly beneath the photometer unit, and the other on the side opposite to the photometer eyepiece. The chambers are mounted onto the photometer by means of a dark slide assembly,which enables the tubes to be protected from strong sources of light.

The power supplies for the thermoelectrically refrigerated photomultiplier tube chambers, are rather massive and so it was decided to mount them at the base of the telescope pier. Because of this, about 10 metres of cable were needed to supply the power from the power supplies to the "cold boxes". Consequently the power supplies delivered 5.4 volts at 8 amps, instead of the advertised 6 volts at 9 amps. Fortunately, this did not affect the operation of the thermo-electric coolers, and they were still able to maintain the "cold boxes" at -20°C in an ambient temperature of 20°C. In the dome, in winter and at night, the ambient temperature would be about 0°C and so we were able to cool our photomultiplier tubes to considerably less than -20°C, probably about -30°C.

4.2.2 The Semi-Automatic System used in 1971 and 1972

The filter slides each contained six locations which could be occupied by a filter. These positions were numbered 1 to 6 and a filter could be selected by moving the appropriate filter wheel until the corresponding number was directly beneath the illuminating light. The filter wheels are mounted underneath the photometer on either side of the lower cold box, as can be seen in Plate 4.2. The filters were optical interference filters supplied by Baird Atomic Inc. The spectral characteristics of each filter in each position in the filter slide, corresponding to each channel are listed in Table 4.2.1.

The photomultiplier tubes used were 9558A S-20 tubes supplied by E.M.I. Their ticket voltages were 920 and 960 volts. Consequently it was decided to operate both tubes from the same E.H.T. unit at 920 volts. It was hoped that by operating both tubes from the same E.H.T. unit, any drift in the relative gains of the two tubes would be minimised.

TABLE 4.2.1

Narrow Band Interference Filters used for JGT 2-channel Hα and Hβ Photometry

Channel	Filter Position No.	Peak Wavelength (Å)	% Transmission	½ Width of Filter (Å)
1	1	4866	76	31
	2	4900	84	212
2	1	4862	75	30
	2	4900	84	213
1	3	6571	54	35
	4	6579	51	125
2	3	6566	55	37
	4	6579	51	125

Filter Positions 5 and 6 in both channels were unused.

Attached to each cold box, is a Keithley Pre-amplifier together with an integrator designed by Dr. I.G. van Breda. The observer has a choice as to whether the output signal from the photomultiplier tube is integrated or counted as a series of pulses.

In the case of pulse counting, the signal is fed into the Keithley Pre-amplifiers. Here the signal is amplified and it is then fed into the Harwell Pulse Counters. These are housed in the large electronics rack immediately above the E.H.T. units, as can be seen in Plate 4.3 The output from the pulse counters is then displayed digitally by the unit at the top of the electronics rack. There are two displays each giving the number of counts detected in a given time interval, in each channel. The time interval over which pulses are counted, or over which a signal is integrated, is set by means of a knob in the central portion of the electronics rack. This sets a timer, and times of 10secs, 30secs, or 60secs. can be selected. The displays at the top of the electronics rack can be used to display the Channel 1 and Channel 2 readings, or they can be used to display sidereal time in one and universal time in the other. The sidereal and universal time is furnished by two oscillators, which increment the two counters at the appropriate frequency.

The Harwell Pulse Counters are fitted with a discriminator. This has the effect of predetermining the minimum pulse height at which a pulse is counted or ignored. Consequently, a lot of the noise, which tends to be in the form of small pulses anyway, can be cut out. It is in this facility that the advantage of pulse counting over integrating, lies. The discriminator levels were chosen so that no pick-up was obtained, from the electronics or telescope drive.

In the event of integrators being used, the result of the signal integrated over the pre-selected time interval is displayed digitally at the end of the time. Some difficulty was encountered due to damp reducing the input impedance of the operational amplifiers used in the integrating units. This difficulty was resolved, at the suggestion of Mr. D.M. Carr, by placing a small heating coil in each integrating unit. An integration or a pulse count may be started or

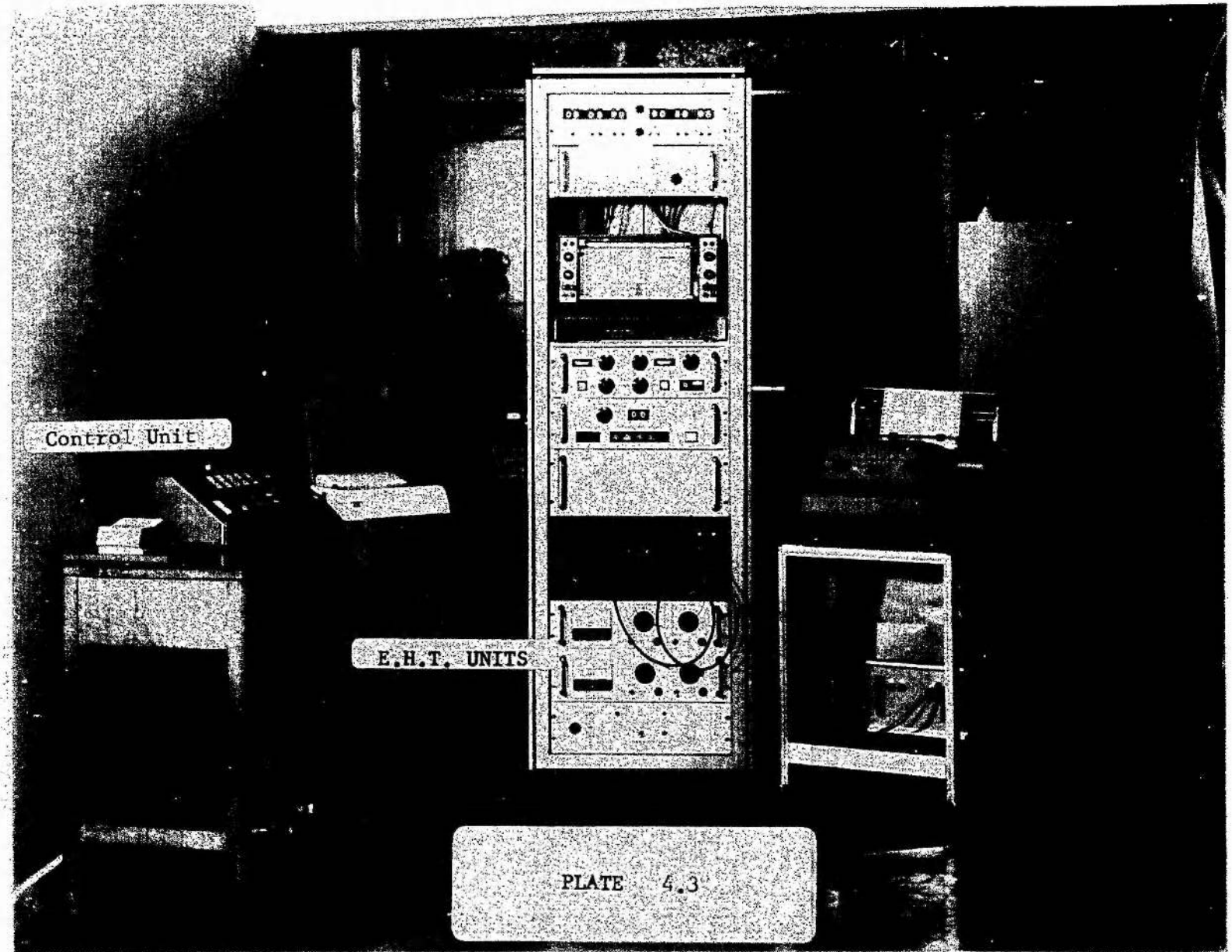

PLATE 4.3

stopped by means of pressing the appropriate button attached to the photometer (See Plate 4.1) or by pressing the appropriate button on the control unit, (See Plate 4.3).

There is an automatic gain selector which operates with the integrators. Normally, the integrators operate on Gain 3, which is a gain of about 400, but if the signal is strong enough to produce a deflection of 10^6 or more, Gain 2, which is a gain of about 20, will be selected. Furthermore, if the signal is strong enough to produce a deflection of 10^6 or more with Gain 2, Gain 1, which is a gain of 1, will be selected. These gain steps were calibrated against one another for both channels. This was done by supplying a signal from a battery and making a manual selection of the gains.

In making an integration or a pulse count, the observation can be repeated a number of times, the number being determined by the setting of the programming board at the back of the electronics rack. When an integration or a pulse count has been completed, the sidereal time, is output to the teletype. If integrators are used then the gain is also output. If pulse counting is used the gain is output as zero. The number of the observation, which is displayed in the display at the centre of the electronics rack, is also output. There are also facilities, not implemented during the observing season 1971/72, for outputting the filter number in each channel, together with the status of the observation made in each channel, that is whether it is a star observation or a sky observation. As these facilities were not implemented, a dummy number is output onto the teletype. If the teletype punch is left switched on, then punched output can be obtained. There is also an additional facility for the universal time output in addition to everything else, but this was not used.

It was found by experience that the apparatus behaved in a more satisfactory way, if the E.H.T. and "cold box" power supplies were left on permanently. In the case of the E.H.T., when this has just been switched on, there are significant electrical transients. These manifest themselves as transient ion movements within the photomultiplier tubes, and this results in a significant contribution to the dark current. After an hour or so, these die down and become

negligible in comparison with the thermal and cosmic ray dark counts. If the coolers are switched off, then some thawing tends to occur within the cold boxes, and condensation on the photomultiplier tube pins can occur. This results in a noisy resistance between the pins which can result in an increase in dark count by several orders of magnitude.

4.2.3 The Observations made with the Semi-Automatic System, and their Reduction.

Beginning in December 1971, Hα and Hβ photometry was carried out for the programme stars selected, using the J.G.T. and the equipment described in §4.2.1. and §4.2.2. This was continued on every available night, except on good dark nights, when the telescope was allocated for direct photography, until the 25th April 1972, when the nights were considered to be too short to be of much use. In December 1971 and January 1972, no useful observations were made on the account of bad weather and instrumental difficulties.

A list of Hα and Hβ standard stars was compiled from the lists of Andrews (1968) and Crawford and Mauder (1966) respectively. Since the main time-consuming operation with the J.G.T. was the actual problem of setting it on a star quickly and accurately, it was decided that Hα and Hβ photometry of the programme and standard stars should be done together. As a result, the standard stars selected were restricted to those which were common to the two lists. The sequence in which the observations on a given star were made, was analogous to that used by Sinnerstad, Arkling, Alm and Bratthund (1968), and is indicated in Table 4.2.2. A ten second integration time was used, and each observation was automatically repeated once. In deciding upon this sequence, it was hoped

that it would enable one to correct, as far as possible, for any differential drift between the two channels.

The advantage of two-channel narrow band photometry over single channel narrow band photometry is that it is independent of the atmospheric extinction and even variations in atmospheric extinction during the course of integrations. This can be seen from equation (4.1.2); since the bandwidths are small, Iw and In will be reduced in the same proportion. Consequently, observations can be made in non-photometric weather, and even in partially cloudy conditions.

The star number is entered manually on the teletype, and prefixed with a character which will identify it as a programme or a standard star. Any comments or information relevant to the observations being made are also entered manually on the teletype, again being prefixed with an appropriate character that will identify them as such. If the integrators were to be used, then the integrator zero-points for each channel, and for each gain step, were measured at the beginning of each night. This block of data had to be preceded by a manually entered character, followed by a "carriage return" and "line feed", that would identify the subsequent data block, up to the next star number, as integrator zero measurements. The end of each night was denoted by manually entering a "/*". This was immediately followed by the date of the next night. In cases where the sequence of observations was different from that described above, the sequence was entered in the record immediately following the star name.

Needless to say, mistakes were made in trying to follow the above procedure. Furthermore, the teletype punch often mis-punched characters, or omitted to punch characters altogether. Consequently if the tapes were to be used for computer reduction of the data, a considerable amount of editing was needed. It was eventually decided that the best way of doing this was to load all the paper tapes onto a magnetic tape and then edit by copying from one

Table 4.2.2

The Sequence in which the Observations were made in 1971-72 using the Semi-Automatic System

Observation (No. and Type)		Channel 1	Channel 2
1st Star			
1	Sky	W(β)	W(β)
2	Sky	N(β)	N(β)
3	Star	N(β)	N(β)
4	Star	N(β)	W(β)
5	Star	W(β)	W(β)
6	Star	W(β)	N(β)
7	Star	W(β)	N(β)
8	Star	W(β)	W(β)
9	Star	N(β)	W(β)
10	Star	N(β)	N(β)
11	Sky	N(β)	N(β)
12	Sky	W(β)	W(β)
13	Sky	W(α)	W(α)
14	Sky	N(α)	N(α)
15	Star	N(α)	N(α)
16	Star	N(α)	W(α)
17	Star	W(α)	W(α)
18	Star	W(α)	N(α)
19	Star	W(α)	N(α)
20	Star	W(α)	W(α)
21	Star	N(α)	W(α)
22	Star	N(α)	N(α)
23	Sky	N(α)	N(α)
24	Sky	W(α)	W(α)
2nd Star			
25	Sky	W(α)	W(α)
26	Sky	N(α)	N(α)
27	Star	N(α)	N(α)
	etc. as above		
33	Star	N(α)	W(α)
34	Star	N(α)	N(α)
35	Sky	N(α)	N(α)
36	Sky	W(α)	W(α)
37	Sky	W(β)	W(β)
	etc. as above		
48	Sky	W(β)	W(β)
3rd Star			
49	Sky	W(β)	W(β)
	etc. as above		

N - Denotes Narrow Filter, W - Denotes Wide Filter

magnetic tape to another, and correct each record as it was copied. For this purpose a trivial Fortran programme was written for the *Honeywell-316* computer of the University Observatory, St. Andrews, hereafter referred to as the "H-316". The programme was written so that a record from paper tape, which was terminated by the characters "carriage-return", and "line-feed", were read in and then written onto magnetic tape in an 80-byte record, padding the record with blanks if necessary. Each time a record is read in, an integer located in the labelled common area of memory, is incremented by one, and its location in core can be easily found by reference to the memory map, and consequently it can be read off the computer console in octal.

Data was written on magnetic tape in ASCII code. As the editing had to be done with the University of St. Andrews IBM 360/44, hereafter referred to as the 360/44, and the software written for this computer accepts characters in EBCDIC, another Fortran programme was written for the 360/44 to translate the ASCII data to EBCDIC data. The actual translation of the characters was executed by means of a subroutine written in PL360, made available by the kind courtesy of Mr. J.R. Stapleton of the University of St. Andrews Computing Laboratory. The number of records on the ASCII tape was read from a card. Then each 80 byte ASCII record was read in turn, into an array containing one character per byte. Each character in the buffer was then translated and then the entire record output onto a second magnetic tape as an 80-byte EBCDIC record. When all the records on the Honeywell Magnetic Tape had been translated and transferred onto the second tape, an end-of-file mark was written on this second tape.

The editing of the information on the magnetic tape so produced was then carried out by means of the Context Editor. This was written for the 360/44 by Mr. I. Sommerville, of the University of St. Andrews Department of Computational Science.

A rather more sophisticated Fortran programme was written to analyse the data on the edited magnetic tapes. In the first instance, if the integrators are being used, the integrator zeros are read

in and averaged for each gain. Then the programme read all the data for one star into core and averaged each observation with the repeats of it which immediately followed. If the gain read in is non-zero, then the observation is an integrator observation, and so the appropriate zero point correction is made, and the reading is multiplied by the factor necessary to reduce all readings to the same gain. Then the appropriate subtractions were made, correcting each star observation for the contribution of the sky background. The next step was to average all the observations for a given star which had the same filter configuration. That is, if a star observation was made in which the filters in each channel were both Hβ narrow filters and the same observation was made again at a later stage in the sequence, these two observations would be averaged at this stage. Then the Hα and Hβ observations were separated.

Thus we eventually reach a stage, at which we have the observations listed below for both Hα and Hβ, provided of course that the original sequence of observations was complete. Here N denotes narrow filter and W denotes wide filter. The subscripts in the case $N_{\psi\phi}$ are used to denote the channel number (ψ) and the observation number (ϕ).

Observation No.	Channel One	Channel Two
1	N_{11}	N_{21}
2	N_{12}	W_{22}
3	W_{13}	W_{23}
4	W_{14}	N_{24}

The arithmetic operations indicated below are now performed. The arrow indicates "set equal to "

$$N_{21} \rightarrow N_{21} \times \frac{N_{12}}{N_{11}} \qquad \text{---------- (4.2.3.1)}$$

This has the effect of correcting the narrow filter reading for channel two, for any instrumental drift or changing sky transparency between observations one and two.

$$W_{23} \rightarrow W_{23} \times \frac{W_{14}}{W_{13}} \qquad \text{---------- (4.2.3.2)}$$

This similarly corrects the wide filter reading for channel two, for any effects of instrumental drift or changing sky transparency, which may have occurred between observations three and four.

$$W_{22} \rightarrow (W_{22} + W_{23})/2 \qquad \text{----------(4.2.3.3)}$$

$$N_{21} \rightarrow (N_{21} + N_{24})/2 \qquad \text{----------(4.2.3.4)}$$

These two numbers, together with the star number and an indicator to indicate whether it is a programme star or a standard star, are output onto a card in the correct format for the Hβ reductions programme (see § 4.2.4). These two figures, when the appropriate dead time correction has been made, give an instrumental alpha/beta index corresponding to the filters used in channel 2, together with the other instrumental characteristics of channel 2.

Similarly for channel one, the following arithmetic operations are performed;

$$W_{13} \rightarrow W_{13} \times \frac{W_{22}}{W_{23}} \qquad \text{----------(4.2.3.5)}$$

$$N_{11} \rightarrow N_{11} \times \frac{N_{24}}{N_{21}} \qquad \text{----------(4.2.3.6)}$$

$$N_{11} \rightarrow (N_{11} + N_{12})/2 \text{ ----------(4.2.3.7)}$$

$$W_{13} \rightarrow (W_{13} + W_{14})/2 \text{ ----------(4.2.3.8)}$$

N_{11} and W_{13} will give an instrumental alpha/beta index for the filters and instrumental characteristics of channel one. These two figures, together with the star number are also output onto a card in the correct format for the Hβ reduction programme.

In practice, four sets of data cards are required from this programme, one for each channel, for both Hα and Hβ. Consequently, four different output device numbers were allocated to them. The programme was run four times, and in each case three of these output device numbers were suppressed by the operating system, and the fourth was connected to the card punch.

4.2.4 Final Reduction of the Semi-Automatic System Data

The final reductions were carried out by means of an Hβ reductions programme. This programme was originally written for a CDC 6400 by Mrs B. Woyman of Kitt Peak National Observatory. It has been modified for use with the 360/44 by Dr. P.W. Hill. The programme was written for the reduction of pulse counting data. It is conceivable that two or more pulses will fail to be resolved and will thus be counted as one pulse. The statistical analysis of this is given by Evans (1955), Chapter 28, and here it is shown that in the first approximation, the true number of counts observed in unit time is given by

$$N = n(1 + n\rho) \text{ ----------(4.2.4.1)}$$

where n = Observed number of counts per unit time and ρ = the resolving power of the system, or the dead time.

Initially a dead time of 50 nanoseconds was assumed. Using this, the observed counts were corrected according to the relationship (4.2.4.1), for each channel. Then the instrumental beta index was calculated for each star according to the relationship (4.1.2).

The standard beta indices for the standard stars had already been read in. The programme assumes that a linear relationship exists between the standard and the instrumental beta indices for the standard stars, and it now proceeds to determine this linear relationship, so that the beta indices of the programme stars can be reduced to the standard system. This transformation is calculated by one or both of two methods. The first method is by the method of least squares (see for example, Barford (1967) p.56). The second method assumes a value for the slope of the transformation and then proceeds to calculate the zero point. In this particular case, all the nights on which five or more standards were observed, the transformation was deduced by the method of least squares. It is justified to use an assumed deadtime correction, since no useful observations were made with the integrators, and so these nights were dropped.

The night which gave the best transformation was then selected and the data for this night were then re-used by the programme several times to calculate a new transformation, and in each case a different dead time correction was applied. It was eventually found that a dead time correction of 67ns, applied to both the narrow and wide deflections in both channels, gave the best transformations. Choosing this dead time correction as the correct one, the data for all nights on which five or more standards were observed, were then rerun with the programme. From the transformations so deduced, a mean slope was calculated for each pair of filters, that is, for each channel. This was achieved by taking a mean of the individual slopes, and weighting each of the individual slopes by the error in the transformation (See Barford (1967) page 62).

Using the mean slope calculated for channel one filters, all the channel one data was now reduced, including the night on which only two, three or four standards were observed. This was also done for channel two data. The programme uses the calculated transformation to compute the standard beta indices of the programme stars. The difference between these, when the transformation was calculated by

the method of least squares and when the method of mean slopes was used, was typically around $0^m.002$. So for nights in which five or more standards were observed, the results of the least squares method were used, as these were marginally better, and are listed in Table 4.2.4.1. For the other nights, the transformations are listed in Tables 4.2.4.2 and 4.2.4.3.

The channel one and channel two beta indices, for each star on each night, were now averaged and the standard deviation, σ', calculated. The mean beta index for all the observations of each star was then deduced. This is a weighted mean, weighted by the value of each of the corresponding standard deviations (See Barford (1967), page 62). The standard deviation of the weighted mean was also calculated by the method given by Barford. The unweighted mean was also calculated, and the standard deviation σ of the unweighted mean was deduced from the definition of the standard deviation. The Bessel criterion of variability were then applied. That is, if $\sigma \geqslant 2\sigma'$ it is concluded that there is a possibility that the star exhibits variability in Hβ. On the other hand, if $\sigma \geqslant 3\sigma'$ then the star is probably variable in Hβ.

No further attempt was made to reduce the Hα observations, as it was felt that there were insufficient results to be of any use, since this was the only stage at which Hα photometry was performed.

Unfortunately, too few standards were observed on each night to see if there was any systematic variation in the residuals, with for example, zenith distance, hour angle and declination. However, with the observations that were taken later, using the CAMAC system, in which a large number of standards were observed each night, it was found that there were no systematic effects in the residuals.

Table 4.2.4.1

Hβ Photometry Transformations: Semi - Automatic System 1972

Channel One Filters

Night	Transformation	Mean Error in Transformation
Feb 4/5	$\beta = 0.2338 + 1.1385\ \beta_{ins}$	0.0141
Feb 14/15	$\beta = 0.0084 + 1.2382\ \beta_{ins}$	0.0143
Mar 3/4	$\beta = 0.4894 + 1.0198\ \beta_{ins}$	0.0028
Mar 5/6	$\beta = -0.2163 + 1.3499\ \beta_{ins}$	0.0130
Mar 15/16	$\beta = -0.2125 + 1.3457\ \beta_{ins}$	0.0108
Mar 20/21	$\beta = 0.4741 + 1.0218\ \beta_{ins}$	0.0191
Mar 22/23	$\beta = 0.3400 + 1.0862\ \beta_{ins}$	0.0187
Mar 23/24	$\beta = 1.1467 + 1.1467\ \beta_{ins}$	0.0166
Mar 24/25	$\beta = -0.0649 + 1.2738\ \beta_{ins}$	0.0182
Mar 27/28	$\beta = 0.2189 + 1.1445\ \beta_{ins}$	0.0086
Mar 28/29	$\beta = 0.1364 + 1.1819\ \beta_{ins}$	0.0043
Apr 2/3	$\beta = -0.1313 + 1.2968\ \beta_{ins}$	0.0197
Apr 14/15	$\beta = 0.1913 + 1.1552\ \beta_{ins}$	0.0087

Channel Two Filters

Night	Transformation	Mean Error in Transformation
Feb 4/5	$\beta = 0.2756 + 1.1229\ \beta_{ins}$	0.0118
Feb 14/15	$\beta = 0.0867 + 1.2128\ \beta_{ins}$	0.0086
Mar 3/4	$\beta = 0.6926 + 0.9316\ \beta_{ins}$	0.0045
Mar 5/6	$\beta = 0.1466 + 1.1897\ \beta_{ins}$	0.0110
Mar 15/16	$\beta = -0.0663 + 1.2848\ \beta_{ins}$	0.0127
Mar 20/21	$\beta = 0.0151 + 0.9707\ \beta_{ins}$	0.0151
Mar 22/23	$\beta = 0.4279 + 1.0518\ \beta_{ins}$	0.0167
Mar 23/24	$\beta = 0.4415 + 1.0437\ \beta_{ins}$	0.0184
Mar 24/25	$\beta = 0.1791 + 1.1713\ \beta_{ins}$	0.0202
Mar 27/28	$\beta = 0.3404 + 1.0969\ \beta_{ins}$	0.0107
Mar 28/29	$\beta = 0.1980 + 1.1652\ \beta_{ins}$	0.0079
Apr 2/3	$\beta = 0.1001 + 1.1992\ \beta_{ins}$	0.0176
Apr 14/15	$\beta = 0.2601 + 1.1310\ \beta_{ins}$	0.0141

Table 4.2.4.2

Hβ Photometry Transformations: Semi - Automatic System 1972

(Mean slopes option for nights on which 2, 3 or 4 Standards were observed)

Channel One Filters

Night	Transformation	Mean Error in Transformation
Jan 23/24	$\beta = 0.3048 + 1.1080\ \beta_{ins}$	0.0062
Jan 24/25	$\beta = 0.3206 + 1.1080\ \beta_{ins}$	0.0175
Feb 8/9	$\beta = 0.2828 + 1.1080\ \beta_{ins}$	0.0005
Feb 13/14	$\beta = 0.2949 + 1.1080\ \beta_{ins}$	0.0184
Feb 15/16	$\beta = 0.2953 + 1.1080\ \beta_{ins}$	0.0120
Feb 22/23	$\beta = 0.3030 + 1.1080\ \beta_{ins}$	0.0023
Mar 2/3	$\beta = 0.2986 + 1.1080\ \beta_{ins}$	0.0185
Mar 4/5	$\beta = 0.2771 + 1.1080\ \beta_{ins}$	0.0233
Mar 11/12	$\beta = 0.2873 + 1.1080\ \beta_{ins}$	0.0217
Mar 13/14	$\beta = 0.2939 + 1.1080\ \beta_{ins}$	0.0112
Mar 14/15	$\beta = 0.3177 + 1.1080\ \beta_{ins}$	0.0052
Mar 26/27	$\beta = 0.2950 + 1.1080\ \beta_{ins}$	0.0203
Mar 29/30	$\beta = 0.2976 + 1.1080\ \beta_{ins}$	0.0068
Mar 30/31	$\beta = 0.3013 + 1.1080\ \beta_{ins}$	0.0117
Apr 1/2	$\beta = 0.3277 + 1.1080\ \beta_{ins}$	0.0146
Apr 4/5	$\beta = 0.2963 + 1.1080\ \beta_{ins}$	0.0049
Apr 8/9	$\beta = 0.3119 + 1.1080\ \beta_{ins}$	0.0272
Apr 12/13	$\beta = 0.2812 + 1.1080\ \beta_{ins}$	0.0180
Apr 13/14	$\beta = 0.3244 + 1.1080\ \beta_{ins}$	0.0135
Apr 18/19	$\beta = 0.2965 + 1.1080\ \beta_{ins}$	0.0077
Apr 19/20	$\beta = 0.2989 + 1.1080\ \beta_{ins}$	0.0033
Apr 20/21	$\beta = 0.3104 + 1.1080\ \beta_{ins}$	0.0102
Apr 22/23	$\beta = 0.2959 + 1.1080\ \beta_{ins}$	0.0055

Table 4.2.4.3

Hβ Photometry Transformations: Semi - Automatic System 1972

(Mean slopes option for nights on which 2, 3 or 4 Standards were observed)

Channel Two Filters

Night	Transformation	Mean Error in Transformation
Jan 23/24	$\beta = 0.4048 + 1.0700\ \beta_{ins}$	0.0055
Jan 24/25	$\beta = 0.4477 + 1.0700\ \beta_{ins}$	0.0792
Feb 8/9	$\beta = 0.4016 + 1.0700\ \beta_{ins}$	0.0230
Feb 13/14	$\beta = 0.4005 + 1.0700\ \beta_{ins}$	0.0163
Feb 15/16	$\beta = 0.3999 + 1.0700\ \beta_{ins}$	0.0115
Feb 22/23	$\beta = 0.3561 + 1.0700\ \beta_{ins}$	0.0013
Mar 2/3	$\beta = 0.4026 + 1.0700\ \beta_{ins}$	0.0152
Mar 4/5	$\beta = 0.3877 + 1.0700\ \beta_{ins}$	0.0133
Mar 11/12	$\beta = 0.3936 + 1.0700\ \beta_{ins}$	0.0207
Mar 12/13	$\beta = 0.3968 + 1.0700\ \beta_{ins}$	0.0114
Mar 26/27	$\beta = 0.3963 + 1.0700\ \beta_{ins}$	0.0188
Mar 29/30	$\beta = 0.4058 + 1.0700\ \beta_{ins}$	0.0057
Mar 30/31	$\beta = 0.4005 + 1.0700\ \beta_{ins}$	0.0147
Apr 1/2	$\beta = 0.4164 + 1.0700\ \beta_{ins}$	0.0020
Apr 4/5	$\beta = 0.3888 + 1.0700\ \beta_{ins}$	0.0157
Apr 8/9	$\beta = 0.4123 + 1.0700\ \beta_{ins}$	0.0285
Apr 12/13	$\beta = 0.3733 + 1.0700\ \beta_{ins}$	0.0203
Apr 13/14	$\beta = 0.4192 + 1.0700\ \beta_{ins}$	0.0090
Apr 18/19	$\beta = 0.3974 + 1.0700\ \beta_{ins}$	0.0188
Apr 19/20	$\beta = 0.3977 + 1.0700\ \beta_{ins}$	0.0036
Apr 20/21	$\beta = 0.4132 + 1.0700\ \beta_{ins}$	0.0168
Apr 22/23	$\beta = 0.3909 + 1.0700\ \beta_{ins}$	0.0064

4.2.5. Changes made to the Photometer for use with the Camac System in Autumn 1973.

The modifications made to the photometer can be seen from a comparison of Plates 4.1 and 4.2 with Plate 4.4. The "cold boxes" were sent away to E.M.I. for upgrading. This involved rewiring the base in which the photomultiplier tube was mounted, so that the cathode was held at ground. In this way, interference is reduced when pulse counting. A thermometer was also mounted on each cold box, to enable the temperature to be monitored.

Another change, which was not really relevant to this programme was the replacement of the wheels for the positioning of the filter slides, with "push-pull" rods. The position of the filter slide was encoded and a digital read-out of the position of the filter slide was supplied. In addition a small thermometer was mounted above the photometer eyepiece, from which it was hoped that any changes in the filter temperature could be noted.

The electronics rack and the photometer-telescope interface were intended for use with another photometer which was being built by the University Observatory at St. Andrews, for ultimate use on the 40" telescope at the South African Astronomical Observatory at Sutherland. The intention in using the electronics rack in 1971/1972 was merely to test it under observing conditions. Thus it became necessary to replace the electronics rack and photometer telescope interface.

The latter was replaced by another which was essentially the same. The integrators and Keithley Pre-amplifiers, which also went to Sutherland, were replaced by two SSR amplifier and discriminator units, one for each channel. Thus the facility for integrating the signals from the photomultipliers, was not replaced. To keep the possible radio frequency pick up to a minimum, the output from the photomultiplier to the SSR was in the form of a piece of doubly shielded coaxial cable, which was made as short as possible. The discriminator setting for the SSR, was found by selecting that

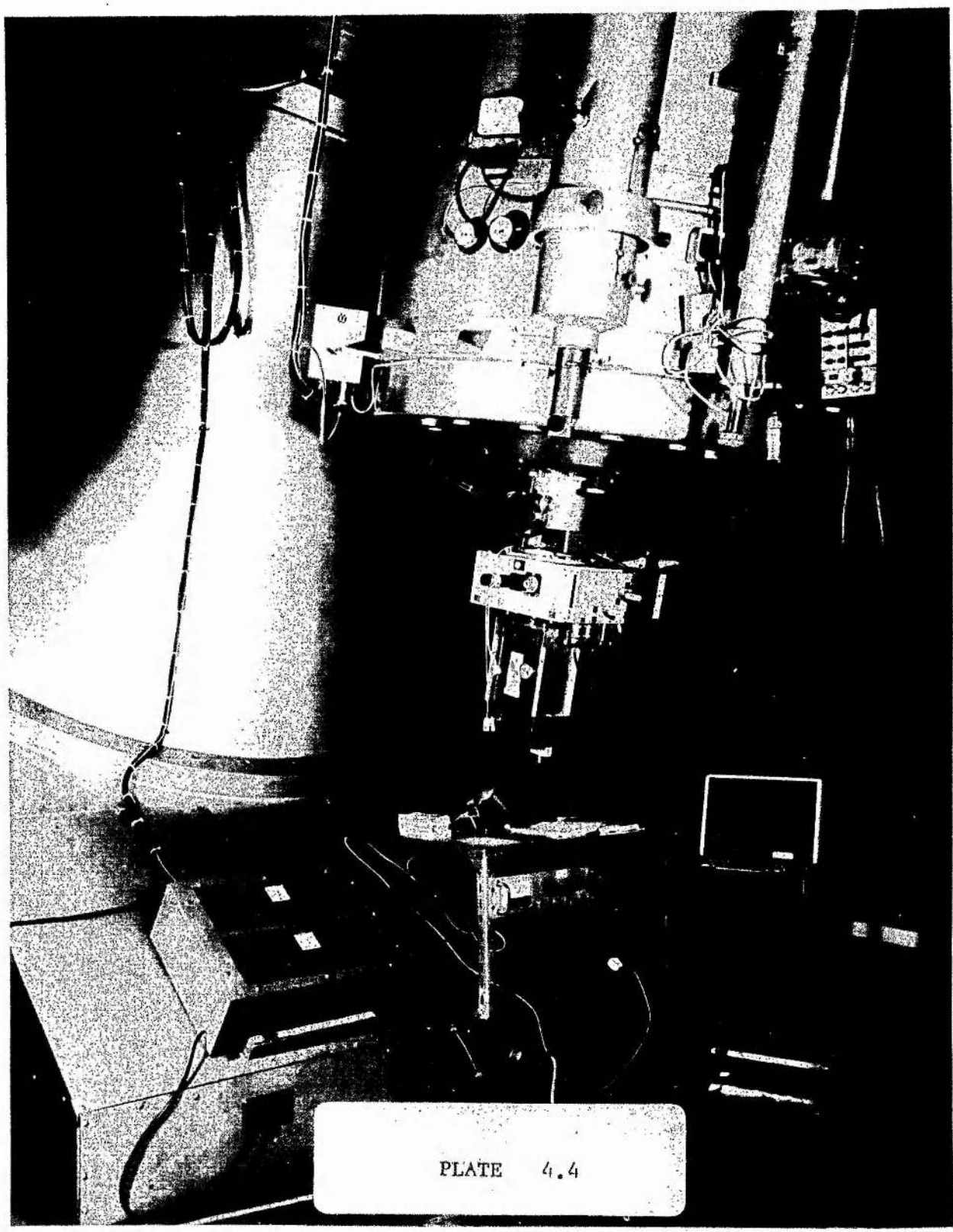

PLATE 4.4

which gave the best signal to noise ratio, for the optimum tube operating voltage.

This was determined by setting the discriminators to zero, that is no discrimination, mounting an artificial light source. and varying the EHT until the optimum signal to noise ratio is obtained. The best discriminator setting was then found by measuring the signal to noise ratio at a number of different discriminator settings, and selecting that which gave the highest signal to noise ratio. The optimum tube operating voltage was found to be 1080 volts.

A further improvement in the signal to noise ratio was made by placing toroidal magnets in the "cold boxes". This has the effect of defocussing the noise-photoelectrons, so that a large proportion of them never reach the photocathode. The signal, on the other hand, which is a narrow beam, is largely unaffected. This had the effect of reducing the dark count by a factor of ten, but scarcely affecting the signal. However, it has been shown by Kelly and Kilkenny (1973) that this use of toroidal magnets gives rise to large variations in the sensitivity across the photocathode. Thus if there are significant flexure effects, this could seriously affect the usefulness of reducing the dark counts by means of toroidal magnets. Fortunately, it was found, by repeated observations of the same standard star at different zenith distances, that there was no flexure effect and the sensitivity remained constant.

4.2.6 The Camac System

The hardware used for this system is shown in Plates 4.4 and 4.5. The system has been described in detail elsewhere by van Breda (1972), Stephens and van Breda (1972) and by van Breda et al (1974). The output leads from the SSR amplifiers are two 80 metre

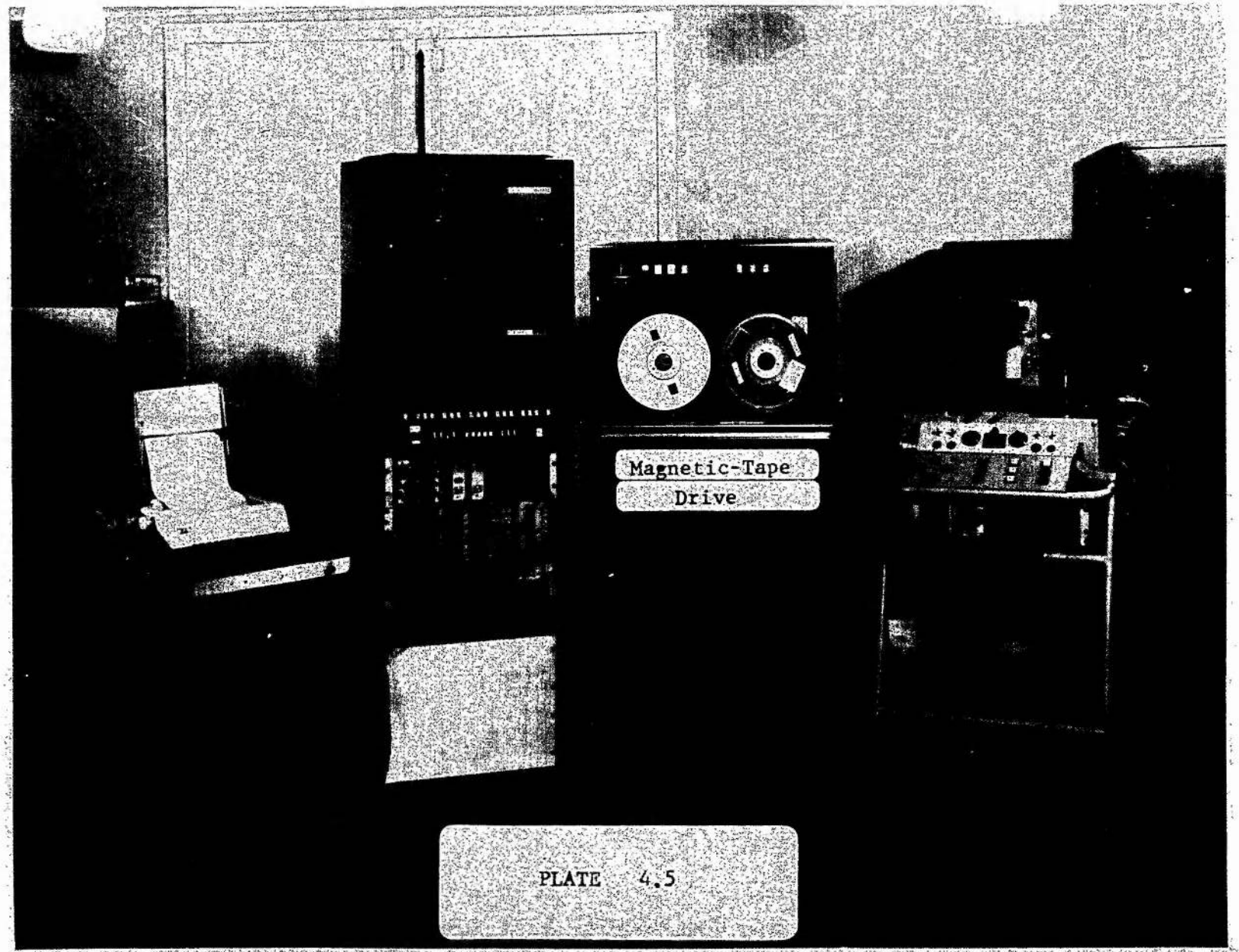

PLATE 4.5

lengths of doubly screened coaxial cable. Each cable runs to a line driver and an optical isolator. The signal from each optical isolator is then fed into a register of a CAMAC-Quad Scaler. This is a Camac Module with four 24-bit data registers, with inhibit and overflow outputs. The Quad-Scaler is mounted in a Camac crate which is linked to the H-316 computer. One of these registers in the Quad Scaler is driven by a 1Hz Oscillator, and this serves as a universal time clock. The remaining register in the Quad-Scaler is used as a timer. It receives pulses from a 1KHz or 1 MHz Oscillator.

The principle of photometry using the Camac System, is that pulses from the photometer channels, amplified by the SSR amplifiers are counted in a given time interval by two of the registers of the Quad-Scaler. It was decided, in the light of Dr. P.W.Hill's observing with the 16" and 36" telescopes at Kitt Peak, (see Sections 4.3 and 4.4), that the sequence of observations used with the Semi Automatic System should be abandoned. This was because such a complicated observing sequence easily lends itself to erroneous observing, and consequently loss of observing time. Instead, it was decided that the system of instrumental ß indices would be defined by having a narrow filter permanently in one channel, and the wide filter permanently in the other. The channel one filters of the Semi Automatic System were used. Furthermore, an 80-20 beam splitter was used, so that 80% of the light from the telescope was incident on the narrow filter, and 20% on the wide filter.

It was decided that the H-316 should be programmed to perform four sequences of pulse counts on a given star, always expecting the narrow filter counts in channel one and the wide filter counts in channel two. The number of counts in each of the four sequences can be anything from one to ten and is selected by the observer before the observation is begun. The programme was also written in such a way that the integration time can be selected by the observer. The integration time chosen was in general dependent on the magnitude of the star being observed, and the general weather conditions prevailing at the time. This is because, as

the star becomes faint, the signal becomes of the same order of magnitude as the noise. Consequently it becomes increasingly important to measure the signal and the noise more precisely. That is, it is necessary to know the number of counts per second to a greater precision. The method used to achieve this was to pulse count for longer intervals. In general the integration time was chosen according to the table below :

Magnitude of the Star being Observed	Integration Time Chosen
$m \leqslant 8.0$	1 sec
$8.0 < m \leqslant 10.5$	5 secs
$10.5 < m \leqslant 12.5$	10 secs
$m > 12.5$	20 secs

If the timer was being driven by the 1KHz oscillator, then the integration time can be any integral number of seconds from 1 to 999. On the other hand, if the timer is being driven by the 1 MHz oscillator, then the integration time can be any number of milliseconds from 1 to 999.

The programme was written in such a way that it required that the first and fourth sequences in an observation be observations of the sky background, and that the second and third sequences be observations of the star. The computer programme was designed so that, if the observer so chose, the beta index would be calculated after each sequence of observations, and be displayed with the beta indices obtained for all previous sequences of observations of the same star. This enables the results to be checked for consistency.

Before calculating the beta index, all the counts are corrected for deadtime errors. The observer has to enter the deadtime that he requires. An approximate value for this was obtained by plotting

the logarithm of the pulse count obtained from the Camac System, as a function of the logarithm of the reading from an integrating system, for a number of different currents passing through a small bulb, mounted temporarily in the interface between the photometer and the telescope. Eventually a more accurate value of the dead time correction was determined, by the same method that was used for the Semi-Automatic System, described in Section 4.2.4. These dead time corrections were found to be 105nS for Channel One and 167nS for Channel Two.

It was decided that the H-316 programme, that was to perform the operations described above, should be written in Fortran rather than DAP-16, which is the H-316 assembler language. This has the advantage that it would make the programme, to some extent at least, computer-independent. Furthermore, it was easier to handle the computations involved in Fortran. To get around the difficulties associated with using Fortran, which lie essentially in the sphere of performing input/output operations to and from the Camac Crate, Dr. P.W. Hill wrote a Fortran callable subroutine in DAP-16, which enabled Fortran Input/Output to and from the Camac Crate, and fitted the specifications given by Stevens and van Breda (1972). However, this did not completely resolve the difficulties, as the 24-bit data word from the Camac Crate had to be stored as two 16-bit Fortran integers. Consequently Dr. P.W. Hill wrote two more Fortran callable assembler subroutines. One took a floating point number and expressed it as two 16-bit integers, and the other performed the reverse of this. Thus it was now possible to perform input/output operations to the Camac Crate using Fortran statements. The H-316 Fortran I/O package was also modified by Dr. P.W. Hill, so that the Fortran I/O number 9 would perform I/O on the 4010 Tetronix terminal. This was connected to the H-316 I/O bus by means of a 7061 teletype interface. This is a Camac module that resides in the Camac Crate.

The principle of performing a pulse count over a pre-determined time interval was devised by Dr. P.W. Hill, although the actual

Fortran software was written by myself. Initially, the contents of the registers and the overflow flags, of Channels 1 and 2 and the timer are cleared. Next, -1 is loaded into channel 2 register and this is incremented by one, thus producing an overflow, and consequently an overflow signal which is fed into a gate. The gate then produces a signal which inhibits channels one and two from counting. In the event of any counts being accumulated in channel one, between the clearing and the inhibiting, channel one is now cleared again. The integration time is now entered into the timer, and then the overflow flag in channel two is cleared, which enables counting to begin. An interrupt character from the 4010 is polled for. If no recognisable interrupt is found, then the timer overflow flag is examined. If this has not been set, that is the count is not complete, then the H-316 will go back and look for interrupt characters from the 4010. This will continue until either the count is complete or until it is interrupted.

The overflow flag in the timer, when it is generated, will cause the gate to inhibit channel one and channel two from counting. These two registers and the clock register are then read. If the sequence has now been completed, the computer will display the computed sidereal time, channel one and channel two counts, and then await a start character from the terminal. If not, it will go through the cycle again, to perform the next count, and at the same time display the previous counts.

At the end of the sequence of observations, the beta index is calculated, if required, and then the data is written onto magnetic tape. This is done in 40 byte records. The first record, which is also printed on the teletype as a summary, contains the star number the average narrow filter and wide filter counts, corrected for sky background but not for deadtime effects, and the instrumental beta index if calculated. The remaining records written onto the magnetic tape are the actual counts made during

the observation, together with the sidereal time of the count, which is calculated from the universal time in the universal clock.

After this the computer awaits the star number of the star being observed in the next observation, or if the same star is being repeated, the appropriate repeat signal. The star number is keyed in manually from the Tetronix terminal, and prefixed with a character that identifies it as a programme or standard star. There are also facilities for entering comments on the terminal, which in turn are copied onto the teletype and also onto magnetic tape.

4.2.7. The Observations made with the Camac System and their Reduction

Several nights in September and October 1973 were devoted to the observing of Hβ standards. These were taken from Crawford and Mander (1966). This was to ensure that good transformations, between the instrumental and standard β systems were obtainable. As a check against flexure effects, all the accessible standards were observed several times during the course of a night, each observation being made at a significantly different zenith distance.

No systematic variation in the residuals was detected from repeated observations of the same standard at many different zenith distances. Good linear transformations were obtained, although there was some discrepancy for standard beta indices less than 2.560. This is hitherto unexplained. It seems to be independent of the filters, and repeatable from night to night. It might conceivably be as a result of the curvature in Hβ transformations discussed by Kilkenny (1975), or it may be due to incorrect inclination of the beam splitter to the incoming beam.

The other strange effect noted, was that systematically different instrumental beta indices were obtained if the star image was placed in different parts of the diaphragm. The first reaction was that

this was due to the magnets, but the effect persisted after the magnets had been removed. It is also observed for the other pair of filters. It was therefore concluded that the effect was due to non-uniformities in the transmission of the beam splitter. However, the effect was again observed using the 50-50 beam splitter, but the size of the difference in the instrumental beta indices was different. It is conceivable that the 50-50 beamsplitter had similar non-uniformities to the 80-20 beamsplitter. Another possibility is that the effect is due to incorrect inclination of the beam splitter to the incoming beam.

The 80-20 beamsplitter was replaced and the 5mm diaphragm was replaced with a 1mm diaphragm. Thus it was hoped that if the star image was kept as close as possible to the centre of the 1mm diaphragm, the difficulty discussed above would be avoided. On nights with poor seeing, however, the photometry would not be so accurate. This probably explains why the transformations obtained using this Camac System are not as good as those obtained by Dr. P.W. Hill at Kitt Peak, where a comparable number of standards were observed in a night. Being satisfied that acceptable transformations were obtainable using the Camac System, every available night in November and December 1973 was used to observe faint programme stars. Because the data was written onto magnetic tape in 40-byte records, only two full nights of observations could be written onto a single 1200ft reel of magnetic tape. Thus it was necessary to write a programme to copy this data onto another tape, blocking it at the same time into 4000 byte records. This programme was written in Fortran for the 360/44. The H-316 observing programme keeps count of the number of records it writes onto magnetic tape, and so the number of records on a H-316 tape to be blocked is known, and is read in from a card by the 360/44. The first 100 records are taken and written as a 4000 byte record, the next 100 records as the second 4000 byte record, and so on. If necessary, the last 4000 byte record is padded with blanks, and

this is followed with an end-of-file mark. During this transfer process, each character is translated from ASCII to EBCDIC using the same subroutine that was used for the data from the Semi-Automatic System.

This blocking process enables data to be stored on 5" of magnetic tape, which previously required about 100". Consequently many reels of H-316 magnetic tape can be stored on a single reel. So when it comes to transferring the data from the second and subsequent H-316 tapes, a facility in the programme for skipping over previously written data until the end of file mark is reached, is invoked. In this way, the end of file mark is overwritten, and another is written at the end of the current data transfer.

A Fortran programme for the 360/44 was now written, which would enable one 4000 byte record from the archive tape to be read at a time. The characters in this 4,000 byte record were now taken 40 at a time, and the first character of each 40 was examined to see if it was an H, C, P or K. The H and C denoted comments, and a string of 40 characters beginning with an H may contain the date of the night on which the observations were made. Consequently if the first character was an H, the next 39 characters were searched to see if the string "1973" occurred, and if so the record was output as an 80 byte record onto another magnetic tape, the last 40 bytes being padded with blanks. If this was not the first date to be output, then this record was preceded by an 80 byte record of blanks. This blank record is an end of night indicator required by the Hβ reductions programme described in §4.2.4.

The strings of characters beginning with a P or a K denote the summary record of the observation of a star. Consequently, the contents of this record were output onto the magnetic tape, in the correct format for the Hβ reductions programme. The standard stars are denoted by "K", and the programme stars by "P". When the current 4000 byte record has been exhausted, the next

one is read in and the process is repeated. This is continued until the last 4000 byte record has been read in, and processed, whereupon a record of blanks and an end of file mark is written on the output tape. Unfortunately the method of detecting the beginning and end of a night is by no means foolproof, and the 360/44 context editor had to be used to correct this.

A modification was made to the IIβ reductions programme so that it would read stellar observational data from 80 byte records on a magnetic tape, instead of from cards. The control data and the standard star data were still read in from cards. All the data was then reduced, and the correct deadtime correction was determined in the same way as before. Then using this correct deadtime correction, all the data was reduced again. The transformations obtained are listed in Table 4.2.7.1.

In practice the observation of each programme star was repeated two or three times and so the standard deviation of the observation of a star in each night can be calculated, when the average is taken. The average of all the observations for all the nights on which a given star was observed is now taken and the standard deviation calculated in the same way as before. A check for variability was also made in the manner described in §4.2.4. For further analysis of this data, see § 4.5.

Table 4.2.7.1

Hβ Photometry Transformations: CAMAC System 1973

Night	Transformation	Mean Error in Transformation
Nov 5/6	$\beta = 2.3462 + 1.1918\ \beta_{ins}$	0.0151
Nov 6/7	$\beta = 2.3281 + 1.3007\ \beta_{ins}$	0.0240
Nov 7/8	$\beta = 2.3288 + 1.3212\ \beta_{ins}$	0.0143
Nov 9/10	$\beta = 2.3642 + 1.2390\ \beta_{ins}$	0.0139
Nov 10/11	$\beta = 2.3474 + 1.2988\ \beta_{ins}$	0.0154
Nov 12/13	$\beta = 2.3171 + 1.3691\ \beta_{ins}$	0.0218
Nov 13/14	$\beta = 2.3436 + 1.3263\ \beta_{ins}$	0.0177
Nov 14/15	$\beta = 2.3778 + 1.2100\ \beta_{ins}$	0.0091
Nov 15/16	$\beta = 2.3907 + 1.2009\ \beta_{ins}$	0.0168
Nov 16/17	$\beta = 2.3664 + 1.2799\ \beta_{ins}$	0.0161
Nov 18/19	$\beta = 2.3708 + 1.2248\ \beta_{ins}$	0.0129
Nov 19/20	$\beta = 2.3680 + 1.2690\ \beta_{ins}$	0.0106
Nov 20/21	$\beta = 2.3098 + 1.3610\ \beta_{ins}$	0.0430
Dec 3/4	$\beta = 2.2855 + 1.1934\ \beta_{ins}$	0.0203
Dec 4/5	$\beta = 2.3218 + 1.1004\ \beta_{ins}$	0.0290
Dec 5/6	$\beta = 2.3393 + 1.1712\ \beta_{ins}$	0.0073
Dec 6/7	$\beta = 2.2935 + 1.3442\ \beta_{ins}$	0.0169
Dec 8/9	$\beta = 2.3205 + 1.2597\ \beta_{ins}$	0.0141
Dec 10/11	$\beta = 2.3517 + 1.1339\ \beta_{ins}$	0.0084
Dec 11/12	$\beta = 2.3237 + 1.2288\ \beta_{ins}$	0.0120
Dec 12/13	$\beta = 2.3113 + 1.2079\ \beta_{ins}$	0.0107
Dec 13/14	$\beta = 2.3228 + 1.2392\ \beta_{ins}$	0.0131
Dec 14/15	$\beta = 2.3402 + 1.2319\ \beta_{ins}$	0.0116
Dec 15/16	$\beta = 2.3428 + 1.1343\ \beta_{ins}$	0.0148
Dec 16/17	$\beta = 2.3302 + 1.2019\ \beta_{ins}$	0.0106

4.3 Two Channel Hβ Photometry using the Kitt Peak 36" Telescope

The observations reported here were carried out by Dr. P.W. Hill in September 1972. Consequently my discussion of the photometer and the observing technique will be very brief.

The two channel photometer attached to the 36" telescope at the Kitt Peak National Observatory, hereafter referred to as the K.P.N.O., is similar in the essential details to the two-channel "People's Photometer", just described. The principle of operation is exactly the same. One difference is in the interface between the photometer and the telescope. Instead of containing a wide field eyepiece, it contains an off-set guider. This means that during a long integration, any drift of the star image that would tend to take it out of the diaphragm can be noted and corrected for with the telescope slow motions. This telescope has an advantage over the J.G.T. in that it can be set quickly and accurately, making it possible to observe a large number of stars each night.

Another important difference is that dry ice was used as a coolant for the photomultiplier tubes, which were different from those used with the J.G.T. Since this means that the tubes were maintained at -78°C, the dark count obtained was of the order of a few counts per second. That is, the signal to noise ratio was as good, if not better than that obtained later with the Camac System System and using magnets. The instrumental beta index system was defined by having the narrow filter in one channel, and the wide filter in the other. An 80-20 beamsplitter was again used, so that 80% of the light from the telescope was incident on the narrow filter. This enhanced the accuracy of the photometry still further.

A pulse counting system was used. The signal from the photomultiplier tube was fed into an SSR amplifier and discriminator, in the same way that was later used in St. Andrews for the CAMAC System. The output from the SSR then goes to a pulse counting

register and timer. The pulse counts were made for ten seconds. At the end of each pulse count, the registers were read and the data was written onto magnetic tape. There was also a facility for "keying-in" the star number, and this was also written onto magnetic tape. The readings obtained were printed out on a strip printer.

The diaphragm in the photometer gave a field of 17.7". The photomultiplier E.H.T. was -1800 volts. The details of the photomultipliers, SSR amplifiers and filters used in each channel are given below in Table 4.3.1.

TABLE 4.3.1.

		Channel 1	Channel 2
Photomultiplier		FW-130 S-20 096806	FW-130 S-20 066823
SSR-Amplifiers		5-1856	5-2001
Filters	Peak Wavelength	4859Å	4860Å
	% Max.Transmission	60.0%	73%
	Bandwidth	29Å	173Å

The sequence of observations that were made on a given star was as indicated in Table 4.3.2. This was the same as the sequence that was later used for the Camac System in St. Andrews, except that each sequence consisted of a single 10 second pulse count.

TABLE 4.3.2

	Channel 1	Channel 2
Sky	Narrow	Wide
Star	Narrow	Wide
Star	Narrow	Wide
Sky	Narrow	Wide

The data that was stored on magnetic tape whilst the observations were being made, was now used by the K.P.N.O. CDC 6400 computer. The programme, already written by an observatory staff

member, produced the data on punched cards in the correct format for the Hβ reductions programme described in §4.2.4. That is, the star readings were corrected for sky background, but not for deadtime effects.

As described before, in the case of the J.G.T. data a number of runs of the Hβ reductions programme were to determine the correct deadtime correction for the apparatus. The preliminary runs were made with the K.P.N.O. CDC 6400, but the final runs were made with the adapted version of the programme running on the 360/44. Dr. P.W. Hill then examined the results to see if there were any flexure effects. He plotted the residuals in the standards, as various functions of hour angle, zenith distance, right ascension and declination. In the case of each of the four nights on which observations were made, it was noticed that

$$\Delta\beta = k \tan(\delta - \phi) \qquad \text{----------(4.3.1)}$$

where

$\Delta\beta$ = Residual of the β index in the standard stars

k = Constant

δ = Declination of the star

and ϕ = Latitude of the Observatory (i.e. K.P.N.O)

The constant k was determined graphically for each of the four nights. The next step was to introduce modifications into the Hβ reductions programme that would make this correction for the flexure effects. This was undertaken by Dr. P.W. Hill, and a subroutine for extracting the declinations of the programme stars from a disk file was by myself. This made a considerable improvement to the transformations obtained for each night. They are listed in Table 4.3.3. The values for the constant k obtained for each night are as listed below in Table 4.3.4.

Table 4.3.3

Hβ Photometry Transformations: Kitt Peak 1972

16" Telescope

Night	Transformation	Mean Error in Transformation
Sep 25/26	$\beta = 0.2074 + 1.0717\ \beta_{ins}$	0.0074
Sep 26/27	$\beta = 0.1363 + 1.1010\ \beta_{ins}$	0.0034
Sep 27/28	$\beta = 0.3592 + 1.0034\ \beta_{ins}$	0.0082

36" Telescope

Night	Transformation	Mean Error in Transformation
Sep 15/16	$\beta = 2.6370 + 1.0938\ \beta_{ins}$	0.0038
Sep 16/17	$\beta = 2.6371 + 1.0950\ \beta_{ins}$	0.0059
Sep 17/18	$\beta = 2.6382 + 1.0930\ \beta_{ins}$	0.0044
Sep 20/21	$\beta = 2.6250 + 1.0931\ \beta_{ins}$	0.0040

TABLE 4.3.4

Night (1972)	k	No. of Standards
15/16 Sept	0.0120	20
16/17 Sept	0.0156	17
17/18 Sept	0.0135	16
20/21 Sept	0.0105	22

Further analysis of the data and the results is presented in §4.4.

4.4 Single Channel Hβ Photometry using the Kitt Peak 16" Telescope

The observations reported here were carried out by Dr. P.W. Hill in September 1972. Consequently my discussion of the photometer and the observing technique will be very brief.

The single channel photometer attached to the 16" Telescope at the K.P.N.O. is fairly simple in its construction and operation. It contains a single Oke window photomultiplier (FW 130-036928-S20), which is cooled with dry ice. The E.H.T. applied was -1800 volts.

There is an eyepiece attachment for centering the required star in the diaphragm. A diaphragm giving a field of view of 28" was used. As with the 36", the telescope can be set quickly and accurately, enabling a large number of stars to be observed in a night. There is a filter slide containing a narrow Hβ filter and a wide Hβ filter. The characteristics of these filters is given below in Table 4.4.1.

TABLE 4.4.1

	Narrow Filter	Wide Filter
Peak Wavelength	4858Å	4861Å
Percentage max. Transmission	60%	71%
Bandwidth	29Å	175Å

A pulse counting system was again used. Each pulse count was made for a period of 10 seconds. The result was then output on a small strip printer. The sequence in which the observations were made is indicated below in Table 4.4.2.

TABLE 4.4.2

Order	Filter	Sky/Star
1	Wide	Sky
2	Narrow	Sky
3	Narrow	Star
4	Wide	Star
5	Narrow	Star
6	Narrow	Sky
7	Wide	Sky

The disadvantage of a single channel system, apart from considerations of efficient use of observing time, is that good photometric weather is needed if satisfactory photometry is to be accomplished. On the other hand, within a two channel system, good Hβ photometry can be obtained, even in partially cloudy conditions.

The star number of the star being observed had to be written on the strip printer output by hand. The standard stars observed were again taken from the list of Crawford and Mander (1966). The star readings were corrected for the sky background by hand, and the data was then punched up on to cards in the correct format for the Hβ reductions programme. The deadtime correction was determined in the manner previously adopted. The transformations that were finally obtained with the correct deadtime correction, are listed in Table 4.4.3. After carrying out the same analysis that was used for the 36" data, Dr. P.W. Hill concluded that there were no systematic errors due to flexure effects.

The beta indices obtained for each programme star on both the 16" and 36", were now averaged and the standard deviation was calculated. The standard deviation of each individual result was derived from the accuracy of the transformation for the night in question. The criterion of variability discussed in Section 4.2.4 was then applied.

TABLE 4.4.3

The Deadtime corrections for the different systems of Hβ Photometry

System	Channel 1	Channel 2
Camac System	105.3 nS	166.5 nS
Semi Automatic System	66.6 nS	66.6 nS
16" Data	71.4 nS	71.4 nS
36" Data	50 nS	50 nS

4.5 A Comparison of the Different Sources of Hβ Photometry

When we have four sources of observational Hβ indices, as well as several sources of published data, it is necessary to make a detailed comparison of the systems used, in order that a uniform system can be derived and used. The Hβ Photometry from the JGT Semi-Automatic System is listed in Table 4.5.1, the photometry for the Camac System in Table 4.5.2 and the K.P.N.O. Photometry in Table 4.5.3.

Unfortunately, Crawford et al. (1971) do not quote errors for their photometry. However, Crawford and Mander (1966) do quote an r.m.s. deviation of $0^m.006$ for a single star. Since the magnitudes of the stars listed in the 1971 paper are comparable to those of the standards listed in the 1966 paper, and the same equipment was used in both cases, it is reasonable to assume the same errors for the Hβ photometry in the 1971 paper.

For the star HR 1220 Crawford et al. (1971) obtain $\beta=2.588$. This compares very favourably with $\beta=2.589$ obtained with the Camac System. Unfortunately this was the only comparison star that was successfully observed. It would have been useful to have had a few more. No further refinements to the Camac System results seemed justified at the moment. A comparison of programme star β indices obtained by Crawford et al (1971) and those obtained with the JGT Semi Automatic System together with those obtained at Kitt Peak are listed in Table 4.5.4.

The difference between each of the experimental systems of beta indices, and the beta index obtained by Crawford et al. (1971) was plotted as a function of the published β index, as shown in Fig. 4.5.1. Bearing the experimental errors in mind, it appears that there is some curvature present, and this would suggest curvature in the original Hβ transformations, of the type discussed by Kilkenny (1975). However, in the case of the Semi Automatic System data, this will be difficult to check, because the number of standards is so small. In the case of the K.P.N.O. data, the

Table 4.5.1

Hβ Photometry: Results for the Semi - Automatic System

Star	β	σ(β)	N	R	Star	β	σ(β)	N	R
HD 169798	2.640	0.001	6		HD 170028	2.668	0.004	9	
HD 170051	2.681	0.001	9		HD 170075	2.744	0.011	5	1
HD 170111	2.680	0.001	9		HD 170736	2.541	-	1	
HD 171532	2.807	-	1		HD 173087	2.708	0.002	4	
HD 173170	2.751	0.001	8		HD 174179	2.645	0.004	5	
HD 174585	2.659	0.003	2		HD 185780	2.599	0.011	6	
HD 186618	2.587	0.007	12		HD 186994	2.567	0.001	11	
HD 187879	2.583	0.001	4		HD 188209	2.553	0.003	4	
HD 188252	2.595	0.003	9		HD 188439	2.568	0.006	9	
HD 189775	2.666	0.001	9		HD 189818	2.603	0.006	12	
HD 189957	2.595	0.008	13		HD 190025	2.656	0.003	8	
HD 190427	2.595	0.009	8	1	HD 190944	2.430	0.013	6	2
HD 191781	2.544	0.030	12		HD 198781	2.574	0.020	11	
HD 198895	2.500	0.001	7	3	HD 207017	2.644	0.005	8	4
HD 205139	2.576	0.002	4		HD 206327	2.603	0.006	6	
HD 207198	2.583	0.004	7		HD 207308	2.590	0.003	8	
HD 208218	2.583	0.002	6		HD 208682	2.498	0.007	7	3
HD 213087	2.572	0.005	2		HD 213405	2.672	-	1	
HD 2083	2.642	-	1		HD 6675	2.578	0.009	3	
HD 25443	2.616	0.007	3		HD 25638	2.604	0.005	3	
HD 25639	2.635	0.003	3		HD 41161	2.591	0.002	4	
HD 58784	2.659	0.012	13	5	HD 60525	2.711	0.004	2	
HD 60848	2.495	0.001	7	3	HD 60868	2.826	0.006	7	
HD 61234	2.833	0.004	6		HD 62072	2.879	0.009	3	
HD 64513	2.846	0.009	4		HD 64745	2.784	0.001	6	
HD 64854	2.560	-	1		HD 65176	2.450	0.025	2	3

N - denotes the No. of observations R - denotes a remark corresponding to

1) A possible variable
2) An emission line star, possibly variable
3) An emission line star
4) A binary star
5) A probable variable

Table 4.5.2

Hβ Photometry: Results for the CAMAC System

Star	β	σ(β)	N	R	Star	β	σ(β)	N	R
LS2 39 02	2.656	0.005	4		BD 43 3371	2.619	0.001	4	
LS3 45 01	2.696	0.018	1		BD 42 3570	2.616	0.001	4	
BD 44 3365	2.577	0.002	2	1	BD 46 2877	2.585	0.001	5	
BD 48 3054	2.627	0.001	4		LS3 50 01	2.670	0.042	1	
BD 49 3292	2.669	0.003	5		LS3 52 01	2.667	0.001	5	
LS3 50 03	2.595	0.007	2		LS3 51 01	2.644	0.001	3	
BD 52 2795	2.681	0.003	4		LS3 53 02	2.763	0.005	1	
LS3 54 01	2.679	0.003	1		LS3 54 01	2.657	0.004	3	
BD 54 2358	2.547	0.002	2		BD 53 2481	2.666	0.001	4	
BD 55 2467	2.677	0.002	2		BD 55 2443	2.834	0.005	1	2
LS3 57 03	2.661	0.021	1		LS3 57 04	2.615	0.003	2	
BD 58 2236	2.593	0.002	5		BD 58 2237	2.631	0.001	5	
LS3 58 03	2.706	0.001	4		LS3 58 05	2.715	0.002	2	
BD 59 2333	2.665	0.001	3		LS3 59 06	2.629	0.001	4	
LS3 59 07	2.654	0.005	2		BD 59 2344	2.504	0.005	1	3
BD 59 2350	2.643	0.001	5		BD 58 2268	2.632	0.011	1	
BD 61 2158	2.630	0.002	5		BD 61 2163	2.650	0.001	6	
LS3 64 01	2.905	0.002	1	2	LS3 64 04	2.670	0.001	4	
BD 64 1677	2.626	0.001	4		BD 65 1774	2.627	0.005	2	
BD 66 1521	2.592	0.001	3		BD 66 1548	2.653	0.002	3	
BD 67 1489	2.613	0.001	5		LS3 67 03	2.603	0.007	2	
BD 68 1373	2.633	0.001	5		LS3 68 01	2.609	0.003	2	
LS3 68 03	2.665	0.003	4		BD 67 1531	2.599	0.012	2	
BD 67 1538	2.659	0.001	4		BD 67 1550	2.606	0.001	4	
BD 67 1546	2.634	0.001	4		BD 68 1386	2.657	0.010	1	
BD 59 0804	2.618	0.001	6		LS5 58 22	2.656	0.013	3	
LS5 57 60	2.689	0.005	7		LS5 54 14	2.674	0.001	5	
LS5 53 30	2.671	0.002	5		LS5 51 22	2.605	0.001	6	
BD 52 0913	2.659	0.001	4		LS5 54 15	2.893	0.013	3	4
LS5 50 12	2.815	0.016	2	4	BD 50 1129	2.646	0.003	4	

Star	β	σ(β)	N	R
BD 48 1263	2.640	0.001	8	
LS5 47 29	2.701	0.019	1	
BD 43 1349	2.643	0.001	10	
BD 37 1415	2.671	0.002	8	
BD 26 1206	2.614	0.001	4	
LS5 23 73	2.648	0.005	3	
BD 24 1337	2.689	0.003	4	
BD 22 1458	2.629	0.002	2	5
HR 1220	2.589	0.001	2	6

Star	β	σ(β)	N	R
LS5 47 28	2.696	0.002	2	
LS5 44 38	2.669	0.003	5	
BD 43 1355	2.677	0.001	5	
BD 35 1332	2.614	0.001	3	
LS5 26 25	2.691	0.001	3	
BD 24 1306	2.581	0.002	2	
BD 22 1407	2.702	0.004	3	
BD 23 1436	2.636	0.004	2	

N - denotes the No. of observations

R - denotes a remark corresponding to :

1) Also HD 191781
2) Wrong star may have been observed in this case
3) A probable emission line star
4) The wrong star may have been observed. The result suggests variability.
5) Also HD 48549
6) Observed as a check only

Table 4.5.3

Hβ Photometry: Results from 16" and 36" Telescopes at Kitt Peak

Star	β	σ(β)	N	R	Star	β	σ(β)	N	R
HD 169798	2.670	0.002	4		HD 170028	2.687	0.002	4	
HD 170051	2.703	0.008	4		HD 170111	2.695	0.003	4	
HD 170650	2.628	0.006	4		HD 170263	2.850	0.008	3	
HD 172397	2.773	0.009	3		HD 172421	2.740	0.009	2	
HD 174261	2.711	0.004	4		HD 174298	2.628	0.006	4	
HD 174585	2.662	0.004	4		HD 174586	2.788	0.002	2	
HD 174664	2.730	0.008	4		HD 175081	2.768	0.013	4	
HD 175803	2.668	0.011	4		HD 176254	2.653	0.011	4	
HD 176803	2.725	0.004	2		HD 176818	2.625	0.006	4	
HD 176914	2.624	0.003	4		HD 176940	2.772	0.007	4	
HD 177006	2.690	0.002	3		HD 177593	2.688	0.006	4	
HD 178540	2.697	0.007	4		HD 178591	2.753	0.014	4	
HD 178849	2.692	0.005	4		HD 178912	2.627	0.009	3	
HD 179506	2.754	0.007	4		HD 180124	2.691	0.004	2	
HD 180844	2.688	0.004	4		HD 181164	2.654	0.014	4	
HD 181492	2.692	0.007	4		HD 182615	2.790	0.001	3	
HD 182975	2.659	0.012	2	1	HD 183129	2.653	0.004	2	2
HD 183535	2.612	0.016	3		HD 183649	2.674	0.001	2	
HD 185780	2.585	0.005	4		HD 185842	2.652	-	2	3
HD 186485	2.814	0.012	4		HD 186618	2.594	0.009	5	
HD 186814	2.798	0.023	3		HD 186994	2.593	0.006	3	
HD 187035	2.674	0.009	4		HD 188252	2.606	0.001	4	
HD 188439	2.580	0.008	5		HD 188461	2.643	0.005	4	
HD 188891	2.607	0.003	4		HD 189775	2.692	0.005	5	
HD 189818	2.624	0.008	4		HD 189957	2.577	0.011	5	
HD 190025	2.683	0.004	3		HD 190254	2.683	0.015	3	
HD 190427	2.573	0.010	3		HD 190901	2.890	0.016	3	
HD 191124	2.916	0.022	3	4	HD 191781	2.544	0.023	4	
HD 192035	2.575	0.018	4		HD 192575	2.611	0.003	3	
HD 193550	2.656	0.009	2		HD 196421	2.635	0.010	3	
HD 197344	2.856	0.006	2		HD 197751	2.701	0.004	2	

Star	β	σ(β)	N	R	Star	β	σ(β)	N	R
HD 197911	2.623	0.004	3		HD 198739	2.697	0.005	2	
HD 198781	2.578	0.011	4		HD 199308	2.645	0.008	3	
HD 199739	2.658	0.010	3		HD 202107	2.658	0.006	2	
HD 204150	2.634	0.010	3		HD 205139	2.574	0.007	3	
HD 206327	2.651	0.004	3		HD 207017	2.660	0.013	3	
HD 207308	2.605	0.003	3		HD 207951	2.645	0.011	4	
HD 208106	2.650	0.007	3		HD 208185	2.643	0.005	3	
HD 208218	2.591	0.004	4		HD 208440	2.625	0.006	3	
HD 208761	2.619	0.010	3		HD 208904	2.670	0.010	4	
HD 208947	2.665	0.012	5		HD 209162	2.752	0.010	3	
HD 207198	2.685	0.006	3		HD 209452	2.668	0.014	5	
HD 209789	2.697	0.011	3		HD 210386	2.605	0.007	3	
HD 213087	2.557	0.010	4		HD 213405	2.605	0.018	3	
HD 213481	2.593	0.009	4		HD 213571	2.697	0.002	3	
HD 216992	2.670	0.015	4		HD 217224	2.636	0.006	3	
HD 220172	2.633	0.007	3		HD 220787	2.650	0.008	3	
HD 222568	2.612	0.007	4		HD 223036	2.529	0.008	2	5
HD 223959	2.663	0.015	3		HD 224395	2.667	0.005	4	
HD 225190	2.714	0.004	2		HD 225573	2.698	0.004	3	
HD 225882	2.624	0.002	3		HD 226070	2.856	0.005	3	
HD 2083	2.610	0.008	4		HD 3366	2.676	0.006	4	
HD 4460	2.619	0.010	2		HD 5553	2.595	0.009	2	
HD 6675	2.586	0.008	4		HD 7852	2.638	0.012	4	
HD 12740	2.579	0.001	2		HD 13544	2.582	0.015	2	
HD 14863	2.738	0.005	3		HD 16393	2.742	0.005	4	
HD 16440	2.602	0.009	3		HD 17179	2.653	0.011	3	
HD 17218	2.611	0.011	2		HD 17929	2.704	0.011	3	
HD 20710	2.801	0.005	3		HD 21267	2.805	0.005	3	
HD 21806	2.624	0.010	4		HD 21930	2.830	0.005	3	
HD 22828	2.824	0.034	5	6	HD 23036	2.686	0.048	3	6
HD 23254	2.692	0.011	4		HD 25090	2.602	0.011	3	
HD 25443	2.583	0.004	3		HD 26684	2.715	0.003	3	
HD 29441	2.542	0.012	2		HD 30677	2.565	0.009	2	
HD 35250	2.688	0.018	4		HD 34233	2.718	0.005	5	

Star	β	σ(β)	N	R	Star	β	σ(β)	N	R
HD 36083	2.718	0.009	2		HD 36662	2.697	0.017	3	
HD 37838	2.729	0.011	4		HD 38410	2.724	0.006	3	
HD 38775	2.814	0.011	3		HD 40160	2.668	0.012	3	
HD 40694	2.671	0.001	2		HD 40784	2.708	0.012	3	
HD 41161	2.584	0.007	3		HD 41258	2.730	0.019	2	
HD 41541	2.732	0.008	3		HD 41689	2.608	0.014	3	
HD 41765	2.733	0.016	2		HD 42614	2.763	0.016	2	
HD 42782	2.692	0.006	5		HD 44512	2.728	0.002	2	
HD 46552	2.756	-	2	7	HD 48029	2.607	0.013	6	
HD 48532	2.698	0.007	4		HD 48549	2.632	0.019	4	
HD 49763	2.677	0.015	4		HD 50003	2.702	0.004	4	
HD 50320	2.687	0.010	4		HD 50767	2.613	0.006	3	
HD 51560	2.687	0.001	3		HD 54352	2.716	0.014	2	
HD 57291	2.650	0.009	3		HD 58784	2.662	0.018	3	
HD 58973	2.670	0.010	3		HD 59882	2.602	0.008	3	
HD 66594	2.650	0.010	2		HD 66665	2.592	0.005	2	
HD 66713	2.730	0.013	2						

N - denotes the No. of observations

R - denotes a remark corresponding to:

1) l = 35.25, b = -8.92: Not a programme star
2) l = 36.15, b = -8.65: Not a programme star
3) l = 36.58, b = -12.12: Not a programme star
4) A possible variable
5) l = 113.49, b = -6.93: Not a programme star
6) A probable variable
7) Both observations identcal

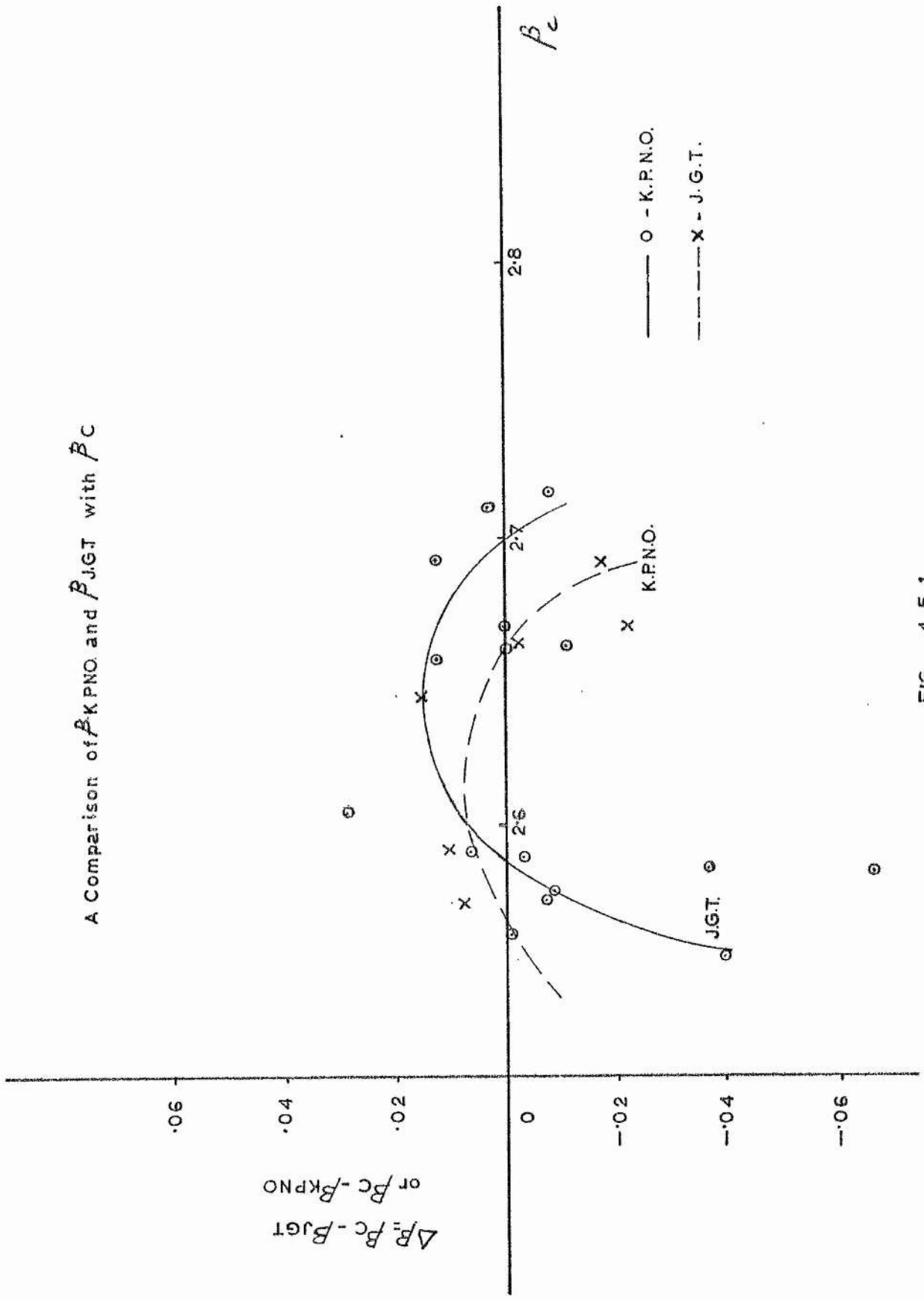
A Comparison of β_{KPNO} and β_{JGT} with β_C
$\Delta\beta = \beta_C - \beta_{JGT}$ or $\beta_C - \beta_{KPNO}$
β_c
0 - K.P.N.O.
X - J.G.T.
K.P.N.O.
J.G.T.
2·8
2·7
2·6
·06
·04
·02
0
-·02
-·04
-·06

FIG. 4.5.1.

residuals are so small that they are almost certainly due to random errors. The apparent discontinuity at β=2.55 in the Hβ transformations derived from the Camac System, needs further investigation.

TABLE 4.5.4

STAR	β_C (Crawford et al. 1971)	β_{JGT} (Semi Automatic System)	$\beta_{K.P.N.O.}$ (16" + 36")
HD 170111	2.692	2.680	2.695
HD 170650	2.643	--	2.628
HD 173087	2.712	2.708	--
HD 174179	2.657	2.645	--
HD 174585	2.660	2.659	2.662
HD 187879	2.580	2.583	--
HD 188209	2.552	2.553	
HD 188439	2.597	2.568	2.580
HD 189775	2.668	2.666	2.692
HD 198781	2.585	2.574	2.578
HD 205139	2.567	2.576	2.574
HD 207198	2.544	2.583	--
HD 208947	2.654	2.665	--
HD 213087	2.565	2.572	2.567
HD 25638	2.568	2.604	--
HD 25639	2.569	2.635	--
HD 34233	2.710	2.718	--

Thus there may well be a case for looking at possible curvature corrections to the transformations. This could be achieved by modifying the Hβ reductions programme, so that instead of just fitting a straight line, a number of polynomials of different order, up to a chosen maximum order, could be fitted, and then the polynomial giving the best fit selected. A programme modification such as this

Table 4.5.5

Hβ Photometry: Published Data (Crawford, Barnes & Golson (1971))

Star	β	N	Star	β	N
HD 170111	2.692	5	HD 170650	2.643	4
HD 173087	2.712	3	HD 174179	2.657	2
HD 174585	2.660	3	HD 174959	2.707	3
HD 175426	2.666	3	HD 176502	2.667	3
HD 176582	2.692	2	HD 176819	2.640	3
HD 176871	2.687	3	HD 177003	2.675	2
HD 177109	2.594	2	HD 178329	2.690	3
HD 178475	2.652	3	HD 180163	2.634	5
HD 181409	2.610	3	HD 182568	2.667	3
HD 184171	2.656	2	HD 187879	2.580	3
HD 188209	2.552	3	HD 188439	2.597	3
HD 188665	2.715	3	HD 189775	2.668	2
HD 197770	2.596	3	HD 198781	2.585	4
HD 199661	2.682	3	HD 202214	2.602	3
HD 204770	2.696	3	HD 205139	2.567	3
HD 206165	2.560	Std.	HD 207198	2.544	3
HD 208947	2.654	2	HD 213087	2.565	1
HD 25638	2.568	3	HD 25639	2.569	3
HD 34233	2.710	3			

All standard deviations were assumed to be $0^{m}.006$

N - denotes the No. of observations

could be achieved by incorporating a subroutine for fitting polynomials in the above manner, already written and used for radial velocity reductions, as discussed by Hill (1971). Any corrections so derived would be small and would make very little difference to the resulting stellar distances. There would certainly be no difference in the analysis of galactic structure derived from these results.

Consequently it was decided that it would suffice, for the time being, to take the weighted mean according to the standard deviation of the individual β indices using the method described by Barford (1967, page 62). The results thus obtained are listed in Table 7.2.1. The relevant β indices published by Crawford et al. (1971) are listed in Table 4.5.5.

Haug (1970a) has investigated the effect of temperature variations on the coefficients of his transformations and finds a relationship of the form,

$$\beta_s = (0.77 - 0.004t)\ \beta' + (0.80 + 0.008t) \qquad \text{---------4.5.1,}$$

where β_s is the beta index on the Standard System, and β' is the instrumental beta index and t is the filter temperature in °C.

This relationship was valid for $7.5°C < t < 16.5°C$ and $2.56 < \beta < 2.84$. It may well prove possible to improve the data by implementing a temperature correction of this type, if the filter temperature at each observation were available. For the Camac System data, if it is assumed that the filters are at the same temperature as the air in the photometer, it may be possible to deduce the filter temperature, from the photometer temperature readings made at the beginning and end of each night and assuming a linear interpolation between the two.

A further improvement may be made by using the programme stars with the best night to night agreement, as additional standard stars, and so derive new and hopefully, improved transformations. This should give improved β indices. The application of Hβ photometry

to derive the distances of the programme stars, is discussed in §7.2.

CHAPTER FIVE

Spectroscopy

5.1 Introduction

- 5.1.1 Radial Velocity Determinations
- 5.1.2 Spectral Type Determinations
- 5.1.3 Spectrophotometry of the Programme Stars

5.2 The Spectroscopic Observations undertaken with the 120cm. Telescope, Spectrograph C, at l'Observatoire de Haute Provence (l'O.H.P).

5.3 The Measurement of Radial Velocities from the l'O.H.P. Plates

5.4 The Spectroscopic Observations undertaken with the Isaac Newton Telescope (I.N.T), Cassegrain Photographic Spectrograph.

5.5 The Measurement of Radial Velocities from the I.N.T. Plates

5.6 A Discussion of the Radial Velocities Obtained and their Comparison with Published Radial Velocities where available.

5.7 The Determination of Spectral Types of Programme Stars from the l'O.H.P. and I.N.T. Plates.

5.8 A Discussion of the Spectral Types Obtained and their Comparison with Available Published Spectral Types.

5.1 Introduction

5.1.1 Radial Velocity Determination

The development of the techniques of radial velocity measurement has been discussed in some detail by Petrie (1962). The change of wavelength with velocity along the line of sight was discovered by Doppler in 1842. In 1866 Huggins attempted to measure the shifts in stellar spectral lines visually, but was unsuccessful. Maxwell (1868) was the first person to present the subject of stellar radial velocity determinations in a definite analytical form. The photographic method of recording stellar spectra was firmly established by Draper and this made the development of the techniques of radial velocity measurement possible.

Vogel (1900) was the first to design and use a prismatic spectrograph. Vogel noticed that the shift in the spectral lines was very small, and had to be measured accurately to 1μ in order to obtain accurate radial velocities. This imposes severe restrictions upon the mechanical and optical tolerances of a spectrograph as the relative positions of the comparison and star beams has to be maintained to a few thousandths of an Angstrom. Vogel also noted that as exposure times in stellar spectroscopy are usually long, temperature changes can occur, resulting in changes in the refractive index of the prism material. Image defects are also caused by lens aberrations and inhomogeneities in the prisms are likely to cause a shift of the stellar spectral lines with respect to the comparison spectral lines. Realising all these possible sources of error, Vogel was able to improve his spectrograph.

The first attempt to develop a standard method for the measurement and reduction of stellar spectrograms was that of Curtiss (1904). This uses the interpolation formula derived by Hartmann (1901) which gives the wavelength of a spectral line, for a prismatic spectrograph,as

$$\lambda = \lambda_o + \frac{K}{n - n_o} \qquad \text{---------- (5.1.1.1),}$$

where n is the measure of the line (read off from the measuring machine), and λ_o, n_o and K are three constants, provided that the zero point for the measures is always the same, which are referred to as the Hartmann Constants. The constants are dependent upon the spectrograph used, and in the case of n_o, on the choice of the zero point, for the measures as well. The use of this interpolation formula saves the need for producing a separate calibration curve for each spectrogram, which simplifies the reduction procedure.

So, in practice, a large number of comparison spectral lines are measured, and as these have known wavelengths, the Hartmann constants can be calculated from any three of them. In order to obtain the required accuracy, this is done several times. Then for each set of measures obtained, the position of each star line and comparison line is predicted from its laboratory wavelength. The differences between these computed positions and the actual measured positions for the comparison lines are now plotted as a function of the measured positions. From the resulting curve, corrections to the measured positions of the star lines can be derived; the differences between these and the positions predicted from the laboratory wavelength are the shifts in position, Δn, of the star lines due to the Doppler Shift.

A discrepancy between the measured and predicted positions of the comparison lines will occur, due to small systematic measuring errors, and also because equation (5.1.1.1) is not an exact relation between n and λ. The systematic measuring errors are discussed by Curtiss (1904), and are due to temperature variation during the course of measuring and non-uniformities in the pitch of the screw of the measuring machine. Another source of error arises from the errors in the published values of the laboratory wavelengths of both the comparison and star lines. The procedure described above corrects for these systematic errors.

Expressing equation (5.1.1.1) in the form $n = n(\lambda)$ and differentiating gives

$$\Delta n = \frac{-K\Delta\lambda}{(\lambda - \lambda_o)^2} \quad ,$$

$$\therefore \quad \Delta\lambda = -\frac{(\lambda - \lambda_o)^2 \, \Delta n}{K} \qquad \text{----------(5.1.1.2)} \quad .$$

It can be shown, from the Special Theory of Relativity, that in the case where the velocity (v) is very much less than the velocity of light (c), as is the case for stellar radial velocities, then the Doppler hift $\Delta\lambda$ is

$$\Delta\lambda = \frac{v}{c}\lambda \qquad \text{----------(5.1.1.3)} \quad .$$

Thus substitution for $\Delta\lambda$ in equation (5.1.1.2) gives

$$v = \frac{-c(\lambda - \lambda_o)^2 \, \Delta n}{K\lambda} \qquad \text{---------- (5.1.1.4).}$$

This enables the Doppler Shift in a stellar spectral line to be calculated by substitution for Δn, λ, λ_o and K. Having corrected for any systematic errors in the radial velocity derived for each stellar line, the average velocity can be evaluated, together with the corresponding standard deviation. In the case of prismatic spectrographs, the spectral lines are curved if the slit jaws are parallel, and in this case, a curvature correction has to be added to this average radial velocity before proceeding to evaluate the heliocentric radial velocity.

The first attempt to employ a diffraction grating in a spectrograph was made by Plaskett (1913), but unfortunately the quality of the

gratings available at that time did not permit very successful results. The use of gratings in spectrographs was eventually pioneered by Merrill (1931). In the case of a grating spectrograph, the Hartmann Formula is found to be

$$\lambda = \lambda_o + Kn \quad \text{----------(5.1.1.5)},$$

where n, λ_o and K represent the same quantities as in equation (5.1.1.1). Again λ_o and K, the Hartmann Constants, depend only on the spectrograph used, provided that the zero point for the measures is always the same. In this case the Hartmann Formula is linear. Thus, if a large number of positions are recorded for comparison lines of different wavelengths, λ_o and K can be determined by means of a Least Squares Fit (See Barford, 1967, p.56).

Differentiating equation (5.1.1.5) gives

$$\Delta\lambda = K\Delta n \quad \text{---------- (5.1.1.6)},$$

and eliminating $\Delta\lambda$ between equations (5.1.1.3) and (5.1.1.6) gives

$$v = \frac{Kc\Delta n}{\lambda} \quad \text{---------- (5.1.1.7)},$$

Grating Spectrograph Spectra can be measured and reduced in a manner similar to that already described for prismatic spectrograph spectra, by the appropriate use of equations (5.1.1.5) and (5.1.1.7) instead of equations (5.1.1.1) and (5.1.1.4).

The geocentric radial velocities are dependent upon the time of observation, and the position of the observatory on the earth's surface. Thus it is useful to correct the radial velocities for the earth's diurnal and annual motion and so determine the heliocentric radial velocities.

The radial velocity correction, V_{re}, for the earth's orbital motion about the sun was derived by Schlesinger (1899) and is given by

$$V_{re} = -V \cos\beta \sin(\lambda_s - \lambda) + V e \sin(\Gamma - \lambda) \cos\beta \quad \text{----------} \quad (5.1.1.8),$$

where λ = Ecliptic Longitude of the Observed Star,

β = Ecliptic Latitude of the Observed Star,

λ_s = Longitude of the Sun at the epoch for which λ and β are determined

Γ = Longitude of the Sun at perigee and is given by

$$\Gamma = 281^\circ 13' 15''.00 + 6189''.03T + 1''.63T^2 + 0''.012T^3$$

----------(5.1.1.9),

and V is given by

$$V = \frac{2\pi a}{\rho(1-e^2)^{\frac{1}{2}}} \approx 29.974 \text{ Km/sec} \quad \text{----------} \quad (5.1.1.10),$$

where T = the number of tropical centuries since 1900.0,

e = the eccentricity of the earth's orbit = 0.0167,

ρ = the number of seconds in a solar year = 31470758,

a = the Semi Major axis of the earth's orbit.

The rotational velocity correction, V_{rer}, for the rotation of the earth is given by Lang (1974) as

$$V_{rer} = V_e \sin h \cos \delta \cos \psi \quad \text{----------(5.1.1.11)},$$

where V_e = the equatorial rotational velocity of the earth,

h = the hour angle of the star, which is taken as positive for objects east of the meridian and negative for objects west of the meridian.

δ = the declination of the celestial object, and

ψ = the latitude of the observatory.

The radial velocity corrections V_{re} and V_{rer} are calculated using these formulae and added to the geocentric radial velocity to give the heliocentric radial velocity. In a similar way the velocity of the interstellar calcium can be determined by measuring the Doppler Shift of the interstellar CaII (K) line, and if it can be resolved from Hε, the CaII (H) line. The heliocentric interstellar calcium velocities were calculated in the same way as the heliocentric stellar radial velocities.

5.1.2 Spectral Type Determinations

The fact that stars of different visual colours have different spectra was first noted by Rutherfurd (1863). Secchi (1868) made the first attempt at classifying the spectra. The stars were divided into four groups with the colours white, yellow, orange and red. These were coupled with the respective spectral features of strong absorption lines of hydrogen, strong calcium lines, strong metallic lines, broad absorption lines and more luminous on the violet side. With the introduction of the spectrograph large numbers of stellar spectra became available and consequently the opportunity for establishing spectral classification on a firm basis arose. Pickering and Fleming (1897) and Pickering (1899) introduced the system of letters to denote a wider variety of colour and spectral types. This system became well established with the development of the Henry Draper Catalogue (Maury and Pickering 1897; Cannon and Pickering, 1918-1924), and was extended in that finer classification divisions were made. This was done by placing a digit 0,1,2----------9, after the capital letter of

the class, and this became known as the Mt. Wilson system.

A further improvement to the system of spectral classification was made by Morgan et al,(1943) who introduced the system of placing the Roman Numerals I, II -----V after the letter and digit. This serves the purpose of denoting the luminosity of the star. This system was revised by Johnson and Morgan (1953), and is what is now referred to as the MK (Morgan-Keenan) system. A further revision of the MK Spectral Classification System has been made by Morgan and Keenan (1973). Here they publish a new list of fundamental standards for the system.

Thus the spectra obtained for radial velocity determinations can be classified in the MK system, by comparing these spectra with the spectra taken with the same spectrograph of spectral type standards that Johnson and Morgan used to establish the MK system.

5.1.3 Spectrophotometry of the Programme Stars.

One of the quantities of interest is the variation in the gas to dust ratio as a function of galactic longitude and latitude. The best that can be achieved with present day observing techniques is the measurement of column densities of the gas and dust along the line of sight to each star. This will then give a measure of the average gas to dust ratio along each line of sight.

The dust along the line of sight gives rise to interstellar reddening. This is given by the parameter E_{B-V}, which is deduced from UBV photometry (see §2.2 and §7.2). The gas density along the line of sight can be measured in two ways. The first is to measure the strength of the neutral hydrogen 21cm line in the direction of the stars, This has already been done by Kilkenny and Schmidt-Kaler in September 1974, using the Bonn Radio Telescope. The reductions of the data are currently being undertaken by Dr. Kilkenny.

The second method involves measuring the equivalent width of the interstellar CaII (K) line at 3933Å, from the spectra obtained for radial velocity determinations. The technique used is the same as that used in the accurate measurement of intensities in stellar spectra,

the study of which has long been known to be fundamental for the study of stellar atmospheres. The problem of obtaining equal densities on a photographic plate to define equal intensities in a source were first studied by Hartmann (1899).

A detailed description of the methods of performing spectrophotometric calibrations is given by Wright (1962), and so only a brief summary will be given here. In principle, two regions of equal density on the same photographic plate, or on two separate plates, may be considered to have been produced by two sources having equal intensity, if in both regions the sensitivity of the emulsion is identical, if they have been given identical exposure and development, if they correspond in wavelength and polarization, and if the same light path and optics have been used.

For relative, rather than absolute, intensity measurements, the last requirement may be relaxed, which is fortunate because it is often impractical to produce the calibration with the spectrograph on the telescope. An incandescent lamp is usually used as source in spectrophotometric calibrations, and another source, such as mercury or cadmium, is used to provide the wavelength calibration.

The measurement of the intensity on a photographic plate is done, in principle, by shining a light on the plate, and the transmission that occurs is a function of the grain density on the plate. Thus, if a device can be arranged which measures the transmission of the plate at different points on it, the variation in grain density can be measured. This was first achieved by Moll (1921)and it was a principle similar to this that was used by Lindblad (1922), in his spectrophotometric determination of absolute magnitudes (§4.1).

The variation in density on a photographic plate can be digitized and the results analysed by means of on-line computer. This is attainable by means of the St. Andrews University Observatory Joyce-Loebl Microdensitometer, which has been linked to the H316 by means of a Camac crate as described by van Breda et al.(1974). Software is currently being written which, it is hoped, will enable the equivalent width of the CaII (K) line in a stellar spectrogram to be measured.

It is hoped that the equivalent width of the Hγ line will also be measured. Then using the calibration of Balona and Crampton (1974), the absolute magnitudes of the stars can be determined. This system for determining absolute magnitudes was developed by Petrie (1953a, 1965), and it has the advantage over Hβ photometry, in that such obstacles as blends can be allowed for. It is hoped that it will eventually enable the Hβ absolute magnitudes to be checked for possible effects of Hβ emission.

5.2 The Spectroscopic Observations undertaken with the 120cm Telescope, Spectrograph C, at 1'Observatoire de Haute Provence (1'O.H.P).

In 1972 the "Commission des Programmes" of 1'Observatoire de Haute Provence, hereafter referred to as 1'O.H.P, made a very generous allowance of 32 nights of observing time to the writer. This was for the use of the 120cm telescope with the Spectrograph C. The nights allocated were from 16th to 30th August 1972, from 18th to 24th October 1972 and from 9th to 18th June 1973, With the exception of the night 11/12 June 1973, the weather in June 1973 was perfect. Consequently advantage was taken, at this time, to observe the fainter programme stars whose magnitudes ranged from $9^m.5$ to $10^m.2$, which had not been previously observed on the Isaac Newton Telescope, hereafter referred to as the I.N.T, (See §5.4.).

In August and October 1972 there were nine cloudless nights, but the seeing was not always as good as 2". Of the remaining thirteen nights, the sky was completely overcast for half the night and clear for the other half, apart from the occasional flurry of cloud, with poor seeing, on seven nights. On the remaining nights the transparency was poor due to cirrus clouds.

Priority was given to observing programme stars of earlier spectral type, because they are probably more luminous and thus more distant than later type B stars of the same apparent magnitude. Consequently spectral features such as the interstellar CaII (K) line will be more distinct. It was also necessary to give priority to observing faint stars in good weather, because in partially cloudy conditions, exposure times become prohibitively long.

Bearing this in mind, an attempt was made to obtain four spectra of those stars for which radial velocities were required. Since it was hoped that absolute magnitudes could be determined from the equivalent width of the Hγ line, as many Hγ standards as possible, taken from the lists of Petrie (1953a) and Crampton et al.(1973), were observed on each night. Those stars were selected that had "a", "b" or "c" classification given by Wilson (1963), so that they could be

used as radial velocity standards and also as a check for possible flexure effects. These stars are listed below in Table (5.2.1).

TABLE 5.2.1.

A list of stars used as Hγ and radial velocity standards at 1'O.H.P

Star (HD)	Radial Velocity (Wilson,1963)	Hγ Equivalent Width
20315	-5(c)	9.3
20365	0(c)	6.3
23302	+12.4(b)	6.7
34759	+5(c)	7.5
177003	-19(c)	5.9
180163	-8.2(a)	4.6
184171	-21.8(a)	
206165	-13.2(b)	

By the use of the stars in Table (5.2.1) as radial velocity standards, it was hoped that maximum use could be made of the available observing time, but it eventually turned out that this was a mistake. Some late type stars, which were radial velocity standards, should have been included. These would not only have accurate published radial velocities, but also radial velocities that could be measured accurately because of the superior quality of the spectral lines in late-type stars.

A further attempt to economise in observing time was made by restricting the observations of bright program stars, radial velocity standards and spectral type standards, to times at which the transparency of the atmosphere was poor, ot to times when there was a great deal of broken cloud about, meaning that the exposure times would have to be short.

A list of bright spectral type standards was prepared from the list of Johnson and Morgan (1953) and is given in Table (5.7.1).

Unfortunately the revised list of Morgan and Keenan (1973) was published after the observing period, although its contents were taken into account during the classification.

The Spectrograph C is used at the Newtonian Focus of the 120cm telescope, and has been described in detail by Boulon (1957, 1963), and so only a very brief description will be attempted here. The spectrograph consists of a slit with parallel jaws, the width of which can be adjusted by means of an attached thumb-screw. As suggested by Boulon (1963) a slit width of 40μ was chosen. This gives a curved-line spectrum of 76Å/mm at Hγ. The spectrograph was orientated with respect to the telescope in such a way that any movement of the telescope in right ascension, resulted in the star image drifting along the slit. The advantage of this orientation was that any errors or fluctuations in the speed of the telescope drive are much larger in right ascension than in declination, and consequently it is much easier to keep the star image trailing on the slit.

The focus of the spectrograph was set in accordance with the findings of previous observers (Boulon, 1963). The spectrograph prism was orientated with respect to the incident beam from the slit so that the wavelength range obtained on the photographic plate was from 3,900Å to 5,000Å. There is also an attached mask in the form of a "V" which is placed over the slit to restrict the width of the stellar spectrum. All stellar spectra obtained with this spectrograph were of the same width.

There is a wooden drum mounted on the spectrograph containing a number of arc tubes with different gaseous materials in them. The observer can select his comparison spectrum by rotating the drum to the appropriate position, and in this case an iron arc comparison spectrum was chosen. A mask is placed over the star spectrum whils the comparison spectrum is being exposed. As suggested by Boulon (1963) the iron-arc was exposed for 1½ mins. both before and after the exposure of the stellar spectrum.

An attached exposure meter consists of a photomultiplier tube, to which a small fraction of the starlight is directed. This produces

an electrical charge in a capacitor and the potential difference across this capacitor is indicated on a voltmeter, which is calibrated in tenths of the full scale deflection. When full scale deflection is attained, a counter is incremented by one and the capacitor is discharged. This process now repeats itself and at the end of the stellar spectrum exposure, the number of counts, together with any fraction of a count indicated by the voltmeter deflection, is a measure of the amount of light that has been incident on the photographic plate during the exposure. Thus in principle it is possible to reproduce exposures accurately in different conditions of atmospheric turbulence and transparency, and, by a trial and error approach, the number of exposure meter counts that gives the correct exposure for the spectrum of each star can be determined.

In practice, however, it was noticed that, when observing a star of magnitude around 9.2, the exposure will not accumulate any counts, which suggests that the charge on the capacitor is leaking away as fast as it is being created by the photomultiplier. Consequently, the exposure meter proves to be rather unreliable, especially for faint stars and conditions of poor transparency and "seeing".

The drive-rate of the 120cm telescope is controlled by an oscillator, the frequency of which can be altered. The larger the difference between the oscillator frequency and the sidereal rate, the faster the star image will drift along the spectrograph slit. The sign of the frequency difference can be reversed by pressing the appropriate button and this gives a convenient method of guiding a star image on the slit. The frequency difference was selected in accordance with the length of exposure to be made. For very short exposures, the star image was moved along the slit with the right ascension "slow-motion" controls. During the exposure, the star image was kept on the slit by means of the declination "slow-motion" controls, to avoid guiding errors. The universal time was recorded at the beginning and end of each exposure, to enable the subsequent determination of the heliocentric radial velocity (See §5.1.1 and 5.3).

Kodak IIaO plates, prebaked for 48 hours at 50°C to enhance their sensitivity, were used. The baked plates are normally stored in a

refrigerator, and are allowed to warm up to the ambient temperature before being used. This avoids large plate expansion whilst the exposure is in progress, and hence radial velocity errors. The plates were developed in MWP_2 at 19°C for 10 minutes, in complete darkness. They were then washed in distilled water and "fixed" in sodium thiosulphate solution for 30 minutes.

The apparatus for carrying out the spectrophotometric calibrations consists of a 200cm optical bench, with a piece of hardboard, painted white and inclined at 45° to the optical bench, at one end, which scatters light from any light sources mounted on the optical bench into a collimator, which is also inclined at 45° to the hardboard. On entering the collimator, the light is passed through a slit, the jaws of which are curved, and a prism, and then onto a photographic plate. A standard tungsten filament lamp and a cadmium vapour lamp were placed at distances of 100cm and 170cm respectively from the hardboard.

Initially the spectrophotometric calibrations were attempted on the same plate as the stellar spectra. The plate was exposed to light from the tungsten filament lamp for 2 mins, displaced slightly, and then exposed to the cadmium vapour lamp for 20 mins. However in some cases, this procedure resulted in the loss of a few stellar spectra, and so it was decided to place the spectrophotometric calibration on a separate plate, and develop it with the plate containing the stellar spectra. In some cases, no spectrophotometric calibration was obtained and it is hoped that the average calibration will be representative, as all the plates came from the same batch, and the developing conditions were identical. Thus it is now, in principle, possible to measure the equivalent widths of the interstellar CaII(K) line and the Hγ absorption line. As discussed in §5.1.3, this will not be undertaken until the software has been written.

5.3 The Measurement of Radial Velocities from the 1'O.H.P. Plates

The spectra were measured with a Hilger and Watts measuring machine, which is essentially a travelling microscope. The plates were mounted on the microscope in a jig constructed for the purpose, with the emulsion side uppermost. This avoids any errors due to refraction in the glass of the plate, resulting from possible variations in the thickness of the glass, and reduces the chance of the plate becoming damaged by scratches. The microscope was focussed on the spectrum, the focus being correct when there is no parallax between the crosswires and the image. The spectrum was then aligned so that it is strictly parallel to the direction of motion invoked by rotating the drum, with the red end on the left when viewed in the eyepiece. The drum was then set to 60.000mm. and the iron arc line λ4202, was aligned with the vertical crosswire. The plate holder was then clamped in position.

The iron arc and star lines were then measured in order of decreasing wavelength, by aligning each line in turn with the vertical crosswire, and in doing so taking care always to approach the alignment by moving the drum in the same direction so as to avoid backlash errors. The curvature in the spectral lines makes the alignment difficult. To minimise the random errors in measuring, an aligning procedure was adopted. In measuring a star line the vertical crosswire was aligned with the centre of it, whereas in measuring a comparison line the vertical crosswire was aligned on the point on the comparison line nearest to the star spectrum. In doing this some systematic error will be introduced into the radial velocity, but since the same aligning procedure was adopted for all spectra, it should be feasible to evaluate this systematic error from the comparison between published and measured radial velocitiesm for radial velocity standard stars.

Two settings were made on each arc line and four settings on each star line. In each case the mean of the readings obtained from the drum and the attached vernier were recorded. The very strong and very weak arc lines were not measured, as they tended to give inaccurate results. The arc lines selected for measuring are listed in Table (5.3.1) and the wavelengths quoted are those given by Edlén (1955).

All visible star lines were measured, but those taken into account in the final average radial velocity were chosen according to the criterion given by Petrie (1953b). The wavelengths of the star lines used were the I.A.U. recommended wavelengths for OB stars (Pearce 1932), and are listed in Table (5.3.2). The line λ4202 was measured to ensure that there was no large error in positioning it on 60.000 mm.

After completing the measures in this direction, hereafter referred to as the forward direction, the plate was turned around and all the measures repeated in exactly the same way, except that they are now measured in order of increasing wavelength, and this is hereafter referred to as the reverse direction of measurement. This corrects for personal errors in setting on the absorption lines of the stellar spectrum and the emission lines of the arc spectrum, and also for errors arising from the fact that the horizontal crosswire may not be strictly parallel to the edge of the star spectrum. A forward measurement is calculated from the reverse measurement and averaged with the forward measurement obtained previously.

TABLE 5.3.1

A Table of the Wavelengths of the Iron Arc Lines used for Radial Velocity Determinations

(all wavelengths in Å)

4957.4844	4383.5469	4118.5469
4891.2500	4352.7344	4071.7400
4871.6875	4325.7617	4030.7549
4859.7461	4315.0859	4005.2458
4736.7773	4282.4023	3969.2610
4602.9414	4260.4766	3956.6809
4528.1484	4235.9414	3930.2988
4494.5664	4202.0273	3922.9082
4427.3086	4143.8672	
4415.1250	4132.0586	

The values of the corrected forward measurement were used to derive the three Hartmann Constants, by the method given in (§5.1.1) using a programme for the 360/44 written by Dr. Kilkenny. This was done for the measures obtained from several spectra, and the values of the Hartmann Constants obtained were in good agreement. Consequently the means were taken and adopted as the values of the Hartmann Constants which are listed in Table (5.3.3) with Boulon's (1963) values for comparison.

The difference between these values and the values obtained by Boulon (1963) may be due to the few changes that were made to the Spectrograph when the exposure meter was added. As a check, the radial velocity was calculated from the measures obtained from a spectrum of HD 206165, for both sets of Hartmann Constants, as described in §5.1. The star HD 206165 is a B2Ib supergiant and has a "b" classification for its radial velocity given by Wilson (1963). A reasonable result was obtained from both sets of Hartmann Constants, although the calculated values gave a slightly better result. Re-measuring the spectrum, and reducing the new data gave a similar result for each individual line. This gave some confidence in the measuring and reduction technique.

So adopting the calculated Hartmann Constants, a Fortran Programme written by Hill (1971) for the 360/44, was used to reduce all the 454 spectra obtained at 1'O.H.P. The programme follows, essentially, the method of reduction outlined in §5.1, except that a polynomial is fitted to the differences between the actual measured positions and the computed positions, as a function of the measured position. Polynomials of all degrees up to seven are fitted, and that which gives the best fit was selected.

In this way the radial velocity for each line is calculated. Taking the spectral type of the star (§5.6) and Table (5.3.2) into account, the average radial velocity from all the individual line velocities was calculated. This was done using a simple BASIC programme written for the Dunsink Observatory NOVA 2/10 computer. The standard deviation of the mean, together with the residuals of each line velocity, were calculated. If the residual of any line was more than twice the standard deviation, it was excluded and the mean recalculated. This iteration was continued until the residuals were all less than twice the standard deviation.

TABLE 5.3.2

A Table of the Wavelengths of the Star Lines used for Radial Velocity Determinations

Line	Wavelength (Å)	Spectral Type Range	Comments
H	4861.3244	BO-B8	(1)
	4340.4648	BO-B8	
	4101.7344	BO-B9	(2)
	3970.0750	BO-B9	(3)
HeI	4921.9258	BO-B9	as H4861
	4471.4766	BO-B9	(4)
	4387.9258	BO-B8	
	4120.8086	BO-B9	
	4026.1890	BO-B9	(4)
	3964.7268	BO-B5	
SiIV	4116.1016	BO-B3	
	4088.8618	BO-B3	
SiIII	4567.8398	BO-B3	
	4552.6211	BO-B3	
SiII	4130.8750	B3-B9	
	4128.0508	B3-B9	
MgII	4481.2266	B3-B9	(5)
CII	4267.1563	BO-B9	
OII	4069.7939	BO-B3	(6)
NII	3994.9958	BO-B5	
HeII	4685.7383	O	(7)
	4541.6094		
	4199.8594		
CaII(H)	3968.4648	O-B3	(8)
CaII(K)	3933.6638	O-B3	(9)

Notes on Table (5.3.2)

(1) This tends not to be a good line because the spectrograph focus is imperfect and the emulsion sensitivity poor.

(2) If NIII 4097 is present then this line is blended with NIII 4103

(3) If the interstellar CaII(K) line is present, then this line is blended with the interstellar CaII(H) line. If any OII line is present, then Hε is blended with OII 3973.

(4) Feast et. al. (1957) indicate that for radial velocity determinations using the Radcliffe Observatory 74" Telescope 2 prism Cassegrain Spectrograph, the following velocity corrections should be applied for O9 to B3 stars :

(i) Luminosity class III-V - apply a correction of +4kms/sec to the velocity obtained from the HeI 4026 line.

(ii) Luminosity class V - apply a correction of +10km/sec to the velocity obtained from the HeI 4471 line.

Since these corrections are due to blends in the lines, any such luminosity corrections will be functions of the spectrograph and dispersion used. The possibility of applying analogous corrections in this analysis is considered in §5.6.

(5) Blended with AlIII earlier than B3

(6) The only OII line retained by Petrie

(7) The occurrence of the lines 4541Å and 4199Å imply blending of the Balmer lines and HeI 4026. In the hottest stars only these two lines remain unblended.

(8) This interstellar line is measured in the few cases in which it can be resolved from Hε.

(9) This line is measured if it is very sharp, in which case it is probably interstellar.

TABLE 5.3.3

The Calculated Hartmann Constants for the 1'O.H.P. 120cm Telescope Spectrograph C and those obtained by Boulon (1963)

Hartmann Constant	Calculated Value	Boulon's Value
λ_0	2279.934	2269
K	55530.433	56048
n_o	-31.1096	*

* Not quoted by Boulon because it is dependant on the position of the plate on the measuring machine. In using Boulon's values for λ_0 and K, the calculated value of n_o was adopted.

Adopting this mean value in the case of each spectrum, the heliocentric radial velocities were evaluated by the method indicated previously (§5.1.1), using a Fortran programme modified for the 360/44 by Dr. Hill. The accuracy of these radial velocities, and possible systematic corrections, are discussed later (§5.6).

5.4 Spectroscopic Observations undertaken with the Isaac Newton Telescope using the Photographic Cassegrain Spectrograph

In 1972 the "Large Telescope Users Panel" granted eight nights of observing time on the Isaac Newton Telescope (hereafter abbreviated to I.N.T), for the use of the Photographic Cassegrain Spectrograph, to Dr. P.W. Hill, who made the application on my behalf. This comprised four nights in November 1972, from 20th to 23rd inclusive, and four nights in December 1972, from 18th to 21st inclusive. Six of these nights were good, with long clear periods, one night was completely lost and on the remaining night, the transparency was so poor that only bright spectral type standards could be observed.

Apart from some of the brighter stars which were not observed at 1'O.H.P. for reasons of time, priority was given to the fainter stars in the observing programme in order to take full advantage of the telescope aperture, although some overlap with stars already observed at 1'O.H.P. was allowed for. The practice adopted at 1'O.H.P. of restricting the observing of the brighter stars to the occasions on which the transparency was poor, was again adhered to.

As many as possible of the stars listed in Table (5.2.1) were observed each night for the reasons already given (§5.2). In addition, realising the mistake made with the 1'O.H.P. observing programme, two late-type radial velocity standards, listed below in Table (5.4.1) were observed. These were selected from the list given by Pearce (1955). A number of spectral type standards, again taken from the list of Johnson and Morgan (1953) were observed and are listed in Table (5.7.2). These were used in the spectral classification of spectra of the programme stars as discussed later (§5.7).

The Cassegrain Spectrograph is attached to the telescope on the underside of the primary mirror. There is a facility for rotating the spectrograph about the optical axis of the telescope, and this was used to orientate the spectrograph so that any movement of the telescope in right ascension, resulted in the image of the star drifting along the slit. The reasons for doing this were discussed, in connection with the 1'O.H.P. spectrograph, in §5.2.

The Cassegrain Photographic Spectrograph for the I.N.T. has been described by Harding and Candy (1971). The spectrograph possesses three cameras, with which spectra of different dispersions can be obtained. For radial velocity measurements, Camera 2 with diffraction grating "A", giving a dispersion of 60Å/mm, was suitable. The angle of the grating was set to be 30.5°, which gave a wavelength range of 3,800Å to 4800Å for the stellar and comparison spectra. A slit width of 200μ was selected, this becoming an effective width of 20μ when projected onto the photographic plate.

The star image was swept with an oscillatory motion along the slit by means of an oscillating glass block. This glass block can be replaced by one of a different thickness, thus altering the size of the sweep, and hence the necessary exposure time (see §5.2). The size of star image sweep was selected according to the magnitude of the star, using a larger sweep for a brighter star. In the cases of very bright standard stars, an appropriate neutral density filter was used, so that a reasonable exposure time would result.

The arc aperture selected is that which is appropriate to the size of the star image sweep chosen. The switch which operates the arc, for the purpose of placing a comparison spectrum on the plate, is interlocked to the slit shutter, the arc aperture position and to the star "field/guide" switch. When these have been correctly set, the arc is switched on and timed automatically. Twelve seconds was chosen as the arc exposure time. Moving the "field/guide" switch to "guide", selecting the appropriate star aperture and re-opening the slit shutter enabled the star exposure to begin. This was timed automatically by a photoelectric exposure meter, which was set according to the camera, grating and length of star sweep used. The principle of operation of this exposure meter is similar to that used at 1'O.H.P, although it is much more sensitive, proving to be quite satisfactory for 11th magnitude stars.

In the case of very faint stars, the exposures were lengthened by 10% of that indicated by the exposure meter. This was to correct for reciprocity failure in the emulsion. To correct for any small movement, expansion or contraction of the plate during the course of the stellar exposure, the arc exposure was repeated at the end of the stellar exposure. The plates used in this observing run were Kodak IIaO,

baked for 48 hours at 50°C.

The spectrophotometric calibrations were placed on plates specially cut for the purpose. The spectrograph used for this is a diffraction grating spectrograph, but otherwise it is in principle similar to that used at l'O.H.P. and discussed previously (§5.2). The grating was set at an angle of 5°.2 in order that the wavelength range obtained is the same as that obtained from the stellar spectrograph . A neutral density filter of 0.6 was used. The plate was exposed to a mercury arc for 2 mins, then to a quartz-halogen lamp for 12 mins, and finally to the mercury arc for a further 2 mins. The mercury arc acts as a wavelength calibration of the continuous spectrum produced by the quartz-halogen lamp.

To ensure identical processing conditions, the spectrophotometric calibration plate was then developed in microphen at 20°C for 6 mins, together with the stellar spectrograms for which it is to serve as a calibration. The plates were then rinsed in distilled water and fixed for 25 minutes. They were then rinsed in cold flowing tap water for a further 30 minutes, wetted with a dilute solution of acetic acid, which acts as a wetting agent, rinsed in distilled water and left to dry.

5.5 The Measurement of Radial Velocities from the I.N.T. Plates

The measuring procedure used for the I.N.T. plates was essentially identical with that used for the 1'O.H.P. plates. Since the I.N.T. spectrograph is a grating spectrograph, the star and comparison lines are straight. Thus it is a simple matter to align the horizontal crosswire parallel to the edge of the star spectrum. Then the star and comparison lines can be easily measured, in order of increasing or decreasing wavelength, as appropriate. As in the case of the 1'O.H.P. plates, all visible star lines were measured and the strong or weak lines were avoided.

In the case of the I.N.T. plates, an argon/copper arc spectrum was chosen in preference to an iron arc spectrum, because the distribution of lines as a function of wavelength was more uniform. The wavelengths used are those supplied by the Royal Greenwich Observatory (private communication), and are listed in Table (5.5.1) The star line wavelengths used, as for the 1'O.H.P. plates, are those listed in Table (5.3.2). The line 4182Å was set initially on the crosswires at the position of 60.000 mm.

For a grating spectrograph, the Hartmann Formula (equation 5.1.1.5) is a linear relation. Consequently the Hartmann Constants can be determined by performing a linear least squares fit. This was done for the measures obtained from a number of I.N.T. spectrograms, using a BASIC programme written by Dr. Hill for the Nova 820 computer at the University Observatory, St. Andrews. In all cases, the results obtained were in good agreement, and so the averages were taken, adopted as the Hartmann Constants, and are

$$\lambda_0 = 7908.346 \quad \text{and} \quad n_o = -62.11298$$

The procedure described in §5.2 that was used to perform a manual reduction of the plate measures was used also for the I.N.T. plates. A slight modification was then made to the computer programme (Hill, 1971), that would enable it to reduce measures from plates taken with a grating spectrograph. Essentially, equations (5.1.1.1) and (5.1.1.4) were replaced by equations (5.1.1.5) and (5.1.1.7) respectively. Good agreement between the manual and computer

TABLE 5.5.1

A Table of the Wavelengths of the Argon/Copper Arc Spectral Lines used in the Radial Velocity Determinations (all wavelengths in Å)

4806.0664	4385.0781	4097.1484
4732.0781	4352.2266	4044.4199
4649.0586	4331.2500	4033.8298
4598.7695	4309.2500	4013.8699
4530.5664	4251.1875	3974.4800
4502.9492	4181.8789	3968.3599
4474.7695	4164.1797	3946.0999
4448.8789	4158.5898	3932.5898
4433.8281	4131.7266	3925.7100

reductions was obtained, and so the remaining measures were reduced using the computer programme. The heliocentric radial velocity was then calculated in the same way as that used for the 1'O.H.P. plates. The results obtained are discussed in the next section.

5.6 A Discussion of the Radial Velocities Obtained and their Comparison with Published Radial Velocities where available

A mean radial velocity was calculated for each star from the velocities determined from the individual 1'O.H.P. spectra of that star. Each spectrogram velocity was weighted by its standard deviation, the mean and the standard deviation in the mean being evaluated using the method of Barford (1967, page 62), using a BASIC programme written for the Dunsink Observatory Nova 1220 computer. This was also done, independently, for the CaII(K) line velocities. In a case where there is only one spectrogram for a star, then the standard deviation of the CaII(K) velocity (σ_k) is taken as the mean σ_k for each spectrogram. This is deduced on the assumption that if σ' is the σ_k obtained from n plates, then the mean σ_k per plate is $\sigma'\sqrt{n}$. The standard error in the stellar and interstellar radial velocities was calculated from their standard deviations σ by the relation

$$s = \sigma(n-1)^{-\frac{1}{2}} \quad \text{- - - - - - - - - - - - - - (5.6.1)}$$

It was decided to adopt the system of velocities developed by Wilson (1963), and to compare the measured velocities with the velocity given in Wilson's catalogue wherever possible. Consequently for the stars chosen as radial velocity standards, the difference between the measured and the observed velocity was taken. A mean difference was then evaluated, weighting the differences according to the standard deviation of each difference, using the method of Barford (1967, page 62). The resulting relation is

$$V_{Wilson} = V_{1'O.H.P.} - (16.6 \pm 2.3) \text{ Km/sec} \quad \text{---------- (5.6.2)}$$

A systematic correction of 0.7Km/sec is expected due to curvature of the spectral lines (Boulon, 1963). Thus the remaining correction of -17.3Km/sec is probably due to systematic measuring errors already discussed (§5.3).

This correction was applied to all the stellar and interstellar velocities obtained from the 1'O.H.P. plates. The standard errors in these velocities were all incremented, as a result of this, by ± 2.3 km/sec. This is probably rather pessimistic, but as the calculation of the standard error by equation (5.6.1) is probably optimistic in view of the small number of plates per star, incrementing the errors in this way is probably justified.

Similarly, the mean stellar and interstellar velocities were evaluated for each star, for which spectra were obtained with the I.N.T. In the case of some I.N.T. plates, CaII(H) is also sufficiently prominent to be measured, and in these cases the mean CaII velocity can be evaluated for each plate from the velocity of the H and K lines. By comparison of the measured and published radial velocities for the late type radial velocity standards (Table 5.4.1), it was found that,

$$V_{Wilson} = V_{INT} + (1.9 \pm 0.3) \quad Km/s \text{ - - - - - - - - - - } (5.6.3),$$

This correction is probably a characteristic of the spectrograph, and was applied to all I.N.T. stellar and interstellar velocities.

Both sets of radial velocities were now investigated for flexure effects, but no systematic variation with hour angle or declination was found. In the case of the 1'O.H.P. spectra, where a flexure effect might be expected on account of the light telescope structure, it seems that the large random errors completely swamp any small systematic error. In the case of the I.N.T. radial velocities, we would not expect any large systematic error on account of the rigid structure of the telescope and spectrograph.

There is also a possibility of systematic errors arising in cases of the velocities obtained from certain stellar lines, due to blending, and this correction would be dependant on the spectral type of the star and on the spectrograph used. This effect was first discussed by Feast et al.(1957). It is clear from the above

discussion and from the size of the corrections, which were derived by Feast et al. for the two-prism spectrograph used on the 74" telescope at Radcliffe, that there is no hope of determining these for the 1'O.H.P. spectra. In the case of the I.N.T. spectra, this effect should be detectable, and consequently the residual in the radial velocity of each star line was plotted as a function of wavelength, for two I.N.T. spectra of HD 177003, a B3 V star and are illustrated in Fig (5.6.1) and Fig (5.6.2). From these it can be seen that no line exhibits a significantly larger residual than the others, and so it appears that there is no justification for applying a luminosity correction of the type discussed by Feast et al. (1957).

The stellar and CaII radial velocities obtained from 1'O.H.P. and I.N.T. plates, as well as those published, are listed, for all the programme stars, in Table (5.6.1). The standard errors in these quantities are also given. The CaII velocity is taken as the velocity of the interstellar gas, unless otherwise indicated.

It will be noticed, except in the case of variable stars which are discussed later in this section, that the errors in the I.N.T. radial velocities compare favourably with those quoted for published radial velocities, for comparable spectra and a comparable number of them. This is not the case for the 1'O.H.P. spectra. There are a number of possible explanations for this.

The focus of a spectrogram is often imperfect, and seems to be better in some than in others. This has been confirmed by Lloyd-Evans (1973) and Hilditch (1974), both noticing this with spectra they had obtained on previous expeditions. That is, there does not seem to be adequate compensation for temperature changes in the spectrograph focus. Another difficulty arose from incorrect exposure times for

Table 5.6.1

Stellar and Interstellar K - Line Radial Velocities of Programme Stars Published and Measured from L'OHP and INT Plates

	Star	RV	δ(RV)	N	V_c	δ(V_c)	N	S	R
HD	169798	-17.2	±1.2	4				1	
HD	170028	-24.8	±1.2	5				1	
HD	170051	-24.4	±1.2	5				1	
HD	170111	-18.0	±2.5	12	-13.1	±1.2	12	1	1
		-11.9	±9.5	4	-27.1	±21.6	2	L'OHP	
HD	170263	45.2	±3.0	1				L'OHP	
HD	170650	16.1	±6.5	4				L'OHP	
		-17.0	±5.0	7	-17.6	±1.2	8	1	2
HD	172421	2.4	±17.5	1				L'OHP	
HD	173087	-19.0	±2.5	8				1	
HD	174179	-15.0	±1.2	5	-15.0	±1.2	5	1	
HD	174261	-15.2	±1.2	5				1	
HD	174298	-15.1	±1.2	4	-15.0	±1.2	4	1	
HD	174585	-16.5	±1.2	8	-16.0	±2.5	8	1	
HD	174567	-2.7	±1.7	5				5	
		-27.3	±9.0	4				L'OHP	
HD	174959	-20.7	±1.2	5	-16.0	±1.2	1	1	3
HD	175081	-26.0	±5.0	6				1	1
HD	175426	-25.8	±0.5	74	-17.0	±2.5	1	1	
		-51.3	±8.3	4				L'OHP	
HD	175803	-30.0	±2.5	8	-4.0	±2.5	8	1	
		-56.6	±6.7	5				L'OHP	
HD	176254	-6.9	±1.2	6	-14.2	±1.2	6	1	
HD	176502	-19.0	±1.2	6				1	
HD	176582	-14.0	±2.5	10				1	
		18.1	±4.6	5	-18.2	±49.4	1	L'OHP	
HD	176803	-17.0	±2.5	9				1	
HD	176818	-9.0	±2.5	25	-18.0	±2.5	1	1	1
		-80.1	±19.5	2	-106.2	±49.4	1	L'OHP	
HD	176819	-10.3	±1.2	19	-17.0	±2.5	1	1	4

Star	RV	δ(RV)	N	V_c	δ(V_c)	N	S	R
HD 176871	-14.0	± 2.5	14	-13.0	±2.5	1	1	3
	34.1	± 3.6	5				L'OHP	
HD 176914	-5.5	± 1.2	5				1	
HD 176940	-12.9	±.23.6	1				L'OHP	
HD 177003	-19.0	± 2.5	13				1	
	-22.7	± 0.1	14				6	
	-18.3	± 2.1	18				L'OHP	
HD 177006	-7.0	± 3.5	5	-17.0	±6.9	4	2	
HD 177109	-22.9	± 1.2	6	-16.9	±1.2	7	1	
HD 177593	-23.7	± 1.2	5				1	
HD 178329	-21.2	± 0.5	45	-14.0	±2.5	1	1	4
	7.9	± 8.2	5	13.8	±49.4	1	L'OHP	
HD 178475	-18.0	± 2.5	14	-14.0	±2.5	1	1	3
HD 178540	-19.0	± 2.5	9				1	
HD 178849	-8.0	± 2.5	7				1	1
HD 178912	-15.0	± 2.3	10	-11.0	±3.7	6	2,3	
HD 179506	21.6	± 7.6	2				L'OHP	
	-53.3	± 7.6	1				INT	
HD 180124	-77.0	± 17.5	1				L'OHP	
	-23.1	± 8.6	1				INT	
HD 180163	-17.8	± 2.1	18	-3.7	±9.9	8	L'OHP	
	-8.2	± 0.5	63	-12.6	±1.2	60	1	3
	-13.0	± 2.7	1	-22.3	±12.7	1	INT	
HD 180844	-30.2	± 1.2	8				1	
HD 181164	-7.6	± 1.2	5	-13.8	±1.2	4	1	
HD 181409	10.0	± 2.5	7	-19.0	±2.5	5	1	
	73.3	± 5.4	4				L'OHP	
HD 181492	-18.6	± 1.2	4				1	
HD 182568	-21.0	± 2.5	11	-15.0	±2.5	1	1	
HD 182615	23.5	± 10.4	2				L'OHP	
HD 183339	-22.0	± 2.5	6				1	
HD 183535	14.0	± 4.1	4	-18.0	±1.3	3	2,3	
HD 183649	-45.4	± 9.4	1	-84.7	±49.4	1	L'OHP	
HD 184171	-21.8	± 0.5	29	-20.0	±2.5	4	1	
	-29.3	± 2.8	16	-41.5	±8.9	2	2	

Star	RV	δ(RV)	N	V_c	δ(V_c)	N	S	R
HD 185780	-5.0	±5.0	10	-17.0	±2.5	5	1	5
	-56.4	±5.8	4	-65.7	±6.9	3	L'OHP	
HD 186485	20.7	±22.5	1				L'OHP	
HD 186618	10.0	±2.1	4	-5.0	±0.9	4	2,3	
	30.4	±12.5	3	-10.6	±31.1	3	L'OHP	
HD 186814	-27.6	±8.0	1				L'OHP	
HD 186994	14.0	±11.4	6	-11.0	±1.9	6	2,3	
HD 187035	65.4	±2.6	5	-2.8	±21.8	3	L'OHP	
HD 187879	-3.9	±1.2	30	-16.2	±1.2	88	1	
HD 188209	-6.2	±1.2	10	-10.2	±1.2	18	1	
HD 188252	-18.3	±1.2	4	-10.0	±2.5	5	1	
HD 188439	-65.0	±2.5	9	-12.8	±1.2	6	1	
HD 188461	-12.9	±1.2	4	-15.0	±2.5	4	1	
HD 188665	-25.0	±2.5	11				1	
	-51.1	±7.6	4				L'OHP	
HD 188891	-38.9	±12.3	3	-48.0	±22.1	3	L'OHP	
	-24.0	±5.0	7				1	1
HD 189160	49.0	±2.4	2				L'OHP	
HD 189775	-16.2	±1.2	12				1	
HD 189818	-3.2	±1.2	4	-6.0	±2.5	3	1	
HD 189957	43.0	±1.9	6	-14.0	±1.4	6	L'OHP	
HD 190025	-14.0	±5.0	6	-7.9	±2.0	5	1,7	6
HD 190254	35.6	±10.6	3	52.2	±10.2	2	L'OHP	
HD 190427	-1.4	±1.0					4	
HD 190901	-39.3	±6.1	4				L'OHP	
HD 191124	-34.3	±12.2	3				L'OHP	
HD 191781	-13.0	±3.5	3	-9.0	±10.0	1	2,3	
	9.7	±6.0	4	24.2	±21.9	3	L'OHP	
HD 192035	1.0	±2.9	5	-17.0	±1.1	5	2,3	
HD 192575	-37.5	±1.2	7	-23.6	±1.2	4	1	
HD 196421	-17.0	±2.8	4	-19.0	±2.3	4	2,3	
HD 197770	-15.0	±2.5	12	-14.4	±1.2	8	1	
	-29.1	±7.4	4	-22.6	±23.7	4	L'OHP	

Star	RV	δ(RV)	N	V_c	δ(V_c)	N	S	R
HD 197911	6.5	±9.7	3	12.9	±12.9	2	L'OHP	
HD 198739	0.1	±8.6	3				L'OHP	
	0.1	±4.4	1	-12.9	±12.7	1	INT	
HD 198781	-27.3	±1.2	4	-20.9	±1.2	3	1	
HD 199308	-23.0	±0.5	4	-18.0	±4.3	4	2,3	
HD 199661	-19.0	±2.5	5				1	
	-18.7	±6.1	5				L'OHP	
HD 199739	-4.4	±12.4	3				L'OHP	
	-4.7	±6.8	1	-0.7	±12.7	1	INT	
HD 202214	-16.2	±1.2	14	-19.0	±1.2	14	1	
HD 204150	-37.0	±5.0	1	-8.0	±5.0	1	1	
	-39.0	±9.2	4	-17.3	±39.2	3	L'OHP	
HD 204770	3.0	±2.5	19				1	
HD 205139	-14.5	±1.2	13	-16.2	±1.2	12	1	
	-7.2	±6.3	4	-29.5	±15.4	3	L'OHP	
HD 206165	-13.2	±1.2	13	-22.2	±1.2	8	1	
	-19.2	±4.2	5	-16.6	±2.0	3	INT	
	7.9	±2.3	19	14.7	±11.2	19	L'OHP	
HD 206327	-30.0	±2.5	3	-18.0	±5.0	1	1	
	-15.2	±6.8	5	0.4	±49.4	1	L'OHP	
HD 207198	-42.9	±19.1	1				L'OHP	
	-18.4	±1.2	7	-19.0	±2.5	5	1	
HD 207308	-23.0	±2.5	2	-21.0	±2.5	2	1	
HD 207951	8.0	±15.0	1	-12.0	±5.0	1	1	
	-17.8	±12.4	2	-5.5	±22.7	2	L'OHP	
HD 208106	-24.0	±15.0	1	-10.0	±5.0	1	1	
	-71.9	±14.3	4	-4.2	±14.3	4	L'OHP	7
	3.0	±10.8	5	-13.0	±1.8	4	2,3	
HD 208185	-16.0	±15.0	1				1	
	-24.0	±6.0	5	-10.0	±2.4	5	2,3	
HD 208218	-21.8	±1.2	6	-16.9	±1.2	6	1	
HD 208440	-14.0	±5.0	4	-9.0	±2.5	2	1	
HD 208904	-5.0	±3.0	5	-13.0	±0.6	5	2,3	
	-7.9	±15.6	3	-44.9	±10.7	2	L'OHP	

Star	RV	δ(RV)	N	V_c	δ(V_c)	N	S	R
HD 208947	2.4	±1.2	32	-9.4	±1.2	23	1	
HD 209789	-9.7	±18.1	4	-12.1	±13.6	3	L'OHP	7
HD 210386	-13.0	±2.3	3	-13.0	±1.8	3	2,3	
	-16.0	±4.6	4	-10.9	±22.2	4	L'OHP	
HD 213087	-14.7	±1.2	10	-10.5	±1.2	3	1,7	
HD 213405	10.0	±8.7	4	-17.0	±2.7	4	2,3	1
HD 213481	11.7	±11.2	4	1.2	±9.5	2	L'OHP	
HD 213571	-17.9	±1.2	6	-19.0	±2.5	5	1	
HD 216992	-7.7	±11.8	3	-13.9	±49.4	1	L'OHP	
	-13.2	±2.1	1	-29.7	±12.7	1	INT	
HD 217224	-4.9	±1.8	19				2,8	4
	-52.7	±12.8	3	-6.5	±15.7	2	L'OHP	
HD 222568	-14.0	±2.1	4	-13.0	±1.5	4	2,3	
HD 223959	16.2	±10.1	4	-55.0	±52.5	2	L'OHP	
HD 224395	-27.0	±2.1	5	-24.0	±5.0	5	2,3	
HD 2083	-5.0	±2.5	5	-8.7	±1.2	4	1	
	-56.6	±6.2	5	44.2	±33.7	4	L'OHP	
HD 3366	-15.1	±1.2	4	-23.1	±7.0	2	1,7	
HD 6675	-5.0	±0.9	4	-10.0	±1.4	3	2,3	
	-35.1	±7.2	5	-11.9	±7.2	4	L'OHP	
HD 7852	-10.1	±5.8	6	-16.6	±37.5	2	L'OHP	
HD 16393	-49.4	±13.2	2				L'OHP	
HD 16440	-16.5	±19.4	3	-86.7	±49.4	1	L'OHP	
HD 17179	26.9	±8.8	5	-79.5	±49.4	1	L'OHP	
HD 17929	-58.9	±1.3	3	25.4	±49.4	1	L'OHP	3
HD 21267	-20.8	±15.2	2				L'OHP	
HD 21806	-22.0	±4.5	3	-11.0	±0.5	3	2,3	
HD 21930	26.3	±6.6	4				L'OHP	
HD 23254	-13.0	±2.6	4	8.0	±9.1	2	2,3	8
HD 25090	-3.0	±2.5	4	-1.1	±1.2	1	1	
HD 25443	-1.6	±1.2	4	-8.9	±3.4	1	1	
HD 25638	-9.7	±0.4	15	-7.4	±1.3	10	2,9	1
HD 25639	-17.1	±1.4	44	-8.2	±0.8	8	2,9	1

Star		RV	δ(RV)	N	V_c	δ(V_c)	N	S	R
HD	26684	5.7	±5.0	3				7	9
		32.9	±7.9	4	39.6	±21.0	4	L'OHP	3
HD	34233	-3.0	±2.5	5				1	
HD	35250	6.8	±12.0	4				L'OHP	
		-17.5	±7.1	2	30.8	±30.8	1	INT	
HD	38258	-2.9	±1.2	5				1	
HD	38410	28.3	±2.1	6	14.4	±49.4	1	L'OHP	8
HD	40160	8.5	±2.6	8				2	
HD	40784	-3.5	±12.7	4	126.9	±49.4	1	L'OHP	8
HD	41161	5.0	±5.0	7	13.2	±1.2	7	1,7	10
HD	41541	4.6	±1.2	10				1,7	8
HD	41689	33.6	±2.7	6	8.0	±10.4	3	1,2,3	
HD	42782	3.0	±3.5	6				2,3	
HD	42783	62.2	±21.0	2				L'OHP	
		-6.0	±6.7	1	11.2	±12.7	1	INT	3
HD	46552	154.5	±11.6	3	-112.1	±49.4	1	L'OHP	3
		-42.3	±5.5	1	15.0	±12.7	1	INT	
HD	48029	17.3	±12.4	3	50.8	±49.4	1	L'OHP	
HD	48532	3.0	±3.5	4	0.0	±7.7	3	2,3	
HD	48549	-2.6	±15.3	3				L'OHP	
HD	50767	-51.4	var	5				4	
HD	53879	-17.2	±31.2	1				L'OHP	
HD	54532	18.5	±3.2	1	12.2	±12.2	1	INT	3
HD	57291	6.8	±1.2	7				1	
HD	58784	36.0	±9.7	4	21.0	±2.7	2	3	11
HD	58973	-3.1	±1.2	7				1	
HD	59882	44.7	±1.9	5				4	
		36.4	±17.7	2				L'OHP	
HD	66594	13.0	±5.0	4	9.0	±4.0	4	3	
HD	66665	18.0	±2.0	7	-8.1	±1.2	2	3	
HD	225573	-3.7	±13.1	1				L'OHP	
		-25.0	±6.2	3	-31.0	±0.5	3	3	
HD	225822	31.2	±7.0	4	23.4	±7.4	4	L'OHP	

Star	RV	δ(RV)	N	V_c	δ(V_c)	N	S	R
BD 48 3504	-63.5	±11.5	3	19.0	±47.6	3	L'OHP	2
	-25.6	±4.8	1	-6.0	±3.2	1	INT	
BD 53 2481	27.5	±5.6	5	-9.1	±10.7	4	L'OHP	3
BD 55 2443	19.5	±4.1	2	26.0	±15.2	2	L'OHP	8
BD 55 2553a	24.0	±11.9	1	7.0	±49.4	1	L'OHP	
BD 58 2236	25.5	±23.3	1	8.9	±49.4	1	L'OHP	
	-17.0	±2.1	5	-20.0	±1.7	4	3	12
BD 58 2268	-45.5	±13.8	3	-1.3	±3.5	3	L'OHP	
	8.0	±1.5	4	-11.0	±2.6	3	3	13
BD 59 2350	-46.6	±9.6	2	-15.8	±9.6	2	L'OHP	
	-14.4	±7.0	1	-15.7	±12.7	1	INT	
BD 59 2384	-56.6	±5.4	5	-15.3	±7.9	5	L'OHP	
BD 61 2158	8.4	±6.0	3	-7.8	±8.3	3	L'OHP	
BD 61 2163	-12.2	±6.5	1				INT	
BD 65 1774	-27.6	±5.5	3	-24.8	±18.3	3	L'OHP	
BD 67 1550	14.6	±5.3	1	-2.0	±9.7	1	INT	
BD 68 1386	-43.5	±3.9	1	-19.8	±12.7	1	INT	
BD 64 1677	-24.9	±4.3	1	-12.2	±12.7	1	INT	
BD 67 1489	-106.4	±6.8	1	-25.9	±11.4	1	INT	
LS3 57 04	-75.1	±5.1	2	-36.0	±3.8	2	INT	
LS5 23 73	38.8	±6.0	1	5.5	±2.0	1	INT	3
LS5 54 14	-19.8	±12.7	1	-38.6	±12.7	1	INT	
BD 59 0804	-47.5	±4.2	2	-14.3	±3.6	2	INT	
BD 68 1373	-36.2	±3.6	2	-31.4	±11.3	2	INT	
BD 67 1531	-20.3	±5.2	3	-18.0	±2.9	3	INT	2
LS3 59 06	-31.1	±5.1	2	-39.3	±4.7	2	INT	
BD 48 1263	5.4	±2.5	4	-5.5	±3.7	4	INT	
BD 22 1407	31.5	±7.3	2	6.1	±8.5	2	INT	2
BD 37 1415	17.5	±2.7	5	-0.2	±7.0	5	INT	2
BD 50 1129	-12.8	±8.3	2	-13.7	±5.7	2	INT	
BD 24 1306	38.2	±9.5	1	3.7	±12.7	1	INT	
BD 43 1355	-44.1	±5.3	1	-1.9	±12.7	1	INT	
BD 23 1436	15.6	±12.1	1	17.8	±12.7	1	INT	

Star	RV	δ(RV)	N	V_c	δ(V_c)	N	S	R
HD 235197	30.0	±6.0	3	-6.0	±2.1	2	3	14
HD 235253	-14.0	±9.3	3	-16.0	±3.7	3	3	2
HD 235259	-26.0	±3.8	4	-25.0	±2.5	5	3	14
HD 239436	-10.0	±7.5	4	-17.0	±2.0	4	3	2
HD 235271	0.0	±0.5	2	-8.0	±1.3	2	3	
HD 235298	-7.0	±3.3	4	-15.0	±2.6	4	3	2
HD 235363	-26.0	±13.3	4				3	15
HD 239595	-11.0	±5.3	3	-15.0	±3.7	3	3	
HD 239600	-18.0	±1.1	4	-24.0	±3.8	3	3	
HD 239605	-20.0	±2.4	2				3	
HD 239618	-8.0	±3.7	4	-27.0	±3.1	3	3	16
HD 260611	7.0	±2.3	4	14.0	±3.2	4	3	

Notes:

RV, Vc and N denote the stellar radial velocity, the interstellar CaII radial velocity and the number of observations respectively. All radial velocities are given in km/sec.

S denotes the source of the radial velocities, and if published it is referenced by:

1) Wilson (1963)
2) Abt & Biggs (1972)
3) Petrie & Pearce (1962)
4) Abt, Levy & Gandet (1972)
5) Hube (1972)
6) Kodaira (1971)
7) Plaskett & Pearce (1931)
8) Fitzgerald (1964)
9) Plaskett (1924)

R denotes a remark corresponding to:

1) Spectroscopic Binary (SB)

2) The radial velocity of this star may be variable.

3) The CaII line(s) in this spectrum may be stellar.

4) This star is a spectroscopic binary, the orbital elements can be found in the reference given, or in a reference cited therein. (ORB)

5) A spectroscopic binary with a radial velocity range of 87 km/sec.

6) A spectroscopic binary with a radial velocity range of 45 km/sec.

7) The radial velocity of this star is probably variable

8) The radial velocity of this star is variable

9) A spectroscopic binary with a radial velocity range of 36 km/sec.

10) A spectroscopic binary with a radial velocity range of more than 200 km/sec.

11) As for 8) above

12) Also HD 239605b

13) Also HD 239676, a spectroscopic biary

14) The spectrum contains diffuse lines

15) The radial velocity of this star is variable, owing to its binary nature.

16) The radial velocity is variable, emission lines are observed in the stellar spectrum. Also BD 59 2344

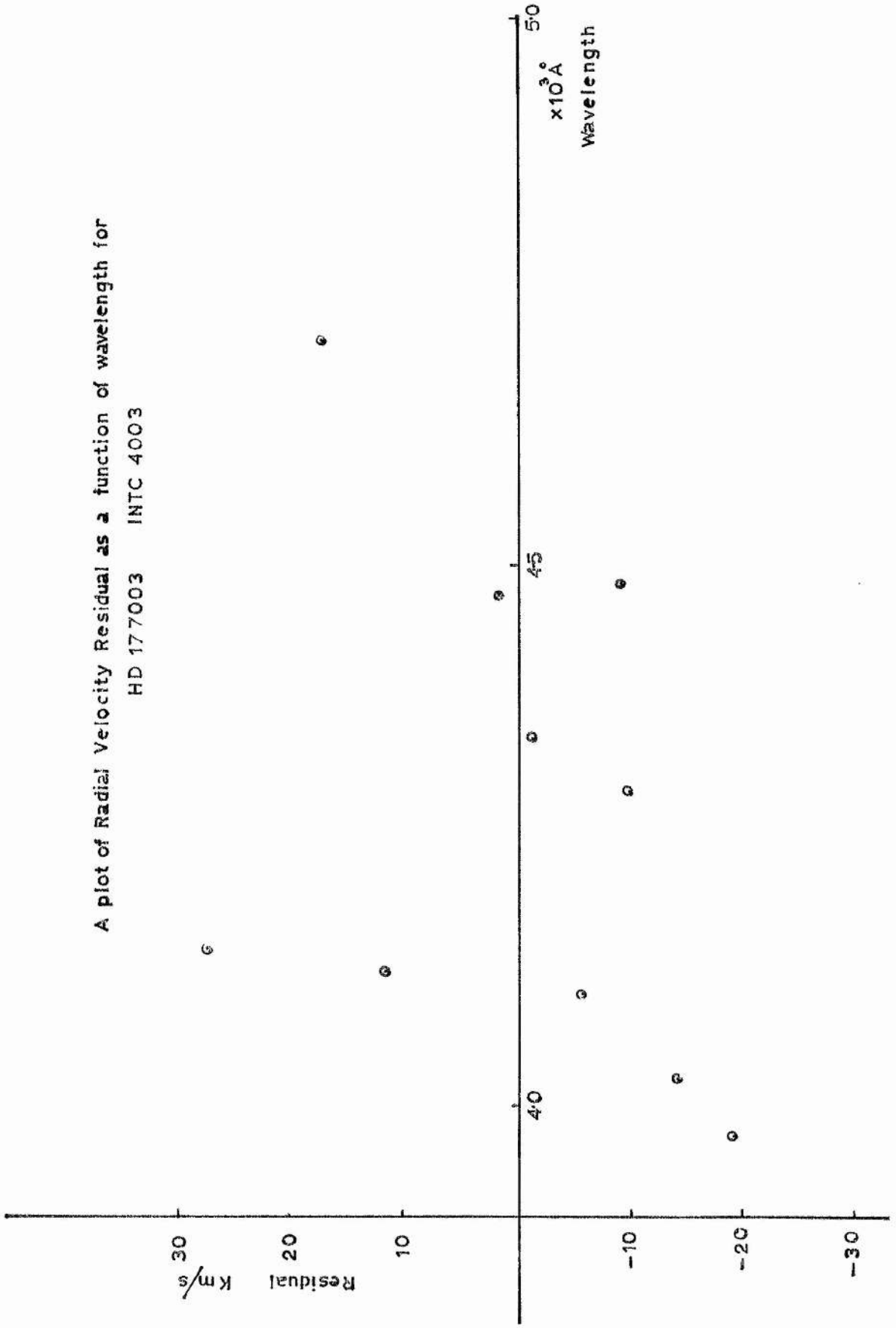
A plot of Radial Velocity Residual as a function of wavelength for
HD 177003 INTC 4003
Residual km/s
30
20
10
-10
-20
-30
40
45
50
x10³Å
Wavelength

FIG. 5.6.1.

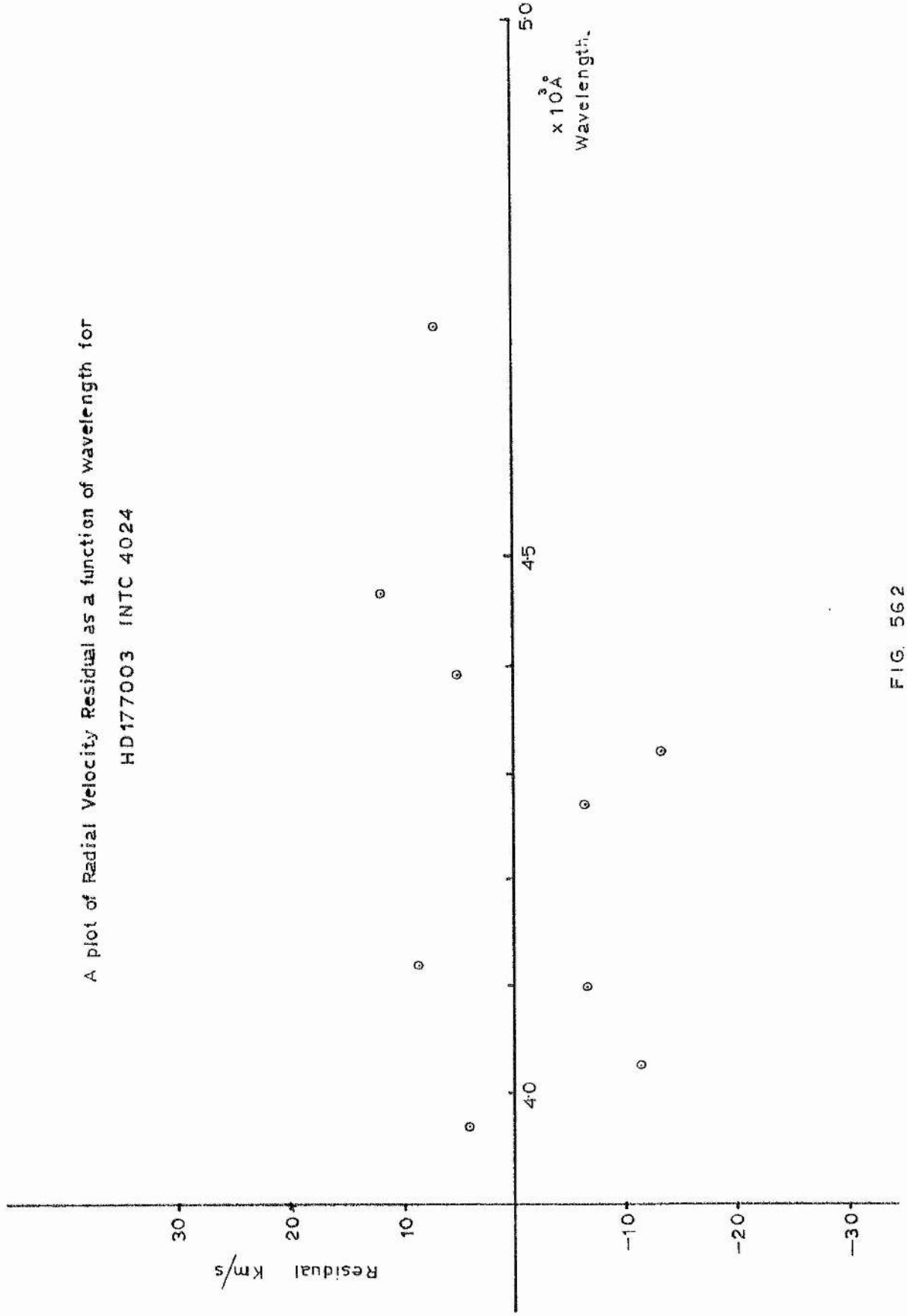
A plot of Radial Velocity Residual as a function of wavelength for
HD177003 INTC 4024
Residual km/s
30
20
10
-10
-20
-30
4·0
4·5
5·0
x 10³ Å
Wavelength

FIG. 562

some of the spectra, due to partially cloudy conditions, coupled with the inadequate operation of the exposure meter discussed earlier (§5.2).

Difficulties in observing bright stars at 1'O.H.P. in 1972 without the use of neutral density filters, were encountered. This meant very short exposure times, and consequently large guiding errors, resulted for the bright stars used as radial velocity standards. For June 1973, neutral density filters were available, by the kind courtesy of Professor D.W.N. Stibbs, who had constructed these filters for a previous expedition.

The usual sources of error in radial velocity determinations are discussed by Abt and Smith (1969). Another source of apparent error is the actual variability of the stellar radial velocity itself. This is discussed by Petrie (1960), who concludes that 51°/₀ of all B stars have a variable radial velocity. The possible variability of the radial velocities was tested for in the same way that the variability of the β index was tested for (§4.2.4). In the case of the 1'O.H.P. radial velocities, no star was found to have a variable radial velocity, although many of these stars were found to have variable radial velocities when the available published data were searched. It is probable that the large error in the velocity obtained from a single plate, makes the 1'O.H.P. radial velocities less sensitive to radial velocity variability than those obtained on other spectrographs. Three of the stars observed on the I.N.T. were found to be possible variables. If a 1'O.H.P. stellar radial velocity did not agree with either a published or an I.N.T. radial velocity, within the limits of experimental error, then it was concluded that this star was a possible velocity variable. These stars are listed in Table (5.6.2). In cases where the same disagreement arises for the CaII radial velocities, the CaII line was assumed to be stellar in origin, and originating from at least one of the components of a binary or multiple system. It is possible that there is an interstellar component of the CaII line blended with the stellar component.

TABLE 5.6.2

Stars with Radial Velocities which are Possibly Variable found by the Comparison of two Independent Radial Velocity Sources

HD 174567	HD 186618	HD 2083
HD 175426	HD 188665	HD 6675
HD 175803	HD 191781	HD 42783
HD 176582	HD 197770	HD 46552
HD 176871	HD 206327	HD 225573
HD 179506	HD 207198	BD 58°2236
HD 180124	HD 207951	BD 59°2350
HD 181409	HD 208106	
HD 185780	HD 217224	

Wherever possible, the published radial velocity was taken from the Catalogue of Wilson (1963), except where a classification "e" was given. If there was no other source of radial velocity, then this radial velocity was adopted and an error of ± 15Km/sec was decided upon as reasonable error in a single plate measurement of a radial velocity of a B star. If there was no radial velocity in Wilson's Catalogue, the weighted mean radial velocity calculated from data given by Abt and Biggs (1972) was used, taking the number of plates on which each given radial velocity is based as a weighting factor. The radial velocities published by different observatories are compared by Petrie (1963) who has shown that Lick Observatory radial velocities exhibit a large systematic error for faint B stars. Consequently these were excluded when calculating the means. If radial velocities were not in the Catalogue by Abt and Biggs, other sources were used as indicated in Table (5.6.1).

Some of the CaII velocities have been determined by the Mount Wilson Coude Spectrograpy (Sanford, 1949), where only one plate was needed for an accurate result. Consequently the CaII velocities

were averaged in the manner described by Barford (1967, Page 62).

The radial velocities obtained could be improved by remeasuring all the plates, and then have all the plates measured a third time by someone other than the writer. This will serve to lessen all personal errors in the measuring. It would also be worthwhile to re-observe all the stars, for which the 1'O.H.P. plates are the only source of radial velocities, using a modern spectrograph.

5.7 The Determination of Spectral Types of Programme Stars from 1'O.H.P. and I.N.T. Plates

In all cases a stellar spectrum of a star of unknown spectral type was compared with a stellar spectrum of a star of known spectral type. Wherever possible, two spectra taken with the same spectrograph were compared. If the programme star spectrum was identical in appearance with the standard star spectrum, then it was concluded that the programme star was of the same spectral type as the standard star. It was often found that a programme star had to be compared with several standard stars of nearly the same spectral type, and some interpolation had to be done to determine the spectral type. The "Atlas of Stellar Spectra", by Morgan et al. (1943) was used as a guide in these cases.

The comparisons were made by means of a Hilger and Watts Spectrocomparator. The plate with the programme star spectrum and the plate with the standard star spectrum are attached, by means of their respective plate-holders, to two separate moveable mountings. The positions of these mountings are adjusted so that the magnified images of both spectra appear on a screen, with the corresponding lines of the two spectra aligned. This enabled a direct line for line comparison of the two spectra.

The spectral type standards observed at 1'O.H.P. and on the I.N.T. are listed in Tables (5.7.1) and (5.7.2) respectively. The daggers adjoining the spectral types in these tables, indicate that this star has been listed as a standard in the Revised MK System (Morgan and Keenan, 1973), and these were used in preference to the other standards. The Spectral types of Standard stars that are available for spectral classification are illustrated in Tables 5.7.3 and 5.7.4. The spectral types obtained are discussed, together with the published MK Spectral types in the next section.

TABLE 5.7.1

Spectral Type Standards Observed at 1'O.H.P

HD	Spectral Type	HD	Spectral Type	HD	Spectral Type
2905	B1 Ia	164354	B5 Ib$^+$	202850	B9 Ia
4142	B5 V	176437	B9 III	204172	B0 Ib
12953	A1 Ia	184915	B0.5III	208057	B3 V
14818	B2 Ia	184930	B5 III	209481	O9 V
22928	B5 III	190603	B1.5 Ia	209975	O9.5 Ib
32630	B3 V$^+$	191263	B3 V	210839	O6f
120315	B3 V$^+$	196867	B9 IV	212593	B9 Iab
123299	A0 III	198478	B3 Ia	214680	O9 V$^+$
147394	B5 IV$^+$	199478	B8 Ia	214993	B2 III
				218440	B2 V

TABLE 5.7.2

Spectral Type Standards Observed on the I.N.T

HD	Spectral Type	HD	Spectral Type	HD	Spectral Type
886	B2 IV$^+$	28446	B0 III	139006	A0 V
2905	B1 Ia	30614	O9.5 Ia	147394	B5 IV$^+$
3901	B2 V	35497	B7 III	198478	B3 I
12301	B8 Ib	35600	B9 Ib	199478	B8 I
13267	B5 I	36371	B5Iab	204172	B0 Ib
14372	B5 V	41117	B2 Iab$^+$	209481	O9 V
21291	B9 Ia	42087	B2.5 Ib	209975	O9.5 Ib
22928	B5 III	87737	A0 I	212593	B9 Iab
23180	B1 III$^+$	90994	B6 V	214993	B2 III
23288	B7 IV	91316	B1 I	218537	B3 V
23850	B8 III$^+$	103287	A0 V$^+$	222173	B8 V
24398	B1 Ib$^+$	120315	B3V$^+$		
24760	B0.5 III$^+$	123299	A0 III		

TABLE 5.7.3

Spectral Types of Standards that are available for the Spectral Classification of 1[illegible] H.P. Spectra

	Ia	Iab	Ib	II	III	IV	V
O9							**
O9.5			*				
BO			*		*		
BO.5							
B1	*						
B1.5	*						
B2	*				*		*
B2.5							
B3	*						**
B5			*		*	**	*
B6							
B7							
B8	*						
B9	*	*			*	**	
AO							

TABLE 5.7.4

Spectral Types of Standards that are available for Spectral Classification of I.N.T. Spectra

	Ia	Iab	Ib	II	III	IV	V
O9			*				*
O9.5	*						
BO			*		*		
BO.5					**		
B1	*	*			**		
B1.5							
B2		**			*	**	*
B2.5			*				
B3		*					**
B5		*			*	**	*
B6							*
B7					*	*	
B8		*	**		**		*
B9	*	*	*				
AO		*			*		**

5.8 A Discussion of the Spectral Types Obtained and their comparison with Available Published Spectral Types

The published spectral types, together with those determined from 1'O.H.P. and I.N.T. plates, are presented in Table(5.8.1). The references from which published spectral types were obtained, are listed at the end of the table. It can be seen that in cases where the writer has classified stars, for which published spectral types already exist, the spectral types obtained are in reasonable agreement with the published ones. A typical error seems to be plus or minus one luminosity class, and plus or minus one colour class.

In cases where two or more different spectral types are available for a given star, the difficulty of selecting one in preference to the others is encountered. The ease with which a spectrum can be classified depends on the width of the spectrum, as well as the dispersion used. The spectra of faint programme stars obtained with the I.N.T. are considerably narrower than the corresponding spectra of the spectral type standard stars. Thus difficulties in classifying the I.N.T. spectra were encountered, which did not arise in the case of the 1'O.H.P. spectra. Consequently in the event of a discrepancy between 1'O.H.P. and I.N.T. spectral classifications, the I.N.T. classification was given a lower weight. The final selection of MK spectral types is discussed later (§7.1).

Table 5.8.1

Spectral Types of the Programme Stars: Observed and Published

Star	MK	S	O
HD 169798	B2 V	5	B3 (HD)
HD 170028	B3 I	3	B3 (HD)
HD 170051	B2 V	5	B3 (HD)
HD 170111	B3 V	H	B3 (HD)
	B3 V	4	
HD 170263	B9 V	H	B8 (HD)
HD 170650	B6 IV	4	B5 (HD)
HD 172421	B5 IV	H	B8 (HD)
HD 173087	B3 V	1 *	B5 (HD)
	B5 V	4	
HD 174179	B3 IVp	4	B3 (HD)
HD 174261	B5 I	3	B5 (HD)
HD 174298	B1 V	5	B3 (HD)
HD 174585	B3 IV	4	B2 (HD)
HD 174714	B5 III	2	B8 (HD)
	B6 III	2 *	
HD 174959	B6 IV	4	B5 (HD)
HD 175081	B5 n	2	B3 (HD)
HD 175426	B2 V	H	B3 R (HD)
HD 175803	B3 V	2	B3 (HD)
	B2 V	H	
HD 176254	B2 IV	5	B3 (HD)
HD 176502	B4 IV	4	B5 (HD)
HD 176582	B5 IV	4	B5 (HD)
	B5 V	H	
HD 176818	B3 V	H	B3 (HD)
HD 176819	B2 IV-V	4	B3 (HD)
HD 176871	B5 V	3	B3 (HD)
	B5 V	H	
HD 176914	B5 I	3	B5 (HD)
HD 1[illegible]	B9 V	H	B8 (HD)
HD 177003	B3 V	1	B3 (HD)
	B3 V	2 *	
	B2.5 IV	4	
	B3 V	H	
	B3 V	I	
HD 177109	B5 IV	4	B3 (HD)
HD 177593	B5 I	3	B5 (HD)
HD 178329	B3 V	4	B3 (HD)
	B3 V	H	
HD 178475	B7 IV	1	B5 R (HD)
	B7 IV	2	
	B7 IV	3	
HD 178849	B3 V	5	B3 (HD)
HD 179506	B9 V	H	B8 (HD)
	B8 V	I	
HD 180124	B2 V	H	B8 (HD)
	B2 V	I	
HD 180163	B4.5 III	1	B3 R (HD)
	B2 IV	1 *	
	B2 IV	2 *	
	B2 V	H	
	B2 V	I	
HD 181409	B2 IV	4	B3 (HD)
	B3 IV	H	
HD 182568	B3 IV	1	B3 R (HD)
	B3 IV	2	
	B3 IV	3	
HD 182615	B9 V	H	B8 (HD)
HD 183339	B7 IV	5	B8 (HD)
HD 183649	B2 V	H	B8 (HD)
HD 184007	A0 V	5	B9 (HD)

Star	MK	S	O
HD 184171	B3 IV	1	B3 (HD)
	B3 IV	2	
	B3 IV	3	
	B2 V	H	
HD 185780	B0.5 II	H	B2 R (HD)
HD 186485	B9 V	H	B8 (HD)
HD 186618	B0 III	H	B2 (HD)
HD 186814	B8 V	H	B8 (HD)
HD 186994	B0 III	2	B0 R (HD)
HD 187035	B5 V	H	B8 (HD)
HD 187879	B1 IV	2	B2 R (HD)
	B1 III	4	
HD 188209	O9.5 Ia	1	B0 (HD)
	O9.5 Ia	2	
	O9.5 III	1	
	O9.5 III	2	
	O9 I	2	
	O9 III	1	
	O9 III	2	
	O9.5 Iab	6	
	O9.5 Ia	4	
HD 188252	B2 III	2	B2 (HD)
HD 188439	B0.5IIIp	2	B2 (HD)
	B0.5 II	1	
	B0.5IIIn	4	
HD 188665	B5 V	1	B5 (HD)
	B5 V	4	
	B5 V	H	
HD 188891	B2 II	H	B3 (HD)
HD 189160	A0p	2	B8 (HD)
	B9 V	H	
HD 189775	B5 III	4	B5 (HD)

Star	MK	S	O
HD 189957	B0 III	2	B3 (HD)
	O9.5III	5	
HD 190254	B2 III	H	B8 (HD)
HD 190427	B0 III	5	B3 (HD)
HD 190901	B9 V	H	B8 (HD)
HD 191124	A0 V	H	B8 (HD)
HD 191781	B0 Ibp	1	B (HD)
	B0 Ibp	2	
	ON9.7Iab	6	
	O9.5 Ia	H	
HD 192575	B0.5 V	5	B3 (HD)
HD 196421	B2 IV	5	B5 (HD)
HD 197770	B2 IV	1	B3 (HD)
	B2 IV	2	
	B2 III	4	
	B2 V	H	
HD 197911	B2 V	H	B5 R (HD)
HD 198739	B8 II	I	B8 (HD)
HD 198781	B0.5 V	1	B0 (HD)
	B0.5 V	2	
HD 199308	B2 IV	5	B3 (HD)
HD 199661	B2.5 IV	4	B3 (HD)
	B3 III	H	
HD 199739	B2 II	H	B8 (HD)
	B2 II	I	
HD 202214	B0 II	1	B2 (HD)
	B0 V	1 *	
	B0 II	2	
	B0 V	2	
HD 204150	B2 III	H	B3 (HD)
HD 204770	B7 V	4	B5 (HD)

Star	MK	S	O
HD 205139	B1 II	1	B0 (HD)
	B1 Ia	2	
	B1 II	2	
	B0.5 III	H	
HD 206165	B2 Ib	1	B2P R (HD)
	B2 I	2	
	B2 Ib	2	
	B2 Ib	H	
HD 206327	B3 III	H	Oe5 R (HD)
HD 207198	O9 II	1	B2 (HD)
	O9 II	2	
	O9 III	3	
	O9 Ib-II	6	
	B0.5 V	H	
HD 207308	B0.5 V	2	B2 (HD)
HD 207951	B2 V	5	B8 (HD)
	B1 V	H	
HD 208106	B1 V	H	B3 (HD)
HD 208185	B2 V	2	B3 (HD)
HD 208218	B1 III	1	B1 (HD)
	B1 III	2	
HD 208440	B1 V	5	B8 (HD)
HD 208761	B2 III	H	B5 (HD)
HD 208904	B2 V	H	B3 (HD)
HD 208947	B2 V	2	B3 (HD)
	B3 V	2	
HD 209789	B2 V	H	B8 R (HD)
HD 210386	B1 III	H	B5 (HD)
HD 213087	B0.5 Ib	1	B0 R (HD)
	B0.5 Ib	2	
	B0 II	2	
HD 213405	B0.5 V	1	B0 (HD)
HD 213481	B0 I	H	B8 (HD)

Star	MK	S	O
HD 213571	B2 IV	5	B5 (HD)
HD 216992	B3 II	H	B8 (HD)
	B3 V	I	
HD 217224	B5 II	H	B8 (HD)
HD 222568	B1 IV	2	B3 (HD)
HD 223959	B5 II	H	B8 (HD)
HD 2083	B1 V	1	B2 (HD)
	B1 IV	2	
	O9.5 III	H	
HD 3122	B4 V	H	B9 (HD)
HD 6675	B0.5 III	1	B0 (HD)
	B0.5 III	2	
	B0.5 Ib	2	
	O9.5 II	H	
HD 7852	B2 III	H	B8 (HD)
HD 16393	B8 V	H	B8 (HD)
HD 16440	B7 II	2	B8 (HD)
	B5 III	H	
HD 17179	B0.5 V	H	B8 (HD)
HD 17929	B5 V	H	B8 (HD)
HD 21267	B8 V	H	B8 (HD)
HD 21806	B1 V(N)	5	B3 R (HD)
HD 21930	A2 V	H	B8 (HD)
HD 25090	B0.5 III	5	B5 (HD)
HD 25443	B0.5 III	1	B2 R (HD)
	B0.5 III	2	
HD 25638	B0 II	2	B0 R (HD)
HD 25639	B0 III	2	B0 R (HD)
HD 26684	B5 I	3	B5 (HD)
	B0.5 III	H	
HD 34233	B3 IV	1	B3 (HD)
	B3 IV	2 *	
HD 35250	B8 II	H	B8 (HD)

Star	MK	S	O
HD 38410	B5 III	H	B8 (HD)
HD 40784	B5 III	H	B8 (HD)
HD 41161	O9n	2 *	B0 (HD)
	O8 V	5	
HD 41689	B2 I	3	B3 (HD)
HD 42783	B5 III	H	B8 (HD)
	B5 III	I	
HD 46552	B5 III	H	B8 (HD)
	B5 III	I	
HD 48029	B2 IV	H	B8 R (HD)
HD 48532	B2 V	2	B3 (HD)
HD 48549	B2 V	H	B8 R (HD)
HD 50767	B2 V	5	B3 (HD)
HD 53879	B2 III	H	B8 (HD)
HD 54352	B5 III	I	B8 (HD)
HD 58784	B3 III	5	B2 (HD)
HD 59882	B2 II	H	B3 (HD)
HD 64854	B2 III	8	B8 (HD)
HD 66594	B3 V	5	B5 (HD)
HD 66665	B0.5 III	1	B3 (HD)
	B0.5 III	2	
HD 225882	B2 III	H	B2 (HDE)
HD 225573	B9 V	H	B5 (HDE)
BD 48 3054	B0 V	H	OB (LS)
	B0 V	I	
BD 53 2481	B5 V	H	OB⁻(LS)
BD 55 2523a	B2 III	H	OB⁻(LS)
LS3 57 04	B3 Ib	I	OB (LS)
BD 58 2236	B2V	H	OB1(LS)
LS3 59 06	B1 III	I	OB (LS)
BD 59 2350	B1 V	H	OBr(LS)
	B0 V	I	
BD 58 2268	B2 V	H	OB⁻(LS)

Star	MK	S	O
BD 59 2384	B1 II	H	OB (LS)
BD 61 2158	B0.5 V	H	OB⁻(LS)
LS3 64 04	B3 II	I	OB⁻(LS)
BD 64 1677	B0.5 IV	I	OB⁻(LS)
BD 65 1774	B2 II	H	OB⁻(LS)
BD 67 1489	B5 III	I	OB⁻(LS)
BD 68 1373	B2 III	I	OB⁻(LS)
BD 67 1531	B0.5 V	I	OB⁻(LS)
BD 67 1550	B2 II	I	OB1(LS)
BD 68 1386	B2 Ib	I	OB1(LS)
BD 59 0804	B5 III	I	OB⁻(LS)
LS5 54 14	B0 III	I N	OB⁻(LS)
BD 52 0913	sd O ?	I N	OB (LS)
BD 50 1129	B2 III	I	OB⁻(LS)
BD 48 1263	B2 Ib	I	OB⁻(LS)
BD 43 1349	B3 III	8	OB1(LS)
BD 43 1355	B3 III	I	OB1(LS)
BD 37 1415	B3 V	I	OB⁻(LS)
LS5 23 73	B5 V	I	OB⁻(LS)
BD 24 1306	B5 II	I	OB⁻(LS)
BD 22 1407	B0 II	I	OB⁻(LS)
BD 23 1436	B3 III	I	OB⁻(LS)
HD 197406	WN7	9 N	Ma (HD)
BD 34 3631	B2 V	10	
BD 46 1043	B3 V	11	
BD 45 1169	B3 V	11	
AAO 50 108	B5 V	11	
AAO 50 164	B2 III	11	
AAO 50 165	B5 V	11	
AAO 50 274	B5 V	11	
HD 46592	B5 V	11	(HD)
AAO 50 363	B5 V	11	
HD 257432	B3 V	11	B9 (HDE)

Star	MK	S	O	Star	MK	S	O
HD 260611	B3 III	8	B3 (HDE)	AAO 99 312	B2 V	8	
HD 45337	B5 V	8	A0 (HD)	AAO 99 326	B3 V	8	
AAO 99 226	B3 V	8		BD -0 1848	B2 V	8	
AAO 99 263	B2 V	8					

Notes:

MK denotes MK Spectral Type

O denotes other catalogued spectral types, the catalogue being referenced in parentheses as:

HD/HDE - Henry Draper Catalogue (Cannon & Pickering, 1918 - 1924) and Henry Draper Extension (Cannon, 1924 - 1936)

LS - " Luminous Stars in the Northern Milky Way " (§ 3.3)

S indicates the source of the MK Spectral Type as given below:

H) Spectroscopic Observations at 1' O.H.P.

I) Spectroscopic Observations on the I.N.T.

1) Blanco et al. (1968)

2) Jaschek et al. (1964)

3) Abt & Biggs (1972)

4) Crawford et al. (1971)

5) Kennedy & Buscombe (1974)

6) Walborn (1972)

7) Crampton et al. (1973)

8) Chuadze (1973)

9) Hiltner (1955)

10) Neckel (1967)

* This reference suggests that this star is a binary, the companion being comparitively faint.

N Only one plate available and this is underexposed, hence the spectral type is uncertain.

Table 5.8.2

Star Number Cross Reference Table

N.B. AAO - represents " Abastumani Astrophysical Observatory No. "

No.	Other No.
BD 46 1043	AAO 25 007
BD 43 1349	AAO 25 663
HD 46592	AAO 50 316
HD 260611	AAO 50 714
BD -0 1848	AAO 99 426
BD 45 1169	AAO 25 137
HD 257432	AAO 50 450
HD 45337	AAO 50 746
HD 64854	AAO 99 520

CHAPTER SIX

UBV Photometry

6.1 Introduction

The intensity of radiation from a black body at a given wavelength was shown, by Planck (1901), to be a smooth function of that wavelength, which exhibited a well defined maximum. The wavelength at which this maximum occurs is dependant upon the temperature of the black body. Stars show a similar behaviour to black bodies, and so the colour of a star is a direct indication of its surface temperature.

If the magnitude of a star in bandwidths centred on different wavelengths can be observed, the temperature of the star and hence its spectral type on the HD catalogue system (Cannon and Pickering, 1918-1924) can be obtained. The wavelengths and their corresponding bandwidths must be chosen in such a way that the differences in magnitude obtained, are as sensitive as possible to the intensity distribution as a function of wavelength. Obviously, the more wavelengths chosen, the more precisely this function can be determined, but for practical reasons the number should be kept to a minimum.

The first attempts to measure stellar temperatures by visual comparison with an artificial black body were made by Wilsing and Sheiner (1909) and also by Wilsing et al. (1919). These were not successful because of the failure to allow for atmospheric extinction, coupled with personal errors in making the visual comparisons. An advance was made by Sampson (1922), who devised a photoelectric device for measuring the intensity at a given wavelength from objective prism spectra. Since the intensities were measured relative to a pre-chosen stellar spectrum on the plate, the effects of atmospheric extinction and instrumentation could be eliminated. This was followed with further work by Sampson (1925, 1930) and an attempt to establish a system of colour standards by Greaves et al. (1929). The discovery of interstellar reddening by Trumpler (1930a) and his subsequent investigations of it, (1930b, c), made further progress possible, and the North Polar Sequence became well established, mainly through the work of Seares and Joyner (1944, 1945). The next development was the establishment of the UBV system by Johnson and Morgan (1953).

The advantage of this photometric system was that it enabled the measurement of interstellar reddening directly, by photometric means alone, and without reference to stars for which the reddening is assumed to be zero. The system uses the revised zero point of the visual magnitude scale of the North Polar Sequence, and takes the MK system of spectral classification as standard. V, B and U are defined as the observed magnitudes through the yellow, blue and ultraviolet filters, reduced to outside the earth's atmosphere, respectively and including a zero point correction to satisfy the conditions B-V = 0 and U-B = 0 for an AOV star.

The added advantage of this system is that B and U are attenuated by the interstellar medium, whereas V is attenuated to a a much lesser extent. Consequently the colour index (B-V) for a star of known spectral type, gives a direct measure of the interstellar reddening. Since (U-B) is very much less sensitive to reddening, the intrinsic colours, that is the colours that would be observed if there were no reddening, can be determined by the method indicated previously (§2.2).

The method of reducing the observed deflections y, b and u, which are measured through the yellow, blue and ultraviolet filters respectively, to the colours V, B-V, and U-B is given by Hardie (1962) and by Schulte and Crawford (1961). A summary is given here, together with modifications suggested by Hill (1974) and adopted in this analysis.

The increase in intensity of a beam of intenisty I, a fraction τdx of which is absorbed by a piece of material of thickness dx is

$$dI = -I\,\tau dx,$$

$$\therefore \text{Log } I = \text{Log } I_o - \tau x,$$

where I and I_o are the initial and final intensities respectively. In magnitudes this becomes

$$m_o = m - 2.5\,\tau x$$

or $$m_o = m - k\,X \qquad \text{---------- (6.1.1)},$$

where X is the airmass, defined as unity at the zenith of the observer, and k is the appropriate extinction coefficient, m is the magnitude of the star as observed outside the atmosphere and m_o is the observed magnitude of the star. The zenith distance of a star is given by the relation

$$\sec z = (\sin \phi \sin \delta + \cos \phi \cos \delta \cos h)^{-1} \qquad \text{----------(6.1.2a)},$$

where ϕ is the latitude of the observer, δ is the declination of the star and h is the hour angle of the star.

If $X \leqslant 10$, it can be calculated to an accuracy of better than 1% by using the polynomial approximation

$$X = \sec z - 0.0018167(\sec z-1) - 0.002875\,(\sec z-1)^2 - 0.0008083\,(\sec z-1)^3 \qquad \text{---------- (6.1.2b)}.$$

It can be seen from equation (6.1.1) that if m is observed for different values of X, m_o and k can be determined from a least squares fit (Barford, 1967, page 56). Considerable improvement can be made if measures over many nights are grouped so that the constancy of m_o for a non-variable star can be used as an additional constant in the determination of k.

By analogy with equation (6.1.1), the extinction is treated in a differential manner for the colour indices giving

$$C_o = C - k_c X \qquad \text{---------- (6.1.3)},$$

where C_o and C are the colour indices for the star as seen inside

and outside the atmosphere respectively. The quantity k_c is the extinction coefficient appropriate to the colour index C and is simply the difference between the corresponding magnitude coefficients. Since some of the variations in the magnitude extinction coefficients are common to both, and the colour sensitivity of equipment tends to be more constant than the absolute sensitivity, k_c can be determined more accurately than k, by the above method.

The light received in any photometric band is not monochromatic. Thus the extinction coefficients used are actually those for a monochromatic beam at some predominant wavelength, which depends on the colour of the star. Thus k and k_c are functions of C, and King (1952) has shown them to be of the approximate form

$$k = k' + k''C \quad \text{- - - - - - - - - - - - - - - - -(6.1.4)},$$

and $$k_c = k_c' + k_c''C \quad \text{- - - - - - - - - - - - - - - - -(6.1.5)},$$

Substitution in equations (6.1.1) and (6.1.3) gives

$$m_o = m - k'X - k''CX \quad \text{- - - - - - - - - - - - - - -(6.1.6)},$$

and $$C_o = C - k_c'X - k_c''CX \quad \text{- - - - - - - - - - - - - -(6.1.7)},$$

To determine k', k'', k_c' and k_c'' two stars with widely differing colour indices, which form a close optical pair, can be observed at a number of different airmasses. Since these two stars will have substantially the same positions, it can be seen from equations (6.1.6) and (6.1.7) that their differential measures of magnitude and colour are related by

$$\Delta m_o = \Delta m - k''\Delta CX \quad \text{- - - - - - - - - - - - - - - - (6.1.8)},$$

and $$\Delta C_o = \Delta C - k_c''\Delta CX \quad \text{- - - - - - - - - - - - - - - - (6.1.9)},$$

Thus a least squares fit of Δm versus ΔCX and of ΔC versus ΔCX, will provide lines whose slopes are k'' and k_c''. Then using the same data, it follows from equations (6.1.6) and (6.1.7) that k' and k_c' can be determined by a least squares fit of $(m-k''CX)$ versus X and of $C(1-k_c''X)$ versus X.

On a good photometric night, the extinction coefficients are solely a function of the location of the observatory. Initially, the extinction coefficients were assumed from a previous determination, made along the lines indicated above, by another observer. Using these assumed extinction coefficients and substituting in the equivalent forms of equations (6.1.6) and (6.1.7), the preliminary magnitude v, and the preliminary colours Cy and Cu may be derived. The magnitudes and colours on the UBV system are then related to these by the relations (Schulte and Crawford, 1961),

$$B-V = a + b.Cy \quad - - - - - - - - - - - - - - - \quad (6.1.10),$$

$$V = z + f.(B-V) + v \quad - - - - - - - - - - \quad (6.1.11),$$

and $$U-B = c + d.Cu \quad - - - - - - - - - - - - - - \quad (6.1.12),$$

These relations are known as the colour equations, and a, b, c, d, f and z are constants, known as colour equation coefficients, and are dependant on the instrumental characteristics of the telescope, the photometer and the filters. Suppose that a UBV photometric standard star is observed at several different airmasses, and in between each observation of this star, two other UBV standard stars, in the same region of the sky if possible to minimise extinction errors, are observed.

Subtracting the corresponding colour equations for the reference star and an adjacent comparison star gives

$$(B-V)_s - (B-V)_c = b.\Delta Cy \quad \text{- - - - - - - - - - - - - - - - -(6.1.13)},$$

$$V_s - V_c = f.[(B-V)_s - (B-V)_c] + \Delta v \quad \text{- - - - - - - - - - (6.1.14)}$$

$$\text{and} \quad (U-B)_s - (U-B)_c = d.\Delta Cu \quad \text{- - - - - - - - - - - - - -(6.1.15)}.$$

Letting $z' = V_c - f(B-V)_c$,

$$a' = (B-V)_c$$

and $$c' = (U-B)_c,$$

gives $$(B-V)_s = a' + b.\Delta Cy \quad \text{- - - - - - - - - - - - -(6.1.16)},$$

$$V_s = z' + f.(B-V)_s + \Delta v \quad \text{- - - - - - - - - - -(6.1.17)}$$

and $$(U-B)_s = c' + d.\Delta Cu \quad \text{- - - - - - - - - - - - - - (6.1.18)}.$$

The mean outside atmosphere magnitude and colours for the reference star, $\overline{V}_c$, $\overline{Cy}_c$ and $\overline{Cu}_c$, can be derived by the application of the equivalent forms of equations (6.1.6) and (6.1.7) and averaging the results. Substituting into equations (6.1.10), (6.1.11) and (6.1.12) gives

$$(B-V)_s = a + b.\overline{Cy}_c ,$$

$$V_s = z + f.(B-V)_s + \overline{V}_c$$

and $$(U-B)_s = c + d.\overline{Cu}_c .$$

Equating the left hand sides of these equations with the left hand sides of equations (6.1.16), (6.1.17) and (6.1.18) gives

$$a + b.\overline{Cy}_c = a' + b.\Delta Cy ,$$

$$\therefore \quad a = a' + b.(\Delta Cy)' \quad - - - - - - - - - - - \quad (6.1.19) ,$$

$$z + f.(B-V)_s + \overline{v}_c = z' + f.(B-V)_s + \Delta v ,$$

$$\therefore \quad z = z'' + \Delta v \quad - - - - - - - - - - - - - - - - \quad (6.1.20) ,$$

and $$c' + d.\Delta Cu = c + d.\overline{Cu}_c ,$$

$$\therefore \quad c = c' + d.(\Delta Cu)' \quad - - - - - - - - - - - \quad (6.1.21) ,$$

where $$z'' = z' - \overline{V}_c = -f.(B-V)_c \quad - - - - - - - - - - - \quad (6.1.22) ,$$

$$(\Delta Cy)' = \Delta Cy - \overline{Cy}_c \quad - - - - - - - - - - - - - \quad (6.1.23) ,$$

and $$(\Delta Cu)' = \Delta Cu - \overline{Cu}_c \quad - - - - - - - - - - - - - \quad (6.1.24) .$$

The application of least squares fits to equations (6.1.19), (6.1.20) and (6.1.21) gives the values of a, b, c, d, f and z. These were then used to determine the extinction coefficients for each night, from the observations of the standard stars, by a reverse process. These improved values of extinction coefficients can then be used to derive improved values for the colour equation coefficients, and this iteration can be continued until no further

improvement in the extinction or colour equation coefficients is obtained. The UBV colours for the programme stars can then be evaluated by substitution in equations (6.1.10), (6.1.11) and (6.1.12).

In practice, this method does not yield good consistent results. Stock (1969), has pointed out that equation (6.1.7) does not give an accurate value of (U-B). That is to say the extinction in (U-B) is not solely a function of the colour of the star, and the Balmer Decrement, D, seems to be a useful second parameter. For $(B-V) \leqslant 0.60$

$$D = -1.285\ Cy_{o} + 0.784 + Cu_{o} \quad - - - - - - \quad (6.1.25)\ ,$$

otherwise $D = -1.983\ Cy_{o} + 1.203 - Cu_{o}$ - - - - - - (6.1.26) .

The equation (6.1.7) becomes, in the case of the colour (U-B) ,

$$Cu_{o} = Cu - (k'_{Cu} + k''_{Cu}.\ Cu + PD)\ X \quad - - - \quad (6.1.27)\ ,$$

where P is a constant.

The value of D is determined from the value of (B-V) according to equation (6.1.25) or (6.1.26). The calculation can be repeated, using equation (6.1.27) instead of equation (6.1.7), several times with a different value of P chosen on each occasion, and the process continued until the value of P which gives the least scatter in the final results, is found. This is then adopted as the correct value for P.

A further correction can be made by introducing time dependant zero point corrections, z_{v}, z_{Cy} and z_{Cu}, appropriate to the magnitude v and the colours Cy and Cu, which arise through instrumental drift and changing atmospheric transparency, so that

equations (6.1.6), (6.1.7) and (6.1.27) become

$$V_o = V - k'X + z_V \quad - - - - - - - - - - - - \quad (6.1.28) ,$$

$$Cy_o = Cy - (k'_{Cy} + k''_{Cy})\, X + z_{Cy} \quad - - - - \quad (6.1.29) ,$$

and $$Cu_o = Cu - (k'_{Cu} + k''_{Cu} + PD)\, X + z_{Cu} \quad - - - \quad (6.1.30) .$$

These zero points are determined by fitting a polynomial to the residuals in the standard star observations as a function of the sidereal time of observation, in the manner in which polynomials were fitted for the radial velocity reductions (§5.3).

The resulting polynomials were integrated as functions of sidereal time between the limits of t_1 and t_2, where t_1 and t_2 are the sidereal times at the beginning and end of the night, respectively. Dividing these integrals by $(t_2 - t_1)/2$ gives the mean zero point corrections for the night. Interpreting the instrumental drift as being equivalent to an extinction variation, and for all practical purposes the two are indistinguishable, the zero point corrections can be treated as a contribution to the primary extinction coefficients (k', k_{Cy} and k'_{Cu}). In this way improved extinction coefficients can be obtained and used to effect a further improvement in the colour equation coefficients in the manner described above. Final values of V, B-V, U-B, for the programme stars observed during the night can be obtained from equations (6.1.10), (6.1.11) and (6.1.12).

6.2 Single Channel UBV Photometry using the 16" Telescope at Kitt Peak

The observations reported here were carried out by Dr.P.W.Hill in September and October 1972, and so the description of the photometer and the observing technique will be very brief. The photometer contains a diaphragm in the focal plane which gives a 28" field of view. On leaving the diaphragm, the light is passed through a filter, which is one of three on a filter slide, and is then directed on to the photocathode of a IP21 photomultiplier. The use of this photomultiplier is discussed by Dewitt and Seyfert (1950). It is mounted in an appropriate housing, and cooled with dry ice. The E.H.T. applied was 900 volts.

The characteristics of the filters used are listed in Table (6.2.1). The signal from the photomultiplier is fed into an integrator, which integrates the signal over a predetermined time interval, which in this case was 20 seconds. Two integrators, numbered #30 and #31 , were available for photometry with this photometer, though only one of these was needed.

Each integrator zero was adjusted by first ensuring that the lead from the photomultiplier was disconnected, and then examining the digital voltmeter (DVM) reading after an integration. By means of a "zero adjust control", an adjustment was made until this reading became zero. The gain steps of each integrator were then calibrated in a similar manner to that already described for the Semi Automatic System integrators (§4.2.2). The gain steps obtained are given in magnitudes in Table (6.2.2) for both integrators.

The integrator #30 was found to be unstable and suffered from a large zero point drift. Consequently its use was discontinued after 3 nights. The figures quoted for integrator #31 are the mean values obtained as a result of two calibrations, made on 10th September 1972 and on 1st October 1972, since both were in very close agreement.

TABLE 6.2.1

The Filters Used for UBV Photometry at Kitt Peak

Filter (1mm x 1mm Schott)	Peak Wavelength	Bandwidth	Maximum Transmission
U (UG2)	3750Å	740Å	81%
V (Corning 3384)	5700Å	1000Å	87%
B (Corning 5030 + 99.13)	4350Å	1230Å	81%

TABLE 6.2.2

The Measured Integrator Gain Steps

Gain Step / Integrator	A	B	C
#30	0.000	2.500	5.020
#31	0.000	2.496	5.016

A list of standard stars for observation was made from the list of Johnson et al. (1966). The stars listed in the usual source of UBV standards, Johnson and Morgan (1953) were found to be too bright. The stars adopted as standards are listed in Table (6.2.3). The running number of the standard, that is 1 to 44, is the number assigned for the purposes of the reduction programme (§6.3).

TABLE 6.2.3

The UBV Standard Stars Used

No.	HR	V	B-V	U-B	No.	HR	V	B-V	U-B
1	6806	6.40	+0.87	+0.59	23	107	6.04	0.44	-0.06
2	6958	6.43	-0.04	-0.26	24	201	6.15	1.62	2.00
3	7144	6.15	0.97	0.71	25	243	6.37	1.07	0.88
4	7173	6.76	0.25	-0.44	26	307	6.00	1.51	1.85
5	7784	6.23	0.06	0.03	27	401	6.21	0.23	0.09
6	7847	6.18	1.01	0.74	28	444	6.59	-0.04	-0.11
7	7993	6.45	0.07	-0.77	29	507	6.19	1.54	1.89
8	8291	6.11	0.07	0.08	30	627	6.35	0.33	-0.43
9	8421	6.12	1.60	1.77	31	825	6.26	0.88	0.50
10	8427	6.27	-0.06	-0.71	32	904	6.11	1.77	2.07
11	8473	6.37	-0.06	-0.18	33	983	6.17	-0.02	-0.25
12	8733	6.17	-0.15	-0.80	34	1029	6.09	-0.07	-0.50
13	8800	6.66	-0.05	-0.68	35	1047	6.24	0.13	-0.25
14	9048	6.21	-0.07	-0.19	36	1553	6.11	0.08	-0.44
15	9092	6.32	+0.18	+0.14	37	1573	6.06	0.41	0.44
16	9097	6.24	0.33	-0.54	38	1925	6.23	0.84	0.51
17	2	6.29	1.10	1.02	39	2228	6.52	0.27	0.09
18	8	6.14	0.75	0.33	40	2230	6.09	0.90	0.62
19	11	6.43	-0.14	-0.48	41	2240	6.25	0.45	-0.39
20	14	6.05	1.38	1.16	42	2584	6.29	0.04	0.06
21	67	6.17	0.94	0.73	43	2613	6.35	-0.11	-0.47
22	72	6.46	0.68	0.29	44	2627	6.49	0.22	-0.75

At the beginning of each night, the date which consisted of the day number and month number, was entered on four thumb switches which were encoded. Before a sequence of observations on each star, the star number was entered on another six encoded thumb switches. A gain step was then selected appropriate to the magnitude and colour of the star, which would give a reasonable reading on the DVM. Two

status switches were then set or reset, so as to give the status of the observation. One indicated whether a star or sky observation was being made, and the other indicated whether a standard or a programme star was being observed. An integration was then begun and at the end of this, the output from the integrator was displayed on the DVM.

The declination, hour angle, sidereal time, date, star number, DVM reading, gain step used and filter slide position were output onto paper tape. Unfortunately the declination and hour angle encoders were not operating correctly, and so the data output for these quantities were meaningless. The data registers were now cleared and the logic was reset so as to be ready to start another observation. The sequence in which the observations were made is given in Table (6.2.4). This was the sequence finally adopted; on the first night a different sequence was used.

On the night of 11/12 September 1972, when conditions were particularly favourable, a sequence of standard stars was observed, for the colour equation determination. This was done in the manner described previously (§6.1). Unfortunately, the weather did not permit the repeating of these observations on another night.

The paper tapes produced were decoded by a standard Kitt Peak programme on the K.P.N.O. *CDC 6400* and written onto 7-track magnetic tape. Unfortunately this was not readable on the 360/44 9-track magnetic tape drives. Consequently, the contents of the magnetic tape were copied onto 10 reels of paper tape, using the K.P.N.O. *CDC 6400* computer. The paper tapes were punched in a CDC code, and a line printer listing of the data on the magnetic tape was also produced. Dr. Hill entered every detail in his observing book, and this proved invaluable in the subsequent editing operations (§6.3).

TABLE 6.2.4

The Sequence of Observations used for UBV Photometry

No. of Observation	Filter	Star/Sky
1	B	Sky
2	B	Star
3	V	Star
4	V	Sky
5	U	Sky
6	U	Star
7	U	Sky
8	V	Sky
9	V	Star
10	B	Star
11	B	Sky

6.3 Reduction of the UBV Photometry

A difficulty arose with reading the *CDC 6400* paper tapes on the 360/44 because there were no distinct end of record characters at the end of each 80 byte record. Further complications arose, owing to the fact that occasionally, one or more characters were missing in a record. For example, if one character were missing in a record, then the character that should have appeared at the beginning of the next record appeared at the end of the current record.

It was eventually decided to copy the paper tapes in chronological order onto magnetic tape, by simply reading the paper tape at 80 characters a time, and then output them onto magnetic tape as EBCDIC characters in an 80 byte record. This programme was written for the 360/44, and incorporated a routine for translating the CDC code to EBCDIC written by Hill (1973).

If the end of the paper tape was sensed before the current 80 byte buffer was full, the remainder of the buffer was filled with blanks, before being output. An end of file mark was then written. In loading the remaining paper tapes, the magnetic tape was wound on until the end of file mark was detected. The data transfer then took place in the same way, overwriting the end of file mark.

An editing programme was written for inserting a specified number of given characters at a specified point in the file, and shifting all the subsequent characters along, and characters which have to be moved from the end of the record are inserted at the beginning of the next record. This was done by copying from one magnetic tape to another. In this way all missing characters on the original paper tapes were inserted. It was found, however, that some characters in the file were incorrect and needed replacing. Furthermore some records required replacement or deletion. Both of these tasks were carried out by a second editing programme written for the 360/44

Since the hour angle and declination encoders were not operational at the time at which the observations were made, another

programme was written for the 360/44 to produce a magnetic tape with these quantities corrected. The star number and sidereal time were read from the existing magnetic tape. Programme stars were located by their HD number on a disk file, from which the right ascension and declination were obtained. In the case of a standard star, the HR number was read from the magnetic tape and used to locate the appropriate right ascension and declination, from an area of core reserved for standard star data, which had previously been read in from a deck of cards.

The coordinates were precessed to the epoch of 1972.7, at which the observations were undertaken. The difference between the right ascension and sidereal time with the appropriate sign adjustment, gave the hour angle. A new magnetic tape was produced containing the original data with the hour angle and declination, for 1950, corrected. Two more programmes were written for the 360/44. The first calculated the average DVM reading for each filter, corrected for sky background together with the average sidereal time and hour angle at which the observation was made. These were then output with the star number and an indication as to whether the star was a programme or standard star, onto a disk file, with one 80 byte record for each observation. The second programme created a second disk file, with the HR number of each standard star replaced with the appropriate sequence number given in Table (6.2.5).

The UBV reductions programme, originally written by Mrs B. Weymann for the CDC 6400 at K.P.N.O., was extensively modified by Dr. Hill for running on the 360/44. The final version of the programme read the data from the disk file, created in the manner described above, and carried out the reductions using the method indicated previously (§6.1). Standard No. 9 (HR 8421) was found to have a large residual which could not be removed. Consequently the reductions were repeated, treating this star as programme star, and this improved the results considerably. There is a facility in the programme for repeating the reductions and excluding all standard stars whose residuals exceed a certain limit. For the final run of the programme, this limit was set to ±0.050.

The weighted mean of each extinction coefficient was calculated, from the values obtained for each extinction coefficient on all the nights on which observations were made, using the method given by Barford (1967, page 62). This was done using a programme written for the St. Andrews University Observatory Nova 820 computer. The mean extinction coefficients were then used to derive improved colour equation coefficients, and these in turn were used to repeat the reductions and derive new extinction coefficients. The process was now repeated, and the iteration continued until no further improvement was obtained in either the colour equation coefficients, or in the results themselves. The final extinction coefficients, colour equation coefficients and r.m.s. (root mean square) errors in V, B-V, and U-B are tabulated in Tables (6.3.1), (6.3.2) and (6.3.3) respectively. For the purposes of this iterative procedure described above, P was treated as a colour equation coefficient.

The photometric results are compared with the published results and discussed later (§6.4).

TABLE 6.3.1

The Extinction Coefficients

Extinction Coefficient (Symbols defined in §6.1)	Initial Value (K,P.N.O)	Final Value (PWH/AELG)
k'	0.160	0.148
k'_{Cy}	0.100	0.099
k''_{Cy}	-0.020	-0.022
k'_{Cu}	0.340	0.318
k''_{Cu}	-0.020	-0.027

TABLE 6.3.2

The Colour Equation Coefficients

Colour Equation Coefficient (Symbols defined in §6.1)	Initial Value (PWH/AELG)	Final Value (PWH/AELG)
a	1.173	1.152
b	1.034	1.031
c	-0.912	-0.956
d	0.944	0.926
f	7.087	7.058
z	-0.004	-0.004
p		0.013

TABLE 6.3.3

The R.M.S. Errors in the UBV Photometry

Night (1972)	No. of Standards	Δ V r.m.s.	Δ(B-V) r.m.s.	Δ(U-B) r.m.s.
Sept 3/4	6	0.0109	0.0005	0.0068
Sept 4/5	6	0.0109	0.0063	0.0019
Sept 5/6	13	0.0294	0.0136	0.0216
Sept 6/7	13	0.0192	0.0062	0.0091
Sept 7/8	8	0.0041	0.0015	0.0088
Sept 10/11	12	0.0213	0.0057	0.0179
Sept 11/12	27	0.0126	0.0064	0.0110
Sept 12/13	15	0.0177	0.0072	0.0112
Sept 13/14	3	0.0213	0.0052	0.0080
Sept 28/29	16	0.0181	0.0068	0.0126
Sept 29/30	17	0.0104	0.0046	0.0183
Sept 30/31	17	0.0195	0.0099	0.0175
Oct 1/2	20	0.0167	0.0093	0.0215
Oct 2/3	9	0.0155	0.0049	0.0077
Oct 7/8	10	0.0114	0.0050	0.0115

6.4 A Comparison of the Different Sources of UBV Photometry

The final results obtained from the photometric observations made at the K.P.N.O. are listed in Table (6.4.1) and designated "K.P.N.O" as their source. The results listed are the means, taken by giving each observation an equal weight. In addition the available published data is given for comparison; the list of appropriate references, and cross-reference numbers being given at the end of the table. The number of observations upon which each result is based is given by N. If no value of N is given, there is no indication in the reference quoted, nor in any of the references cited therein, of the number of observations.

In the event of two more sources of UBV photometry being given in the catalogue by Blanco et al. (1968), the result quoted is the mean of the results given, each observation being given an equal weight. In a few cases Blanco et al. quote photometry on the "Cape Photometric System", defined by Cousins et al.(1961). In this event the U-B values quoted were derived from Table II in the paper by Cousins and Stoy (1963). The observational errors in the published data can be obtained from the references indicated. The typical errors in V, B-V and U-B are $\pm 0^{m}.02$.

A comparison was now made between the different sources of UBV photometry, searching for systematic errors. None were found except in the case of the K.P.N.O. (U-B) and the (U-B) obtained by Guetter (1974). The mean relation between these two was found to be

$$(U-B)_{KPNO} = (U-B)_{Guetter} + 0.028 \quad - - - - - - - - - - \quad (6.4.1)$$

The system of colour indices to which the correction should be applied can, in theory, be determined by a comparison of both systems with the other systems. Unfortunately there is insufficient overlap with other systems to do this.

Table 6.4.1

UBV Photometry of Programme Stars: Results and Published Data

	Star	V	B-V	U-B	N	S	R
HD	169798	6.798	-0.102	-0.613	3	K.P.N.O.	
		6.76	-0.12			4	
HD	170028	6.901	-0.131	-0.592	3	K.P.N.O.	
HD	170051	7.118	-0.106	-0.567	3	K.P.N.O.	
		7.12	-0.11			4	
		7.09	-0.10	-0.59	3	5	
HD	170111	6.501	-0.104	-0.586	3	K.P.N.O.	
		6.52	-0.11	-0.59	3	3	
HD	170263	8.616	-0.011	-0.131	3	K.P.N.O.	
HD	170650	5.907	-0.089	-0.511	3	K.P.N.O.	
		5.89	-0.10	-0.52	3	3	
HD	173297	7.667	-0.017	-0.329	3	K.P.N.O.	
HD	172421	7.672	-0.016	-0.407	3	K.P.N.O.	
HD	173087	6.46	-0.12	-0.56	3	1	1
HD	174179	6.05	-0.13	-0.67	3	3	
HD	174261	7.133	-0.015	-0.483	3	K.P.N.O.	2
HD	174298	6.557	-0.056	-0.793	3	K.P.N.O.	
		6.54	-0.08	-0.81	3	5	
		6.56	-0.08			4	
HD	174585	5.956	-0.218	-0.713		1	3
		5.90	-0.16	-0.72	3	3	
HD	174586	7.625	-0.020	-0.100	3	K.P.N.O.	
HD	174959	6.08	-0.11	-0.49	3	3	
HD	175081	7.330	-0.086	-0.384	3	K.P.N.O.	
		7.33	-0.08	-0.37	3	5	
HD	175426	5.57	-0.15	-0.67	3	3	
		5.56	-0.15	-0.67	3	5	
HD	175803	8.005	0.010	-0.576	3	K.P.N.O.	
		8.02	0.00	-0.57	3	5	
		8.02	0.12			4	
HD	176254	6.738	0.042	-0.545	3	K.P.N.O.	
		6.74	0.03	-0.56	3	5	

Star	V	B-V	U-B	N	S	R
HD 176502	6.21	-0.16	-0.66	3	3	
HD 176582	6.40	-0.17	-0.71	3	3	
HD 176803	7.342	0.059	-0.311	2	K.P.N.O.	
HD 176818	7.042	0.126	-0.591	3	K.P.N.O.	
HD 176819	6.68	0.02	-0.70	2	3	
HD 176871	5.68	-0.08	-0.55	3	3	
HD 176914	7.037	-0.081	-0.699	3	K.P.N.O.	4
HD 176940	8.308	0.126	-0.197	2	K.P.N.O.	
HD 177003	5.38	-0.166		2	1	
	5.37	-0.19	-0.76	3	3	
HD 177006	7.255	-0.138	-0.623	3	K.P.N.O.	
	7.30	-0.13			4	
HD 177109	6.38	-0.12	-0.63	3	3	
HD 177593	7.304	-0.106	-0.506	3	K.P.N.O.	
HD 178329	6.49	-0.16	-0.65	3	3	
	6.46	-0.16	-0.65	3	5	
HD 178475	5.26	-0.113	-0.541	8	1	
	5.28	-0.11	-0.51	3	3	
HD 178540	6.612	-0.015	-0.505	2	K.P.N.O.	

Star	V	B-V	U-B	N	S	R
HD 178591	7.142	-0.035	-0.225	2	K.P.N.O.	
HD 178849	7.035	-0.138	-0.625	3	K.P.N.O.	
	7.00	-0.12	-0.64	3	K.P.N.O.	
HD 178912	8.335	-0.163	-0.815	2	K.P.N.O.	
	8.2				4	
HD 179506	7.919	-0.038	-0.381	2	K.P.N.O.	
HD 180124	7.197	-0.004	-0.524	2	K.P.N.O.	
HD 180163	4.39	-0.15	-0.65	8	1,3	5
HD 180844	7.231	-0.114	-0.553	2	K.P.N.O.	
HD 181164	7.533	-0.024	-0.704	2	K.P.N.O.	
HD 181409	6.59	-0.19	-0.91	3	3	
HD 181492	6.824	-0.084	-0.588	3	K.P.N.O.	6
	6.82	-0.09	-0.59	3	5	
HD 182568	4.98	-0.12	-0.71	3	3	
	4.97	-0.09	-0.72		1	
	4.97	-0.127		2	1	
HD 182615	7.977	-0.052	-0.197	2	K.P.N.O.	
HD 183339	6.57	-0.14	-0.54	22	1	
	6.56	-0.13	-0.54	3	2	

	Star	V	B-V	U-B	N	S	R
HD	183535	8.641	-0.159	-0.914	2	K.P.N.O.	
		8.66	-0.17			4	
HD	183649	8.813	-0.119	-0.616	3	K.P.N.O.	
HD	184171	4.73	-0.136	-0.67	2	1	
		4.72	-0.15	-0.62	3	3	
		4.74	-0.13	-0.67	2	2	
HD	185780	7.742	-0.080	-0.895	3	K.P.N.O.	
		7.75	-0.10	-0.93	3	5	
HD	186485	8.540	-0.012	-0.117	3	K.P.N.O.	
HD	186618	7.759	-0.189	-0.965	3	K.P.N.O.	
		7.77	-0.21	-0.99	3	5	
		7.81	-0.19			4	
HD	186814	9.23	0.029	0.021	2	K.P.N.O.	
HD	186994	7.508	-0.126	-0.933	3	K.P.N.O.	
		7.55	-0.13			4	
		7.50	-0.10		3	5	
HD	187035	8.833	-0.037	-0.449	2	K.P.N.O.	
HD	187139	8.178	0.018	-0.173	2	K.P.N.O.	
HD	187879	5.68	-0.04	-0.78	3	3	

	Star	V	B-V	U-B	N	S	R
HD	188209	5.62	-0.07	-0.97	11	1	
		5.65	-0.09	-0.98	3	3	
HD	188252	5.916	-0.186	-0.848	4	K.P.N.O.	
		5.68	-0.14			4	7
HD	188439	6.30	-0.10	-0.86		1	
		6.30	-0.12	-0.93	3	3	
HD	188461	6.988	-0.157	-0.762	3	K.P.N.O.	4
		6.98	-0.15	-0.78	3	5	
HD	188665	5.12	-0.129	-0.550	12	1	
		5.14	-0.15	-0.55	2	3	
HD	188891	7.30	-0.01	-0.74	1	1	
HD	189775	6.14	-0.19	-0.66	2	3	
HD	189818	7.326	-0.176	-0.829	2	K.P.N.O.	
HD	189957	7.805	0.019	-0.848	3	K.P.N.O.	
		7.22	-0.06			4	
		7.81	0.00	-0.88	3	5	
HD	190025	7.530	-0.077	-0.544	3	K.P.N.O.	
HD	190254	8.676	-0.017	-0.513	3	K.P.N.O.	
HD	190427	8.347	0.174	-0.731	3	K.P.N.O.	
		8.35	0.14	-0.76	3	5	

Star	V	B-V	U-B	N	S	R
HD 190901	9.650	0.186	-0.131	2	K.P.N.O.	
HD 191124	9.325	0.117	-0.058	2	K.P.N.O.	
HD 191781	9.536	0.642	-0.412	3	K.P.N.O.	
	9.54	0.64	-0.41	2	1	
HD 192035	8.186	0.072	-0.786	3	K.P.N.O.	
	8.18	0.05	-0.82	6	5	8
	8.19	0.06			4	
HD 192575	6.82	0.15	-0.67	3	5	
	6.827	0.177	-0.662	3	K.P.N.O.	
	6.7				4	
HD 193550	7.856	0.135	-0.311	2	K.P.N.O.	
HD 196421	8.077	0.099	-0.623	3	K.P.N.O.	
	8.09	0.08			4	
HD 197344	8.587	0.177	0.112	2	K.P.N.O.	
HD 197751	7.666	0.068	-0.305	2	K.P.N.O.	
HD 197406	10.3	0.57	-0.45	2	9	
HD 197770	6.32	0.33	-0.48	2	1	
	6.31	0.34	-0.47	3	3	

Star	V	B-V	U-B	N	S	R
HD 197911	7.661	0.049	-0.728	3	K.P.N.O.	
	8.3				4	
	7.65	0.04	-0.77		10	
HD 198739	7.986	0.034	-0.412	3	K.P.N.O.	
HD 198781	6.45	0.07	-0.77	2	1	
	6.44	0.05	-0.77	2	3	
HD 199308	7.504	0.160	-0.626	3	K.P.N.O.	
	7.52	0.14			4	
	7.51	0.13	-0.64	3	5	
HD 199661	6.23	-0.17	-0.69	2	3	
HD 199739	7.957	0.471	-0.252	3	K.P.N.O.	
HD 202107	7.921	0.143	-0.564	3	K.P.N.O.	
HD 202214	5.64	0.121	-0.765	9	1	
	5.64	0.10	-0.76	2	3	
HD 204150	7.692	0.022	-0.720	3	K.P.N.O.	
	7.69	0.01	-0.74	3	5	
	7.72	0.45			4	
HD 204770	5.43	-0.11	-0.43	3	3	

	Star	V	B-V	U-B	N	S	R
HD	205139	5.55	0.11		4	1	
		5.53	0.13	-0.74	3	3	
HD	206165	4.74	0.29	-0.53	7	1	
		4.73	0.28	-0.57	1	3	
HD	206327	8.681	0.181	-0.562	3	K.P.N.O.	
HD	207198	5.94	0.31	-0.64	6	1	
		5.95	0.30	-0.63	3	3	
HD	207308	7.496	0.252	-0.571	3	K.P.N.O.	
		7.50	0.25			4	
		7.48	0.24	-0.61	3	5	
		7.49	0.25	-0.57		2	
HD	207951	8.18	0.14	-0.57		2	
HD	208106	7.370	0.152	-0.546	3	K.P.N.O.	4
		7.42	0.13	-0.57	6	5	
		7.35				4	
		7.4	0.14	-0.54		2	
HD	208185	7.381	0.135	-0.598	4	K.P.N.O.	4
	(a)	7.38	0.11	-0.53		2	9
	(ab)	7.37	0.10	-0.67		2	

	Star	V	B-V	U-B	N	S	R
HD	208218	6.703	0.245	-0.550	3	K.P.N.O.	
		6.64	0.23	-0.49		2	
HD	208440	7.947	0.077	-0.715	4	K.P.N.O.	
		7.90	0.08	-0.73		2	
HD	208761	7.659	0.050	-0.747	3	K.P.N.O.	
		7.61	0.06	-0.75		2	
HD	208904	7.547	-0.009	-0.602	3	K.P.N.O.	
		7.54	-0.01	-0.60	3	5	
		7.5				4	
HD	208947	6.40	-0.06	-0.69	3	3	
HD	209178	8.683	0.232	-0.447	3	K.P.N.O.	
HD	209452	8.271	0.149	-0.386	3	K.P.N.O.	
HD	209789	8.967	0.197	-0.396	3	K.P.N.O.	
HD	210386	8.004	0.327	-0.536	3	K.P.N.O.	
		8.00				4	
HD	213087	5.46	0.37	-0.59	2	1	
		5.52	0.36	-0.59	1	3	
HD	213405	7.95	0.47	-0.44	2	1	
HD	213481	8.201	0.553	-0.326	3	K.P.N.O.	

Star	V	B-V	U-B	N	S	R
HD 213571	7.157	0.045	-0.604	5	K.P.N.O.	
	7.14	-0.04	-0.63	3	5	
	7.1				4	
HD 216992	8.036	0.147	-0.436	3	K.P.N.O.	
HD 217224	8.218	0.329	-0.458	3	K.P.N.O.	
HD 222568	7.667	0.427	-0.424	6	K.P.N.O.	
	7.67	0.40	-0.48	3	5	
	7.72	0.45			4	
HD 223959	8.393	0.120	-0.480	5	K.P.N.O.	
HD 224395	7.838	0.130	-0.499	7	K.P.N.O.	
	7.89	0.16			4	
HD 2083	6.89	0.03	-0.83	2	1	
HD 3366	6.948	-0.009	-0.618	4	K.P.N.O.	
	6.95	0.00	-0.65	3	5	
HD 6675	6.90	0.31	-0.64	2	1	
HD 7852	8.851	0.340	-0.420	3	K.P.N.O.	
HD 14863	7.769	0.069	-0.397	3	K.P.N.O.	
HD 16393	7.598	0.032	-0.318	3	K.P.N.O.	
HD 16440	7.880	0.709	0.070	3	K.P.N.O.	
HD 17179	7.859	0.243	-0.450	2	K.P.N.O.	

Star	V	B-V	U-B	N	S	R
HD 17929	7.858	0.297	-0.160	3	K.P.N.O.	
HD 20710	7.605	0.094	-0.184	3	K.P.N.O.	
HD 21267	7.991	0.017	-0.277	3	K.P.N.O.	
HD 21806	7.757	0.323	-0.538	5	K.P.N.O.	
	7.76	0.30			4	
	7.56	0.28	-0.59	3	5	
HD 21930	8.435	0.193	0.009	3	K.P.N.O.	
HD 22828	7.137	-0.047	-0.216	3	K.P.N.O	
HD 23036	8.093	-0.010	-0.344	3	K.P.N.O.	
HD 23254	8.064	0.052	-0.455	5	K.P.N.O.	
	8.08	-0.01			4	
HD 24116	8.54	0.21	-0.22		2	
HD 25090	7.312	0.339	-0.552	5	K.P.N.O.	
	7.32	0.29	-0.60	3	5	
HD 25443	6.74	0.33	-0.62	2	1	
HD 25638	7.1	0.40			4	
HD 25639	6.9				4	
HD 26684	6.727	-0.034	-0.481	4	K.P.N.O.	
HD 26801	7.74	0.00	-0.13	2	1	10
HD 32747	7.81	0.11	-0.22	2	1	

Star		V	B-V	U-B	N	S	R
HD	34233	6.12	-0.033	-0.47	3	1	
		6.12	-0.02	-0.48	4	3	
HD	35250	8.235	0.213	-0.337	3	K.P.N.O.	
HD	36083	7.491	0.062	-0.250	3	K.P.N.O.	
HD	36662	8.541	0.111	-0.333	3	K.P.N.O.	
		8.55	0.09			4	
HD	37838	8.205	0.092	-0.050	3	K.P.N.O.	
HD	38258	7.471	0.034	-0.116	3	K.P.N.O.	
HD	38410	8.744	-0.069	-0.442	3	K.P.N.O.	
HD	38439	7.982	-0.16	-0.306	3	K.P.N.O.	
HD	38775	8.387	0.287	0.135	3	K.P.N.O.	
HD	40160	7.510	-0.081	-0.637	4	K.P.N.O.	
HD	40694	8.321	0.095	-0.295	3	K.P.N.O.	
HD	40784	8.344	0.019	-0.364	3	K.P.N.O.	
HD	41161	6.763	-0.077	-0.937	3	K.P.N.O.	
		6.77	-0.11	-1.00	3	5	
HD	41258	8.401	0.118	-0.162	2	K.P.N.O.	
HD	41541	7.034	0.037	-0.037	3	K.P.N.O.	
HD	41689	8.428	-0.062	-0.823	3	K.P.N.O.	
		8.44	-0.08	-0.88	3	5	

Star		V	B-V	U-B	N	S	R
HD	41765	8.064	0.021	-0.322	3	K.P.N.O.	
HD	42614	8.038	0.020	-0.253	3	K.P.N.O.	
HD	42734	9.11	0.01	-0.21	2	1	
HD	42782	7.175	-0.161	-0.620	3	K.P.N.O.	
HD	42783	7.521	-0.039	-0.408	3	K.P.N.O.	
HD	44512	8.338	0.029	-0.286	3	K.P.N.O.	
HD	46552	7.740	-0.061	-0.329	3	K.P.N.O.	
HD	48029	8.602	-0.088	-0.839	2	K.P.N.O.	
HD	48532	8.5				4	
		8.679	-0.078	-0.556	3	K.P.N.O.	
HD	48549	8.684	-0.113	-0.700	3	K.P.N.O.	
HD	49763	9.379	-0.139	-0.658	3	K.P.N.O.	
HD	50003	8.059	-0.088	-0.397	2	K.P.N.O.	
HD	50320	8.465	-0.138	-0.506	2	K.P.N.O.	
HD	50767	7.697	-0.208	-0.839	2	K.P.N.O.	
HD	53879	9.663	-0.091	-0.602	3	K.P.N.O.	
HD	54352	9.566	-0.349	-0.409	1	K.P.N.O.	
HD	54538	9.923	-0.081	-0.431	1	K.P.N.O.	
HD	56032	8.99	-0.10	-0.34	2	1	

Star	V	B-V	U-B	N	S	R
HD 57291	6.875	-0.163	-0.719	1	K.P.N.O.	
	6.8				4	
HD 58383	7.41	-0.09	-0.31	3	1	11
HD 58784	8.59	-0.07		4	1	
	8.567	-0.068	-0.607	1	K.P.N.O.	
HD 58973	7.851	-0.127	-0.616	1	K.P.N.O.	
HD 59882	8.802	-0.142	-0.926	1	K.P.N.O.	
	8.81	-0.19	-0.92	6	5	
HD 64854	9.27	-0.06			8	
HD 66594	7.57	-0.14	-0.52	8	1	
HD 66665	7.80	-0.26	-1.04		1	
HD 225882	9.668	0.009	-0.685	3	K.P.N.O.	
HD 225573	8.928	-0.025	-0.384	3	K.P.N.O.	
	8.92	-0.03			4	
HD 226070	10.189	0.206	0.168	3	K.P.N.O.	
HD 235253	9.06	0.00			4	12
HD 235259	8.87	0.02			4	B5
HD 239436	8.51	0.26			4	B5
HD 235271	9.0				4	B5
HD 235298	8.4				4	B5

Star	V	B-V	U-B	N	S	R
HD 235363	8.42	0.53			4	13
HD 239595	9.27	0.31	-0.46		4	14
HD 239600	8.87	0.14	-0.58		4	B3
	8.87	0.15	-0.60		11	B2 V
HD 239605a	8.07				4	15
HD 239605b	9.23	0.28			4	16
HD 239618	8.45	0.50	-0.42		11	17
	8.64	0.44	-0.44		4	B3 e
HD 239626	9.29	0.35	-0.57		11	18
HD 239649	9.31	0.19	-0.49		11	B1 V
HD 239675	9.16	0.30	-0.25		11	B3 V
HD 239676	9.06	0.52	-0.38		11	19
HD 239681	9.34	0.27	-0.60		11	20
BD 61 2213	8.98	0.18	-0.45		11	B3V + B5V
BD 61 2214	9.85	0.23	-0.35		11	B3 V
BD 61 2215	9.34	0.19	-0.49		11	B3 V
BD 61 2218	10.03	0.14	-0.51		11	B3 V
BD 34 3631	10.16	-0.11	-0.88		9	B2 V
BD 35 1332	9.30	0.25	-0.68		6	
BD 46 1043	9.44	0.19			8	21

Star	V	B-V	U-B	N	S	R
BD 45 1169	9.96	0.28			8	21
BD 43 1349	8.98	0.31			8	21
AAO 50 108	10.88	0.30			8	
AAO 50 164	10.78	0.10			8	
AAO 50 165	10.81	0.21			8	
AAO 50 274	12.49	0.30			8	
HD 46592	8.78	0.07			8	21
AAO 50 363	12.23	0.11			8	
HD 257432	10.13	0.08			8	21
HD 260611	8.79	0.10			8	21
HD 45337	9.12	-0.02			8	21
AAO 99 226	12.48	0.13			8	
AAO 99 263	11.91	0.23			8	

Star	V	B-V	U-B	N	S	R
AAO 99 312	12.68				8	
AAO 99 326	12.03	0.01			8	
BD -0 1848	10.90	0.21			8	21
HD 64854	9.27	-0.06			8	21
LS1 69 06	9.35	0.32	-0.32	3	7	
LS1 68 21	10.81	0.70	-0.07	3	7	
LS1 68 20	11.76	0.68	0.20	3	7	
LS1 68 19	11.30	0.63	-0.09	3	7	
LS1 64 100	11.40	0.56	-0.28	3	7	
LS1 64 97	11.28	0.53	-0.33	3	7	
LS1 63 198	12.78	-0.08	-0.99	3	7	
LS1 62 235	11.73	0.52	0.05	3	7	
LS1 61 325	11.81	0.55	-0.23	3	7	

Notes to Table 6.4.1:

S denotes the source of the UBV photometry which corresponds to the list given below:

1) Blanco et al. (1968)
2) Kennedy & Buscombe (1974)
3) Crawford et al. (1971)
4) Crampton et al. (1973)
5) Guetter (1974)
6) Drilling (1975)
7) Haug (1970)
8) Chuadze (1973)
9) Hiltner (1955)
10) Crampton & Fisher (1974)
11) Simonson III (1968)

R denotes a remark which corresponds to the list given below:

1) Binary: V = 8.05 for the companion.
2) Binary: The companion is comparitively faint.
3) A 111 observations are reported in this reference.
4) Possibly variable
5) Binary: V = 8.58 for the companion
6) As for 4) above
7) Possibly variable with a long period
8) RX - Cyg: Apparently non variable
9) Binary
10) Triple System: Faint Companions
11) Binary: V = 9.52 for the companion
12) Also BD 49 3292 (B5)
13) Binary: A B5 Primary with a G - Type companion
14) Also BD 59 2331 (B3)
15) Also BD 58 2237 (B3)
16) Also BD 58 2236 (B5n)
17) Also BD 59 2344 (B2 Ve)

18) Also BD 59 2350 (B0 V)

19) Also BD 58 2268 (B1 V)

20) Also BD 59 2384 (B1 V)

21) See Table 5.8.2

N.B. A spectral type given in the remarks column indicates that this spectral type is given in the reference cited.

HD 239600 ≡ BD 59 2333

One possible explanation for the discrepancy would be that the U filter, used at the K.P.N.O. or by Guetter (1974), has a red leak which has not been corrected for. This would make (U-B) algebraically larger than it should be. If the omission lies in the K.P.N.O reductions, then the discrepancy might be accounted for. If this is the case, some dependence of $[(U-B)_{KPNO} - (U-B)_{Guetter}]$ on $(U-B)_{Guetter}$ and E_{B-V} (defined in §2.2) would be expected. To test this a multiple linear regression analysis is needed. A Schott UG2 filter was used on both occasions. In addition, both photomultiplier tubes used have virtually zero sensitivity in the red, and so any differences due to red leak would be very small.

Consequently it was felt that there is no justification for correcting $(U-B)_{KPNO}$ at present, especially as the agreement with the systems is good. Further analysis of the Kitt Peak data is needed to ensure the best attainable accuracy. The effect of red leak on the (U-B) index has been discussed in more detail by Ažusienis and Straižys (1969). They have found that it is not possible to accurately determine the red leak correction without a knowledge of the interstellar reddening.

Thus V, (B-V) and (U-B) would have to be determined, without a red leak correction, and used to determine E_{B-V} (§2.2). Then using the value of E_{B-V} for each star, a red leak correction appropriate to each star could be calculated and used to redetermine V, (B-V) and (U-B). This would enable a redetermination of E_{B-V}, and the whole procedure repeated. The iteration could be continued until no further improvement in the results is obtained.

It has been shown by Gutierrez-Moreno and Moreno (1970, 1972) that the colour transformations are dependent upon the interstellar reddening. This is a fairly small effect, the correction being typically $\sim 0^m.02$ in (B-V) and (U-B). Consequently, it can be ignored for the present, since its inclusion will not radically change the conclusions drawn from this work.

However, to obtain the best possible results, all the data listed in Table (6.4.1) would have to be corrected for the effects of reddening on the colour transformations. To accomplish this with

published data, without access to the original observations, would be difficult. For the Kitt Peak observations, the reductions programme discussed previously (§6.3) could be modified so that a determination of the interstellar reddening could be made for each star, and this used to derive improved UBV colours. Those in turn could be used to derive an improved value for E_{B-V} and then a redetermination of the UBV colours would be possible. This iteration could be continued until no further improvement is obtained.

A further improvement to the photometric accuracy can be made by taking the programme stars which have the best night to night agreement in the UBV colours obtained, and use these as additional standard stars. Thus it should be possible to derive more accurate extinction and colour equation coefficients, and hence improved UBV colours for the remaining programme stars.

In view of these potential improvements, the weighted values of V, B-V and U-B were taken for each star in turn. Each quantity was weighted by the number of observations upon which it depended. If the number of observations was unavailable, then it was assumed to be one and the published colours weighted accordingly. These results are listed in Table (7.2.1) and are discussed further later (§7.1). In all cases UBV colours and magnitudes were adopted where available in preference to BV photometry. No account of published BV photometry was taken in obtaining an average V or (B-V).

CHAPTER SEVEN

A Discussion of the Available Data, Stellar Associations, Distant Stars and High Velocity Stars

7.1 The Adoption of Final β Indices, UBV Colours, Absolute Magnitudes, Intrinsic Colours, MK Spectral Types, Stellar and Interstellar Radial Velocities, Proper Motions and CaII (K) Equivalent Widths.

7.2 The Determination of Stellar Distances, Galactocentric Distances, Space Motions and the Standard Deviations in these Quantities.

7.3 Associations of OB Stars :

- 7.3.1 Introduction
- 7.3.2 NGC 1502
- 7.3.3 Cepheus OB2
- 7.3.4 Other Associations
- 7.3.5 Interesting Groups of Stars

7.4 High Velocity and Possible Runaway Stars

7.5 Distant and Possibly Subluminous Stars

7.1 The Adoption of Final β Indices, UBV Colours, Absolute Magnitudes, Intrinsic Colours, MK Spectral Types, Stellar and Interstellar Radial Velocities, Proper Motions, and CaII(K) Equivalent Widths

The UBV colours and magnitudes were adopted by calculating the means, weighted by the number of observations as already indicated (§6.4), and listed in Table (7.2.1). The star HD 177347 is classified as a B8 star in the HD Catalogue (Cannon & Pickering, 1918-1924), and since it is brighter than $V = 7^{m}.00$, it was omitted from the observing list. It was eventually reincluded because Crampton & Fisher (1974) have found the spectral type to be B3V, and the UBV photometry that they give are listed in Table (7.2.1). The star HD 208185 is a binary (§3.2.2), and since the separation is only 2" the photometry must be treated with suspicion. For this reason the second result denoted by "a", of the three given in Table (6.4.1), was adopted as this is thought to be the result of light from the primary alone.

A difference of $0^{m}.2$ in V between the results obtained by Dr. Hill, at K.P.N.O., and Guetter (1974) for the star HD 21806, would be explained if this star were a long period variable. Since Crampton et al. (1973) obtain a V magnitude which compares very well with the K.P.N.O. result, it is conceivable that the star observed by Guetter (1974) was not HD 21806. Consequently the K.P.N.O. UBV colours and magnitude were adopted for this star.

The most likely MK spectral type of each programme star was selected from Table (5.8.1), and the corresponding value of $(B-V)_{o}$ obtained from Johnson (1963, page 214). The parameter Q was then calculated using the method already described (§2.2). This was not done in the case of HD 54352, for which only one UBV observation is available, and this gave a peculiar result which may have been due to the wrong star having been observed. In cases where there were no MK spectral types available, Q was calculated using the Johnson

& Morgan (1953) formula, which is equation (2.2.5). A comparison of the values of Q obtained from equations (2.2.5) and (2.2.7) for stars with published MK spectral types, showed that the error in Q as a result of using equation (2.2.5) was not likely to exceed $0^m.005$. The adopted value of Q is listed in Table (7.2.1).

The weighted mean value of β was calculated by the method already described (§4.5). For HD 183339, the value β = 2.706 is quoted from Crawford et al.(1973). In the cases of HD 25638 and HD 25639, the β indices in Table (4.5.1) depart from what is to be expected from stars of these MK spectral types, and so they were not considered in adopting the final β indices for these stars. In fact these two stars constitute a visual binary, and the two components are themselves spectroscopic binaries, a fact discovered by Plaskett (1924). This may explain the large difference in the observed values of β and these stars are reconsidered later (§7.3.2).

The adopted values of β are listed in Table (7.2.1). In the cases for which both β and Q were available, the absolute magnitude and the intrinsinsic colour, $(B-V)_o$, were determined using the method already described (§2.2). In the event of no β index being available, or if β < 2.54 in which case the star is probably an emission line star, the catalogue by Petrie & Lee (1966) was searched for Hγ equivalent widths. If found, they were listed in Table (7.2.1) in the same column as the β index, but followed by a colon, and the quoted absolute magnitude was also adopted. If the parameter Q had been derived for these stars, then $(B-V)_o$ was obtained from Fig (2.2.1).

The absolute magnitudes and intrinsic colours, obtained by Haug (1970b), were adopted for the programme stars that were included in his list. The absolute magnitude and $(B-V)_o$ based on the MK spectral type were adopted if no other source existed. These were obtained from Blaauw (1963) and Johnson (1963, page 214) respectively, and followed by a colon when included in Table (7.2.1).

The β index obtained for HD 213571 is unexpectedly large if the spectral type is B2, as indicated by the UBV photometry. Conversely, in the cases of BD 59°2350 and HD 239595, the photometry suggests that these stars are more luminous than would be supposed from the MK spectral type. Consequently the absolute magnitudes given by Blaauw (1963), derived from the MK spectral types, were adopted for the time being.

The absolute magnitude and Q have been determined photometrically for the majority of the stars listed in Table (7.2.1). This presents the opportunity of obtaining photometric spectral types to check the spectroscopic spectral types discussed earlier (§5.8). The colour class was obtained from Q, using the calibration in Fig. (7.1.1). The luminosity class was then obtained by matching the colour class and photoelectric absolute magnitudes in the appropriate calibration given by Blaauw (1963). In each case the MK spectral types determined in this way were corrected to the nearest colour and luminosity classes, and are hereafter referred to as the photometric MK spectral types. These were then compared with the spectroscopic MK spectral types listed in Table (5.8.1), in which the typical error is plus or minus one luminosity and colour class. So if the photometric and spectroscopic MK spectral types are in agreement to within these limits, the spectroscopic MK spectral type was adopted. If not, it was assumed that the stellar spectrum was misclassified, and the photometric MK spectral type was adopted. In the event of two or more different spectroscopic MK spectral types being available from different sources, the photometric MK spectral type was used to select one in preference to the others. The photometric MK spectral type was adopted in the event of no other spectral classification being available. The adopted spectral types are listed in Table (7.2.1).

In cases where there is only one source for the radial velocity of a star, the velocity obtained from this source was adopted as the stellar radial velocity. In other cases the adopted radial velocity is the weighted mean, which is obtained by weighting each result by its standard deviation, using the method prescribed by

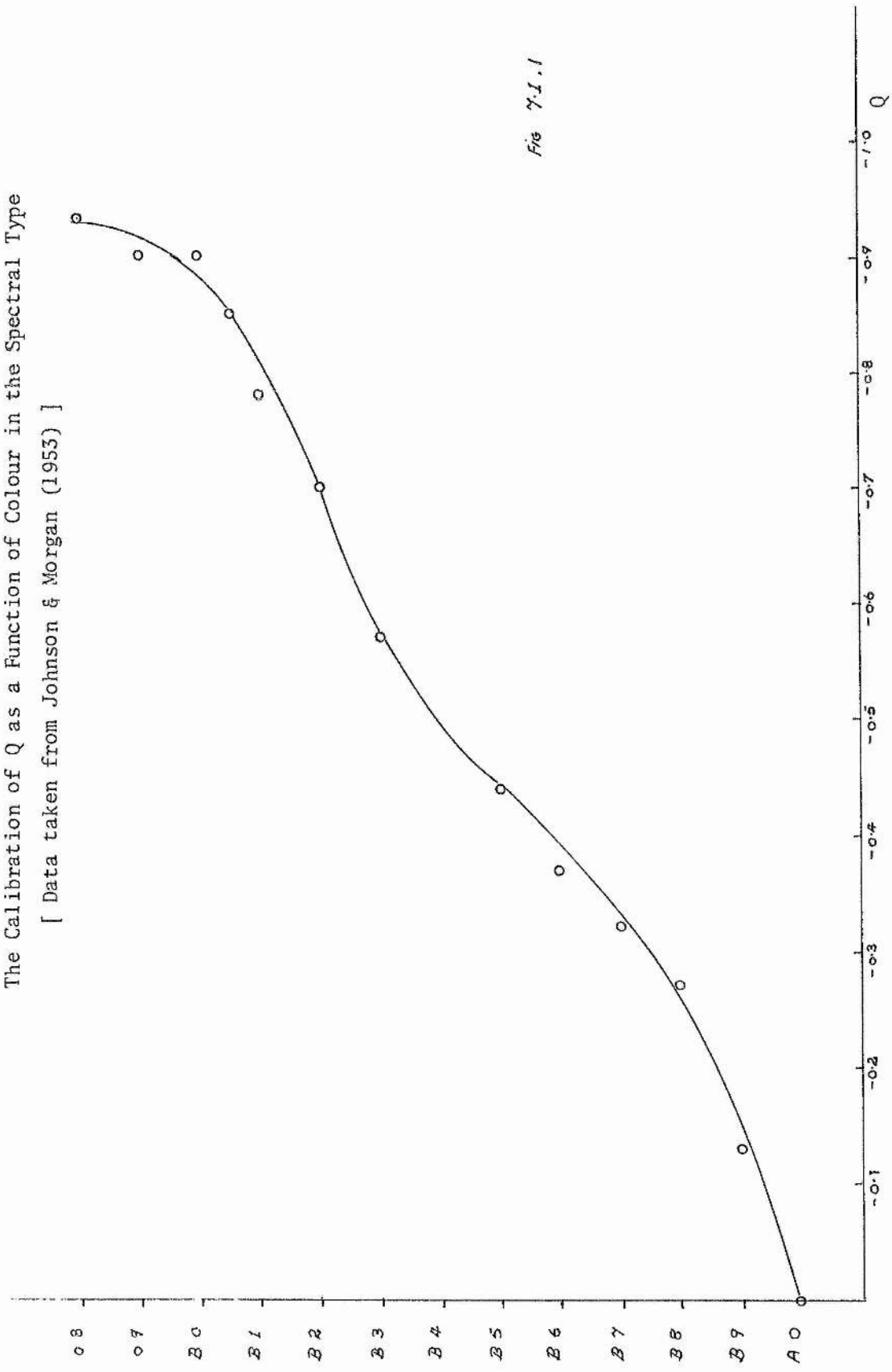

Fig 7.1.1

The Calibration of Q as a Function of Colour in the Spectral Type

[Data taken from Johnson & Morgan (1953)]

Barford (1967, page 62). The 1'O.H.P. plates were all underexposed in the cases of HD 170650, HD 170111, HD 176818 and HD 178329 and the resulting radial velocities were discarded. In a similar way, the adopted values of the interstellar CaII(K) radial velocities were determined, although care was needed in these cases, as stars of colour class B5 tend to have stellar CaII lines, which combine with any interstellar line to give a single spectral feature. Because of this possible blending, the CaII velocity cannot be combined with other stellar lines to yield an improved stellar radial velocity.

The adopted radial velocities are also listed in Table (7.2.1), although no interstellar CaII radial velocities are given for the B5 stars, except in cases where the star appears to be luminous, and the CaII(K) line appears to be strong and narrow on the plates. In these cases it is almost certainly an interstellar feature predominating over the stellar line.

The proper motions listed in the Table (7.2.1) are all obtained from the Smithsonian Astrophysical Observatory Star Catalogue (1966). They are only given for those stars for which radial velocity and distance determinations are available. The only two such stars for which no proper motions at all can be found are HD 187035 and HD 35250. Indeed an extensive search of the literature failed to produce a proper motion for these stars.

Equivalent widths of the interstellar CaII(K) lines have not as yet been measured from the spectra obtained by the writer, in collaboration with others, as already explained (§5.1.3). However, CaII(K) equivalent widths have been determined for some of the programme stars by Petrie and Lee (1966) and Beals & Oke (1953). The equivalent widths listed in Table (7.2.1) are in km/sec., and the equivalent widths of Petrie & Lee were expressed in km./sec. in the system of Beals & Oke by the relation

$$W(\mathrm{CaIIK})_{\mathrm{Beals}} = 76.3 W(\mathrm{CaIIK})_{\mathrm{Petrie}} + 0.6 \quad - - - - \quad (7.1.1),$$

in which 76.3 is the conversion factor from $\mathring{A}$ to km/sec, and 0.6

is the mean of the residuals calculated from

$$\Delta W = W(CaIIK)_{Beals} - 76.3W(CaIIK)_{Petrie},$$

for the stars in common with the two lists.

7.2 The Determination of Stellar Distances, Galactocentric Distances, Space Motions and the Standard Deviations in these Quantities.

The colour excess, E_{B-V}, was determined for each star, where possible, by substitution in equation (2.2.1). The distances, distances from the galactic plane, galactocentric distances and space motions, were then derived, where possible, using the method already described (§2.3 and §2.4). These calculations were carried out, initially using a programme written for the 360/44 by Dr. Kilkenny, and subsequently using a similar programme written for the Dunsink Observatory Nova 1220, which had the additional facility of being able to determine the standard deviations in each calculated quantity, using the method already described (§2.5).

These calculated quantities and their standard deviations, where necessary, are listed in Table (7.2.1). The following of a figure by a colon indicates that the determination was based on an absolute magnitude or a $(B-V)_o$, or both, obtained from the spectroscopic MK spectral type. Values of $(B-V)_o$ were obtained from MK spectral types only when (B-V) was available and (U-B) was not. In these cases, stellar distances were derived from V, B-V and the MK spectral type. The resulting distance was used to determine the space motion if the radial velocity and proper motions were known, these being enclosed in parentheses in Table (7.2.1).

In these cases, the standard deviations $\sigma(M_V) = 0^m.5$ and $[(B-V)_o] = 0^m.05$ were assumed in the calculation of standard deviations in the distances and space motions. This gave a standard deviation in the reddening of $\sigma(E_{B-V}) = 0^m.05$. If the distance determination was based on UBV and Hβ photometry, the assumptions $\sigma(M_V) = 0^m.2$ and $\sigma[(B-V)_o] = 0^m.02$ were made. This gave a standard deviation in the reddening of $\sigma(E_{B-V}) = 0^m.02$. The standard deviation in the galactocentric distance was 0.8kpc and slightly more for the more distant stars. This is to be expected because the standard deviation in the distance of the sun from the galactic centre is 0.8kpc (§2.5).

Table 7.2.1

Data for the Programme Stars

	Star	l	RV	μ_α	μ_δ	V	B-V	$(B-V)_o$	β	r	R	U	V	W	S	V_{CaII}
	MK	b	σ(RV)	σ(μ_α)	σ(μ_δ)	M_V	U-B	E_{B-V}	Q	σ(r)	z	σ(U)	σ(V)	σ(W)	σ(S)	W_{CaII}
HD	169798	50.83	-17	-21	-5	6.80	-0.10	-0.20	2.650	0.54	9.68	7	-31	39	50	
	B2 V	15.59	6	12	12	-2.2	-0.61	0.10	-0.543	0.02	0.15	18	17	31	26	20.4
HD	170028	54.28	-25	-14	-5	6.90	-0.13	-0.20	2.681	0.41	9.77	-1	-23	16	28	
	B4 V	16.79	7	12	12	-1.4	-0.59	0.07	-0.508	0.02	0.12	15	13	24	17	
HD	170051	54.50	-24	-21	0	7.10	-0.10	-0.19	2.684	0.44	9.76	-7	-25	33	41	
	B4 V	16.85	7	8	7	-1.4	-0.58	0.09	-0.493	0.02	0.13	11	10	18	15	16.6
HD	170111	54.53	-18	-6	1	6.51	-0.11	-0.20	2.686	0.32	9.83	-7	-5	8	11	-13
	B3 V	16.79	11	7	5	-1.3	-0.59	0.09	-0.518	0.01	0.09	11	8	13	11	
HD	170650	52.33	-17	-2	-6	5.90	-0.09	-0.17	2.636	0.54	9.69	2	-11	-2	12	-18
	B3 III	15.18	6	4	4	-3.0	-0.52	0.08	-0.453	0.02	0.14	9	7	13	8	
HD	174179	61.48	-15	8	-2	6.05	-0.13	-0.21	2.649	0.38	9.82	-7	4	-12	14	-15
	B3 IVp	14.56	10	7	6	-2.2	-0.67	0.08	-0.576	0.02	0.10	11	9	14	13	
HD	174298	54.36	-15	-17	3	6.55	-0.07	-0.28	2.628	0.60	9.67	-7	-14	43	46	-15
	B1 V	11.23	5	10	10	-3.0	-0.80	0.21	-0.747	0.03	0.12	18	16	28	27	14.3
HD	174585	62.65	-17	3	-8	5.96	-0.22	-0.23	2.661	0.37	9.84	3	-4	-10	10	-16
	B3 IV	14.62	7	4	3	-1.9	-0.71	0.01	-0.567	0.02	0.09	8	6	10	9	

	Star	l	RV	μ_α	μ_δ	V	B-V	$(B-V)_o$	β	r	R	U	V	W	S	V_{CaII}
	MK	b	σ(RV)	$\sigma(\mu_\alpha)$	$\sigma(\mu_\delta)$	M_V	U-B	E_{B-V}	Q	σ(r)	z	σ(U)	σ(V)	σ(W)	σ(S)	W_{CaII}
HD	175426	66.93	-26	-2	-3	5.57	-0.15	-0.21	2.666	0.77	9.90	-6	-11	-2	12	-17
	B3 V	15.50	8	3	3	-1.8	-0.67	0.06	-0.565	0.01	0.07	8	5	8	6	
HD	175803	51.25	-33	14	8	8.01	0.01	-0.21	2.668	0.63	9.62	-51	12	-27	59	-4
	B3 V	7.87	9	7	9	-1.7	-0.57	0.22	-0.573	0.03	0.09	17	12	23	18	15.8
HD	176254	52.19	-7	20	-10	6.74	0.04	-0.20	2.653	0.41	9.75	2	10	-40	41	-14
	B2 IV	7.73	4	13	12	-2.1	-0.55	0.24	-0.567	0.02	0.06	14	14	25	24	
HD	176502	70.89	-19	5	0	6.21	-0.16	-0.21	2.667	0.35	9.89	-11	-1	-6	12	
	B4 IV	16.00	8	4	3	-1.7	-0.66	0.05	-0.554	0.02	0.10	8	6	9	8	
HD	176582	69.52	-7	-3	12	6.40	-0.17	-0.24	2.692	0.30	9.90	-18	11	12	24	-18
	B3 V	15.35	10	5	4	-1.2	-0.71	0.07	-0.599	0.02	0.08	10	7	10	9	
HD	176818	53.27	-9	-3	-12	7.04	0.13	-0.25	2.625	0.58	9.67	-1	-1	5	6	-18
	B2 IV	7.56	13	11	9	-3.0	-0.59	0.38	-0.674	0.03	0.08	19	17	29	28	
HD	176819	52.67	-10	6	18	6.68	0.02	-0.27	2.629	0.56	9.67	-47	32	9	58	-17
	B2 IV	7.26	8	7	6	-3.0	-0.70	0.29	-0.711	0.03	0.07	11	11	19	11	
HD	176871	57.62	2	-9	-9	5.66	-0.08	-0.19	2.687	0.20	9.89	15	8	6	18	
	B5 V	9.66	11	6	5	-1.2	-0.55	0.11	-0.497	0.01	0.03	9	6	9	9	
HD	176914	59.57	-6	-8	30	7.04	-0.08	-0.23	2.624	0.90	9.58	-110	46	83	146	
	B2 IV	10.55	5	22	16	-3.2	-0.70	0.15	-0.649	0.04	0.16	46	48	84	61	
HD	177003	80.65	-22	29	4	5.37	-0.19	-0.26	2.675	0.22	9.97	-16	1	-18	24	
	B3 V	19.29	9	6	5	-1.5	-0.76	0.05	-0.632	0.01	0.07	9	7	10	10	

	Star	l	RV	μ_α	μ_δ	V	B-V	$(B-V)_o$	β	r	R	U	V	W	S	V_{CaII}
	MK	b	σ(RV)	σ(μ_α)	σ(μ_δ)	M_v	U-B	E_{B-V}	Q	σ(r)	z	σ(U)	σ(V)	σ(W)	σ(S)	W_{CaII}
HD	177006	63.27	-7	12	14	7.26	-0.14	-0.20	2.690	0.45	9.81	-37	25	-5	45	-17
	B4 V	12.21	10	9	10	-1.2	-0.62	0.06	-0.522	0.02	0.10	16	12	20	15	
HD	177109	64.46	-23	-8	3	6.38	-0.12	-0.14	2.594	1.75	9.39	-50	-18	58	78	-17
	B3 II	12.63	6	7	6	-4.9	-0.63	0.02	-0.551	0.08	0.38	34	3]	53	46	
HD	177347	57.30	-24	-29	-28	6.98	-0.03	-0.18		0.36	9.81	40	-44	18	62	-10
	B3 V	9.00	7	11	8	-1.3	-0.53	0.15	-0.508	0.02	0.06	11	11	18	16	
HD	177593	65.12	-24	5	-17	7.30	-0.11	-0.17	2.688	0.48	9.81	17	-16	-26	35	
	B5 V	12.46	6	12	13	-1.3	-0.51	0.06	-0.440	0.02	0.10	20	16	27	23	
HD	178329	72.17	-21	-3	-6	6.48	-0.16	-0.21	2.690	0.35	9.90	1	-9	-2	9	-14
	B3 V	14.97	7	5	5	-1.4	-0.65	0.05	-0.542	0.02	0.09	9	7	10	7	
HD	178475	67.24	-18	-5	-1	5.27	-0.11	-0.16	2.652	0.30	9.89	-4	-5	4	8	
	B5 III	12.66	11	1	1	-2.3	-0.53	0.05	-0.460	0.01	0.07	9	6	7	7	
HD	178540	56.87	-19	-15	-5	6.61	-0.02	-0.19	2.697	0.26	9.86	4	-12	12	17	
	B4 V	7.60	9	22	13	-1.0	-0.51	0.17	-0.496	0.02	0.03	13	15	25	20	
HD	178849	66.10	-8	3	-4	7.03	-0.13	-0.21	2.692	0.38	9.86	0	6	-5	8	
	B3 V	11.81	9	6	5	-1.1	-0.63	0.08	-0.542	0.02	0.08	10	7	12	9	
HD	178912	64.75	-15	-23	-2	8.34	-0.16	-0.25	2.627	1.62	9.43	22	22	125	138	-11
	B3 IV	11.10	9	10	11	-3.0	-0.82	0.09	-0.692	0.07	0.31	56	43	74	69	21.9
HD	180124	57.77	-34	5	-10	7.20	-0.00	-0.20	2.691	0.36	9.82	-6	-20	-17	27	
	B4 V	6.45	9	5	5	-1.2	-0.52	0.20	-0.518	0.02	0.04	9	7	10	9	

Star	l	RV	μ_α	μ_δ	V	B-V	$(B-V)_o$	β	r	R	U	V	W	S	V_{CaII}
MK	b	σ(RV)	σ(μ_α)	σ(μ_δ)	M_V	U-B	E_{B-V}	Q	σ(r)	z	σ(U)	σ(V)	σ(W)	σ(S)	W_{CaII}
HD 180163	70.61	-9	0	3	4.39	-0.15	-0.19	2.634	0.26	9.92	50	-7	7	3	-13
B2 IV	12.74	7	2	2	-2.8	-0.65	0.04	-0.545	0.01	0.05	6	5	7	6	
HD 180844	65.34	-30	8	-8	7.23	-0.11	-0.19	2.688	0.40	9.84	66	-6	-14	-20	
B4 V	9.62	6	9	6	-1.3	-0.55	0.17	-0.473	0.02	0.07	10	10	16	14	
HD 181164	59.14	-8	3	8	7.53	-0.02	-0.27	2.654	0.57	9.72	-27	17	5	33	-14
B2 V	6.12	4	11	8	-2.1	-0.70	0.25	-0.689	0.03	0.06	16	16	27	16	
HD 181409	65.81	21	-17	-32	6.59	-0.19	-0.28	2.610	1.00	9.64	143	-34	-2	148	-19
B2 IV	9.31	8	13	11	-3.7	-0.91	0.09	-0.778	0.04	0.16	37	33	56	37	
HD 181492	64.55	-19	5	-4	6.82	-0.08	-0.20	2.692	0.32	9.87	-5	-3	-9	11	
B3 V	8.60	5	12	13	-1.1	-0.59	0.16	-0.532	0.01	0.05	14	11	18	16	
HD 182568	62.91	-21	17	14	4.98	-0.11	-0.25	2.667	0.18	9.92	-20	3	-6	22	-15
B3 IV	6.63	9	3	3	-1.7	-0.72	0.14	-0.647	0.01	0.02	8	5	7	8	
HD 183339	89.42	-22	-23	11	6.57	-0.14	-0.17	2.706	0.29	10.00	-15	-14	18	27	
B5 V	18.44	9	2	2	-0.9	-0.54	0.03	-0.438	0.01	0.09	8	5	7	7	
HD 183535	69.75	14	-3	-12	8.64	-0.16	-0.29	2.612	2.43	9.44	80	-10	-34	87	-18
B1 V	9.09	10	15	12	-3.7	-0.91	0.13	-0.794	0.11	0.38	103	92	152	113	21.9
HD 183649	68.38	-45	5	18	8.81	-0.12	-0.20	2.674	1.03	9.67	-117	1	19	119	-85
B3 V	8.25	10	15	11	-1.5	-0.62	0.08	-0.532	0.05	0.15	42	39	64	42	
HD 184171	67.97	-22	-3	0	4.73	-0.14	-0.20	2.656	0.20	9.93	-6	-7	1	9	-22
B3 IV	7.43	2	2	2	-2.0	-0.65	0.06	-0.555	0.01	0.03	4	4	5	4	

Star	l	RV	μ_α	μ_δ	V	B-V	$(B-V)_o$	β	r	R	U	V	W	S	V_{CaII}
MK	b	σ(RV)	σ(μ_α)	σ(μ_δ)	M_V	U-B	E_{B-V}	Q	σ(r)	z	σ(U)	σ(V)	σ(W)	σ(S)	W_{CaII}
BD 34 3631	69.16				10.16	-0.11	-0.20:		2.98:	9.36:					
B2 V	6.90				-2.5:	-0.88	0.09:	-0.801	0.32:	0.36:					
HD 185780	74.14	-5	-29	-32	7.75	-0.09	-0.28	2.589	2.34	9.63	355	-110	47	374	-25
B0.5 II	9.06	18	24	14	-4.7	-0.92	0.19	-0.854	0.11	0.37	139	138	222	141	
LS2 39 02	74.01							2.655							
	8.09														
HD 186618	80.48	11	-15	-15	7.76	-0.20	-0.28	2.590	2.64	9.91	161	-10	29	164	-5
B0 III	11.49	7	21	12	-4.6	-0.98	0.08	-0.834	0.12	0.53	141	137	217	144	23.4
HD 186994	78.61	14	-24	14	7.50	-0.12	-0.25	2.571	3.60	9.93	-162	-6	369	403	-11
B1 Ib	10.06	30	26	15	-5.7	-0.93	0.13	-0.840	0.16	0.63	240	231	366	349	28.0
HD 187035	78.59	65			8.83	-0.04	-0.16	2.674	1.07	9.85					
B5 IV	10.00				-1.7	-0.45	0.14	-0.423	0.05	0.18					
HD 225822	73.38	31	2	-18	9.67	0.01	-0.25	2.624	2.44	9.59	120	13	-113	166	23
B2 III	6.66	16	15	11	-3.1	-0.69	0.26	-0.688	0.11	0.28	105	92	147	126	
BD 43 3371	78.36							2.619							
	9.28														
HD 187879	75.21	-4	-8	-6	5.68	-0.04	-0.22	2.582	1.10	9.78	17	-2	13	22	-16
B2 II	7.13	8	4	3	-5.1	-0.78	0.18	-0.748	0.05	0.14	14	12	18	16	9.1
HD 188209	81.01	-6	-4	0	5.64	-0.08	-0.21	2.553	2.37	9.91	-43	8	28	52	-10
O9.5 Ia	10.09	6	7	5	-6.7	-0.98	0.14	-0.917	0.11	0.42	49	43	66	55	26.9

Star	l	RV	μ_α	μ_δ	V	B-V	$(B-V)_o$	β	r	R	U	V	W	S	V_{CaII}
MK	b	σ(RV)	σ(μ_α)	σ(μ_δ)	M_v	U-B	E_{B-V}	Q	σ(r)	z	σ(U)	σ(V)	σ(W)	σ(S)	W_{CaII}
HD 188252	81.82	-18	-5	-5	5.92	-0.19	-0.25	2.603	0.88	9.91	3	-7	1	8	-10
B2 III	10.51	6	5	4	-4.0	-0.85	0.06	-0.719	0.04	0.16	15	12	18	13	
HD 188439	81.79	-65	-20	-7	6.30	-0.11	-0.26	2.582	1.46	9.90	43	-70	47	94	-13
B0.5 II	10.32	9	7	6	-5.0	-0.90	0.15	-0.820	0.07	0.26	35	28	42	33	
HD 188461	76.16	-13	-3	-12	6.98	-0.15	-0.26	2.643	0.64	9.87	19	-5	-12	23	-15
B2 V	7.03	4	7	5	-2.4	-0.77	0.11	-0.663	0.03	0.08	14	12	18	15	
HD 188891	75.54	-26	0	28	7.30	-0.01	-0.74	2.607	1.22	9.77	-170	16	82	189	-48
B2 II	6.19	14	21	13	-3.9	-0.74	0.24	-0.731	0.08	0.15	70	63	100	76	
LS3 45 01	79.83							2.696							
	8.49														
HD 189775	86.04	-16	17	7	6.14	-0.19	-0.20	2.669	0.36	9.98	-28	1	-10	30	
B3V	11.54	7	3	4	-1.7	-0.66	0.01	-0.537	0.02	0.07	8	5	7	8	
HD 189818	91.18	-3	-23	6	7.33	-0.18	-0.24	2.612	1.22	10.09	-25	-8	79	83	-6
B2 IV	14.37	6	6	5	-3.3	-0.83	0.06	-0.693	0.05	0.30	25	21	30	30	
LS3 54 01	88.11							2.679							
	12.65														
HD 189957	77.42	43	-21	17	7.81	0.01	-0.29	2.588	2.01	9.98	-100	58	217	245	-14
B0 III	6.17	6	32	18	-4.6	-0.87	0.28	-0.872	0.09	0.22	171	156	244	230	24.2
HD 190025	78.35	-14	-33	-6	7.53	-0.08	-0.18	2.667	0.63	9.89	35	-16	52	65	-8
B4 IV	6.67	13	16	14	-1.8	-0.54	0.10	-0.493	0.03	0.07	35	27	42	39	

Star	l	RV	μ_α	μ_δ	V	B-V	$(B-V)_o$	β	r	R	U	V	W	S	V_{CaII}
MK	b	σ(RV)	σ(μ_α)	σ(μ_δ)	M_V	U-B	E_{B-V}	Q	σ(r)	z	σ(U)	σ(V)	σ(W)	σ(S)	W_{CaII}
HD 190254	79.69	36	-17	25	8.68	-0.02	-0.19	2.683	0.77	9.89	-66	48	91	122	52
B4 V	7.24	21	19	12	-1.3	-0.51	0.17	-0.498	0.03	0.10	44	37	57	51	
HD 190427	81.04	-1	-30	7	8.35	0.16	-0.27	2.584	2.48	9.92	47	-23	252	252	
B0 III	7.94	5	26	15	-5.0	-0.75	0.43	-0.861	0.12	0.34	214	156	215	214	
BD 42 3570	78.70							2.616							
	6.52														
HD 191781	81.18	-7	19	-7	9.54	0.64	-0.27	2.574	2.54	9.93	-75	38	-179	198	-3
B0 Ib p	6.61	8	26	15	-5.4	-0.41	0.91	-0.880	0.15	0.29	185	162	248	237	29.6
HD 192035	83.33	1	-27	15	8.18	0.06	-0.26	2.575	2.96	10.09	-115	-13	327	347	-17
B0.5 II	7.75	8	10	8	-5.2	-0.80	0.32	-0.843	0.14	0.40	98	78	117	115	25.0
BD 48 3054	84.33	-31													-6
B0 V	8.36														
HD 192575	101.44	-38	-38	-2	6.82	0.17	-0.28	2.611	0.65	10.14	18	-29	26	42	-24
B0.5 V	18.15	7	5	5	-3.7	-0.68	0.45	-0.797	0.03	0.20	14	11	15	13	
BD 46 2877	82.46							2.585							
	6.86														
LS3 50 01	86.35							2.670							
	8.67														
HD 193550	85.46				7.86	0.14	-0.14	2.656	0.68	9.97					
B5 III	7.58				-2.2	-0.31	0.28	-0.390	0.03	0.09					

Star	l	RV	μ_α	μ_δ	V	B-V	$(B-V)_o$	β	r	R	U	V	W	S	V_{CaII}
MK	b	σ(RV)	σ(μ_α)	σ(μ_δ)	M_V	U-B	E_{B-V}	Q	σ(r)	z	σ(U)	σ(V)	σ(W)	(S)	W_{CaII}
HD 235197	87.00							7.6:							-6
	8.00				-1.0										31.1
LS3 54 03	90.24							2.657							
	9.05														
BD 49 3292	87.16	-14			9.06	0.00		2.669							-16
	6.58														
HD 235259	88.00	-26			8.87	0.02		7.0:							-25
	6.60				-1.4										25.8
HD 239436	92.16	-10			8.51	0.26		7.6:							-17
	9.80				-1.0										34.3
LS3 52 01	89.34							2.667							
	7.62														
HD 235271	88.40	0			9.00			5.8:							-8
	6.30				-2.3										30.3
LS3 52 03	88.23							2.595							
	6.48														
LS3 51 01	88.71							2.644							
	6.83														
HD 196421	93.84	-17	-11	-1	8.08	0.10	-0.25	2.635	0.98	10.11	-4	-5	18	19	-19
B2 IV	10.42	7	7	7	-3.0	-0.62	0.35	-0.681	0.05	0.18	28	20	29	28	25.8

Star	l	RV	μ_α	μ_δ	V	B-V	$(B-V)_o$	β	r	R	U	V	W	S	V_{CaII}
MK	b	σ(RV)	σ(μ_α)	σ(μ_δ)	M_V	U-B	E_{B-V}	Q	σ(r)	z	σ(U)	σ(V)	σ(W)	σ(S)	W_{CaII}
HD 235298	88.60	-7			8.40			6.5:							-15
	6.10				-1.8										32.6
HD 197406	89.75				10.30	0.57			9.12	13.16					
WN7	6.50				-6.8	-0.45	0.62		1.15	1.00					
HD 197751	98.91				7.67	0.07	-0.13	2.701	0.42	10.07					
B5 V	12.82				-1.1	-0.31	0.20	-0.345	0.02	0.09					
HD 197770	93.89	-16	-30	6	6.32	0.34	-0.23	2.596	0.63	10.06	1	-10	49	49	-14
B2 II	9.01	10	7	6	-4.5	-0.48	0.57	-0.717	0.04	0.10	17	13	18	18	
HD 197911	98.86	7	-59	12	7.66	0.04	-0.29	2.623	0.83	10.16	6	-1	114	114	13
B2 V	12.64	19	11	8	-3.0	-0.75	0.33	-0.774	0.04	0.18	34	25	36	36	32.8
BD 54 2358	96.76							2.547							
	9.28				-3.7										33.3
BD 53 2481	91.89	28						2.666							
B5 V	7.24														
HD 198512	91.79	-10	-14	3	8.29	0.39	-0.24:		0.94:	10.07:	-10:	1:	37:	39:	-12
B1 Ve	6.43	8	7	7	-3.6:	-0.54	0.63:	-0.828	0.05:	0.11:	27:	19:	27:	27:	27.3
BD 52 2795	91.28							2.681							
	6.49														
HD 235363	92.65	-26			8.42	0.53		3.9:							
	7.15				-3.9										59.3

Star	l	RV	μ_α	μ_δ	V	B-V	$(B-V)_o$	β	r	R	U	V	W	S	V_{CaII}
MK	b	σ(RV)	σ(μ_α)	σ(μ_δ)	M_V	U-B	E_{B-V}	Q	σ(r)	z	σ(U)	σ(V)	σ(W)	σ(S)	W_{CaII}
BD 55 2467	93.31							2.677							
	7.78														
HD 198739	98.71	0	27	-7	7.99	0.03	-0.17	2.697	0.47	10.08	-19	18	-28	39	-13
B5 V	11.69	17	17	14	-1.0	-0.41	0.20	-0.432	0.02	0.09	31	23	32	30	
HD 198781	99.95	-27	-26	-4	6.45	0.06	-0.25	2.577	1.42	10.33	39	-10	40	57	-21
B0.5 V	12.61	5	5	5	-5.3	-0.77	0.31	-0.815	0.07	0.31	29	22	30	29	
HD 198895	93.27	-23			8.32	0.56	-0.26:		0.72:	10.07:					-22
B1 Ve	7.14	4			-3.6:	-0.31	0.82:	-0.729	0.04:	0.09:					21.4
HD 199308	94.20	-23	-20	3	7.51	0.15	-0.28	2.645	0.50	10.05	0	-12	23	26	-18
B2 IV	7.37	3	8	6	-2.4	-0.64	0.44	-0.720	0.02	0.06	14	11	15	14	31.8
HD 199661	94.80	-19	3	13	6.23	-0.17	-0.22	2.682	0.31	10.03	-23	-9	10	27	
B3 V	7.46	7	3	2	-1.4	-0.69	0.05	-0.573	0.01	0.04	5	3	5	5	
HD 199739	94.88	-5	-18	4	7.96	0.47	-0.22	2.658	0.34	10.03	-4	7	17	19	-1
B2 V	7.45	7	7	7	-1.9	-0.25	0.69	-0.580	0.02	10.03	11	7	11	10	
LS3 57 03	96.09							2.661							
	7.83														
BD 55 2523a	95.48	24													7
B2 III	6.06				-3.6										
LS3 57 04	96.82	-75						2.615							-36
B3 Ib	6.55				-5.7										

Star	l	RV	μ_α	μ_δ	V	B-V	$(B-V)_o$	β	r	R	U	V	W	S	V_{CaII}
MK	b	σ(RV)	σ(μ_α)	σ(μ_δ)	M_V	U-B	E_{B-V}	Q	σ(r)	z	σ(U)	σ(V)	σ(W)	σ(S)	W_{CaII}
HD 202107	96.74		-27	-8	7.92	0.14	-0.25	2.658	0.52	10.07					
B2 V	6.42		7	7	-1.9	-0.56	0.39	-0.648	0.02	0.06					
BD 59 2333	98.53	-18	-17	5	8.87	0.14	-0.27	2.665	0.74	10.13	-9	-9	33	35	-24
B2 V	7.98	3	7	7	-1.8	-0.58	0.41	-0.674	0.03	0.10	21	15	21	21	35.7
HD 202214	98.53	-16	0	15	5.64	0.12	-0.29	2.602	0.48	10.08	-35	-11	23	43	-19
B0.5 V	7.99	6	7	7	-4.1	-0.77	0.41	-0.847	0.02	0.07	14	10	14	14	26.9
BD 58 2236	97.80	-17	-20	-2	9.23	0.28	-0.24:	2.593	1.03:	10.19:	18:	-1:	30:	34:	-20
B2 V	7.21	6	7	7	-2.5:		0.52:		0.11:	0.13:	30:	21:	30:	30:	
BD 58 2237	97.76				8.07			2.631							
	7.22														32.6
HD 203025	97.98	-17			6.42	0.22	-0.26:		0.52:	10.08:					-18
B2 IIIe	6.51	1			-3.7:	-0.53	0.48:	-0.691	0.03:	0.06:					
HD 239649	98.85				9.31	0.19	-0.26:		1.98:	10.48:					
B1 V	7.00				-3.6	-0.49	0.45:	-0.629	0.21:	0.24:					
HD 239675	99.47				9.16	0.30	-0.25:		0.71:	10.14:					
B3 V	6.51				-1.7:	-0.25:		-0.471	0.08:	0.08:					
BD 59 2344	98.62	-8	-30	10	8.45	0.50	-0.28:	2.504	0.85:	10.16:	-7:	-3:	72:	72:	-27
B1 Ve	7.56	7	7	7	-3.7:	-0.42	0.78:	-0.776	0.09:	0.11:	25:	18:	25:	25:	30.3
BD 59 2350	99.13	-23	-14	8	9.29	0.35	-0.31	2.643	0.79	10.15	-20	-16	38	46	-16
B1 V	7.54	7	7	7	-2.3	-0.57	0.66	-0.820	0.04	0.10	23	17	23	22	23.5

Star	l	RV	μ_α	μ_δ	V	B-V	$(B-V)_o$	β	r	R	U	V	W	S	V_{CaII}
MK	b	σ(RV)	σ(μ_α)	σ(μ_δ)	M_V	U-B	E_{B-V}	Q	σ(r)	z	σ(U)	σ(V)	σ(W)	σ(S)	W_{CaII}
LS3 59 06	99.22	-31						2.629							-39
B1 III	7.49														
HD 239595	98.50	-11	-18	3	9.27	0.31	-0.28	7.0:	0.55	10.09	-3	0	22	23	-15
B3 V	8.00	9	7	7	-1.3	-0.46	0.59	-0.688	0.03	0.08	17	12	17	17	30.3
LS3 59 07	99.46							2.654							
	7.25														
HD 204150	100.19	-37	77	-15	7.69	0.02	-0.27	2.634	0.82	10.17	-81	-17	-147	169	-8
B2 IV	7.45	6	17	14	-2.8	-0.73	0.29	-0.732	0.04	0.11	54	38	51	52	26.5
HD 203374	100.50	-11	-45	-12	6.69	0.31	-0.29:		0.90:	10.20:	78:	16:	29:	85:	-16
B0 IVe	8.61	15	10	9	-5.0:	-0.74	0.60:	-0.968	0.05:	0.14	36:	26:	36:	36:	27.0
HD 203467	102.74	-18	9	7	5.18	-0.04	-0.11:		0.21:	10.05	-11:	-8:	1:	14:	-14
B3 Ve	10.69	6	4	2	-1.7:	-0.60:		-0.571	0.01:	0.40:	6:	4:	5:	5:	
BD 58 2268	99.49	7	-51	10	9.06	0.52	-0.38	2.632	0.72	10.14	21	17	88	92	-8
B2 V	6.08	24	7	7	-2.8	-0.38	0.80	-0.750	0.04	0.08	24	16	24	24	41.8
BD 59 2384	100.18	-57	-20	1	9.34	0.27	-0.19:		3.75:	11.27:	45:	-22:	129:	139:	-15
B1 II	6.69	13	7	7	-5.0:	-0.60	0.46:	-0.781	0.40:	0.44:	109:	78:	106:	106:	
HD 205139	100.55	-14	-9	3	5.53	0.13	-0.25	2.573	0.84	10.19	-14	-3	20	25	-16
B0.5 III	6.62	5	4	3	-5.3	-0.74	0.38	-0.828	0.04	0.10	13	9	12	12	
BD 61 2158	102.14	8						2.630							-8
B0.5 V	7.68														

Star	l	RV	μ_α	μ_δ	V	B-V	$(B-V)_o$	β	r	R	U	V	W	S	V_{CaII}
MK	b	σ(RV)	(μ_α)	$\sigma(\mu_\delta)$	M_V	U-B	E_{B-V}	Q	σ(r)	z	σ(U)	σ(V)	σ(W)	σ(S)	W_{CaII}
BD 61 2163	102.10	-12						2.650							
	7.34														
HD 206165	102.27	-9	-8	1	4.74	0.29	-0.14	2.560	0.90	10.23	-12	3	14	19	-21
B2 Ib	7.25	5	3	2	-6.4	-0.53	0.43	-0.724	0.04	0.11	11	7	10	10	
HD 206327	102.01	-28	-20	-2	8.68	0.18	-0.27	2.635	0.77	10.20	16	-11	16	25	-18
B2 V	6.76	6	17	14	-2.2	-0.56	0.45	-0.683	0.04	0.10	51	36	47	47	
HD 207198	103.13	-19	-20	3	5.94	0.31	-0.15	2.567	2.16	10.69	7	1	84	84	-19
O9 II	6.98	4	7	7	-7.2	-0.64	0.46	-0.861	0.10	0.26	63	45	61	61	22.7
HD 207308	103.10	-23	-92	-4	7.49	0.25	-0.26	2.597	0.66	10.16	97	5	76	123	-21
B0.5 V	6.81	4	17	14	-4.3	-0.59	0.51	-0.766	0.03	0.08	44	31	40	43	31.1
BD 61 2213	103.90				8.98	0.18	-0.20:		0.78:	10.21:					
B3V+B5V	6.50				-1.7:	-0.45	0.38:	-0.581	0.08:	0.09:					
BD 61 2214	103.90				9.85	0.23	-0.20:		1.08:	10.31:					
B3 V	6.50				-1.7	-0.35	0.43:	-0.518	0.12	0.12:					
BD 61 2215	103.90				9.34	0.19	-0.20:		0.91:	10.26:					
B3 V	6.50				-1.7	-0.49	0.39:	-0.629	0.10:	0.10:					
BD 61 2218	103.90				10.03	0.14	-0.20:		1.34:	10.40:					
B3 V	6.50				-1.7	-0.51	0.34:	-0.612	0.14:	0.15:					
HD 207951	103.23				8.18	0.14	-0.24	2.645	0.71	10.19	-36	0	3	36	-12
B2 V	6.05				-2.3	-0.57	0.38	-0.652	0.02	0.08	49	33	44	49	

Star	l	RV	μ_α	μ_δ	V	B-V	$(B-V)_o$	β	r	R	U	V	W	S	V_{CaII}
MK	b	σ(RV)	$\sigma(\mu_\alpha)$	$\sigma(\mu_\delta)$	M_V	U-B	E_{B-V}	Q	σ(r)	z	σ(U)	σ(V)	σ(W)	σ(S)	W_{CaII}
HD 208106	103.41	-24	-36	-4	7.40	0.14	-0.25	2.650	0.45	10.11	26	-7	15	30	-13
B2 V	6.06	26	17	14	-2.1	-0.56	0.39	-0.655	0.02	0.05	33	22	31	32	26.5
HD 208185	104.21	-24	-5	0	7.38	0.11	-0.22	2.643	0.56	10.15	-5	-12	2	13	-10
B2 V	6.94	15	7	5	-2.4	-0.53	0.33	-0.603	0.03	0.07	17	11	15	12	26.5
HD 208218	103.96	-22	0	22	6.67	0.24	-0.20	2.586	1.03	10.29	-84	-35	82	123	-17
B1 III	6.60	4	7	6	-4.8	-0.52	0.44	-0.687	0.05	0.12	29	20	27	27	
HD 208440	104.02	-14	-30	0	7.92	0.08	-0.28	2.625	0.94	10.27	27	6	38	47	-9
B1 V	6.41	11	17	14	-3.1	-0.72	0.36	-0.772	0.04	0.11	64	44	57	59	
HD 208761	104.43		-6	3	7.64	0.06	-0.29	2.619	0.89	10.26					
B1 V	6.50		4	3	-3.3	-0.75	0.37	-0.788	0.04	0.10					
HD 208904	106.19	-5	18	11	7.54	-0.01	-0.22	2.670	0.52	10.15	-43	-5	11	45	-13
B2 V	8.60	8	7	6	-1.7	-0.60	0.21	-0.592	0.02	0.08	16	11	14	15	25.0
HD 208947	106.56	2	8	-6	6.40	-0.06	-0.26	2.658	0.34	10.10	-21	9	6	24	-9
B2 V	9.00	8	5	4	-1.9	-0.69	0.20	-0.648	0.02	0.05	9	6	8	8	
HD 209178	105.37		-66	-1	8.68	0.23	-0.22	2.685	0.56	10.16					
B3 V	7.17		17	15	-1.5	-0.45	0.45	-0.585	0.03	0.07					
HD 209452	106.81		5	0	8.27	0.15	-0.17	2.668	0.62	10.19					
B4 V	8.70		8	16	-1.7	-0.39	0.32	-0.456	0.03	0.09					
HD 209789	107.64	-10	-27	-9	8.99	0.20	-0.20	2.697	0.80	10.27	32	18	-3	36	-12
B3 V	9.38	40	10	16	-1.8	-0.40	0.40	-0.530	0.04	0.13	44	33	52	42	

Star	l	RV	μ_α	μ_δ	V	B-V	$(B-V)_o$	β	r	R	U	V	W	S	V_{CaII}
MK	b	σ(RV)	σ(μ_α)	σ(μ_δ)	M_v	U-B	E_{B-V}	Q	σ(r)	z	σ(U)	σ(V)	σ(W)	σ(S)	W_{CaII}
HD 210386	106.00	-14	-123	-17	8.00	0.34	-0.28	2.605	0.96	10.30	220	58	82	241	-13
B1 III	6.38	5	17	15	-3.9	-0.54	0.62	-0.780	0.05	0.11	67	47	60	65	31.1
HD 213087	108.50	-15	3	3	5.48	0.37	-0.22	2.567	0.78	10.27	-25	-7	6	27	-11
B0.5 Ib	6.38	5	4	3	-5.9	-0.59	0.59	-0.845	0.04	0.09	14	9	11	13	
HD 213405	108.68	10	-50	-14	7.95	0.47	-0.28	2.605	0.78	10.27	65	50	-2	82	-17
B0.5 V	6.25	19	17	15	-3.9	-0.44	0.75	-0.780	0.04	0.08	56	38	49	50	23.5
HD 213481	109.44	12	-17	-12	8.20	0.55	-0.22	2.593	1.17	10.44	28	49	-34	66	1
B2 II	7.39	20	9	16	-4.6	-0.33	0.77	-0.721	0.08	0.15	53	46	71	55	
BD 65 1774	109.48	-28													-25
B2 II	7.39														
HD 213571	111.42	-18	39	-2	7.16	0.04	-0.26	2.697	0.79	10.31	-53	-16	-33	65	-19
B2 IV	10.53	4	7	5	-3.3	-0.62	0.30	-0.644	0.04	0.15	23	15	18	21	
BD 64 1677	109.10	-25						2.626							-12
B0.5 IV	6.54														
BD 66 1521	110.13							2.592							
	7.83														
BD 66 1548	111.45							2.653							
	7.23														
HD 216992	112.52	-13	8	24	8.04	0.15	-0.20	2.670	0.53	10.21	-38	-22	50	66	-29
B3 V	7.32	3	10	16	-1.7	-0.44	0.35	-0.532	0.03	0.07	25	22	33	29	

Star	l	RV	μ_α	μ_δ	V	B-V	$(B-V)_o$	β	r	R	U	V	W	S	V_{CaII}
MK	b	σ(RV)	σ(μ_α)	σ(μ_δ)	M_V	U-B	E_{B-V}	Q	σ(r)	z	σ(U)	σ(V)	σ(W)	σ(S)	W_{CaII}
HD 217224	112.75	-6	-18	12	8.22	0.33	-0.26	2.636	0.64	10.26	-11	-1	42	43	-7
B2 V	7.81	8	10	16	-2.7	-0.46	0.59	-0.674	0.02	0.09	30	26	40	39	
BD 67 1489	112.61	-106						2.613							-26
B5 III	7.22														
LS3 67 03	113.89							2.603							
	6.49														
LS3 68 01	115.01							2.609							
	7.54														
BD 68 1373	115.20	-36						2.633							-31
B2 III	7.50														
LS3 68 03	115.71							2.655							
	6.57														
BD 67 1531	115.72	-20						2.599							-18
B0.5 V	6.52														
BD 67 1538	116.05							2.659							
	6.66														
BD 67 1546	116.25							2.634							
	6.32														
BD 67 1550	116.46	15						2.606							-2
B2 II	6.78														

Star	l	RV	μ_α	μ_δ	V	B-V	$(B-V)_o$	β	r	R	U	V	W	S	V_{CaII}
MK	b	σ(RV)	σ(μ_α)	σ(μ_δ)	M_V	U-B	E_{B-V}	Q	σ(r)	z	σ(U)	σ(V)	σ(W)	σ(S)	W_{CaII}
BD 68 1386	116.65	-44						2.657							-20
B2 Ib	7.44														
HD 222568	116.50	-14	15	-13	7.67	0.42	-0.26	2.612	0.69	10.32	-20	-3	-46	51	-13
B1 IV	6.36	7	10	16	-3.7	-0.44	0.68	-0.739	0.04	0.08	31	28	44	42	28.1
HD 223959	119.51	16	-11	13	8.39	0.12	-0.21	2.663	0.70	10.35	-22	11	49	54	-55
B3 V	14.09	23	6	9	-1.9	-0.48	0.33	-0.556	0.03	0.17	22	18	28	27	
HD 224395	118.91	-27	-41	-12	7.84	0.13	-0.21	2.667	0.51	10.25	27	4	-25	37	-24
B3 V	10.41	6	15	17	-1.8	-0.50	0.34	-0.575	0.02	0.09	33	26	35	34	18.9
HD 2083	120.91	-12	3	7	6.89	0.03	-0.30	2.610	0.81	10.43	-17	-10	25	32	-9
B1 V	9.03	7	5	4	-3.8	-0.83	0.33	-0.847	0.04	0.13	19	12	14	16	25.3
HD 3366	121.91	-15	69	16	6.95	-0.01	-0.23	2.676	0.35	10.06	-31	-29	23	48	-23
B3 V	10.06	4	13	17	-1.5	-0.62	0.22	-0.623	0.02	0.06	22	17	24	21	
HD 6675	124.48	-6	14	-15	6.90	0.31	-0.28	2.582	1.01	10.60	-47	-7	-68	83	-10
B0.5 III	6.88	3	12	17	-5.0	-0.64	0.59	-0.860	0.05	0.12	55	46	67	63	28.8
HD 7852	125.50	-10	18	1	8.85	0.34	-0.25	2.638	0.82	10.49	-33	-18	9	9	38
B2 V	6.36	15	9	17	-2.6	-0.42	0.59	-0.657	0.04	0.09	38	35	54	38	
LS1 63 198	139.15				12.78	-0.08	-0.34:		32.33:	40.23:					
O9 IV	6.29				-5.6:	-0.99	0.26:	-0.926	1.46:	3.54:					
HD 16440	132.81	-17	32	20	7.88	0.71	-0.08	2.602	1.19	10.84	-7	-29	137	141	-87
B5 II	7.75	38	10	16	-5.0	0.07	0.79	-0.422	0.07	0.16	66	49	70	70	

Star	l	RV	μ_α	μ_δ	V	B-V	$(B-V)_o$	β	r	R	U	V	W	S	V_{CaII}
MK	b	σ(RV)	σ(μ_α)	σ(μ_δ)	M_V	U-B	E_{B-V}	Q	σ(r)	z	σ(U)	σ(V)	σ(W)	σ(S)	W_{CaII}
HD 17179	131.48	27	30	-45	7.86	0.24	-0.23	2.653	0.49	10.32	-87	-6	-71	113	-80
B3 V	12.05	21	15	16	-2.1	-0.45	0.47	-0.620	0.02	0.10	34	24	34	34	
HD 17929	133.89	-59	41	-3	7.86	0.30	-0.14	2.704	0.32	10.22	18	-55	1	58	
B5 V	8.66	4	9	17	-1.1	-0.16	0.44	-0.357	0.02	0.05	19	14	20	15	
LS1 68 19	135.23				11.30	0.63	-0.21:		1.01:	10.72:					
B3 V	9.39				-1.4	-0.09	0.84:	-0.563	0.06:	0.16:					
LS1 68 21	136.06				10.81	0.70	-0.21:		0.79:	10.58:					
B3 V	9.89				-1.6	-0.07	0.91:	-0.599	0.05:	0.14:					
LS1 64 97	138.94				11.28	0.53	-0.27:	-0.726	2.11:	11.66:					
B2 V	6.49				-2.9	-0.33	0.80:		0.12:	0.24:					
HD 21806	139.74	-22	12	-3	7.76	0.32	-0.27	2.624	0.59	10.46	-2	-24	5	24	-11
B1 V(N)	6.50	9	15	12	-3.0	-0.54	0.59	-0.732	0.03	0.07	32	25	36	26	25.0
BD 69 0219	136.61				9.35	0.32	-0.29:		1.90:	11.43:					
B3 II	11.16				-4.0	-0.32	0.61:	-0.556	0.10:	0.37:					
LS1 64 100	140.40				11.40	0.56	-0.26:		1.80:	11.43:					
B2 V	7.60				-2.5:	-0.28	0.82:	-0.699	0.10:	0.24:					
HD 23036	131.60				8.09	-0.01	-0.13		0.60	10.39					
B7 IV	18.58				-1.2	-0.34	0.12	-0.338	0.03	0.19					
HD 23254	141.76	-13	9	2	8.06	0.05	-0.19	2.692	0.48	10.38	2	-10	12	16	8
B5 V	6.21	6	17	14	-1.1	-0.46	0.24	-0.485	0.02	0.05	30	23	34	30	26.5

Star	l	RV	μ_α	μ_δ	V	B-V	$(B-V)_o$	β	r	R	U	V	W	S	V_{CaII}
MK	b	σ(RV)	σ(μ_α)	σ(μ_δ)	M_V	U-B	E_{B-V}	Q	σ(r)	z	σ(U)	σ(V)	σ(W)	σ(S)	W_{CaII}
LS1 61 325	143.09				11.81	0.55	-0.25:		1.83:	11.51:					
B3 V	6.29				-2.0:	-0.23:	0.78:	-0.641	0.10:	0.20:					
HD 25090	143.18	-3	-72	2	7.31	0.32	-0.28	2.602	0.76	10.61	44	84	-67	116	-1
B0.5 III	7.35	6	17	15	-4.0	-0.58	0.60	-0.816	0.04	0.10	47	37	54	45	
HD 25443	143.70	-2	-14	3	6.74	0.33	-0.29	2.594	0.43	10.35	5	13	-1	14	-9
B0.5 III	7.34	3	12	8	-4.4	-0.62	0.62	-0.855	0.02	0.06	17	15	22	15	
HD 25638	143.68	-10	-20	10	7.10	0.40	-0.27:	2.568	1.12:	10.96:	39:	58:	12:	71:	-7
B0 II	7.67	3	9	9	-5.4:		0.67:		0.12:	0.16:	40:	31:	44:	34:	23.0
HD 25639	143.68	-17	-44	-7	6.90			2.569							-8
B0 III	7.67				-5.0:										27.0
BD 59 0804	147.60	-48						2.618							-14
B5 III	7.37														
HD 32343	150.98	-11	-6	-6	5.22	-0.09	-0.19:		0.45:	10.32:	-47:	11:	-14:	51:	
B2 Ve	10.79	6	7	7	-2.5:	-0.73	0.10:	-0.666	0.01:	0.11:	7:	7:	11:	7:	
LS5 57 60	148.96							2.689							
	6.91														
LS5 58 22	149.17							2.656							
	8.92														
LS5 54 14	153.78	-20						2.674							-39
B0 III	6.42														

Star	l	RV	μ_α	μ_δ	V	B-V	$(B-V)_o$	β	r	R	U	V	W	S	V_{CaII}
MK	b	σ(RV)	σ(μ_α)	σ(μ_δ)	M_V	U-B	E_{B-V}	Q	σ(r)	z	σ(U)	σ(V)	σ(W)	σ(S)	W_{CaII}
LS5 53 30	154.59							2.671							
	6.72														
LS5 51 22	156.84							2.605							
	6.03														
BD 52 0913	155.96							2.659							
Sd O ?	7.10														
BD 50 1129	157.88							2.646							-14
B2 III	6.79														
LS5 47 28	161.86							2.696							
	6.24														
BD 48 1263	161.40							2.640							
B2 Ib	6.92														
HD 35250	144.60	-11			8.24	0.21	-0.18:	2.688	0.46:	10.36:					31
B3 V	17.73	27			-1.3:	-0.34	0.39:	-0.468	0.03:	0.14:					
HD 36662	164.86		32	2	8.54	0.11	-0.16:	2.697	0.54:	10.52:					
B5 V	7.04		28	16	-1.0:	-0.33	0.25:	-0.398	0.03:	0.07:					22.7
BD 46 1043	164.96				9.44	0.19	-0.20:		0.95:	10.92:					
B3 V	8.73				-1.7:		0.39:		0.10:	0.14:					
BD 45 1169	166.04				9.96	0.28	-0.20:		1.06:	11.02:					
B3 V	8.57				-1.7:		0.48:		0.11:	0.16:					

Star	l	RV	μ_α	μ_δ	V	B-V	$(B-V)_o$	β	r	R	U	V	W	S	V_{CaII}
MK	b	σ(RV)	σ(μ_α)	σ(μ_δ)	M_V	U-B	E_{B-V}	Q	σ(r)	z	σ(U)	σ(V)	σ(W)	σ(S)	W_{CaII}
BD 43 1369	167.52				8.98	0.31	-0.20:		1.12:	11.09:					
B3 III	7.31				-2.9:		0.51:		0.12:	0.14:					
LS5 44 38	166.55							2.669							
	8.40														
BD 43 1355	168.13	-44						2.677							
B3 III	7.76														
HD 40160	166.04	9	35	-5	7.51	-0.08	-0.22	2.668	0.57	10.54	-7	-43	52	67	
B3 V	11.16	7	15	15	-1.7	-0.64	0.14	-0.583	0.03	0.11	30	24	39	34	
HD 40694	166.57		20	-12	8.32	0.10	-0.13	2.671	0.79	10.76					
B6 III	9.93		26	15	-1.9	-0.30	0.23	-0.351	0.04	0.14					
HD 40784	162.99	-4	-9	17	8.34	0.02	-0.15	2.708	0.55	10.51	19	42	6	47	
B5 V	13.47	28	9	9	-0.9	-0.36	0.17	-0.375	0.03	0.13	26	17	25	19	
HD 41161	164.97	5	12	5	6.77	-0.09	-0.30	2.589	1.44	11.37	6	1	63	64	13
O8 V	12.88	14	8	6	-4.7	-0.97	0.21	-0.900	0.07	0.32	32	31	50	50	19.2
BD 35 1332	176.42				9.30	0.25	-0.30	2.614	1.61	11.60					
B1 V	6.87				-3.5	-0.68	0.55	-0.863	0.08	0.19					
BD 37 1415	174.70	18						2.671							0
B3 V	8.04														
HD 41689	151.92	34	30	-7	8.43	-0.07	-0.28	2.608	3.25	12.79	-86	-162	179	256	8
B1 II	19.34	7	16	14	-4.8	-0.85	0.21	-0.803	0.15	1.08	174	149	222	190	29.6

Star	l	RV	μ_α	μ_δ	V	B-V	$(B-V)_o$	β	r	R	U	V	W	S	V_{CaII}
MK	b	σ(RV)	σ(μ_α)	σ(μ_δ)	M_V	U-B	E_{B-V}	Q	σ(r)	z	σ(U)	σ(V)	σ(W)	σ(S)	W_{CaII}
HD 42782	165.12	3	-3	12	7.18	-0.16	-0.16	2.692	0.47	10.44	8	25	8	27	
B5 V	14.55	9	27	15	-1.2	-0.62	0.00	-0.400	0.02	0.12	26	32	54	34	42.5
LS5 26 25	185.97							2.691							
	6.44														
AAO 50-363	183.76				12.63	0.11	-0.16:		3.57:	13.54:					
B5 V	7.67				-1.0:		0.27:		0.38:	0.48:					
AAO 50-108	182.55				10.88	0.30	-0.16:		1.21:	11.19:					
B5 V	8.77				-1.0:		0.46:		0.13:	0.18:					
HD 257432	184.18				10.13	0.08	-0.20:		1.54:	11.52:					
B3 V	8.26				-1.7:		0.28:		0.16:	0.22:					
HD 45337	184.79				9.12	-0.02	-0.16:		0.86:	10.85:					
B5 V	7.99				-1.0		0.14:		0.09:	0.12:					
AAO 50-165	183.09				10.81	0.21	-0.16:		1.33:	11.32:					
B5 V	8.93				-1.0		0.37:		0.14:	0.14:					
AAO 50-164	182.86				10.78	0.10	-0.24:		4.55:	14.49:					
B2 III	9.00				-3.6:		0.34:		0.49:	0.71:					
BD 24 1337	189.41							2.689							
B5 V	8.45														
LS5 23 73	189.41	39						2.648							
	6.21														

Star	l	RV	μ_α	μ_δ	V	B-V	$(B-V)_o$	β	r	R	U	V	W	S	V_{CaII}
MK	b	σ(RV)	σ(μ_α)	σ(μ_δ)	M_v	U-B	E_{B-V}	Q	σ(r)	z	σ(U)	σ(V)	σ(W)	σ(S)	W_{CaII}
AAO 50 273	183.39				12.49	0.30	-0.16:		2.61:	12.57:					
B5 V	9.91				-1.0:		0.44:		0.27:	0.45:					
BD 24 1306	189.39	38						2.581							4
B5 II	7.14														
HD 46552	181.90	-6	5	11	8.78	0.07	-0.16:		0.64:	10.63:	20:	25:	22:	38:	
B5 V	11.16	6	10	11	-1.0:		0.23:		0.07:	0.11:	22:	18:	30:	23:	
BD 22 1407	191.70	32						2.702							6
B0 II	6.92														
HD 260611	184.99	7	15	3	8.79	0.10	-0.20:		1.34:	11.31:	22:	-19:	77:	82:	14
B3 III	10.26	5	15	11	-2.8:		0.30:		0.20:	0.24:	44:	50:	88:	84:	35.7
HD 48029	195.11	17	11	-10	8.60	-0.09	-0.28	2.607	2.28	12.20	52	-141	45	157	51
B2 IV	6.48	21	7	9	-3.8	-0.84	0.19	-0.775	0.10	0.26	56	41	78	47	
BD 23 1436	190.90	16						2.636							18
B3 III	7.68														
HD 48532	194.29	3	5	15	8.68	-0.08	-0.19	2.698	0.73	10.71	8	43	35	56	
B5 V	7.55	8	8	8	-1.0	-0.56	0.11	-0.499	0.03	0.10	17	15	28	21	20.4
HD 48549	192.45	-3	0	3	8.68	-0.11	-0.22	2.630	1.68	11.62	19	24	3	31	
B2 V	8.49	31	8	8	-2.8	-0.70	0.11	-0.621	0.07	0.21	45	36	62	40	
HD 49763	195.73				9.38	-0.14	-0.21	2.677	1.35	11.29					
B3 V	8.44				-1.5	-0.66	0.07	-0.557	0.06	0.20					

Star	l	RV	μ_α	μ_δ	V	B-V	$(B-V)_o$	β	r	R	U	V	W	S	V_{CaII}
MK	b	σ(RV)	σ(μ_α)	α(μ_δ)	M_V	U-B	E_{B-V}	Q	σ(r)	z	σ(U)	σ(V)	σ(W)	σ(S)	W_{CaII}
HD 50003	198.11		9	-6	8.06	-0.09	-0.14	2.702	0.63	10.60					
B5 V	7.59		7	9	-1.1	-0.40	0.05	-0.338	0.03	0.08					
HD 50320	198.97		-8	-13	8.47	-0.14	-0.16	2.687	0.87	10.82					
B5 V	7.56				-1.3	-0.51	0.02	-0.405	0.04	0.11					
HD 50767	191.72	-51	-6	-19	7.70	-0.21	-0.23	2.613	1.85	11.78	72	-121	-132	193	
B2 III	11.55	35	8	8	-3.7	-0.84	0.02	-0.672	0.08	0.34	51	40	68	56	
HD 53879	207.01	-17	-27	17	9.66	-0.09	-0.24:		3.60:	13.28:	-192:	432:	-277:	548:	
B2 III	7.36	31	12	12	-3.6:	-0.60	0.15:	-0.536	0.38:	0.46:	118:	105:	200:	137:	
HD 57291	213.08	7	5	-16	6.88	-0.16	-0.22	2.650	0.60	10.50	35	-30	-8	47	
B3 IV	8.15	3	11	11	-2.2	-0.72	0.06	-0.596	0.03	0.08	18	16	30	18	
HD 58784	214.82	36	-4	2	8.57	-0.07	-0.21	2.660	0.96	10.80	-21	11	-7	25	21
B3 V	9.08	22	11	11	-1.8	-0.61	0.14	-0.563	0.04	0.15	34	27	48	34	31.3
HD 58973	219.85	-3	-11	4	7.85	-0.13	-0.19	2.670	0.74	10.58	-3	43	-26	50	
B3 V	6.66	3	13	13	-1,7	-0.62	0.06	-0.525	0.03	0.09	27	23	43	30	
HD 59882	222.54	45	-2	0	8.80	-0.17	-0.28	2.602	3.09	12.44	-14	25	-13	31	
B1 IV	6.38	5	13	13	-4.0	-0.92	0.11	-0.804	0.18	0.34	113	93	177	115	
AAO 99-312	220.19				12.68										
B2 V	12.35														
AAO 99-326	220.24				12.03	0.01	-0.20:		4.09:	13.30:					
B3 V	12.61				-1.7		0.21:		0.43:	0.89:					

Star	l	RV	μ_α	μ_δ	V	B-V	$(B-V)_o$	β	r	R	U	V	W	S	V_{CaII}
MK	b	σ(RV)	σ(μ_α)	σ(μ_δ)	M_V	U-B	E_{B-V}	Q	σ(r)	z	σ(U)	σ(V)	σ(W)	σ(S)	W_{CaII}
BD-00 1848	221.07				10.90	0.21	-0.20:		1.81:	11.39:					
B3 V	13.18				-1.7:		0.41:		0.19:	0.41:					
HD 60848	202.53	28	-8	-10					2.54:	12.27:	-9:	-78:	-133:	154:	13
O8 Ve	17.53	8	7	9			0.14:								17.3
AAO 99-226	219.91				12.48	0.13	-0.20:		4.22:	13.38:					
B3 V	14.90				-1.7:		0.33:		0.45:	1.08:					
AAO 99-263	220.86				11.91	0.23	-0.20:		4.04:	13.21:					
B2 V	14.89				-2.5:		0.43:		0.43:	1.04:					
HD 64854	220.70				9.27	-0.06	-0.24:		2.88:	12.25:					
B2 IIIe	14.14				-3.6:		0.18:		0.31:	0.70:					
HD 65875	223.65	42	-18	10	6.56	-0.07	-0.07:		0.45:	10.32:	-47:	11:	-14:	51:	
B3 Ve	14.01	20	7	7	-1.7:	-0.83	0.00:	-0.780	0.02:	0.11:	14:	10:	16:	14:	
HD 66594	225.81	13	-11	-2	7.57	-0.14	-0.15	2.650	0.97	10.68	-16	19	-43	50	9
	13.80	11	13	13	-2.4	-0.52	0.01	-0.425	0.04	0.23	40	30	53	+9	18.1
HD 66665	215.76	18	-8	-28	7.80	-0.26	-0.29	2.592	3.03	12.43	115	-277	-273	406	-8
B0.5 III	19.13	6	12	12	-4.7	-1.04	0.03	-0.856	0.13	0.99	114	84	152	123	

Notes on Table (7.2.1)

BD 34°3631 - The existence of this star, a B2V star, in the region surveyed, escaped the writer's notice until the catalogue of Neckel (1967) was consulted.

HD 198512 - This star was not originally included in the observing list as it was classified "peculiar" in the HD catalogue. However in the "Remarks" at the end of the catalogue, it is mentioned that it is a late O or early B type star and that the spectrum is almost a continuum.

HD 235363 - This star is thought to be a binary, the secondary being a G-star (Crampton et al., 1973). It is assumed that the secondary will be much fainter than the primary, and so have little effect on the observations.

BD 61°2213 - This star is thought to have a secondary component of spectral type B5V. Thus the distance could be in error.

BD 61°2214 - Petrie & Lee (1966) obtain $M_V = -3^m.7$.

HD 34233 - Neckel (1967) quotes a spectral type B3IV for this star with $M_V = -2^m.5$, and a corresponding distance of 0.42kpc.

BD 52°0913 - The spectrum is apparently without absorption lines.

HD 42782 - Petrie & Lee (1966) obtain $M_V = -2^m.8$.

HD 60848 - The distance is quoted from Neckel (1967) and is probably unreliable as the star is a variable (Kukarkin et al., 1969).

HD 66665 - Petrie & Lee (1966) obtain $M_V = -3.8$

HD 197406 - Since this star is a Wolf Rayet, the reddening and distance determinations by Smith (1968) have been adopted.

The distances of the programme stars which were observed by Haug (1970b), were redetermined, using the procedure already described (§2.2), assuming the values for M_V and $(B-V)_o$ quoted by Haug. The reason for this is that Haug (1970b) adopted the relation

$$R = 3.20 + 0.21\ (B-V)_o \quad - - - - - - - - - \quad (7.2.1),$$

which was proposed by Schmidt-Kaler (1965c), whereas in this analysis $R = 3.2$ has been adopted (§2.3). Similarly, the programme star distances determined by Neckel (1967), based on the assumption that $R = 3.1$, were also redetermined. All the programme stars that have been considered by Neckel (1967), with the exception of BD 34°3631, are emission line stars listed by Wackerling (1970), and so they were not observed by the writer. They are discussed in the notes to Table (7.2.1). There are also other stars in the region of the galaxy surveyed by Kepner (1970), which have been considered by Neckel (1967), but are not considered here as they are binaries, in which the difference in magnitude between the two components is small.

7.3 Associations of OB Stars

7.3.1 Introduction

Two or more programme stars having almost equal galactic co-ordinates, distances and space motions are likely to be physically connected in some way. It is possible that they are the most luminous members of a galactic cluster or OB-association. Furthermore, OB associations are of special interest, not only because of their relevance to large scale galactic structure and evolution, but also because they are good indicators of spiral structure (Rohlfs, 1967).

Consequently, the catalogue of Sulentic & Tifft (1970) was searched for galactic clusters in the region of the galaxy under consideration. The Catalogue of Star Clusters and Associations (Alter et al., 1970) was then searched, together with the references cited therein, to establish the nature of these clusters. After eliminating all the clusters which were not OB-associations, only NGC 1502 and NGC 7160 remained.

7.3.2 NGC 1502

The OB-association, NGC 1502 ($l = 143°.70$, $b = 7°.60$), is a small cluster containing only nine stars of type B3 or earlier. The stars HD 25638 and HD 25639, which constitute a visual binary as already discussed (§7.1), are the most luminous stars in the cluster. Two-colour photographic photometry of 50 stars in this cluster, together with spectral types by Trumpler for 31 of them, is given by Zug (1933). These data have enabled Johnson et al. (1961), to derive a distance of 880 ± 150 pc. for the cluster, which agrees within the limits of observational error with the distance of 1120 ± 120 pc, derived in this analysis for HD 25638. Since the estimated distance of this star from the galactic plane is 157 pc, the whole cluster is $\sim$ 150pc. above the galactic plane. It would be worthwhile making Hβ, UBV and radial

velocity observations of the seven B2 and B3 stars, as it is evidently a young cluster.

The stars HD 25090 and HD 25443 have galactic coordinates which would qualify them as candidates for membership of NGC 1502. However, their distances are 760 pc. and 430pc. respectively. Moreover, the values of E_{B-V} obtained for both of these stars are almost the same, being 0.60 ± 0.03 for HD 25090 and 0.62 ± 0.03 for HD 25443. This suggests that the interstellar absorption in the direction of NGC 1502 lies in two distinct layers. One layer lies between the sun and a distance of 400pc., and the other lies between 800pc. and 1100pc., there being virtually no interstellar absorption between 400pc. and 800pc. This confirms the results of Kiefer & Baker (1941).

7.3.3 Cepheus OB2

The cluster NGC 7160 is part of a vast complex of OB stars known as Cepheus OB2, which extends from $l = 96°$ to $l = 106°$, and from $b = +2°$ to $b = +8°$. This can be seen clearly by the concentration of stars around $l = 100°$, $6° < b < 8°$ as depicted in Fig (8.1.1). Cepheus OB2 has been considered in detail by Simonson III (1968). The distance of NGC 7160 ($l = 104°.0$, $b = 6°.5$) was estimated as 840pc. by Johnson et al. (1961). Unfortunately this distance has been incorrectly quoted by Neckel (1967).

The programme stars located in the part of Cepheus OB2 which overlaps the area of the Galaxy under consideration are listed in Table (7.3.3.1). The distances of these stars differ from those given by Simonson III (1968), because a different ratio of total to selective absorption has been adopted and, in most cases, because the B-Q method (§2.2) has been adopted to determine the absolute magnitude and $(B-V)_o$ instead of using the MK Spectral Type. The distances of these stars is plotted as a function of galactic longitude, as depicted Fig (7.3.3.1). Excluded from this diagram, is the distant star HD 239681.

All the stars listed in Table (7.3.3.1) are considered to be members

The Distance - Galactic Longitude Diagram for Possible Members of Cepheus OB2

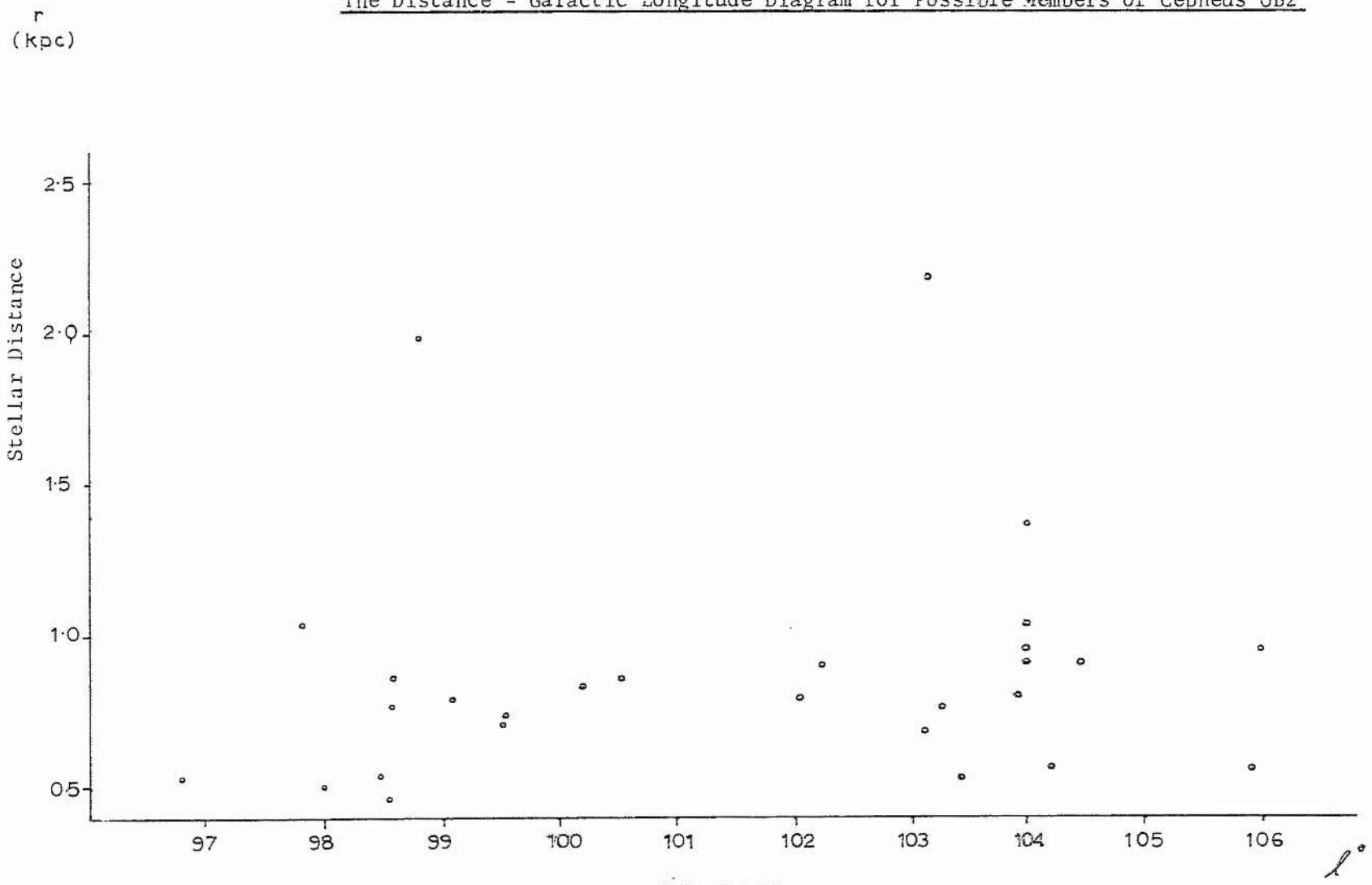

FIG 7.3.31

Table 7.3.3.1

Programme Stars Possibly Connected with Cepheus OB2

Star	l	b	E_{B-V}	r	σ(r)	U	V	W	σ(U)	σ(V)	σ(W)
				pc.	pc.	km/s	km/s	km/s	km/s	km/s	km/s
LS3 57 03	96.09	7.83									
HD 202107	96.74	6.42	0.39	520	24						
BD 58 2236	97.80	7.21	0.52	1030	111	18	-1	30	30	21	30
HD 203025	97.98	6.51	0.48	520	25						
HD 239595	98.50	8.00	0.59	550	28	-3	0	22	17	12	12
BD 59 2333	98.53	7.98	0.41	740	35	-9	-9	33	21	15	21
HD 202214	98.53	7.99	0.41	480	23	-35	-11	23	14	10	14
HD 239618	98.62	7.56	0.78	850	90	-7	-3	72	25	18	25
HD 239649	98.85	7.00	0.48	1980	211						
HD 239626	99.13	7.54	0.66	790		-20	-16	38			
HD 239675	99.47	6.51	0.50	710	77						
HD 239676	99.49	6.08	0.80	720	39	21	17	88	24	16	24
HD 239681	100.18	6.69	0.46	3750	403	45	-22	129	109	78	106
HD 204150	100.19	7.45	0.29	820	37	-81	-17	-147	54	38	51
HD 205139	100.55	6.62	0.38	840	39	-14	-3	20	13	9	12
HD 206327	102.01	6.76	0.45	770	37	16	-11	16	51	36	47
HD 206165	102.27	7.25	0.15	900	43	-12	3	14	11	7	10
HD 207308	103.10	6.81	0.51	660	32	97	5	76	44	31	40
HD 207198	103.13	6.98	0.46	2160	103	7	1	84	63	45	61
HD 207951	103.23	6.05	0.38	710	33	-36	0	3	49	33	44
HD 208106	103.41	6.06	0.39	450	21	26	-7	15	33	22	31
HD 208218*	103.96	6.60	0.44	1030	49	-84	-35	82	29	20	27
BD 61 2213*	103.9	6.5	0.38	780	143						
BD 61 2214*	103.9	6.5	0.43	1080	97						
BD 61 2215*	104.0	6.5	0.39	910	116						
BD 61 2218*	104.0	6.5	0.34	1340	84						
HD 208440*	104.02	6.41	0.36	940	44	27	6	38	64	44	57
HD 208185	104.21	6.94	0.33	560	26	-5	-12	2	17	11	15
HD 208761	104.43	6.50	0.37	890	43						
HD 209178	105.37	7.17	0.45	560	27						
HD 210386	106.00	6.38	0.62	960	49	220	58	82	67	47	60

* - denotes that the star is probably a member of the cluster NGC 7160

of Cepheus OB2 by Simonson III (1968), with the exceptions LS3 57-03, HD 202107, BD 58°2236, HD 209178 and HD 210386. These five additional stars lie within the limits of the association decided upon by Simonson III. The faint star LS3 57-03 is a probable member of this association since $\beta = 2^{m}.661$ for this star, which suggests that it is not very luminous. A possible reason for excluding HD 210386 is that it appears to be a high velocity star, and will be discussed later (§7.4). The distance determinations of the other three stars, and the space velocity components of BD 58°2236, seem to be appropriate for membership of Cepheus OB2.

The star HD 204150 has a very high velocity towards the galactic plane (W = -149 ± 51 km/sec), which is surprising in view of its galactic latitude (b = 7°.45). The distance and reddening determinations place it within the association. However, it is the only star listed in Table (7.3.3.1) with a negative W velocity component, and this makes it unlikely that it was formed within the association. It is possible that this star condensed from a high velocity cloud (§9.5), and that through a near encounter, it has been captured by Cepheus OB2.

The results of a 21cm survey by Kepner (1970) suggest that, at the galactic longitude of Cepheus OB2, an observer is looking longitudinally along the Intermediate Arm. If this interpretation is correct, then the existence of distant luminous stars beyond Cepheus OB2 is to be expected. The stars HD 239649, HD 207198 and HD 239681 appear to be more distant than the other stars listed in Table (7.3.3.1), and the possibility of their being in the Intermediate Arm has to be considered. The occurrence of these stars in the Intermediate Arm at these galactic longitudes would be consistent with the high HI intensity reported by Kepner.

The values of E_{B-V}, on the other hand, suggest that these stars are members of Cepheus OB2, as they are no higher than the reddening values obtained for members of the association. Thus if these three stars do lie in the Intermediate Arm, then it would appear that there would have to be"low absorption windows" in the Local and Intermediate Arms at the galactic coordinates of these stars. The distance of HD 239649 is based on an absolute magnitude determined from its MK spectral type, and if this is in error, due to a misclassification,

the star may be much closer. Similarly, if there is any hitherto undetected emission at Hβ in the spectrum of HD 207198, then this star too will be closer than suggested.

There appears to be a gap in the star concentration at $l \sim 101$, a fact apparently unnoticed by Simonson III (1968). This can be seen from Fig. (7.3.3.1). If this implies a reduction in the dust density, then $E_{B-V} = 0.46$ for HD 239681 at a distance of 3.75kpc is reasonable. The only direct evidence for this is the anomalous velocity star HD 204150, for which $E_{B-V} = 0.29$ at a distance of 820pc.

Indirect evidence in support of small reddening at $l \sim 101°$ is to be found from neutral hydrogen surveys, since there appears to be a correlation between the concentrations of HI and dust (§8.4). Neutral hydrogen surveys by Lindblad (1966) and Weaver & Williams (1973) suggest that the HI density reaches a minimum at $l \sim 101°$, over the galactic longitude range covered by Cepheus OB2. Thus it seems reasonable to believe that there is a "low absorption window" at $l \sim 101°$. The radial velocity of this star is -57 km/sec (HD 239681 = BD 59°2384, Table 7.2.1), which suggests, on the basis of a kinematic distance estimate, using equation (2.4.1.2), that the distance of 3.75 kpc is correct. The possibility that HD 239681 is subluminous, and therefore much closer, can be more or less ruled out.

Among the remaining stars in Table(7.3.3.1) which have not been discussed above, and are not members of NGC 7160, there appears to be little or no correlation between E_{B-V} and distance, suggesting that the greater part of the reddening is caused by dust between the sun and the association, rather than by dust in the association itself. On dividing these remaining stars into five groups as indicated in Table (7.3.3.2), a correlation between E_{B-V} and l, for a given b, was noticed. The reddening attains maxima at $l \sim 99°$ and $l \sim 103°$, and minima at $l \sim 96°$, $l \sim 101°$, and $l \sim 106°$.

This shows that there are small contributions to the interstellar reddening from dust within Cepheus OB2, and that this effect shows a large variation from place to place within the association. The areas of maximum dust concentration correspond to the areas of highest HI concentrations (Weaver & Williams, 1973).

Table 7.3.3.2

A Division of Probable Members of Cepheus OB2 into Groups by their Galactic Coordinates

Group 1: ($96^\circ < l < 101^\circ$; $6.4^\circ < b < 7^\circ$)

Star:	HD 202107	HD 203025	HD 239675	HD 205139
E_{B-V}:	0.39	0.48	0.50	0.38

Group 2: ($101^\circ < l < 106^\circ$; $6.4^\circ < b < 7^\circ$)

Star:	HD 206327	HD 207308	HD 208185	HD 208761
E_{B-V}:	0.45	0.51	0.33	0.37

Group 3: ($96^\circ < l < 106^\circ$; $6^\circ < b < 6.4^\circ$)

Star:	HD 239676	HD 207951	HD 208106
E_{B-V}:	0.80	0.38	0.39

Group 4: ($96^\circ < l < 101^\circ$; $7^\circ < b < 8^\circ$)

Star:	BD 58 2236	HD 239595	BD 59 2333	HD 202214
E_{B-V}:	0.52	0.59	0.41	0.41

Star:	HD 239618	HD 239626	HD 204150
E_{B-V}:	0.78	0.66	0.29

Group 5: ($101^\circ < l < 106^\circ$; $7^\circ < b < 8^\circ$)

Star:	HD 206165	HD 209178
E_{B-V}:	0.15	0.45

Another interesting point, worthy of note, is that in the half of the association for which $l < 101°$, there seems to be an increase of reddening with increasing galactic latitude. This can be seen from a comparison of Group I and Group 4 stars (Table 7.3.3.2). Moreover, no luminous OB stars brighter than the limiting magnitude of the survey ($V \sim 12^{m}.0$) are to be found between $96° < l < 101°$ and $8° < b < 11°.5$. The distances of the stars HD 197751 ($l = 98°.91$, $b = 12°.82$), HD 198739 ($l = 98°.71$, $b = 11°.69$) and HD 197911 ($l = 98°.86$, $b = 12°.64$) are such that they do not exclude the possibility that these stars are associated with Cepheus OB2.

The high latitude neutral hydrogen survey by Heiles & Habing (1974) indicates that the HI concentration reaches a maximum at $b = 10°.6$ for $l = 99°$. As there seems to be a correlation between the dust and HI densities (§8.4), it seems probable that the dust density would also reach a maximum at this point. Thus a dense dust cloud may exist in the region $96° < l < 101°$, $8° < b < 11°.5$, which obscures the luminous stars behind, which may well constitute another cluster within the Cepheus OB2 association. The stars HD 197751, HD 198739 and HD 197911 would then presumably be the high latitude limit of Cepheus OB2. In fact no such dust cloud was found by Lynds (1962) but an HII region is found from Hα surveys. Consequently, searches, using radio techniques for formaldehyde and OH, which are usually found associated with dust clouds, should be carried out. A detailed H109-α survey which could establish the existence of any faint HII regions, would also be useful. The results of such surveys, as they are relevant to the large scale structure of the Galaxy in the region of interest, together with the appropriate references, are considered later, (§8.1, §8.2).

The stars HD 239595, BD 59°2333 and HD 202214 are physically very close together, and appear to be moving as a group. This suggests that these stars had a common origin, although their motion normal to the galactic plane is comparable with that found in the majority of the stars in this association. The stars HD 207308, HD 239676 and HD 239618 have much higher velocities normal to the plane, and it is conceivable that these stars were originally formed in the galactic plane, and were subsequently ejected from it. They are considered

in a more general context later (§7.4., §9.4).

There appears to be some correlation between the distance and E_{B-V} for the stars which are members of NGC 7160, which is a cluster within the Cepheus OB2 complex. This indicates that the greater proportion of the reddening is due to dust in the cluster itself. The distance estimate of BD 61°2218 is almost certainly erroneous on account of the apparently low E_{B-V}. Weak helium lines have been noticed in the spectrum of this star by Simonson III (1968), and it is possible that an incorrect absolute magnitude has resulted from a wrong spectral type being adopted.

The star HD 208218 appears to have a high velocity normal to the galactic plane, and although its galactic coordinates and distance suggest that it is a member of NGC 6160, it is unlikely that this star was formed in the cluster unless the cluster itself turns out to have a comparable velocity normal to the galactic plane. The space motions of HD 208440 are not significantly different from zero, and so a comparison is rather meaningless. Accurate distances and radial velocities must be obtained for the stars BD 61°2213, BD 61°2214, BD 61°2215 and BD 61°2218, before a more detailed analysis of NGC 7160 can be made.

The possible connection between the association Cepheus OB2 and the Intermediate Arm is considered later. It is of vital importance that any such connection should be investigated because of the implications for an understanding of large scale galactic structure. There are additional stars, listed in Table (7.2.1), which lie within the limits of the association given by Simonson III (1968). Observations of these are needed to determine distances and radial velocities. The more luminous of these stars are probably located in the Intermediate Arm.

7.3.4 Other Associations

From a list of known OB-associations (Trans. I.A.U., 12B, 336, 1964), the associations Cyg OB7, Cam OB1, Cyg OB5 and Ceph OB4 might

extend into the region of the Galaxy under consideration. None of the stars listed in Table (7.2.1) have galactic coordinates which would place them in the direction of either Cam OB1 or Ceph OB4. This suggests that these associations may not in fact extend into the region of the Galaxy of interest.

The only possible member of Cyg OB5, among the stars listed in Table (7.2.1), is BD 31°3631. The estimated distance of this star is 2.08kpc, and so it is unlikely to be associated with Cyg OB5, since the listed distance for this association is 1.61 kpc. This suggests that there is either an error in distance determination, or that Cyg OB5 does not extend into the region of the Galaxy of interest.

A list of programme stars which lie in the direction of Cyg OB7 is given in Table (7.3.4.1). No comment is entered into the table for stars which are established members of the association, that is stars whose distances agree with the accepted distance of Cyg OB7. The distance of the peculiar star HD 198512 may be inaccurate, since it has been determined from the spectral type. Thus it is by no means certain that this star is a member of the association.

The stars HD 199661 and HD 199739 are extremely interesting. Here there is a case of two stars with very similar galactic coordinates and distances and very different values for the interstellar reddening, $E_{B-V} = 0^m.69$ for HD 199739 and $E_{B-V} = 0^m.05$ for HD 199661. Furthermore, HD 199309 is more distant than either of these stars, and is not as heavily reddened as HD 199739, although the galactic coordinates are very similar. Thus it seems that HD 199739 has an abnormally high reddening and is probably a "cocoon star". This type of star has been considered in some detail by Kahn (1974).

Both HD 199661 and HD 199739 are too close to be members of Cyg OB7. No information on distance or motion is as yet available for the stars BD 55°2470, LS5 57-02 and LS5 56-04. Consequently nothing can be said about the possibility of their being located in Cyg OB7.

Table 7.3.4.1

Stars in the Direction of Cygnus OB7

Star	l°	b°	Comments
BD 48°3504	84.33	8.36	Possible Intermediate Arm Star, Radial Velocity = -31km/sec.
HD 193550	85.46	7.58	
LS3 50.01	86.35	8.67	Probable member of Cyg OB7, β=2.670
HD 235197	87.00	8.00	Probable member of Cyg OB7, Radial Velocity = 30 km/sec.
BD 49°3292	87.16	6.58	Probable member of Cyg OB7, β = 2.669
HD 235259	88.00	6.60	Probable member of Cyg OB7, M_V = -1.1
LS3 50-03	88.23	6.48	Possible Intermediate Arm Star, β = 2.595
HD 235271	88.40	6.30	Probable member of Cyg OB7, M_V = -2.3 Radial Velocity = 0 km/sec.
HD 235298	88.60	6.10	Probable member of Cyg OB7, M_V = -1.8
LS3 51-01	88.71	6.83	Probable member of Cyg OB7, β = 2.644
LS3 52-01	89.34	7.62	Probable member of Cyg OB7, β = 2.667
HD 197406	89.75	6.50	Probable Perseus Arm member (§8.2).
BD 52°2795	91.28	6.49	Probable member of Cyg OB7, β = 2.681
HD 198512	91.79	6.43	See text
BD 53°2481	91.89	7.24	Probable member of Cyg OB7, β = 2.666
HD 235363	92.65	7.15	Possible member of Cyg OB7, M_V = -3.9
BD 55°2467	93.31	7.78	Probable member of Cyg OB7, β = 2.667
BD 55°2470	93.39	7.78	See text
HD 197770	93.89	7.24	See text
HD 199308	94.20	7.37	See text
LS3 56-04	94.54	6.85	See text
HD 199661	94.89	7.46	See text
HD 199739	94.88	7.45	See text
BD 55°2523a	95.48	6.06	Probably a member of Cyg OB7, M_V = -3.6
LS3 57-02	95.85	7.98	See text

7.3.5 Interesting Groups of Stars

There are several groups of stars, within which the stars have similar galactic coordinates, and if they prove to have similar distances as well, the possibility of there being some physical connection between them exists. These groups are listed in Table (7.3.5.1), in which V_r and V_{obs} are as defined previously (§2.4, §2.5). A number in the final column refers to a remark at the foot of the table. The neutral hydrogen maps of Weaver & Williams (1973), Lindblad (1966) and Heiles & Habing (1974) were consulted in a search for neutral hydrogen features with the same galactic coordinates and radial velocities as the stars listed in Table (7.3.5.1). The radial velocities of the stars in the groups (HD 213481, BD 65°1774) and (HD 199661, HD 199739) are very different, and no HI feature could be found corresponding to the radial velocity of either star in either group. Therefore it seems unlikely that there is any physical connection between the two stars in these two groups.

A neutral hydrogen feature exists at the galactic coordinates of the group (HD 170028, HD 170051, HD 170111) with a radial velocity of about -24kms/sec. This suggests that the first two stars are physically associated and that the third is not. This seems to be verified by the fact that HD 170111 is closer to the sun than the other two.

Among the remaining groups of stellar pairs, the radial velocity of only one of the stars in each pair is known. A neutral hydrogen feature, with the corresponding galactic coordinates and radial velocity, is found. Thus it seems possible that the stars HD 213087, BD 68°1373, BD 67°1531 and HD 222568 are among the more luminous members of a cluster or an OB association. Distance and radial velocity determinations for the other stars in each pair would be needed to confirm this.

Table 7.3.5.1

Interesting Groups of Stars

Star	l	b	r	E_{B-V}	U	V	W	V_r	V_{obs}	
HD 170028	54.28	16.79	410	0.07	-1	-23	16	-14	-25	
HD 170051	54.50	16.85	440	0.09	-7	-25	33	-14	-24	
HD 170111	54.53	16.79	320	0.09	-7	-5	8	-5	-18	
HD 213087	108.50	6.38	780	0.59	-25	-8	6	1	-15	
LS3 64-04	108.59	6.34								
HD 213481	109.44	7.39	1170	0.77	28	49	-34	8	12	
BD 65°1774	109.48	7.39							-28	
HD 199661	94.80	7.46	310	0.05	-23	-9	10	-6	-19	
HD 199739	94.88	7.45	340	0.69	-4	7	17	9	-5	
LS3 68101	115.01	7.54								
BD 68°1373	115.20	7.50							-36	1
LS3 68-03	115.71	6.57								
BD 67°1531	115.20	6.52							-20	2
BD 67°1546	116.25	6.32								
HD 222568	116.50	6.36	690	0.68	-20	-3	-46	1	-14	

Notes

1) BD 68°1373 - The radial velocity of this star corresponds to that expected for a star in the Intermediate Arm.

2) BD 67°1531 - The radial velocity is rather low for a star in the Perseus Arm. Thus it is probably located in the Local Arm and heavily reddened.

7.4 High Velocity and Possible Runaway Stars

Through the work of Oort (1928), it has been thought that a star in the vicinity of the sun will escape from the Galaxy if it has a velocity component of 65km/sec in the direction of galactic rotation, with respect to its local standard of rest. Using a revised model for the galactic mass distribution, it has been shown by Schmidt (1965), that the escape velocity in the solar neighbourhood is 380kms/sec with respect to the galactic centre. The solar velocity with respect to the galactic centre is 250km/sec. According to Schmidt's model, a star with a velocity of 315 km/sec, with respect to the galactic centre, will merely recede to a distance of 24kpc from the centre of the galaxy.

Therefore any star with a space velocity with respect to the galactic centre of 315 km/sec or more, can be considered to be dynamically unstable in its present position. Such stars are of interest because they may act as indicators of galactic evolution. Furthermore, they could play a vital role in any attempt to determine more accurate force laws in, and perpendicular to, the galactic plane.

These stars are termed, "high velocity stars", for the purposes of this analysis, and they appear to fall into two categories. There are those stars which have a large and negative W velocity component, or alternatively, a large and positive U velocity component. These stars are listed in Tables (7.4.1) and (7.4.2). Their space motions preclude the possibility that they will eventually escape from the Galaxy. Consequently they are considered separately from the other high velocity stars which are listed in Table (7.4.3).

In view of the uncertainties in the mass distribution in the outer regions of the Galaxy, and the consequent limitations of Schmidt's Model, it was decided that the stellar "escape" velocities of 315km/sec and 380 km/sec would be adopted for all stars, regardless of galactocentric distance, as though they were in the solar neighbourhood. This will suffice as a first order approximation, because of the large uncertainties in the space motions. To attain the higher degree of

TABLE 7.4.1

Stars with High Velocities Towards the Galactic Plane or Centre

Star	U	V	W	S*	V_{obs}	CaII (RV)	HI(RV)	E_{B-V}	
	km/s	km/s	km/s	km/s	km/s	km/s	km/s		
HD 181409	143	-34	-2	260	21		21	0.09	
HD 183535	80	-10	-34	257	14	-18	14	0.13	
HD 225822	120	13	-113	311	31			0.26	(1)
HD 185780	355	-110	47	385	-5	-25	-5	0.19	
HD 186618	161	-10	29	290	11	-5	11	0.08	
HD 191781	-75	38	-179	347	-7		-3	0.91	
HD 204150	-81	-17	-147	286	-37		-37	0.29	
HD 213405	65	50	-2	305	10	-17	-17	0.75	
HD 213481	28	49	-34	299	12	1	1	0.77	
HD 6675	-47	-7	-68	254	-6	-10	-6	0.59	
HD 17179	-87	-6	-71	267	27	-80		0.47	(1)
HD 25090	44	84	-67	340	-3	-1	-1?	0.60	
HD 50767	72	-121	-132	192	-51			0.02	(2)
HD 53879	-192	432	-277	742	-17		-17	0.15	(3)
HD 60848	-9	-78	-133	207	28	13	28	0.15	(4)
HD 66665	115	-277	-273	299	18	-8	18	0.03	

Notes

(1) The radial velocities for these stars are based on 1'O.H.P. plates.

(2) The small reddening suggests that this star may be subluminous.

(3) The radial velocity of this star is based on one L'O.H.P. plate

(4) See note at the end of Table 7.2.1.

Table 7.4.2

The Galactic Distribution of Stars with High Velocities Towards the Galactic Plane or Centre

	Star	l	b	MK		Star	l	b	MK
HD	181409	65.81	9.31	B2 IV	HD	213481	109.44	7.39	B2 II
HD	183535	69.75	9.09	B1 V	HD	6675	124.48	6.88	B0.5 III
HD	225822	73.38	6.66	B2 III	HD	17179	131.48	12.05	B3 V
HD	185780	74.14	9.06	B0.5 II	HD	25090	143.18	7.35	B0.5 III
HD	186618	80.48	11.49	B0 III	HD	50767	191.72	11.55	B2 III
HD	191781	81.18	6.61	B0 Ib	HD	53879	207.01	7.36	B2 III
HD	204150	100.19	7.45	B2 IV	HD	60848	202.53	17.53	O8 Ve
HD	213405	108.68	6.25	B0.5 V	HD	66665	215.76	19.13	B0.5 III

Table 7.4.3

High Velocity and Possible Runaway Stars

Star	r pc.	z pc.	U km/s	V km/s	W km/s	S^* km/s	E_{B-V}	Esc?
HD 176914	900	164	-110	46	83	250	0.15	?
HD 177109	1750	378	-50	-18	58	255	0.02	No
HD 178912	1620	312	22	-55	125	234	0.09	Yes?
HD 183649	1030	147	-117	1	19	278	0.08	No
HD 188891	1220	147	-170	16	82	327	0.24	?
HD 189957	2010	216	-100	58	217	390	0.28	Yes
HD 186994	3600	630	-162	-6	369	471	0.13	Yes
HD 190254	770	97	-66	48	91	318	0.17	?
HD 190427	2480	343	-7	-23	252	340	0.43	Yes?
HD 188439	1460	261	43	-70	47	191	0.15	No
HD 192035	2960	399	-115	-13	327	420	0.32	Yes
HD 189818	1220	304	-25	-8	79	256	0.06	?
BD 59 2344	850	112	-7	-3	72	257	0.78	?
BD 58 2268	720	77	21	17	88	282	0.80	?
BD 59 2384	3750	436	45	-22	129	259	0.46	Yes?
HD 203374	900	135	78	16	29	277	0.60	No
HD 207308	660	78	97	5	76	283	0.51	?
HD 207198	2160	261	7	1	84	261	0.46	?
HD 208218	1030	118	-84	-35	82	243	0.44	?
HD 216992	530	71	-38	-23	50	224	0.35	No
HD 25638	1120	157	39	58	71	305	0.67	No
HD 41689	3250	-86	-162	179	179	208	0.21	Yes?
HD 40160	570	109	-7	-43	52	211	0.14	No
HD 48029	2280	255	52	-141	45	113	0.19	No

accuracy that would be necessary if the space motion components were more precise, the variation in gravitational potential as a function of galactocentric distance must be considered.

The galactocentric space velocity components in the directions normal to the galactic plane and towards the galactic centre for any star, are the same as they are when observed with respect to the local standard of rest of that star. The galactocentric space velocity component in the direction of galactic rotation was calculated by adding the rotational velocity for each star, determined from its galactocentric distance using the table given by Schmidt (1965). The galactocentric space velocity (S^*) was then determined from its three mutually orthogonal components.

A number of the stars listed in Table (7.4.3) have $S^* > 315$km/s and these may be unstable in their present location. A few have $S^* > 315$km/sec, and these may be unstable in their present location. A few have $S^* > 380$ km/sec, and these may escape from the galaxy altogether. However, for all of these stars $V < 65$km/sec, and so it appears that they are not likely to be unstable as a result of motion in the galactic plane.

Some of these stars may escape as a result of their motion perpendicular to the galactic plane. The variation in the acceleration normal to the galactic plane, K_z, has been determined for different values of z, the distance from the galactic plane, by Oort (1960). The result of fitting a polynomial to these data is

$$K_z = a_1 + a_2 z + a_3 z^2 + a_4 z^3 + a_5 z \quad - - - - - - \quad (7.4.1)$$

where $a_1 = 0.310791$ $\quad a_2 = 2.19231 \times 10^{-2}$,

$a_3 = 2.16328 \times 10^{-5}$, $a_4 = 9.25593 \times 10^{-9}$ and

$a_5 = -1.37845 \times 10^{-12}$

This quartic polynomial gave a better fit than the quadratic

and cubic, which were also tried. The data obtained by Oort (1960) suggest that equation (7.4.1) is fairly representative of K_z up to z = 3kpc. Beyond this a deviation begins to arise, in that $K_z = 0$ when $z = 3.573$ kpc and becomes negative for larger values of z. In reality K_z would be expected to become a better and better approximation to the inverse square law as z increases.

The potential energy of a star at a height z above the galactic plane is equal to the kinetic energy needed for escape. Consequently, if m_* and W_{esc} are the mass and the escape velocity, in a direction normal to the galactic plane of a star then it follows that

$$\tfrac{1}{2} m_* W^2_{exc} = m_* \int_z^{\infty} K_z(z)dz ,$$

$$\text{and so} \quad W_{esc} = \sqrt{2 \int_z^{\infty} K_z(z)dz} \qquad \text{- - - - - - - - - -} \quad (7.4.2).$$

Since equation (7.4.1) does not accurately represent the real situation for large values of z, a very approximate value of W_{esc} has to be calculated, using

$$W_{esc}(z) = \left[2 \int_z^{X} K_z(z)dz \right]^{\frac{1}{2}} \qquad \text{- - - - - - - -} \quad (7.4.3),$$

where X = 3573pc. Substitution for $K_z(z)$ from equation (7.4.1) gives W_{esc} = 73km/sec for z = 0 pc. and W_{esc} = 64 km/sec for z = 1000pc.

The calculated values of W_{esc} will be rather less than the true escape velocity for a given z. Taking this, and the inherent errors in the space velocity components, into account, any star for which $W \gtrsim$ 100 km/sec and for which $S^* \gtrsim$ 380 km/sec must be considered as a probable runaway star. The situation is less certain when 70 km/s $\lesssim W \lesssim$ 100/s and 315 km/s $\lesssim S^* \lesssim$ 380 km/s, or when $W \gtrsim$ 100km/s and $S^* \lesssim$ 380 km. Stars in this category can only be termed possible

runaway stars. The conclusions as to whether each star is escaping or not are entered in Table (7.4.3) in the column on the extreme right.

Certain questions arise concerning the motions of these early type stars normal to the galactic plane, which are connected with their evolutionary lifetimes. For instance, do stars bound within the galaxy describe some form of harmonic motion about the galactic plane, and if so, how many oscillations do they make in a lifetime? A further question that may be asked is what is the origin of motion normal to the galactic plane? The origin of runaway stars is considered by Poveda et al. (1967) and further consideration is given to these questions later (§9.4, §10.1).

The possibility that some, if not all, of these high velocity stars are subluminous cannot be entirely ruled out. However, according to Neckel (1967), they all have reddening appropriate to their distances and galactic coordinates.

The stars listed in Table (7.4.1) have space motions incompatible with their spectral type and distance from the galactic plane. The classical way of explaining this is to consider the possibility of these stars being subluminous, and then proceed to show that the space motions are more reasonable with the revised absolute magnitude. This approach was adopted by Hill (1968) in the case of HD 125924.

A number of the stars listed in Table (7.4.1) appear to be heavily reddened and exhibit strong interstellar CaII(K) lines in their spectra. Consequently they are unlikely to be subluminous and another explanation of their space motions is needed. The neutral hydrogen surveys of Lindblad (1966), Weaver and Williams (1973) and Heiles & Habing (1974) were searched for HI features which have the same galactic coordinates as these stars, with either the stellar or interstellar CaII(K) line radial velocity. The velocities of such features, where found, are indicated in Table (7.4.1).

If the stellar and HI radial velocities are equal, within the limits of observational error, then there is good reason to believe that the neutral hydrogen and the star are associated. This would be unlikely if the star were subluminous, and so these stars are considered to be normal early type stars. Similarly, if the HI and CaII(K)

velocities were equal, then the star was also considered to be normal if there was appreciable reddening. The radial velocities of HD 225822, HD 17179, and HD 53879 are determined from 1'O.H.P. spectra and may be unreliable. This might explain the apparent absence of any HI features associated with these stars.

The space motions of HD 60848 may exhibit exceptional unreliability because of a distance error (see note at the end of Table (7.2.1), and the absence of an associated HI feature may be due to this. A star with a numerically large and variable radial velocity is HD 50767 (Abt et al., 1972). The low E_{B-V} and apparent absence of any associated HI features would suggest a possibility that this star is subluminous. A spectrum showing the confluence of the Balmer Series and ubvy photometry (Strömgren, 1963 and Graham 1970) would be useful additions to the available information on this star.

The neutral hydrogen, which appears to be associated with some of the early type stars listed in Table(7.4.1), is probably the remains of the clouds from which the stars were originally formed. Thus, the neutral hydrogen would be expected to have a similar space velocity to that of the stars themselves. The high velocity clouds, discussed by Davies (1972) and Hulbosch (1975), are a possible source of this neutral hydrogen. The longitude distribution of the stars in Table (7.4.2) corresponds roughly with the distribution of HVC's at $b \sim 10°$, given by Davies (1972). This possibility of star formation at considerable distances from the galactic plane is considered in a more general context later (§9.4, §9.5, & §10.1).

The literature was searched in an effort to locate an HI feature which may be associated with HD 125924. Only a feature whose radial velocity was equal to that of the CaII(K) line was found. This is to be expected if the CaII(K) line is interstellar in origin. The radial velocity of HD 125924 is + 252km/sec (Hill, 1968), resulting in a radial velocity with respect to its local standard of rest of 290 km/sec. This is comparable to the radial velocity of HI in the vicinity of $l \sim 300°$, $b \sim 0°$ which is part of the Magellanic Stream discovered by Mathewson et al. (1974). Thus it is conceivable that this star might be or might have been, associated with the Magellanic Stream. Because of its large space motions (Hill, 1968) this star

would be some distance from its place of creation, which would account for its distance of 3.6 kpc., reported by Hill. This star lies beyond the survey limits of Mathewson et al., and so great importance must be attached to a search for HI features in the vicinity of this star, with heliocentric radial velocities of the order of 250km/sec.

This suggestion is put forward as an alternative to Hill's suggestion that HD 125924 is subluminous. From a detailed analysis of the spectrum of HD 125924, Greenstein & Sargent (1974) conclude that it is a normal B star with an absolute magnitude of -2.9, which agrees well with the value of -3.3 reported by Hill (1968).

7.5 Distant and Possibly Subluminous Stars

The stars with derived distances in excess of 3kpc. are listed in Table (7.5.1). These stars are interesting because of their possible association with the Intermediate or Perseus Spiral Arms. They may be subluminous, in which case their distances have been overestimated.

The stars HD 186994, HD 197406, BD 59°2384, HD 41689, HD 53879 and HD 66665 have already been discussed (§7.3 & §7.4). The distance estimated for LS1 63-198 places it well outside the Galaxy. Consequently, the assumption of an absolute magnitude of -5.6, based on a spectral classification of O9 IV, can hardly be correct. The stars LS1 63-199 and LS1 64-197, which are the closest to LS1 63-198 on the celestial sphere, are much more heavily reddened and very much closer to the Sun. This has been pointed out by Haug (1970b), who also notes that the spectrum of LS1 63-198 has an intense ultraviolet. Thus it would appear that LS1 63-198 is subluminous, and this has been confirmed by Greenstein & Sargent (1974).

There appears to be no justification for considering HD 59882 to be subluminous. From the work of Neckel (1967) and Fitzgerald (1968) it is not possible to say whether this star has a small reddening for its distance or not. The I.U.E. spectra of this star show that it has the characteristics of a normal B star. However, a higher dispersion spectrum, showing the confluence of the Balmer Series would be a useful addition in an effort to verify this.

The distances of the remaining stars are all calculated on the basis of absolute magnitudes obtained from the spectral types, which are subject to errors in classification. Neckel (1967) estimates $E_{B-V} = 0.04 \pm 0.01$ for a distance of 1kpc, in the direction of these stars. Thus it seems probable that they are all normal B stars and useful as spiral tracers.

TABLE 7.5.1

Stars with Estimated Distances in Excess of 3kpc.

Star	l °	b °	E_{B-V}	r kpc.
HD 186994	78.61	10.06	0.13	3.60
HD 197406	89.75	6.50	0.62	9.12
BD 59°2384	100.18	6.69	0.46	3.75
LS1 63-198	139.15	6.29	0.26	32.33
HD 41689	151.92	19.34	0.21	3.25
AAO 50-164	182.86	9.00	0.34	4.55
AAO 50-363	183.76	7.67	0.27	3.57
HD 53879	207.01	7.36	0.15	3.60
HD 66665	215.76	19.13	0.03	3.03
AAO 99-226	219.91	14.90	0.33	4.22
AAO 99-326	220.24	12.61	0.21	4.09
AAO 99-263	220.86	14.89	0.43	4.04
HD 59882	222.54	6.38	0.11	3.09

CHAPTER EIGHT

The Distribution of Stars and the Interstellar Medium.

8.1 The Spatial Distribution of Stars and the Interstellar Medium.

8.2 Galactic Spiral Structure and a Comparison with Radio Results

8.3 Estimates for the Height of the Reddening Layer at Different Galactic Longitudes.

8.4 The Possible Correlation Between Gas and Dust Distributions.

8.1 The Spatial Distribution of Stars and the Interstellar Medium

The galactic latitudes of stars listed in Table (7.2.1) were plotted against their galactic longitudes. This is depicted in Fig.(8.1.1) and shows the galactic distribution of the programme stars. These stars are all thought to be normal B stars, and LS1 63-198 was omitted because it is probably sub-luminous (§7.5). The sample of programme stars contains one WN7 star, HD 197406, and 6B stars more luminous than B5V. Some stars classified as B8 in the HD Catalogue (Cannon & Pickering, 1918-1924) may be earlier than B5, and have been missed because they were omitted from the observing programme. The number of such stars is probably small, and so the sample of programme stars is fairly complete in the magnitude range $4^m.0 \leqslant V \leqslant 8^m.0$, with a number of fainter stars included (§3.2 & §3.3).

At the galactic longitudes $l \sim 130°$ and $l \sim 175°$, there are comparatively few programme stars. Otherwise the stars are thinly distributed across the region, with a fairly dense concentration of stars at $l \sim 100°$, $b \sim 7°$, which is part of Cepheus OB2 as already discussed (§7.3.3). The apparent irregularities in the distribution are characterised by extensive regions in which no programme stars are found. The typical minimum diameter of these regions is $\sim 10°$ and so they are unlikely to be stellar rings of the type discussed by Isserstedt (1968).

The existence of local dust clouds would account for the irregular distribution of programme stars. A list of dark nebulae, taken from the catalogue of Lynds (1962), was therefore prepared and presented in Table (8.1.1) and Table (8.1.2). Dieter (1973) has pointed out that the galactic coordinates given by Lynds (1962) are incorrect. The galactic coordinates given in Table (8.1.1) have been redetermined from the equatorial coordinates given by Lynds.

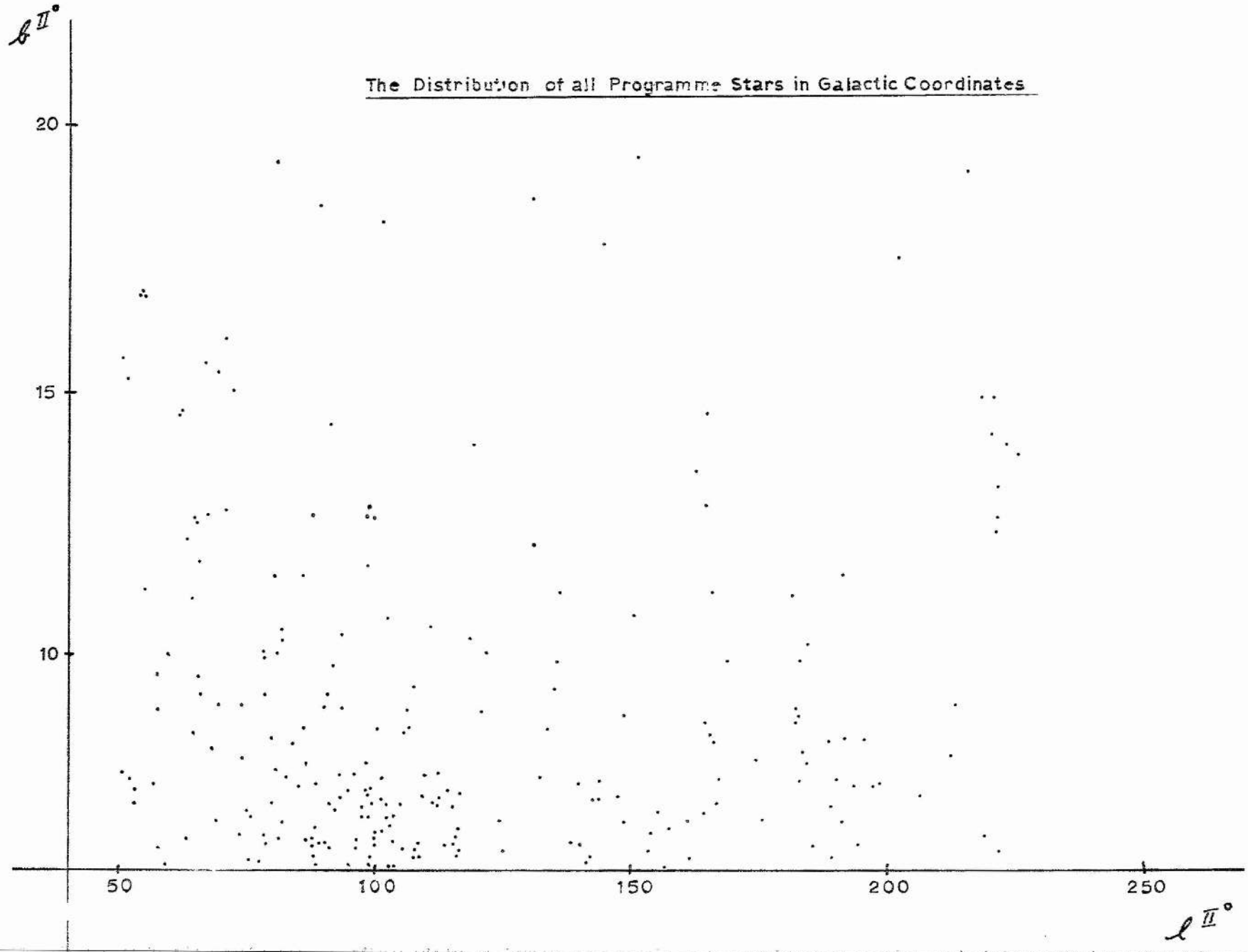
The Distribution of all Programme Stars in Galactic Coordinates
b II°
20
15
10
50
100
150
200
250
l II°

Table 8.1.1

A List of Dark Nebulae in the Region of the Galaxy Under Consideration

L	l	b	A	O	R	L	l	b	A	O	R
706	49.41	16.36	8	4		1089	94.80	13.78	244	3	
712	50.40	6.70	865	2		1094	98.83	14.06	2	5	
719	51.87	6.38	88	2		1100	98.86	13.88	7	5	
734	54.50	6.40	660	2		1108	99.49	6.34	46	3	
759	56.50	6.89	358	1		1122	99.97	14.81	41	4	
777	57.61	6.94	226	1		1125	100.04	8.90	10	5	
890	78.45	6.21	54	3		1135	101.44	6.06	54	3	
903	80.78	6.61	5	5		1140	101.70	6.16	240	2	
905	81.09	6.59	18	4		1145	102.14	8.24	183	3	
1033	93.44	9.69	714	3		1147	102.14	15.29	127	3	*
1036	93.52	9.58	88	5	*	1152	102.37	16.14	25	5	
1037	93.53	6.75	591	3		1155	102.60	15.25	6	6	
1038	93.53	8.20	660	2		1157	102.65	15.75	5	5	
1039	93.58	8.94	79	4		1158	102.66	15.17	111	4	
1041	93.79	9.78	22	5		1162	102.92	10.76	4	3	
1049	94.12	9.35	5	6	*	1167	103.30	13.32	62	2	
1051	94.16	9.29	10	5		1168	103.31	14.21	3	5	
1053	94.18	6.37	33	5	*	1170	103.63	13.84	215	3	
1056	94.35	6.69	36	2		1171	103.71	14.88	2	5	
1058	94.72	6.27	869	3		1172	103.76	13.82	10	6	*
1061	95.36	7.56	618	2		1173	103.88	13.67	6	5	
1065	95.56	6.09	23	5	*	1174	104.15	14.14	294	4	
1067	95.87	6.00	12	5		1176	104.93	11.15	446	1	
1068	95.89	6.59	27	5		1177	105.22	13.06	5	4	
1069	95.90	6.21	18	4		1181	105.36	9.97	8	4	
1071	96.00	8.10	92	5	*	1183	105.42	10.03	90	2	
1076	96.57	10.04	8	5		1199	106.57	12.15	235	2	
1082	96.98	10.07	111	5	*	1213	109.06	6.39	6	5	
1214	109.14	6.57	256	1	*	1273	118.46	6.08	199	2	
1217	110.54	11.79	186	3		1274	118.52	8.54	32	4	*
1219	110.58	12.06	3	5		1304	122.21	6.91	4000	1	

L	l	b	A	O	R	L	l	b	A	O	R
1221	110.67	9.61	20	5		1308	124.59	10.13	1570	1	
1235	112.24	13.88	37	6	*	1333	128.88	13.71	7	6	*
1236	112.56	8.49	44	4		1340	130.15	11.49	1	5	
1241	113.08	17.48	1380	1		1352	132.68	6.50	17	1	
1242	113.15	13.11	793	3		1353	133.14	7.61	2510	1	
1243	113.16	15.60	81	3		1355	133.46	8.68	7	6	
1247	113.66	15.17	167	4		1357	133.52	8.53	4	6	*
1251	114.51	14.65	195	5	*	1358	133.53	9.09	6	6	*
1259	116.93	12.44	35	2	*	1419	153.11	6.59	79	2	
1261	117.20	12.35	30	4		1460	159.59	11.74	181	3	
1262	117.20	12.35	66	6	*	1466	160.04	12.19	124	4	*
1264	117.50	6.03	102	2	*	1467	160.12	12.32	29	3	

Notes:

The column headings are as follows:

L - denotes the number of the dark nebula in the catalogue (Lynds, 1962),

l & b - denote the galactic coordinates of the dark nebula, as discussed in the text,

A - is the area of the dark nebula in square degrees x 10^{5},

O - is the opacity of the dark nebula on the system used by Lynds, and

R - refers to a remark which is indicative of further details to to be found in Table (8.1.2).

TABLE 8.1.2

The Results of Radio Observations of Dark Nebulae

L	Radial Velocity Corrected for the Solar Motion (km/s)					r(kpc)
	H_2CO^1	HI	OH	H_2CO^2	Adopted	
1036				-2.4	-2.4	0.9
1049				(a)		
1053				-1.7	-1.7	0.7
1065				(b)		
1071				(b)		
1082	-39.0	-40.1		(b)	-39.6	4.8
1147	1.8	2.1		2.5	2.1	?
1172	2.2	0.8		2.8	1.9	?
1214				(a)		
1235	-4.7	-7.0		-4.0	-5.3	0.6
	-42.7	-41.1			-41.8	3.7
1251	-5.5	-7.0	-4.0	-5.0	-5.5	0.6
1259				3.7	3.3	?
1262				3.5	3.5	?
1264				(a)		
1274				(c)		
1333	2.6	3.0	3.0	(a)	2.9	?
1357				(a)		
1358				(a)		
1466				(a)		

Notes

The column headings are as follows :

L - as in Table (8.1.2),

H_2CO^1 - Formaldehyde observations by Minn & Greenberg (1973a),

H_2CO^2 - Formaldehyde observations by Dieter (1973),

r - kinematic heliocentric distance, a "?" indicating that the

radial velocity is positive, whereas differential galactic rotation suggests a negative velocity at this galactic longitude.

(a) - denotes that a search for formaldehyde in the velocity range $-5.6 \leqslant V \lesssim 6.8$ was made by Dieter (1973), but no formaldehyde was detected.

(b) - as for (a), the velocity range scanned was $-18.0 \leqslant V \lesssim 6.8$

(c) - as for (a), the velocity range scanned was $-18.0 \leqslant V \leqslant 19.2$

No part of any of the dark nebulae lies along the line of sight to any of the programme stars. Thus, it is possible that the distribution depicted in Fig (8.1.1), within the galactic longitude ranges in which dark nebulae are found, is at least partly due to obscuring dust clouds. Outside this region, the observed stellar distribution may be genuine. The absence of dark nebulae in the regions $134° \leqslant l \lesssim 153°$ and $160° \leqslant l \leqslant 228°$, for $b \geqslant 6°$, was noticed. In the former case there may be some connection with the absence of programme stars in the region $136° \leqslant l \lesssim 141°$.

Recent suggestions that stellar rings may be used as spiral tracers have been supported by photometric observations made by Isserstedt & Schmidt-Kaler (1970). On the other hand, the interpretation of these observations has been questioned by Haug & Kohoutek (1971). A statistical analysis by Uranova (1975) has demonstrated that stellar rings are unlikely to be anything other than optical illusions. If this is the case, then the centres of the dark nebulae may be expected to be nearly coincident with the centres of the stellar rings. In fact there was no correspondence between the centres of the dark nebulae listed in Table (8.1.1) and the stellar rings in the region of the Galaxy under consideration, which were obtained from Isserstedt (1968). This shows, though by no means

conclusively, that stellar rings may be aggregates of young stars. This is directly opposed to the conclusions of Uranova (1975), and as the true nature of stellar rings is unestablished, they are not given any further consideration.

An association between OB stars and neutral hydrogen has been found to exist in M31, by Emerson (1974). For reasons given later (§9.2), it is reasonable to suppose a similar association in our own galaxy. Thus a detailed comparison of the OB star and HI distributions in three-dimensional space, could yield valuable information on galactic structure and evolution. This comparison is discussed later (§8.2, §9.2).

Local interstellar reddening variation with distance and galactic coordinates may, to some extent, explain the two dimensional programme star distribution depicted in Fig (8.1.1). Furthermore, there may be a correlation between the interstellar reddening and neutral hydrogen column density (§8.4). A comparison between the stellar and local neutral hydrogen column densities were inferred from the contour maps obtained by Weaver & Williams (1974a, 1974b). These were checked against the low resolution local neutral hydrogen column density map given by Weaver (1974).

A comparison between stellar and Hα emission distributions is of interest because the latter indicates the presence of hydrogen, ionised by nearby early type stars. These are usually referred to as HII regions (Strömgren, 1948). The distribution of Hα emission with galactic longitude and latitude was obtained from the survey by Sivan (1974). A general comparison of the stellar, HII and local HI distributions, suggests that the region of the Galaxy under consideration may be conveniently considered as seven separate intervals of galactic longitude:

(i) $\underline{40^\circ \leqslant l \leqslant 70^\circ}$

The tenuous filaments of high latitude neutral hydrogen at

$l = 48°$ decrease in abundance, reaching a minimum at $l = 65°$. There is very little local neutral hydrogen for $b > 6°$ at this galactic longitude, but a rapid increase in the local neutral hydrogen column density occurs between $l = 65°$ and $l = 70°$. The distribution of dark nebulae listed in Table (8.1.1) follows the distribution of local neutral hydrogen. This suggests that a correlation between neutral hydrogen and dust densities exists.

The programme stars that occur between $l = 60°$ and $l = 70°$ are either more distant than 1kpc, or lie within 500pc. Stars in the former category are not considered to be local and are discussed later (§8.2). Stars in the latter category are all of type B3V, B4V or B5V, and so may not be associated with neutral hydrogen (Kilkenny et al., 1975).

Extensive HII regions are not found in this galactic longitude interval, which indicates the absence of dense regions of neutral hydrogen containing embedded OB stars, the circumstances in which the hydrogen may become ionised. Only three compact HII regions are known to exist in this galactic longitude interval, and they are included in Table (8.2.1). The occurrence of S94 and S96 at $l \sim 65°$ in the absence of dense local neutral hydrogen suggests that they are not local objects. No distance determination or identification of exciting stars, seems to have been made.

(ii) $\underline{70° < l \leq 96°}$

This region contains the association Cyg OB7 which has been considered elsewhere (§7.3.4). It is convenient to subdivide this region into three:

(a) $70° < l < 88°$, $6° \leq b < 10°$

In comparison with region (i), there is a high concentration of neutral hydrogen, but no perceptible increase in the OB star concentration. Furthermore, there is extensive Hα emission, the individual HII regions having been discussed by Dickel et al.(1969) and are listed in Table (8.2.1). The Hα emission distribution

given by Sivan (1974), shows that there are points in this region where the Hα intensity is diminished. A visual survey for dark nebulae, as carried out by Lynds (1962), would be unsuccessful in a region such as this and the only dark nebulae listed in Table (8.1.1) which are located in this region, are to be found at these points where the Hα intensity is diminished.

Since OB stars are usually associated with neutral hydrogen, a lower Hα emission intensity suggests fewer OB stars and less neutral hydrogen to be ionised. It is probable that this implies less obscuring dust. Thus, points of diminished Hα intensity are possibly "low absorption windows", through which distant stars might be observed. An example of this is HD 191781, and many distant stars are observed at the edge of this region, where the Hα intensity is diminished and there is presumably less obscuration for the same reason.

This suggests a high concentration of OB stars in this region, which are presumably obscured by the dust associated with the neutral hydrogen surrounding the HII regions. A formaldehyde survey of this region, of the kind undertaken by Dieter (1973), to confirm the existence of obscuring dust, would be useful. The remaining programme stars in this region are probably between the sun and the HII regions. This would be consistent with their proximity and low reddening.

(b) $88° \leqslant l \leqslant 96°$, $6° \leqslant b < 10°$

From $l = 88°$ to $l = 96°$, the Hα emission intensity and local neutral hydrogen column densities decrease. Following the argument given in (a), a corresponding decrease in the concentration of OB stars would be expected. However, the lower neutral hydrogen column densities may imply a reduced obscuration due to interstellar dust, and hence the stars in this region are more easily observable. Therefore a real decrease in the concentration of OB stars may be observed as an increased concentration. In fact an increased concentration is observed, which is additional evidence for a correlation between interstellar reddening and

neutral hydrogen column density.

A reduced Hα emission intensity would make the visual detection of dark nebulae more feasible. Thus a higher number of these objects per square degree might be expected. Sixteen dark nebulae located in this region are listed in Table (8.1.1), and so this appears to be the case.

(c) $70° < l \leqslant 96°$, $10° \leqslant b \leqslant 20°$

There is very little local neutral hydrogen, no Hα emission and no dark nebulae in this region. The more distant stars may be associated with distant neutral hydrogen and these are discussed later. The remaining stars are mainly of spectral type B3 or later, and so they may no longer be associated with the neutral hydrogen clouds from which they were formed. Nonetheless, the means by which these stars came to be at high latitudes is worthy of further consideration, and is given later (§9.4, §10.1).

(iii) $\underline{96° < l \leqslant 106°}$

This region contains the association Cepheus OB2, already discussed at some length (§7.3.3). It is convenient to subdivide it into two :

(a) $6° \leqslant b < 8°$

The apparent concentration of OB stars in this region is higher than in any other part of the Galaxy investigated. However, there is no Hα emission and the local neutral hydrogen column density is marginally less than that found, at the same galactic latitudes, in the regions (ii) and (iv) which are on the other side. The highest concentration of dark nebulae is also to be found in this region. It seems probable that this region is comparable to region (ii)b, in that the apparent increased concentration of OB stars is due to the reduced amount of obscuring dust, and that in reality there is a decreased concentration of OB stars.

(b) $8° < b < 20°$

There is an extensive region of Hα emission at $l \sim 99°$, $b \sim 10°$, at which the highest column density of local neutral hydrogen, at this galactic longitude, is found. Following the arguments adopted above in the case of the region (ii)a, it would seem that there is a concentration of OB stars here, totally obscured by dust associated with the neutral hydrogen.

This gives additional support to the suggestion, made earlier (§7.3.3), that Cepheus OB2 extends well beyond $b = 8°$, which is the galactic latitude limit hitherto suggested for it, (Simonson III, 1968). Dark nebulae extend to $b \sim 16°$ at $l \sim 102°.5$, and so the high latitude limit for the extent of Cepheus OB2 may be higher than suggested before (§7.3.3). There are filaments of local neutral hydrogen extending from ($l = 96°$, $b = 6°$) to ($l = 85°$, $b = 13°$) and to ($l = 108°$, $b = 20°$). The high latitude and heavily reddened star HD 192575 ($b = 18°.15$) may be associated with the second of these filaments and not form part of Cepheus OB2.

(iv) $106° < l \leq 115°$

(a) $6° \leq b \leq 8°$

The concentration of stars is less than in region (iii)a, and there is an increased column density of local neutral hydrogen. An extensive region of weak Hα emission is present, between $l = 106°$ and $l = 110°$, which corresponds with the distribution of stars, in that the stars are found in the regions of stronger Hα emission. Furthermore, when $l > 110°$ the local neutral hydrogen column density decreases, and the apparent concentration of OB stars increases. Thus the remarks made above concerning regions (ii) & (iii)a appear to be applicable in this case also.

(b) $8° < b \leq 20°$

Very little local neutral hydrogen, no Hα emission and a few programme stars are present in this region. Those stars of spectral type B2 or earlier appear to have neutral hydrogen features associated with them. The comments on stars later

than B2 in region (ii)c, are also applicable in this case. Numerous dark nebulae are located in this region, some of which may not be local (Table 8.1.2). Among the local dark nebulae, there is evidence for star formation at some distance from the galactic plane (§9.5).

(v) $115° < l \leq 130°$

There is very little local neutral hydrogen in this region; the column density reaching a minimum at $l \sim 120°$. No Hα emission and very few programme stars are found in this region. A number of the stars are earlier than B2, reddened and within 1kpc. These stars have neutral hydrogen features associated with them, and the reddening is probably the result of dust associated with the neutral hydrogen. Thus it would appear that the local interstellar medium is broken up into clouds in this region. There are dark nebulae present, but they may be distant objects.

(vi) $130° < l \leq 180°$

Local neutral hydrogen densities may be inaccurate in the vicinity of $l \sim 180°$, because the kinematic distances become indeterminate (See Fig. 9.3.1). This has to be remembered in dealing with this region and region (vii). This region is conveniently divided into two :

(a) $6° \leq b \leq 13°$

There is an abundance of local neutral hydrogen in this region, with the column density reaching a maximum at $l \sim 175°$. There is also a ridge of higher column density HI at $b \sim 13°$, which extends across the whole region, being denser in places than the neutral hydrogen in the galactic plane. Extensive Hα emission occurs in the vicinity of $l = 143°$, $b = 13°$. Adopting the reasoning used in the case of region (ii)a, there are probably many luminous OB stars in the vicinity of this Hα emission, but are totally obscured by dust.

The high column density of local neutral hydrogen at $l \sim 175°$ suggests that stars will be heavily reddened at this galactic longitude. This is observed in the case of BD 35°1332 which is the only programme star in this vicinity. There are only a few known dark nebulae in this region, contrary to what might be expected from the studies of other regions given above.

(b) $13° < b \leqslant 20°$

There is very little local neutral hydrogen, and no Hα emission in this region. The local programme stars are later than B2, and so may not be associated with neutral hydrogen. Thus the comments on region (ii)c are also applicable in this case.

(vii) $\underline{180° < l \leqslant 228°}$

There are no known dark nebulae or extensive regions of Hα emission. The only known HII region is S274 which is listed in Table (8.2.1). The local neutral hydrogen column density decreases to a minimum at $l \sim 205°$, and beyond this, with $l > 205°$, there is very little local neutral hydrogen, other than a tenuous filament extending from ($l \simeq 210°$, $b \simeq 6°$) to ($l \simeq 215°$, $b \simeq 10°$). The local programme stars earlier than B3 are found associated with HI, whereas many of the later programme stars are not and the comments on region (ii)c are applicable to these.

Kepner (1970) failed to find any intermediate or high velocity neutral hydrogen in this region, and so she did not give it any consideration in her ensuing analysis of intermediate latitude spiral structure. However, this has not been verified by subsequent observers. Davies (1972), Dieter (1972) and Weaver & Williams (1974a, 1974b) have shown that features with velocities around +45km/sec do exist. Furthermore, there are tenuous high velocity clouds with velocities around -100km/sec, but occasionally reaching -250 km/sec. These features would seem to be examples of high velocity clouds which are not participating in differential galactic rotation.

8.2 Galactic Spiral Structure and a Comparison with Radio Results

Kilkenny et al. (1975) have noted that O-B2 stars are better spiral tracers than B3-B5 stars. Consequently, the only B3 stars used as spiral tracers in this analysis, are those more luminous than luminosity class III, the later types being excluded altogether. The heliocentric distance, projected onto the galactic plane, was plotted as a function of galactic longitude for each spiral tracer as depicted in Fig (8.2.1). The only spiral tracer omitted was the WN7 star HD 197406, on account of it being at a much greater distance than any of the others (§7.5). The star LS1 63-198 is almost certainly subluminous (§7.5), and so it has also been omitted.

Further information on galactic spiral structure can be obtained from studies of dark nebulae and HII regions. The distances of HII regions can be determined from two independent methods. One method is to determine the distance of the exciting star by the method already described (§2.2 & §7.2). The other involves a kinematic distance determination from a radial velocity, as described below.

A number of interstellar molecules have been observed in dark nebulae, the OH and H_2CO molecules being the most convenient for kinematic distance determination. Radial velocities of HI, OH and H_2CO dark nebulae listed in Table (8.1.1) were obtained from Minn & Greenberg (1973a). Additional H_2CO velocities were obtained from Dieter (1973). All these radial velocities together with the adopted means and the kinematic distances, derived as described below, are listed in Table (8.1.2). Some of the dark nebulae were observed by Dieter (1973), and no formaldehyde was detected, in which case the velocity range searched was given in Table (8.1.2).

The catalogue prepared by Sharpless (1959), and the lists by Courtes et al. (1966) and Dickel et al. (1969), were searched for HII regions located in the part of the Galaxy under consideration.

Galactic Spiral Structure - a Determination from Intermediate Latitude OB Stars

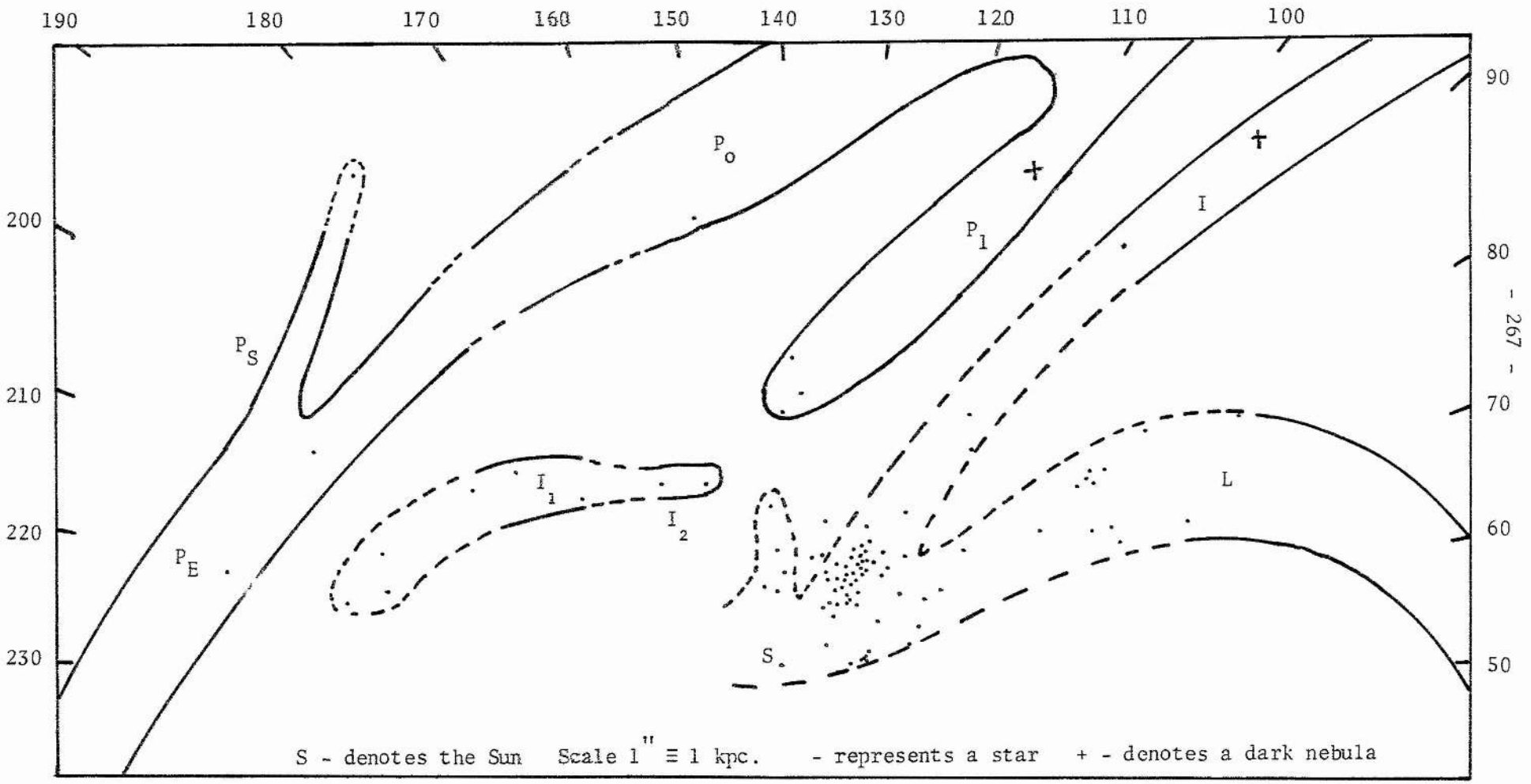

Fig 8.2.1

These HII regions, together with published radial velocities, corrected for the solar motion, and kinematic distances, derived in the manner described below, are listed in Table (8.2.1). The two unnumbered HII regions are listed by Courtes et al., and the details on S129 and S274 from Minn & Greenberg (1973b). The exciting stars of S85 and S130 are as given by Crampton & Fisher (1974). The prefix "DWB" to a HII region number represents the number in the list by Dickel et al. (1969), and the prefix "S" denotes the number in the Sharpless catalogue.

Radial velocities of HII regions and dark nebulae were assumed to be due to differential galactic rotation, after correction for the solar motion (§2.4.3). On the basis of this assumption, equation (2.4.1.2), together with the approximation to the rotation curve previously adopted (§2.4.1), give the heliocentric distance, from which the galactocentric distance was derived using the method already described (§2.3). This method of kinematic distance determination was tested by redetermining the neutral hydrogen kinematic distances quoted by Kepner (1970), from the HI velocities she obtained. Agreement to within 0.01kpc. was obtained, which justifies the method.

The galactic coordinates of S274 do not agree with those of the exciting stars named by Minn & Greenberg (1973b). Since the galactic coordinates agreed with the l^I, b^I given by Sharpless (1959), it was assumed that the wrong exciting stars had been adopted. This is unfortunate since it is the only HII region considered, with a published radial velocity, which appears to be away from the solar neighbourhood.

The only distant dark nebulae are L1082 and L1235, the latter comprising of two dark nebulae, one local and one distant, (Table 8.1.2). The local component of L1235 is of little interest and is not considered. These objects are plotted in Fig. (8.2.1). Although their kinematic distances are subject to observational and systematic errors, they are adopted as spiral tracers in the absence of any alternative in their vicinity. Dark nebulae are potentially regions of star formation (Sume et al., 1975) and so they would be expected to be excellent spiral tracers.

TABLE 8.2.1

A List of HII Regions in the Region of the Galaxy under Consideration

No.	l	b	V_{lsr} (km/s)	r pc	R_c kpc	Exciting Star
S 85	57.43	9.08				HD 177347
S 94	64.91	6.75				
S 96	66.12	7.13				
DWB 17	75.3	6.4				
DWB 47	77.3	7.5				
DWB 56	77.8	6.9				
DWB 69	78.3	6.2				
DWB 75	78.5	6.4				
DWB 91	79.4	6.0				
	80.2	6.0	-2.5	390	10.10	
DWB 123	80.7	6.5				
	81.2	6.1	-5.1	410	10.21	
DWB 145	81.9	6.1				
DWB 148	82.1	6.0				
DWB 171	83.4	7.3				
DWB 172	83.5	7.2				
DWB 177	83.9	6.9				
DWB 178	84.1	6.5				
DWB 179	84.4	6.8				
DWB 186	84.8	6.1				
S 129	98.50	8.00	-9.6	400	10.07	HD 202214
S 130	98.82	12.69				HD 197911
S 133	103.05	9.58				
S 136	105.05	13.23				
S 137	105.60	7.82				
S 150	108.86	6.13				
S 174	120.29	18.44				
S 218	159.50	11.27				
S 274	205.16	14.22	19.0	1800	11.60	See text.

The distribution of spiral tracers closely resembles the pattern of spiral features obtained from 21cm observations by Kepner (1970) and Davies (1972), together with those of others referred to in the latter paper. Therefore these patterns were included in Fig (8.2.1), the distances adopted being those suggested by the spiral tracers. Kinematic distances derived from HI radial velocities were not considered, the differences between these and the adopted distances being discussed later (§9.2). The continuous lines in Fig (8.2.1) represent the observed HI features, which are labelled as shown. The broken lines in Fig (8.2.1) represent suggested extensions to the HI features, largely as a result of the spiral tracer distribution.

If the programme stars hitherto rejected as spiral tracers are plotted in Fig (8.2.1), then no significant change in the spiral pattern results. The only major addition, due to a number of stars at $l \sim 180°$ between 1kpc and 1.5kpc, is the suggestion of a HI feature bridging the gap between the Local Arm, and I_1 and I_2. Such a feature would be consistent with the high concentration of local HI discussed earlier (§8.1).

The Local Arm is well defined by spiral tracers, presumably because of the high interstellar absorption in the direction of $l = 75°$, already discussed (§8.1). The observations made suggest that it extends from the solar neighbourhood in the direction of $l = 75°$. From a more extensive neutral hydrogen survey by Weaver (1971), it would appear that the Local Arm is curved so that this direction becomes $l = 40°$, and that it joins the Sagittarius Arm at about 6kpc from the Sun.

This in turn extends for a further 4kpc in this direction. A region of exceptionally high obscuration in the direction of $l = 40°$ has been discovered by Sherwood (1974). This is consistent with the 21cm observations in that observing longitudinally along a major spiral would give rise to the high interstellar absorption.

The features P_E and P_S in Fig (8.2.1) were discovered by Davies (1972), P_E being the Perseus Arm Extension and P_S a distant

spur protruding from it. It is tempting to suggest that P_E merges with the main branch of the Perseus Arm, P_o, at $l = 180°$. Radio observations cannot confirm this because the radial velocities, due to differential galactic rotation, become zero at $l = 180°$. However the existence of one star, AAO 50-363 (BV5), at approximately the right distance and longitude, supports this belief. Crampton & Georgelin (1975), have concluded that the Perseus Arm is continuous through $l = 180°$, as a result of studying HII regions in the galactic plane.

The features I_1 and I_2 were mapped by Weaver (1971). From the distribution of stars, it appears that they may be connected. Kepner (1970) discovered a feature which she labelled as "Feature Q". This feature extends over the same galactic longitudes as feature I_2, and so confusion between the two may arise. In view of the large HI velocity difference, this is not very probable. Furthermore, the radial velocity and galactic latitude of one of the stars defining I_2, HD 41161, suggests that I_2 could not possibly have any connection with the feature Q.

Simonson III (1975) suggests that there is a dwarf irregular galaxy at $l = 197°.3 \pm 0°.5$, $b = 2°.1 \pm 0°.5$, (17 ± 4)kpc from the Sun, and a satellite of the Milky Way, which provides a satisfactory explanation for Q, as the tidal debris resulting from a perigalactic passage of this galaxy. Consequently Q is not a spiral feature, and is excluded from Fig (8.2.1).

The features P_o, P_1 and I are labelled in manner adopted by Kepner (1970). The stellar distribution suggests that the Intermediate Arm, I, merges with the Local Arm at $l \sim 98°$. The HI observations made by Kepner suggest that I is a very tenuous feature, and because of the association between dust and neutral hydrogen (§8.4), the obscuration of stars observed in I, and through I, will be correspondingly small. This is verified by the low interstellar reddenings observed in the directions of HD 239649, HD 239681, HD 207198 and HD 197406.

The kinematic distance of P_o at the galactic longitude of HD 197406, derived by Kepner, agrees with the distance obtained for this star by Smith (1968). Thus it would appear that HD 197406 is associated with P_o. No mention of the P_1 feature has been made by either Weaver (1971) or Davies (1972). The stars LS1 64-097, BD 69°0219, LS1 64-100 and LS1 61-325 tentatively confirm the existence of this feature in the galactic latitude range $6° \lesssim b < 12°$.

Kepner (1970) reports the existence of a feature, which she refers to as P*, which may be a bridge of HI gas between the P_1 and I features. There is apparently no stellar counterpart to this feature, though the dark nebula L1235 may constitute a part of P*, on account of its high galactic latitude. The remaining features discovered in Kepner's survey, as well as the "Arm X" discovered by Davies (1972), are apparently too distant for even the most luminous of any stars that may be located in these features, to be detected among the stars surveyed.

The stars HD 2083, HD 6675 and HD 7852, at $l \sim 122°$, are apparently not associated with the spiral pattern depicted in Fig. (8.2.1). The region in which these stars are located has already been discussed (§8.1), and it was concluded that any local neutral hydrogen present, was in the form of isolated clouds. As each of these stars appears to have an associated HI feature, the non-participation of these stars in spiral structure is to be expected.

The spiral features delineated by Northern Hemisphere intermediate latitude early type stars are similar to those found from 21cm observations. Furthermore, these early type stars appear to be located at considerable distances from the galactic plane, as summarised in Table (8.2.2). These are consistent with the observations made by Kilkenny et al. (1975). The main branch of the Perseus Arm extends to $\sim$1kpc above the galactic plane, as suggested by Kepner (1970). There are parts of the Local Arm which appear to extend to beyond 0.5kpc.

TABLE 8.2.2

The Distances of Spiral Tracers from the Galactic Plane

Spiral Arm	Feature	Spiral Tracer	z (pc).
Perseus	P_o	HD 197406	1030
		HD 41689	1075
	P_S	AAO 50-164	712
	P_E	HD 53879	461
		AAO 99-263	1039
	P_1	L 1235	890
		LS1 64-097	238
		BD 69°0219	368
		LS1 64-100	238
Intermediate	I	HD 239649	240
		HD 239681	436
		HD 207198	261
		L 1082	840
Local	L	HD 177109	378
(60°<l<85°)		HD 183535	383
		BD 34°3631	358
		HD 185780	367
		HD 186618	525
		HD 186994	630
		HD 225822	283
		HD 188209	415
		HD 189957	216
		HD 190427	343
		HD 191781	293
		HD 192035	399
	I_2	HD 41161	322
		BD 35°1332	193
	I_1	HD 48029	255
		HD 48549	206
		HD 50767	369
		HD 60848	766
		HD 66665	990

On the whole, it appears that the greater the galactocentric distance of a feature, the greater the distance to which it extends from the galactic plane. The notable exception is the feature P_S, although little significance can be attached to one star. Thus, the interpretation of some high velocity features, as vertical extensions to the spiral arms, made by Kepner (1970), seem to be correct. There is also evidence supporting the suggestions by Davies (1972) and Verschuur (1973a, 1973b), that the greater the galactocentric distance, the greater the vertical extension is in the case of the outer spiral arms.

8.3 Estimates for the Height of the Reddening Layer at Different Galactic Longitudes

The variation of interstellar reddening with height above the galactic plane is given by

$$E_{B-V} = \beta \operatorname{cosec} b \, (1 - \exp(-z/h)) \quad - - - - - - - - \quad (8.3.1),$$

if the galactic neutral hydrogen, and the dust associated with it (§8.4), are in hydrostatic equilibrium. In this relation

- z = Distance from the galactic plane,
- b = Galactic Latitude,
- h = a constant, hereafter referred to as the height of the reddening layer, and
- β = constant, which is in fact the value of E_{B-V} that would be obtained for a star if it were located at the galactic pole.

Equation (8.3.1) was derived by Abt & Golson (1962), and they found that their observations of North Equatorial Polar Stars were in agreement with the predictions of this result.

Lanczos (1957) discusses a polynomial approximation for exp(x) which was used to derive an approximate form of equation (8.3.1). An attempt to fit the observed values of E_{B-V} to a polynomial function of the observed values of z, which is of the same form as the polynomial approximation of equation (8.3.1), was made using a regression analysis discussed by Efroymson (1965). This was considered to be unsuccessful due to large scatter in the derived values of β and h, suggesting that equation (8.3.1) does not accurately represent the physical situation for the stars discussed in this analysis.

Consequently equation (8.3.1) was rearranged as

$$h = \frac{z}{(\text{Log}_e \beta - \text{Log}_e (\beta - E_{B-V} \sin b))} \quad - - - - (8.3.2),$$

and h was calculated using an assumed value for β. However, h is only determinate if the condition $\beta > E_{B-V} \sin b$ is satisfied. Thus h was evaluated for a number of different values of β, ranging from $0^m.01$ to $0^m.16$, using the Dunsink Observatory Nova 2/10. The stars were selected at different galactic longitude intervals which corresponded with the apparent distributions of local stars, dust, HI gas, HII regions and dark nebulae, which have been discussed already (§8.1). In this way, it was hoped that any systematic variation in β and h, with galactic longitude, could be taken into account. The adopted value of β was the minimum value satisfying the condition $\beta > E_{B-V} \sin b$, for all programme stars within a selected range of galactic coordinates. Further increases in the value of β gave an increased $\sigma(h)$, the standard deviation in the height of the reddening layer.

The mean h, $\sigma(h)$ and β are listed in Table (8.3.1), in which n represents the number of programme stars within a given range of galactic coordinates. The derived values of $\sigma(h)$ are generally larger than h, for each galactic longitude interval. This suggests that the observations are not represented in a satisfactory way by equation (8.3.1).

Abt & Golson (1962) obtain $\beta = 0^m.057$ and $h = 187$ pc from a fit of their observations of north equatorial pole stars to equation (8.3.1). They obtain a satisfactory fit. However, as they indicate, all their stars are within 550pc, and so the observed reddening would be entirely due to local dust. A graphical fit of observations of intermediate latitude OB stars in the region $260° \leqslant l \leqslant 20°$, $b \geqslant 7°$ has been attempted by Kilkenny (1973), who reports that $\beta = 0.062$ if a value $h = 200$pc, is adopted. There is also considerable scatter in Kilkenny's graphical fit.

TABLE 8.3.1

Heights of the Reddening Layer in Different Galactic Longitude Intervals

Galactic Longitude Interval	n	h pc.	σ(h) pc.	β
$50° < l \leq 70°$	39	239	317	0.04
$70° < l \leq 96°$	37	773	1039	0.11
$96° < l \leq 106°$	41	175	622	0.10
$106° < l \leq 115°$	14	81	128	0.09
$115° < l \leq 130°$	4	73	49	0.08
$130° < l \leq 180°$	31	270	344	0.13
$180° < l \leq 228°$	28	1841	2224	0.10

Thus it would appear that high galactic latitude stars in the solar neighbourhood, such as those observed by Abt & Golson (1962) and Hill & Hill (1966), have colour excesses which are well represented by equation (8.3.1). More distant intermediate latitude stars are not, and so it would appear that a significant proportion of their reddening is due to dust beyond the solar neighbourhood. Furthermore, equation (8.3.1) seems to be invalid beyond the solar neighbourhood, and thus the assumption on which it is based, namely that the galactic gas is in hydrodynamic equilibrium, is invalid.

A closer look at the values of h derived for each star reveals some dependance on the heliocentric and galactocentric distance. This suggests that the high standard deviations are due to systematic errors, rather than random errors. The values of h given in Table (8.3.1) are consistent with the local distributions and spiral features already discussed (§8.1 & §8.2).

With exception of the galactic longitude interval ($50<l\leq70°$), the derived values of β are higher than those obtained by other workers. These will be discussed later (§10.1).

8.4 The Possible Correlation Between Gas and Dust Distributions

Column densities of neutral hydrogen between the observer and a star, hereafter abbreviated to N_H, are not easily determined from 21cm surveys. In fact progress is only possible if it is assumed that no galactic neutral hydrogen lies beyond the star in question, which presumably becomes a better approximation for stars at higher galactic latitudes. Consequently, HI column densities were only considered for stars with $b \gtrsim 10°$, and were obtained from the contour maps published by Heiles (1975). A small feature, such as a local increase in the observed column density, at the galactic coordinates of most stars, gave some confidence in the assumption discussed above.

The r.m.s zero level error of 0.1°K in the corrected neutral hydrogen profiles, gave a column density error of $\pm$ 0.3 x 10^{20} atoms cm^{-2}. Errors incurred through reading the contour maps were estimated to be $\sim$ 0.7 x 10^{20} atoms cm^{-2}, and so the total error is $\sim 10^{20}$ atoms cm^{-2}. The error in E_{B-V} ranges from to $0^m.05$ (§7.2). Errors in N_H due to neutral hydrogen beyond the star are neglected for the moment.

The neutral hydrogen column densities were plotted against the corresponding E_{B-V} reddenings, as depicted in Fig. (8.4.1). The probable error associated with each point, is indicated by the error box on the right hand side. Bearing these errors in mind, together with probable sources of error arising from the above assumption, it can be seen that there may be a linear correlation between N_H and E_{B-V}, and a linear least squares fit, Barford (1967, page 62) was made. The result was

$$N_H \times 10^{-20} = (38.4 \pm 2.7)E_{B-V} + (9.6 \pm 0.5) \quad - - \quad (8.4.1),$$

and the linear correlation coefficient Q, calculated from the equivalent form of equation (9.1.2), was found to be 0.90. Equation (9.1.3) gives $t = 14.6$, and the application of Student's t-test shows that there is a 98% chance of the distribution in Fig (8.4.1) being linear. The straight line drawn in Fig (8.4.1) represents equation (8.4.1).

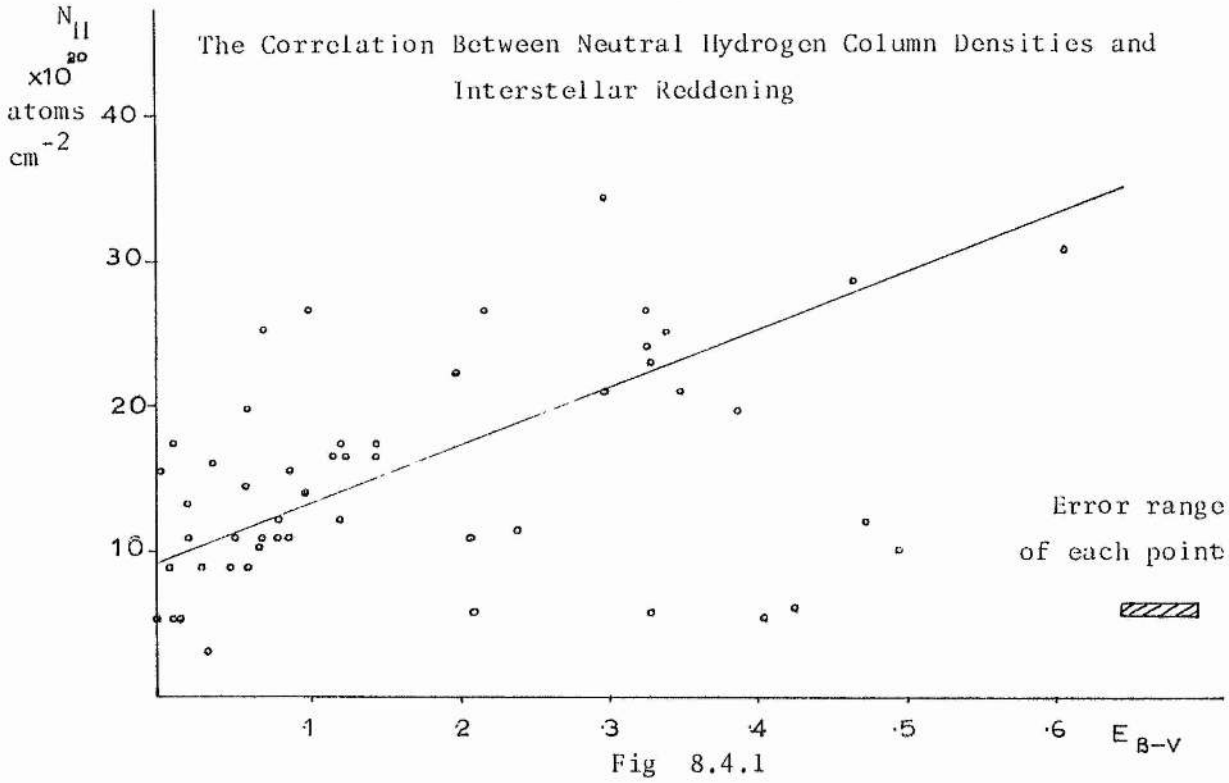

Fig 8.4.1

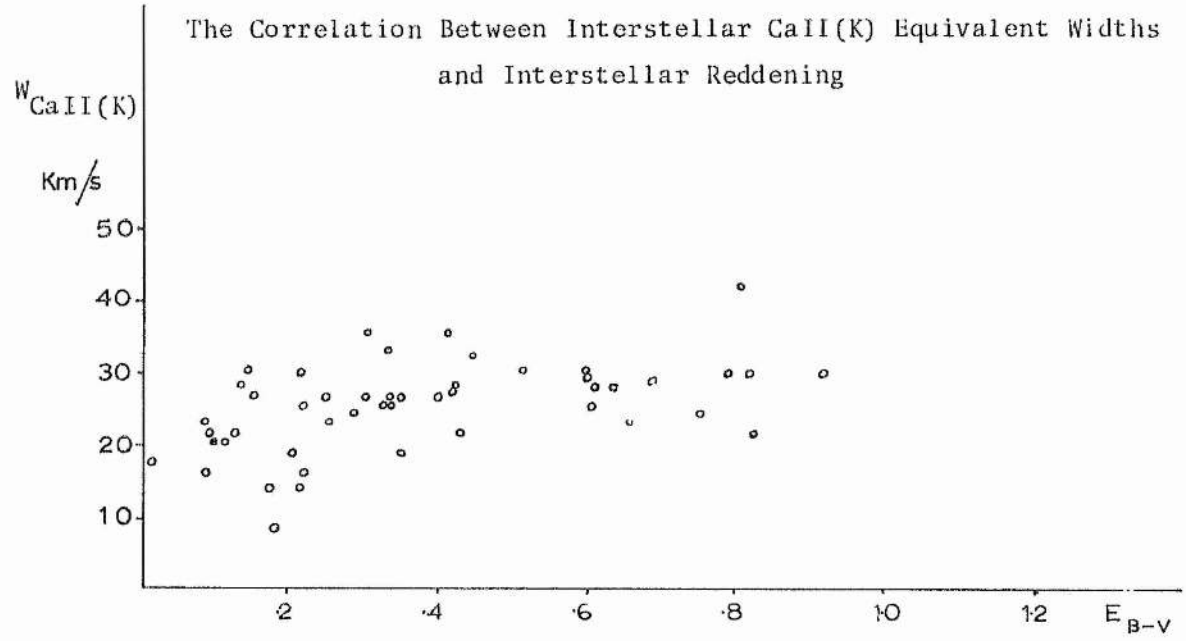

Fig 8.4.2

The stars rejected in the derivation of equation (8.4.1) are listed in Table (8.4.1). The stars HD 32343, HD 203467 and HD 213571 are in the solar neighbourhood, and so the high value of N_H may be due to galactic neutral hydrogen beyond the star. The remaining stars may be associated with concentrations of HI, too small to be resolved in the 21cm surveys. Thus the value of N_H would be too low, which would account for a surprisingly high E_{B-V}.

A quadratic was also fitted to the values of N_H and the corresponding values of E_{B-V}, following the method given by Sokolnikoff & Redheffer (1966, page 675), and the result was

$$N_H \times 10^{-20} = 9.07 + 40.5\ E_{B-V} - 5.93\ E_{B-V}^2 .$$

This gave a larger r.m.s. scatter than equation (8.4.1), and so it was rejected in favour of the linear relation.

The possibility of an association between neutral hydrogen and interstellar dust has been the subject of considerable controversy. Wesselius & Sancisi (1971) have conducted a statistical analysis, and shown that there is no general correlation between gas and dust. However, on consideration of individual regions, they conclude that there is a fairly strong correlation. In particular, a strong correlation was found for the region of the Galaxy considered in this analysis.

High velocity clouds in the Galaxy may explain the absence of a correlation at high galactic latitudes, noted by Wesselius & Sancisi, in the Northern Galactic Hemisphere. Hulsbosch (1975) has proposed that high velocity clouds originate as a result of the infall of extragalactic matter. This suggests a dust density in high velocity clouds between 2×10^{-34}gms cm^{-3}, reported by Schmidt (1975) for the intergalactic medium, and 1.2×10^{-25}gms cm^{-3} for the interstellar medium (Lilley, 1955).

Further consideration to the chemical composition of the interstellar medium was given by Braunsfurt & Rohlfs (1973). They derive the fractional abundance of molecular hydrogen that should be observed as either free gas or coating on interstellar grains, and conclude that if this is not observed, the composition of the interstellar medium is non-uniform.

TABLE 8.4.1

Stars Rejected in Determining the Relation Between N_{H} and E_{B-V}

Star	E_{B-V}	r (kpc)	$N_{H} \times 10^{20}$ atoms cm^{-2}
HD 213571	0.30	0.79	34.12
BD-0°1848	0.41	1.81	5.13
AAO 99 226	0.33	4.22	5.57
AAO 99 263	0.43	4.04	5.57
HD 192575	0.45	0.35	9.59
AAO 99 326	0.21	4.10	5.57
HD 32343	0.10	0.30	26.31
HD 203467	0.07	0.21	25.20

Savage & Jenkins (1972) have derived neutral hydrogen column densities from the interstellar Lyman-α (Lα) line in ultraviolet stellar spectra of nearby OB stars. The interstellar Lα lines are due to neutral hydrogen between the observer and the star in question. Thus, column densities derived in this way are not subject to the uncertainties in 21cm HI column densities, which are discussed above. From Lα column densities in the directions of OB stars in the solar neighbourhood, Kerr and Knapp (1974) derive

$$N_{H} = [\ (51.4 \pm 5.2)\ E_{B-V} - (0.1 \pm 1.9)\ ] \times 10^{20} \quad - - \quad (8.4.2),$$

and similarly Hobbs (1974) derives

$$N_H = (4.8 \times 10^{21}) E_{B-V} \quad - - - - - - - - - \quad (8.4.3)$$

These results suggest a strong linear correlation between gas and dust in the solar neighbourhood, with $N_H = 0$ when $E_{B-V} = 0$. This implies that the constant term in equation (8.4.1) is a mean error, arising from contributions to N_H from galactic neutral hydrogen beyond the stars considered. Thus N_H may be more realistically expressed as a function of E_{B-V} by the relation

$$N_H = (38.4 \pm 2.7) E_{B-V} \times 10^{20} \quad - - - - - - \quad (8.4.4).$$

There appears to be a significant difference between equation (8.4.4) and equations (8.4.2) and (8.4.3). This may be a systematic error or possibly a real difference. Concentrations of galactic dust would be expected at the centres of gravitational attraction, which are the galactic centre and spiral arms. This also applies to the neutral hydrogen, though to a lesser extent as it is more susceptible to Brownian Motion. Thus a higher proportion of dust may be expected at the centres of gravitational attraction, which is precisely where the luminous OB stars are found. The solar vicinity is not a centre of gravitational attraction, as the Sun is located on the inner edge of the Local Arm.

The CaII(K) equivalent widths listed in Table (7.2.1) were plotted against the corresponding E_{B-V}, assuming that this was available, and the result is given in Fig (8.4.2). It can be seen from this that the correlation is rather poor. The linear correlation coefficient was determined, and the Student t-test was applied, as in the case of the $N_H - E_{B-V}$ relation. This showed that there is $\sim$ 80% chance that the relation

$$W_{CaII(K)} = (22.79 \pm 2.08)\ E_{B-V} + (7.41 \pm 4.69)$$

which was derived from a least squares fit (Barford, 1967, page 62) is not due to a random distribution. This correlation is much weaker than that found for the N_{II} - E_{B-V} relation, which supports the results obtained by Hobbs (1975). Consequently, no attempt was made to investigate the galactic gas to dust ratio using the CaII(K) equivalent widths.

CHAPTER NINE

A Kinematic Study of the Programme Stars and the Associated Interstellar Medium.

9.1 A Study of Galactic Rotation from Interstellar Calcium Radial Velocities

The method for determining the mean distance of a column of interstellar material, along the line of sight to a star, was discussed previously (§2.1 & §2.6). To be compatible with the density distribution, adopted by Abt & Golson (1962) and given in equation (8.3.1), equation (2.1.8) was adopted for mean distance determination of interstellar CaII columns. The heights of the CaII layers were assumed to be the same as those derived for the reddening layers at different galactic longitudes (§8.3). The validity of this assumption ia questionable because of the poor correlation between E_{B-V} and the equivalent width of the CaII(K) line.

Corrections to the observed CaII(K) line velocities, due to the solar motion and differential galactic rotation, were determined by the methods already described (§2.3, §2.4, and §2.5). The calculations were carried out using the Dunsink Observatory Nova 2/10. The results and their standard deviations were listed in Table (9.1.1). The values of $\sigma(V_2)$ are large because they reflect the uncertainty in R_o, the distance of the Sun from the Galactic centre.

For $l < 180°$, the values of $\bar{r}$, suggest that most of the interstellar CaII is within 1kpc of the Sun. Values of $\bar{r}_1$ in excess of 1kpc, in this region, are consistent with longitudinal viewing along the Local and Intermediate Arms, where more distant gas is to be expected (§8.2). For $l > 180°$, there is very little local gas (§8.1) and so values of $\bar{r}_1$ in excess of 1kpc should prove to be more common. This is found to be the case and is consistent with the feature I_1, already discussed (§8.2).

The radial velocities of the interstellar calcium lines, corrected for the solar motion, were plotted against galactic longitude. The result is depicted in Fig (9.1.1), and the curves

Table 9.1.1

Calculated Mean Distances and Radial Velocity Corrections for the Observed Interstellar Ca II

Direction of Observed Interstellar Ca II Star		l	b	V_1 km/s	$\sigma(V_1)$ km/s	V_2 km/s	$\sigma(V_2)$ km/s	$\bar{r}_1$ kpc	$\sigma(r_1)$ kpc
HD	170111	54.5	16.8	4.3	4.2	1.9	21.7	0.1	0.3
HD	170650	52.3	15.2	-0.2	3.4	-4.0	21.9	0.2	0.4
HD	174298	54.4	11.2	2.2	2.5	-2.1	23.0	0.3	0.5
HD	174585	62.6	14.6	1.1	7.1	-1.3	24.5	0.2	0.3
HD	175426	66.9	15.5	-0.1	2.5	-1.8	24.0	0.1	0.2
HD	175803	51.2	7.9	13.1	7.1	8.2	23.8	0.3	0.5
HD	176254	52.2	7.7	2.9	3.0	-0.5	22.1	0.2	0.4
HD	176582	69.5	15.4	-1.5	49.4	-3.2	55.1	0.1	0.3
HD	176818	53.3	7.6	-1.2	2.5	-5.6	23.1	0.3	0.5
HD	176819	52.7	7.3	0.0	2.5	-4.4	22.9	0.3	0.5
HD	177006	63.3	12.2	0.0	13.8	-2.9	27.7	0.2	0.4
HD	177109	64.5	12.6	0.1	3.2	-7.7	27.8	0.7	1.0
HD	177347	57.3	9.0	7.1	2.1	4.3	22.9	0.2	0.3
HD	178329	72.2	15.0	2.5	2.5	0.7	24.9	0.2	0.3
HD	178912	64.7	11.1	5.9	9.1	-1.8	29.2	0.6	1.1
HD	180163	70.6	12.7	3.9	28.0	2.4	37.4	0.1	0.2
HD	181164	59.1	6.1	3.0	2.5	-1.1	24.3	0.3	0.5
HD	181409	65.8	9.3	-2.3	5.6	-7.7	26.9	0.4	0.8
HD	181492	64.6	8.6	1.8	2.5	-0.5	24.3	0.2	0.3
HD	182568	62.9	6.6	1.7	2.5	0.2	23.9	0.1	0.2
HD	183535	69.7	9.1	-1.6	2.3	-10.3	30.2	0.9	1.4
HD	183649	68.4	8.2	-68.2	49.4	-73.4	56.1	0.5	0.8
HD	184171	68.0	7.4	-5.2	5.0	-6.6	25.2	0.1	0.2
HD	185780	74.1	9.1	-9.0	5.6	-16.8	32.3	1.1	2.0
HD	186618	80.5	11.5	10.4	1.9	6.1	29.5	1.2	2.1
HD	186694	78.6	10.1	4.5	4.7	-1.7	34.8	1.6	2.7

Direction of Observed Interstellar Ca II Star	l	b	V_1 km/s	$\sigma(V_1)$ km/s	V_2 km/s	$\sigma(V_2)$ km/s	$\bar{r}_1$ kpc	$\sigma(\bar{r}_1)$ kpc
HD 225822	73.4	6.7	39.2	14.8	30.6	36.6	1.1	2.1
HD 187879	75.2	7.1	-0.5	11.3	-4.6	29.4	0.5	1.0
HD 188209	81.0	10.1	5.0	5.1	1.2	29.3	1.1	2.0
HD 188252	81.8	10.5	5.1	5.6	3.2	26.9	0.4	0.8
HD 188439	81.8	10.3	2.3	3.0	-0.4	27.1	0.7	1.3
HD 188461	76.2	7.0	0.6	5.0	-1.9	26.7	0.3	0.6
HD 188891	75.5	6.2	-32.4	38.3	-36.8	47.2	0.6	1.1
HD 189818	91.2	14.4	7.9	4.4	8.5	19.9	0.6	1.0
HD 189957	77.4	6.2	1.4	3.5	-4.2	29.9	1.0	1.8
HD 190025	78.4	6.7	7.4	4.5	5.3	26.7	0.3	0.6
HD 190254	79.7	7.2	67.4	14.4	65.1	30.2	0.4	0.7
HD 191781	81.2	6.6	11.7	10.0	7.7	31.5	1.2	2.2
HD 192035	83.3	7.7	-2.2	2.3	-4.7	30.1	1.4	2.5
HD 192575	101.4	18.1	-11.5	2.5	-10.3	19.4	0.3	1.2
HD 196421	93.8	10.4	-5.8	4.6	-4.8	20.2	0.5	0.9
HD 197770	93.9	9.0	-1.3	3.4	-0.7	20.0	0.3	0.6
HD 197911	98.9	12.6	25.2	18.3	26.6	27.1	0.3	1.6
HD 198739	98.7	11.7	-0.6	12.7	0.2	23.4	0.4	1.0
HD 198781	99.9	12.6	-8.8	2.1	-6.4	21.2	0.5	2.2
HD 199308	94.2	7.4	-5.1	8.6	-4.6	21.6	0.2	0.5
HD 199739	94.9	7.4	12.1	12.7	12.5	23.5	0.2	0.3
BD 59 2333	98.5	8.0	-2.9	4.5	-1.6	20.8	0.3	1.6
HD 202214	98.5	8.0	-6.9	6.6	-6.0	21.0	0.2	1.1
BD 58 2236	97.8	7.2	-7.8	5.4	-6.1	21.5	0.5	2.1
BD 59 2344	98.6	7.6	-15.0	13.6	-13.4	24.7	0.4	1.8
BD 59 2350	99.1	7.5	-3.9	6.6	-2.3	21.6	0.4	1.7
HD 239595	98.5	8.0	-2.9	6.4	-1.9	21.0	0.3	1.2
HD 204150	10 2	7.4	3.6	5.0	5.3	21.4	0.4	1.7
BD 58 2268	99.5	6.1	4.1	6.1	5.6	21.5	0.3	1.6
BD 59 2384	100.2	6.7	-3.6	17.7	2.9	34.8	1.2	4.6

Direction of Observed Interstellar Ca II Star		l	b	V_1 km/s	$\sigma(V_1)$ km/s	V_2 km/s	$\sigma(V_2)$ km/s	$\bar{r}_1$ kpc	$\sigma(\bar{r}_1)$ kpc
HD	205139	100.5	6.6	-4.7	4.2	-2.9	21.5	0.4	1.8
HD	206165	102.3	7.2	-9.2	3.4	-7.0	21.9	0.4	1.9
HD	206327	102.0	6.8	-6.5	5.0	-4.6	21.7	0.4	1.7
HD	207198	103.1	7.0	-8.0	5.6	-2.7	28.2	0.8	3.6
HD	207308	103.1	6.8	-10.0	3.6	-8.2	21.1	0.3	1.5
HD	207951	103.2	6.1	-0.8	5.0	1.2	21.7	0.3	1.6
HD	208106	103.4	6.1	-1.6	5.0	-0.4	20.7	0.2	1.0
HD	208185	104.2	6.9	0.8	5.4	2.4	21.2	0.3	1.3
HD	208218	104.0	6.6	-6.1	3.0	-3.2	23.0	0.5	2.2
HD	208440	104.0	6.4	1.8	3.6	4.5	22.7	0.4	2.0
HD	208904	106.2	8.6	-2.6	1.4	-1.1	19.2	0.2	0.4
HD	208947	106.6	9.0	1.0	5.8	2.1	19.8	0.2	0.3
HD	209789	107.6	9.4	-1.9	23.6	0.3	30.3	0.3	0.6
HD	210386	106.0	6.4	-2.7	3.2	0.4	23.4	0.4	2.1
HD	213087	108.5	6.4	-0.7	2.1	1.8	19.4	0.3	0.7
HD	213405	108.7	6.3	-7.3	5.4	-4.8	20.0	0.3	0.7
HD	213481	109.4	7.4	10.8	13.4	14.2	23.6	0.3	0.8
HD	213571	111.4	10.5	-9.6	5.6	-7.2	19.5	0.3	0.5
HD	216092	112.5	7.3	-19.8	12.7	-17.8	22.5	0.2	0.5
HD	217224	112.7	7.8	2.4	22.2	4.7	29.0	0.3	0.5
HD	222568	116.5	6.4	-5.2	3.0	-2.3	18.0	0.3	0.2
HD	223959	119.5	14.1	-47.3	74.2	-45.0	76.1	0.2	0.2
HD	224395	118.9	10.4	-16.5	11.2	-14.4	20.5	0.2	0.2
HD	2083	120.9	9.0	-1.7	2.5	1.5	17.1	0.3	0.2
HD	3366	121.9	10.1	-16.4	9.9	-14.7	19.4	0.2	0.1
HD	6675	124.5	6.9	-4.4	2.5	0.0	16.6	0.4	0.3
HD	7852	125.5	6.4	-11.2	53.0	-7.3	55.5	0.3	0.3
HD	16440	132.8	7.7	-83.2	49.4	-76.5	52.5	0.5	0.9
HD	17179	131.5	12.0	-75.2	49.4	-72.5	51.7	0.2	0.4
HD	21806	139.7	6.5	-9.6	1.0	-6.1	14.0	0.3	0.5

Direction of Observed Interstellar Ca II Star			V_1	$\sigma(V_1)$	V_2	$\sigma(V_2)$	$\bar{r}_1$	$\sigma(\bar{r}_1)$
	l	b	km/s	km/s	km/s	km/s	kpc.	kpc.
HD 23254	141.8	6.2	8.8	12.9	11.7	18.3	0.2	0.4
HD 25090	143.2	7.4	-0.5	1.3	3.7	13.7	0.4	0.6
HD 25443	143.7	7.3	-8.5	3.4	-6.0	12.8	0.2	0.4
HD 41161	165.0	12.9	8.4	3.2	11.9	17.8	0.6	0.9
HD 41689	151.9	19.3	7.4	18.0	14.5	21.7	0.8	1.0
HD 260611	185.0	10.3	4.2	6.4	2.8	17.0	0.7	1.1
HD 48029	195.1	6.5	38.5	49.4	31.6	50.8	1.1	1.9
HD 58784	214.8	9.1	6.5	3.9	1.1	14.5	0.5	0.8
HD 66665	215.8	19.1	-21.0	1.8	-36.1	24.1	1.4	2.2
HD 25638	143.5	7.7	-6.9	4.1	-0.9	15.6	0.5	0.9
HD 66594	225.8	13.8	-5.4	8.0	-11.1	18.2	0.5	0.8
HD 203374	100.5	8.6	-4.7	2.1	-2.8	21.1	0.4	0.8

Notes

V_1 is the interstellar Ca II radial velocity corrected for the solar motion and $\sigma(V_1)$ is its standard deviation

$\bar{r}_1$ is the mean distance of the column of interstellar Ca II between the observer and each star, $\sigma(\bar{r}_1)$ being its standard deviation

V_2 is V_1 corrected for differential galactic rotation assuming a galactocentric distance based on $\bar{r}_1$, $\sigma(\bar{r}_1)$ being the estimated standard deviation.

A Plot of the Interstellar Calcium Radial Velocities, Corrected for the Solar Motion, as a Function of Galactic Longitude

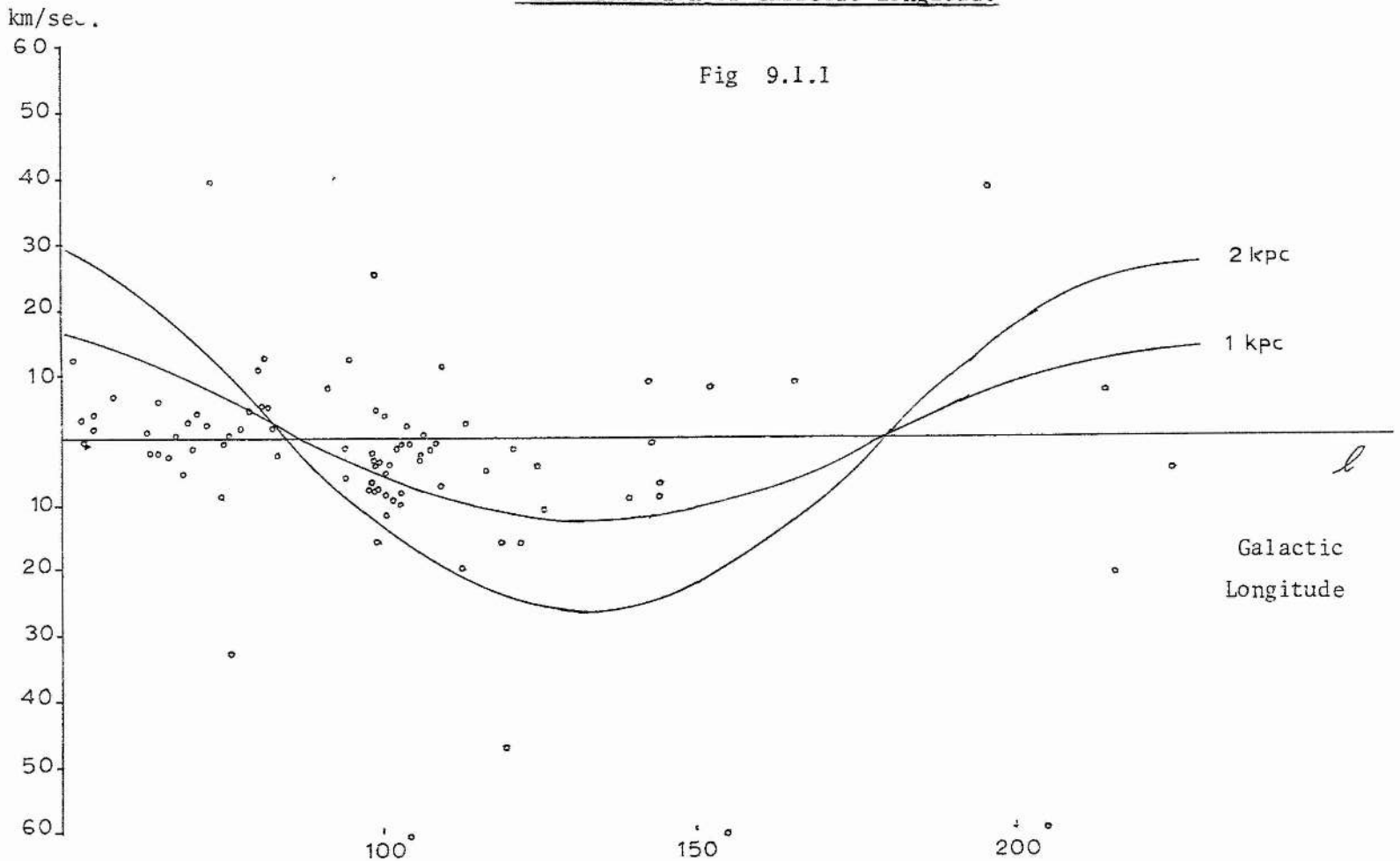

Fig 9.1.1

for interstellar material at 1kpc and 2kpc from the Sun, predicted by differential galactic rotation (equation 2.4.1.2), were included for comparison. If the interstellar calcium does move about the Galactic Centre in circular orbits, then virtually all the interstellar calcium lies within 2kpc. This agrees with the values of $\overline{r}_1$ given in Table (9.1.1).

On correcting V_1 for differential galactic rotation, a small residual radial velocity remains, which is not significantly different from zero. Thus, for each of the ranges of galactic longitude adopted previously (§8.3), the mean residual was calculated, each residual being weighted by its standard deviation, using the method given by Barford (1967, page 64). The mean radial velocity residual ($\overline{V}_2$), the standard deviation of the mean ($\sigma(\overline{V}_2)$), the number of radial velocity residuals contributing to the mean (n) and the corresponding longitude range are listed in Table (9.1.2). Even these averages are not significantly different from zero.

Kinematic information is lost in the averaging process. Consequently it was decided to adopt a correlation analysis, using the model for neutral hydrogen in the galactic plane developed from the density wave theory by Burton & Bania (1974). A useful measure of the relationship between the observed (ΔV_*) and model (ΔV_m) radial velocity residuals is given by the correlation coefficient,

$$Q = \frac{N\Sigma\Delta V_* \Delta V_m - \Sigma\Delta V_* \Sigma\Delta V_m}{\{ [N\Sigma(\Delta V_*)^2 - (\Sigma\Delta V_*)^2] [N\Sigma(\Delta V_m)^2 - (\Sigma\Delta V_m)^2] \}^{\frac{1}{2}}} \quad - - \quad (9.1.1),$$

where N is the number of observations. The significance of the difference of Q from zero was tested using Student's t-test, t being given by

$$t = \left[\frac{Q^2 (N-2)}{1-Q^2} \right]^{\frac{1}{2}} \quad - - - - - - - - - - - - - - - \quad (9.1.2),$$

TABLE 9.1.2

Mean CaII Velocities - corrected for the Solar Motion and Differential Galactic Rotation

$\overline{V}_2$	$\sigma(\overline{V}_2)$	n	l
-2.6	5.5	21	$50° < l \leqslant 70°$
3.1	5.8	22	$70° < l \leqslant 96°$
-1.8	4.5	25	$96° < l \leqslant 106°$
-1.4	7.2	9	$106° < l \leqslant 115°$
-5.5	8.0	7	$115° < l \leqslant 130°$
3.6	4.8	9	$130° < l \leqslant 180°$
-0.7	5.7	5	$180° < l \leqslant 228°$

The probability P of obtaining a value t from a random sample can then be obtained from tables.

For $R_c > R_o$, the Schmidt rotation curve has been expressed by Burton (1971) in the form

$$\omega(R_c) = R_c(C_1 R_c^{-\frac{1}{2}} - C_2 R_c^{-3}) \quad - - - - - - - - \quad (9.1.3),$$

where $C_2 = 1000(C_1/\sqrt{10} - 250)$,

and $C_1 = 885.44$

In an attempt to fit the observations to the density wave theory, Burton & Bania (1974) adopted a value of C_1 given by

$$C_1 = 885.44 + 40k \quad - - - - - - - - - - - - - - - - \quad (9.1.4),$$

where k is a constant. By comparing HI distances with distances determined from supergiants, they found that the best fit between

theory and observations was given by $k = -3.6$.

Burton & Bania have pointed out that their analysis is only valid for the regions $90° \leqslant l \leqslant 165°$ and $195° \leqslant l \leqslant 234°$, and so this restriction was applied. Revised estimates of $\omega(R_c)$ calculated from equation (9.1.3) were used to redetermine the contributions to the radial velocity due to differential galactic rotation, using equation (2.4.1.2). The differences between these and the earlier estimates, constitute the theoretical radial velocity residuals. The correlation between these and the experimental residuals listed in Table (9.1.1), given by equation (9.1.1), was found to be very weak for $k = -3.6$, giving $Q = 0.07$ and $t = 0.66$. This corresponds to a probability of $\sim 31\%$ that the sample of observed radial velocity residuals is entirely random.

Correlations were calculated for a large number of values for k, the best correlation being obtained with $k = 1.34$. This gave $Q = 0.25$ and a corresponding probability of 12% that this correlation could have been obtained from a random sample of observed radial velocity residuals. The fact that this differs from the best estimate of k obtained by Burton & Bania (1974) for supergiants is only marginally significant, in that they obtain $k = -1.7$ for associations and $+3.0$ and -9.0 for HII regions.

The weakness of an analysis of this kind lies in the fact that it is heavily dependant upon a crude method of distance determination. The sources of error in these distances are primarily the result of observing across relatively gas free interarm gaps. Since this arises in only a few cases, the values of $\bar{r}_1$ would be reasonable in most cases. Thus the result of the correlation analysis cannot be rejected on this account, and may be worthy of further consideration.

It can be seen from Table (9.1.1) that the values of V_1 obtained for the interstellar CaII in the directions of the stars HD 188891, HD 190254, HD 183649, HD 223959, HD 16440, HD 17179 and HD 48029 are significantly different from those suggested by differential galactic rotation. A search of the available literature was made

to see if there were any HI features with the same radial velocity.

In a survey by Dieter (1972), an interesting feature corresponding to the interstellar CaII can be found in the direction of HD 190254. This is similarly found, in the cases of the remaining stars, from a survey by Burton & Verschuur (1973). The interstellar calcium velocity found in the direction of HD 223959 is very interesting as it seems to correspond to an intermediate velocity cloud discussed by Hulsbosch (1975). This is considered later (§9.5).

9.2 Neutral Hydrogen Radial Velocities

In this section distances derived from neutral hydrogen radial velocities are compared with those derived from optical spiral tracers. The neutral hydrogen radial velocities of the spiral features I, P_1 and P_0 (§8.2) were obtained for the different galactic longitudes of interest from Fig. 5 (Kepner, 1970). Similarly, the neutral hydrogen radial velocities of the features P_E and I_1 for galactic longitudes $l > 200°$ were obtained from Fig. 3 (Davies, 1972). The heliocentric and galactocentric distances were calculated from the radial velocities using equation (2.4.1.2), in the manner already described (§2.4 and §8.2).

There are some discrepancies between HI spiral features and those suggested by the distribution of stars (§8.2). Only spiral tracers for which there appear to be corresponding neutral hydrogen features are considered in this section. These are listed in Table (9.2.1). The stellar distances and galactocentric distances are those derived previously (§7.2).

It can be seen that there is a general disagreement between the stellar distances derived from photometry, and the neutral hydrogen distances suggested by differential galactic rotation (Schmidt, 1956). If these were largely due to systematic errors in photometry, radial velocities, calibration or reddening correction, then the departures would be expected to be similar for a given heliocentric distance, and not show the dependence on galactic longitude and galactocentric distance, exhibited by the figures in Table (9.2.1). Thus only two conclusions are possible. The distances may be genuinely different, that is the optical and HI spiral arms do not coincide. Alternatively, there may be a systematic velocity difference between the stars and HI gas.

The first suggestion is unacceptable for two reasons. In the first instance our ideas on stellar evolution suggest that very young stars are associated with neutral hydrogen. Thus, if the suggestion of non-coincidence of optical and radio spiral arms were to be accepted a drastic revision of the theory of

Table 9.2.1

A Comparison Between the Observed Neutral Hydrogen Radial Velocities and those Predicted from Differential Galactic Rotation and the Density Wave Theory

Spiral Feature	Probable Stellar Member	l	b	Stellar Distance (kpc.) Heliocentric	Galactocentric	Neutral Hydrogen Radial Velocity (km/s) Observed	Schmidt Model	Density Wave Theory
I	BD 59 2384	100.18	6.69	3.75	11.27	-32	-31	-35
P_1	BD 69 0219	136.61	11.16	1.90	11.43	-20	-24	-27
P_0	HD 41689	151.92	19.34	3.25	12.79	-29	-26	-32
I_1	HD 60848	202.53	17.53	2.54	12.27	20	20	22
	HD 64854	220.70	14.14	2.88	12.25	38	33	37
	HD 66665	215.76	19.13	3.03	12.43	35	31	35
	HD 59882	222.54	6.38	3.09	12.44	40	37	43
P_E	HD 53879	207.01	7.36	3.60	13.28	38	31	36
	AAO 99 326	220.24	12.61	4.09	13.30	55	41	51
	AAO 99 226	219.91	14.90	4.22	13.38	54	41	51
	AAO 99 263	220.86	14.89	4.04	13.21	56	41	50

stellar evolution would be needed. Furthermore, observational evidence indicates that the Milky Way is similar to the Andromeda Nebula (M31). Emerson (1974) has shown that there is a strong correlation between the distribution of neutral hydrogen and OB stars in M31. Therefore, it is reasonable to assume a systematic velocity difference between the stars and gas in the spiral arms.

On this basis the photometrically determined stellar distances were adopted for the spiral features. The expected neutral hydrogen radial velocity for these distances were than calculated using the method already described (§2.4). Neutral hydrogen radial velocities were also predicted using the density wave theory in the manner already adopted for the CaII(K) velocities (§9.1). Since the number of neutral hydrogen radial velocities is small, it was decided that the minimum mean square residual would be adopted as a criterion for the best fit to the observations.

Theoretical neutral hydrogen radial velocities were calculated for a number of different values of k. The value $k = -0.7$ gave the best fit and the predicted velocities are listed in Table (9.2.1). The fact that this value of k differs from those obtained by Burton & Bania (1974), is of little significance because so few neutral hydrogen radial velocities have been considered.

9.3 A Comparison of the Stellar Kinematics with the Theoretical Predictions

The programme stars with space velocities high enough to allow the star to escape from its present location in the Galaxy, or even escape from the Galaxy altogether, have already been considered (§7.4). The remaining programme stars might be expected to participate in differential galactic rotation. Consequently the stellar radial velocities, corrected for the solar motion in the manner already described (§2.4), were plotted against galactic longitude, as depicted in Fig. (9.3.1). Radial velocity curves for stars at 1kpc, 2kpc, 3kpc and 4kpc from the Sun, predicted by differential galactic rotation (equation 2.4.1.2), were included for comparison. The radial velocities corrected for the solar motion and differential galactic rotation, and their standard deviations, are listed in Table (9.3.1). The high velocity stars were included for completeness.

A comparison of Fig (9.1.1) with Fig (9.3.1) suggests that the interstellar calcium adheres to differential galactic rotation more closely than OB stars. This is consistent with the results of Blaauw (1952), who obtained a velocity dispersion of $\sim$6 km/sec for interstellar CaII(K) line radial velocities, and Filin (1957), who obtained a radial velocity dispersion of $\sim$ 10km/sec for B stars. It has been pointed out by Burton (1974), that this difference in radial velocity dispersions is to be expected from the predictions of the density wave theory (Lin et al., 1969). This is because the interstellar medium is more responsive to a spiral gravitational field than stars. Thus there may be reason to believe that the density wave theory, which is successful in explaining spiral structure in the galactic plane, may also explain spiral structure at intermediate galactic latitudes.

The mean radial velocities, corrected for the solar motion and differential galactic rotation, were calculated for each of the galactic longitude ranges previously adopted (§8.3). Each

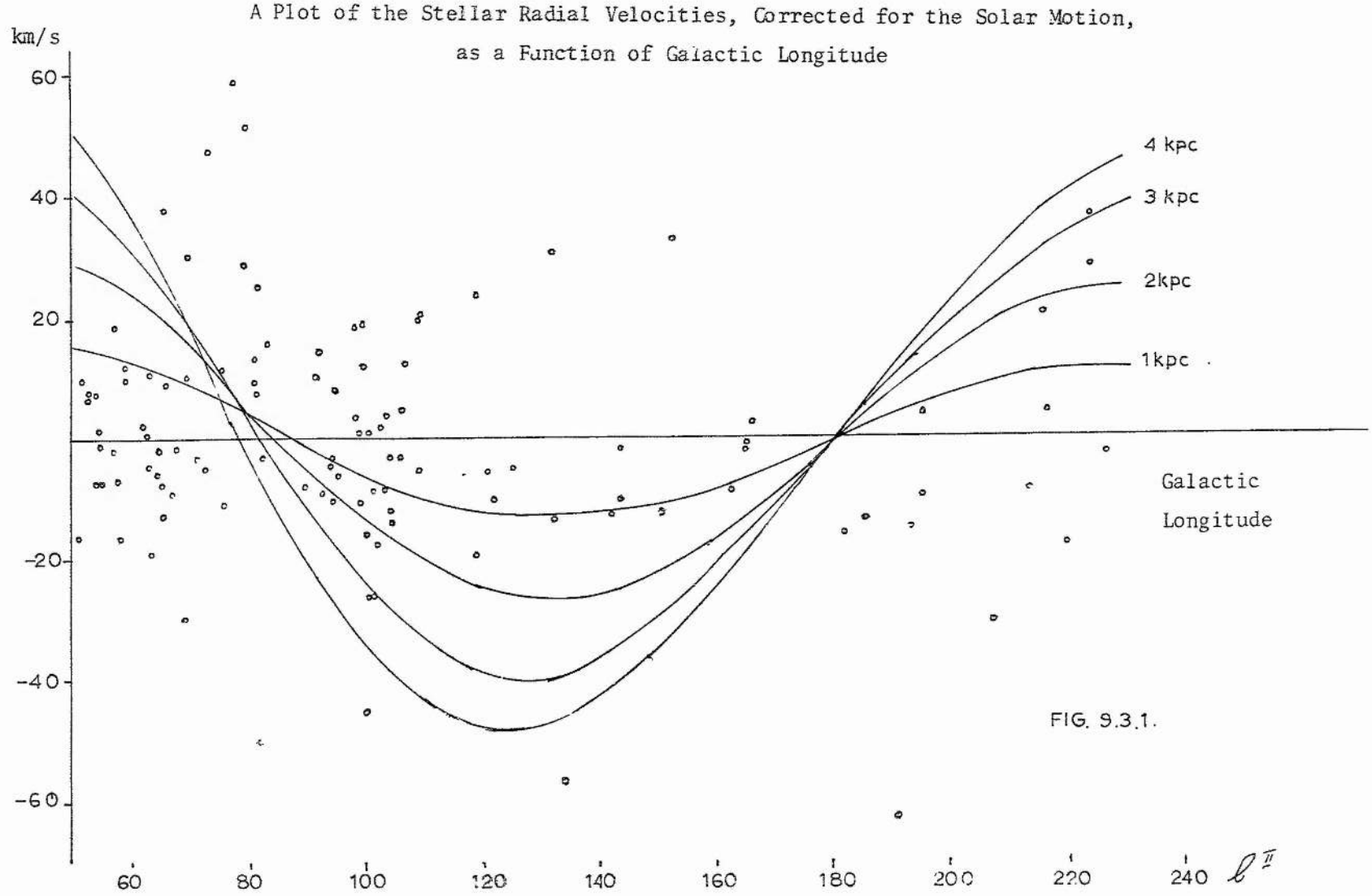
A Plot of the Stellar Radial Velocities, Corrected for the Solar Motion,
as a Function of Galactic Longitude
km/s
60
40
20
-20
-40
-60
4 kpc
3 kpc
2kpc
1kpc
Galactic
Longitude
60
80
100
120
140
160
180
200
220
240
ℓ^{II}

FIG. 9.3.1.

Table 9.3.1

Stellar Radial Velocities Corrected for the Solar Motion and Differential Galactic Rotation

Star	V_1	$\sigma(V_1)$	V_2	$\sigma(V_2)$	Star	V_1	$\sigma(V_1)$	V_2	$\sigma(V_2)$
HD 169798	0.2	2.1	-7.9	20.7	HD 170028	-7.4	3.0	-13.4	21.4
HD 170051	-7.0	3.0	-13.4	21.5	HD 170111	-0.6	9.0	-5.3	23.0
HD 170650	0.4	3.0	-7.7	21.2	HD 174298	2.1	3.0	-6.9	22.2
HD 174585	0.6	4.0	-4.2	23.6	HD 175426	-8.9	4.0	-12.1	24.2
HD 175803	-16.2	8.0	-26.2	22.9	HD 176254	10.2	3.0	3.6	21.6
HD 176502	-2.4	3.0	-5.8	24.6	HD 176582	10.0	8.0	6.8	25.6
HD 176818	8.0	13.0	-1.0	25.5	HD 176819	6.7	5.0	-2.1	22.3
HD 176871	18.7	10.0	15.5	24.5	HD 176914	11.6	3.0	-0.4	23.8
HD 177003	-6.2	0.6	-7.4	24.9	HD 177006	10.0	9.0	4.2	25.4
HD 177109	-5.9	3.0	-23.6	25.3	HD 177347	-6.8	6.0	-12.3	23.4
HD 177593	-6.8	2.5	-12.6	24.2	HD 178329	-4.7	3.0	-8.0	24.9
HD 174179	2.2	8.0	-2.9	24.4	HD 178475	-1.2	10.0	-4.8	26.2
HD 178540	-2.0	8.0	-6.1	23.8	HD 178849	8.8	7.0	4.2	25.2
HD 178912	1.9	8.0	-14.9	26.4	HD 180124	-16.7	9.0	-22.2	24.5
HD 180163	7.7	4.0	4.9	25.0	HD 180844	-13.4	4.0	-18.4	24.6
HD 181164	9.2	3.0	1.0	23.6	HD 181409	37.9	7.0	26.8	25.9
HD 181492	-1.8	3.0	-6.1	24.3	HD 182568	-4.3	9.0	-6.9	25.4
HD 183339	-7.7	7.0	-7.6	20.2	HD 183535	30.4	9.0	13.4	27.8
HD 183649	-28.9	9.0	-39.2	26.9	HD 184171	-5.6	3.0	-8.1	24.9
HD 185780	11.0	17.0	-0.6	31.4	HD 186618	26.0	5.0	23.5	26.4
HD 186994	29.5	30.0	28.2	39.7	HD 225822	47.1	16.0	34.1	31.0
HD 187879	11.8	7.0	4.5	27.1	HD 188209	9.0	4.0	6.3	26.4
HD 188252	-3.2	3.0	-6.2	26.3	HD 188439	-49.9	8.0	-53.3	27.4
HD 188461	2.7	3.0	-1.8	26.2	HD 189775	-1.6	4.0	-2.5	26.4
HD 188891	-10.5	14.0	-18.2	29.8	HD 189818	10.7	3.0	13.2	19.4
HD 189957	58.4	5.0	50.6	27.0	HD 190025	1.3	13.0	-2.4	29.3
HD 190254	50.8	21.0	47.0	33.6	HD 190427	13.7	3.0	11.1	26.5
HD 191781	7.8	7.0	5.5	27.3	HD 192035	15.8	7.0	18.3	20.7

Star	V_1	$\sigma(V_1)$	V_2	$\sigma(V_2)$	Star	V_1	$\sigma(V_1)$	V_2	$\sigma(V_2)$
HD 192575	-25.4	3.0	-22.0	18.6	HD 196421	-3.8	6.0	-1.0	20.3
HD 197770	-3.3	9.0	-1.8	21.6	HD 197911	18.8	19.0	22.7	26.9
HD 198739	12.4	17.0	14.4	25.7	HD 198781	-15.2	3.0	-7.0	18.9
HD 199308	-10.1	1.1	-8.9	19.7	HD 199661	-6.2	6.0	-5.5	20.6
HD 199739	8.2	7.0	9.0	20.9	BD 59 2333	1.1	9.0	4.4	21.3
HD 202214	-4.1	5.0	-2.1	20.1	BD 58 2236	-4.4	5.0	0.3	19.9
BD 59 2344	4.0	7.0	8.0	20.5	BD 59 2350	-11.3	7.0	-7.5	20.5
HD 239595	1.1	9.0	3.4	21.4	HD 204150	-25.7	5.0	-21.4	19.8
BD 58 2268	19.1	24.0	22.7	30.8	BD 59 2384	-44.9	13.0	-13.5	22.1
HD 205139	-2.6	4.0	1.9	19.6	HD 206165	2.0	4.0	7.5	19.4
HD 206327	-16.9	5.0	-12.4	19.7	HD 207198	-7.6	3.0	9.3	18.4
HD 207308	-12.0	3.0	-7.9	19.3	HD 207951	3.6	18.0	8.1	26.2
HD 208106	-13.3	26.0	-10.6	32.3	HD 208185	-13.2	15.0	-9.6	24.2
HD 208218	-11.0	3.0	-3.8	19.0	HD 208440	-3.2	11.0	3.2	21.8
HD 208904	5.4	7.0	9.1	20.0	HD 208947	12.8	7.0	15.2	20.0
HD 209789	0.5	40.0	6.8	44.0	HD 210386	-3.3	5.0	4.0	19.2
HD 213087	-4.9	4.0	1.5	18.8	HD 213405	19.7	19.0	26.2	26.4
HD 213481	21.3	20.0	31.8	26.9	HD 213571	-8.5	3.0	-1.4	18.0
HD 216992	-4.1	2.1	0.8	18.1	HD 217224	3.1	8.0	9.1	19.5
HD 222568	-6.2	7.0	1.0	18.6	HD 223959	23.9	23.0	31.3	28.2
HD 224395	-19.5	5.0	-14.0	17.5	HD 2083	-5.3	6.0	3.9	17.4
HD 3366	-8.4	3.0	-4.5	16.7	HD 6675	0.2	2.1	12.5	15.6
HD 7852	-4.7	15.0	5.3	21.5	HD 16440	-13.0	38.0	2.3	40.3
HD 17179	31.2	21.0	37.1	25.4	HD 17929	-55.6	3.0	-51.6	14.3
HD 21806	-20.6	9.0	-13.3	15.3	HD 23254	-12.2	6.0	-6.3	13.3
HD 25090	-2.4	6.0	6.7	12.8	HD 25443	-1.2	3.0	3.9	11.8
HD 40160	3.2	7.0	6.4	8.3	HD 40784	-7.7	28.0	-4.0	28.5
HD 41161	0.2	14.0	8.9	14.7	HD 41689	33.0	7.0	59.7	8.1
HD 42782	-1.6	9.0	1.1	10.2	HD 46552	-15.3	6.0	-15.8	6.1
HD 260611	-2.8	5.0	-5.7	5.3	HD 48029	5.0	21.0	-8.5	21.1
HD 48532	-9.0	8.0	-13.3	9.2	HD 48549	-14.1	31.0	-22.9	31.2
HD 53879	-31.1	31.0	-60.4	31.3	HD 58784	21.5	22.0	10.3	24.4

Star	V_1	$\sigma(V_1)$	V_2	$\sigma(V_2)$	Star	V_1	$\sigma(V_1)$	V_2	$\sigma(V_2)$
HD 59882	29.2	5.0	-7.8	7.9	HD 66665	5.1	6.0	-25.7	7.8
HD 50767	-62.4	35.0	-71.3	35.2	HD 57291	-7.7	3.0	-14.5	10.8
HD 25638	-9.2	2.1	4.3	11.2	HD 66594	-1.4	11.0	-13.3	17.1
HD 32343	-12.3	2.1	-9.2	9.5	HD 65875	27.4	12.0	22.0	17.7
HD 198512	3.3	8.0	5.1	21.3	HD 203374	1.0	15.0	5.9	24.3

Notes:

V_1 is the stellar radial velocity, in km/s, and corrected for the solar motion. Its standard deviation is $\sigma(V_1)$

V_2 is V_1 corrected for differential galactic rotation, (V_2) being its standard deviation. These quantities are also expressed in km/s.

TABLE 9.3.2

Mean Stellar Radial Velocities - corrected for the Solar Motion and Differential Galactic Rotation

$\bar{V}_2$	$\sigma(\bar{V}_2)$	n	l
-6.3	4.2	33	$50° < l \leqslant 70°$
3.1	4.6	29	$70° < l \leqslant 96°$
-1.3	4.3	25	$96° < l \leqslant 106°$
8.6	7.1	9	$106° < l \leqslant 115°$
2.7	7.0	9	$115° < l \leqslant 130$
8.1	3.3	14	$130° < l \leqslant 180°$
-12.9	2.7	14	$180° < l \leqslant 228°$

radial velocity was weighted by its standard deviation and the means calculated using the method given by Barford (1967, page 62). The means are listed in Table (9.3.2), and it can be seen that some are significantly different from zero, which would suggest that the Schmidt Rotation curve does not adequately describe galactic rotation.

A correlation analysis was adopted to see if the velocity residuals in the programme stars agreed with the predictions made by density wave theory. This shows that the departures from circular motion can be expressed in terms of the peculiar motions, V_R and V_Θ taken to be positive in the directions of increasing galactic radius and azimuth respectively, where

$$V_R = - a_R \cos [\times(R,O)] \quad - - - - - - - \quad (9.3.1)$$

and $$V_\Theta = a_O \sin [\times(R,O)] \quad - - - - - - - - \quad (9.3.2)$$

Following Burton & Bania (1974, the model is simplified by assuming that

$$a_R = a_\Theta = \frac{a}{8.0} \left(2R - \frac{R^2}{8.0} \right) \quad - - - - - - \quad (9.3.3),$$

where R is the galactocentric distance, and

a is a constant.

The angle $\times$ is the phase of the superimposed spiral given by

$$\times = 2\Theta - \phi(R) \quad - - - - - - - - - - - - - - - \quad (9.3.4),$$

where $\phi(R)$ is the radial phase function, and Θ is the galactic azimuth angle given by

$$\sin \Theta = \frac{r \sin l}{R} \quad - - - - - - - - - - - - - - - \quad (9.3.5),$$

where r is the heliocentric stellar distance.

The tilt angle t is related to the angular wave number k(R) by

$$k(R) = \frac{d\phi}{dR} = \frac{-2}{R \tan t} \quad - - - - - - - - - - \quad (9.3.6),$$

Since consideration is being given to stars within a few kiloparsecs of the Sun, the practise of Burton & Bania (1974) can be adopted and t assumed to be a constant independent of R. Therefore, solving the differential equation (9.3.6) gives

$$\phi = \frac{-2}{\tan(t)} \text{Log}_e (R/R') \quad - - - - - - - - - - \quad (9.3.7),$$

where R' is the constant of integration.

Considering the case of $\Theta = 0$. For the Sagittarius Arm $\times = +2\pi$, and for the Perseus Arm $\times = +2\pi$. The working model adopted by Burton & Bania (1974), places these two arms at distances of 8.9 and 11.4 kpc, adopts a tilt angle of 8° and a = 5. Substituting for R in equation (9.3) gives

$$8.9 = R' e^{\pi \tan(t)} \quad - - - - - - - - - - - - \quad (9.3.8),$$

and $$11.4 = R' e^{-\pi \tan(t)} \quad - - - - - - - - - - - - \quad (9.3.9).$$

Multiplying equations (9.3.8) and (9.3.9) gives R' = 10.07. Thus substituting for t and R' in equation (9.3.7) enables $\phi(R)$ to be determined. Hence, using equations (9.3.5), (9.3.4) (9.3.3), (9.3.2) and (9.3.1), V_R and V_Θ can be determined. The residual in the radial velocity, after correcting for the solar motion and differential galactic rotation is given by

$$\Delta V_m = V_\Theta \cos(90° - 1 - \Theta) - V_R \cos(1 + \Theta) \quad - - - \quad (9.3.10)$$

The residual ΔV_m was calculated for each programme star and the correlation coefficient Q determined, using equation (9.1.2), to be 0.23. Student's t-test showed that the probabilty of obtaining this correlation from a random sample of velocity residuals is 11%. Thus it would appear that the density wave theory is valid for intermediate galactic latitudes, as well as for the galactic plane.

The correlation is not as good as that obtained by Burton & Bania (1974) for supergiants in the galactic plane. There are probably several reasons for this. A number of main sequence stars of type B5V have been considered here, and these may be so far from their places of formation that they can no longer be regarded as spiral tracers.

Another possibility is that as the distance from the galactic plane increase, the density wave theory becomes a poorer and poorer representation of the physical situation. Thus the stars near the the galactic plane may give a stronger correlation than those further away. This was tested by calculating Q for different maximum distances from the galactic plane. The correlation was found to become stronger as stars further from the galactic plane were included.

In fact the best correlation was obtained when all stars up to a maximum distance of 1 kpc from the galactic plane were included, in which case only HD 41689 was excluded. This resulted in Q = 0.27 with t = 3.19, giving a probability of this correlation resulting from a random sample of 10%.

It would appear, therefore, that the density wave theory is valid at distances up to 1kpc from the galactic plane. The weaker correlation obtained in this analysis may be due to the fact that only 131 optical spiral tracers have been considered. Burton & Bania (1974) have used 668 optical spiral tracers, and this may result in their obtaining a stronger correlation.

9.4 Stellar Dynamical and Evolutionary Lifetimes

Early type stars appear to exist in considerable numbers at distances up to 1kpc from the galactic plane (§8.2). A similar result has been obtained by Kilkenny et al. (1975), who have conducted a similar survey in the Southern Hemisphere. Early type stars are generally thought to have been formed in the galactic plane, in which case they can only achieve great distances from the galactic plane by virtue of their space motions.

If this is not the case, then either stars are formed away from the galactic plane, or a large proportion of them are subluminous. The latter is not very likely in view of recent work by Greenstein (1971). The former suggestion can be tested by making a comparison of stellar dynamical and evolutionary lifetimes.

The calculation of stellar ages is dependant upon the adopted theoretical model of stellar evolution. Since stars spend most of their lifetime on the main sequence, and undergo little, if any, apparent change during that time, the age of main sequence stars is difficult to determine. An approximate formula for the duration of the main sequence, given by Iben (1972), is

$$t_{ms} \sim 34\ (7M_{\odot}/M)^{1.9} \qquad (9.4.1),$$

where t_{ms} is the duration of the main sequence in millions of years,

M is the mass of the star, and

$M_{\odot}$ is the solar mass.

This formula is valid for $M > 3M_{\odot}$ and can be regarded as representing an upper limit for the age of a main sequence star. It was adopted to calculate t_{ms} for the main sequence stars in this analysis, for reasons of computational simplicity. The masses for the main sequence stars were taken from Schmidt Kaler (1965b), making interpolations for intermediate spectral types where necessary.

Giant and supergiant stars also present difficulties when it comes to determining their ages. This is largely because of uncertainties in their masses, metal content and the extent to which they have evolved from the main sequence. The age of a cluster can be determined by fitting its colour-magnitude diagram to theoretical curves of equal time in the HR diagram. As a result, it seems reasonable to suppose that crude estimates of stellar ages can be made in the same way, provided the stars are young and luminous. This has been done by Barbaro et al. (1969), who have derived a set of isochronous curves in the M_V, $(B-V)_o$ diagram, given in Fig. 2 of their paper. The age of a star may be read off from this diagram, if the absolute magnitude (M_V) and $(B-V)_o$ are known. If the star is well evolved, or $M_V < -4$, then this can be done accurately, otherwise the age will be subject to a larger probable error.

Stellar dynamical lifetimes are difficult to determine with any accuracy because of the large uncertainties in the force law and the component of the space velocities normal to the galactic plane. The force law adopted previously (§7.4) is used again here. Thus the acceleration away from the galactic plane in the direction of increasing z is given by

$$\ddot{z} = -(a_0 + a_1 z + a_2 z^2 + a_3 z^3 + a_4 z^4) \qquad (9.4.2),$$

where a_0, a_1, a_2, a_3, a_4 and a_5 are the same as those in equation (7.4.1).

In the above relation, z is in parsecs and $\ddot{z}$ in cms/sec^2 x 10^{-9}. Making the substitution $\ddot{z} = \frac{d\dot{z}}{dz}\dot{z}$ it follows that

$$\dot{z} = \left[2K - z(a_0 + a_1 z + \tfrac{2}{3} a_2 z^2 + \tfrac{1}{2} a_3 z^3 + \tfrac{2}{5} a_4 z^4)\right]^{\frac{1}{2}}$$

$$\qquad (9.4.3),$$

where K is the constant of integration. This can be evaluated for each star by substituting the observed height above the galactic

plane, and the observed space velocity component. An attempt to derive an expression for z as a function of time, results in the need to evaluate an elliptic integral. Thus it was decided to proceed by numerical integration.

Consider the case of a star moving away from the galactic plane, and at a distance z from it. This distance is divided into a 1000 equal intervals. For each of these, the velocity $\dot{z}$ is calculated from equation (9.4.3), by substituting the value of z corresponding to the point in each interval nearest the galactic plane. The time taken by the star to traverse each interval was then calculated on the assumption that $\dot{z}$ is a constant for that interval. The dynamical lifetime is then the sum of these times.

A star originating in the galactic plane and moving towards it, must have been ejected, attained a maximum distance at which $\dot{z} = o$ and is now "falling back". The dynamical lifetimes of such stars were calculated, in a manner similar to that used above, assuming that no change to the force law had occurred during the trajectory. The time taken by a star to reach its present distance from the galactic plane, assuming that the star is moving away from it, was calculated as before. The integration was continued, by summing the times taken to traverse intervals of the same size, until $\dot{z} = o$. Thus the time taken to reach the maximum distance from the galactic plane can be calculated, and the dynamical lifetime is then twice this less the time taken to traverse the distance from the galactic plane to the present position.

The space motions of the stars HD 191781, HD 204150, HD 225822, HD 53879, HD 66665 and HD 50767 suggest that their distances from the galactic plane exceeded 3kpc at one time. Beyond this distance equation (9.4.2) is no longer valid (§7.4). Thus, the dynamical lifetimes of these stars were calculated on the assumption that they reach their maximum distance from the galactic plane when $\dot{z} = o$, which is not necessarily the case. Thus the calculated dynamical lifetimes of these stars must be regarded as absolute minima. These dynamical lifetimes and evolutionary lifetimes of main sequence stars,

were determined using the Dunsink Observatory Nova 2/10. The results are presented to the nearest 10^6 years in Table (9.4.1), T_c and T_d denoting the evolutionary and dynamical lifetimes respectively.

The stars listed in Table (9.4.1) for which the space velocity component normal to the galactic plane is significantly positive, that is $(W - \sigma(W))>0$, have $T_e > T_d$ in many cases. Thus it appears that these stars were formed in the vicinity of the galactic plane and subsequently ejected from it. However, $T_d > T_e$ or the stars HD 174298, HD 192575, HD 198781, HD 210386 and HD 41161. With the exception of HD 210386, these are all main sequence stars and thus the above result is all the more surprising since the value of T_e, listed in Table (9.4.1), is the upper limit to the evolutionary lifetime.

Unless the force law is different from that expressed in equation (9.4.2), it seems possible that these stars were formed away from the galactic plane. The dynamical and evolutionary lifetimes become comparable when it is assumed that these stars were formed at $\sim$ 100pc from the galactic plane. Their colour classes are all B1 or earlier, and this may be significant.

Similarly there are many stars with $(W - \sigma(W))<0$ and for every one of them, $T_d > T_e$. For some stars, the difference is as large as an order of magnitude. Recalling that T_e is the maximum evolutionary lifetime likely for a main sequence star, this result is even more striking. It appears, therefore, that these stars must have been formed away from the galactic plane. In this case the dynamical lifetimes would be much shorter, and more comparable with the evolutionary lifetime.

Therefore, among the programme stars for which $|W - \sigma(W)|>0$, there are 19 which seem to have been formed away from the galactic plane, and 15 which were probably formed in its vicinity. Among intermediate galactic latitude early type stars, 50% may have been formed away from the galactic plane. The origin of those stars is considered in the next section (§9.5). The possibility that these stars are subluminous does arise, but it would appear from the results of Greenstein (1971), that this is rather unlikely.

Table 9.4.1

The Stellar Dynamical and Evolutionary Lifetimes

Star	T_e	T_d	Star	T_e	T_d	Star	T_e	T_d
HD 169798	19	7	HD 170028	40	14	HD 170051	40	8
HD 170111	29	21	HD 170650	28	37	HD 174298	12	22
HD 174585	12	66	HD 175426	29	40	HD 175803	29	83
HD 176254	37	104	HD 176502	12	53	HD 176582	29	0
HD 176818	8	11	HD 176819	8	2	HD 176871	54	3
HD 176914	8	9	HD 177003	29	72	HD 177006	29	50
HD 177109	17	3	HD 177347	29	9	HD 177593	54	82
HD 178329	29	39	HD 174179	28	64	HD 178475	43	18
HD 178540	40	2	HD 178849	29	53	HD 178912	8	8
HD 180124	40	73	HD 180163	22	25	HD 180844	40	75
HD 181164	19	20	HD 181409	12	56	HD 181492	29	62
HD 182568	5	61	HD 183339	54	6	HD 183535	12	94
HD 183649	29	4	HD 184171	28	18	HD 185780	10	4
HD 186618	10	21	HD 186994	8	7	HD 225822	12	67
HD 187879	10	16	HD 188209	8	23	HD 188252	12	55
HD 188439	10	7	HD 188461	19	66	HD 189775	29	62
HD 188891	17	4	HD 189818	8	0	HD 189957	8	5
HD 190025	40	4	HD 190254	40	5	HD 190427	5	4
HD 191781	5	39	HD 192035	8	1	HD 192575	9	13
HD 196421	8	16	HD 197770	12	2	HD 197911	19	2
HD 198739	54	85	HD 198781	9	11	HD 199308	5	2
HD 199661	29	5	HD 199739	19	2	BD 59 2333	19	3
HD 202214	9	3	BD 58 2236	19	5	BD 59 2344	12	0
BD 59 2350	12	2	HD 239595	29	3	HD 204150	37	49
BD 58 2268	19	1	BD 59 2384	14	6	HD 205139	10	8
HD 206165	8	14	HD 206327	19	10	HD 207198	6	5
HD 207308	9	1	HD 207951	19	36	HD 208106	19	5
HD 208185	19	37	HD 208218	14	2	HD 208440	12	5
HD 208904	19	13	HD 208947	19	15	HD 209789	29	43
HD 210386	10	20	HD 213087	8	1	HD 213405	9	37

Star	T_e	T_d	Star	T_e	T_d	Star	T_e	T_d
HD 213481	12	94	HD 213571	8	93	HD 216992	29	2
HD 217224	19	0	HD 222568	12	116	HD 223959	29	5
HD 224395	29	81	HD 2083	12	6	HD 3366	29	2
HD 6675	8	143	HD 7852	19	17	HD 16440	14	1
HD 17179	29	151	HD 17929	54	38	HD 21806	12	22
HD 23254	54	7	HD 25090	6	142	HD 25443	5	34
HD 40160	29	20	HD 40784	54	7	HD 41161	4	14
HD 41689	14	12	HD 42782	54	1	HD 46552	54	13
HD 260611	28	18	HD 48029	10	13	HD 48532	54	19
HD 48549	19	35	HD 53879	12	24	HD 58784	29	52
HD 58973	29	82	HD 59882	17	60	HD 66665	14	22
HD 50767	17	55	HD 57291	17	57	HD 25638	8	12
HD 66594	37	109	HD 32343	19	62	HD 65875	29	66
HD 198512	12	2	HD 203374	8	2			

9.5 High and Intermediate Velocity Clouds

Recent surveys of high and intermediate velocity clouds in the region of the Galaxy surveyed by Kepner (1970), have been carried out by Meng & Kraus (1970) and Hulsbosch (1975). The high velocity clouds (HVCs) and intermediate velocity clouds (IVCs) in this region are listed in Table (9.5.1), in order of increasing galactic longitude. Meng & Kraus surveyed the region where $b > 10°$ and omitted the regions where $l > 222°$ and $100° < l < 150°$. Hulsbosch surveyed the region where $100° < l < 130°$ for all galactic latitudes. Thus the list of HVCs/ IVCs given in Table (9.5.1) is probably incomplete. Bearing this in mind, the distribution of HVCs/IVCs is displayed as a histogram in Fig. 9.5.1.

There appears to be no correlation between the distribution of HVCs/IVCs and the distributions of programme stars (§8.1), local neutral hydrogen (Weaver, 1974) and HII regions (Sivan, 1974). Correlations of this kind are to be expected if the HVCs/IVCs are local objects, and their absence supports the view that the HVCs/IVCs are distant objects. A comparison of Fig.(9.5.1) with Fig (8.2.1) shows that the distribution of HVCs/IVCs may be connected with galactic spiral structure. There is a very prominent increase in the concentration of HVCs/IVCs where $l < 90°$, and this may be connected with viewing longitudinally along the Local Arm.

In this event the maximum concentration of HVCs/IVCs would be expected at $l \sim 40°$ (§8.2), but from the more extensive map given by Davies (1972, Fig 5), it appears that this maximum occurs for $10° \leqslant b \leqslant 20°$ at $l \sim 60°$. Thus the suggestion that the HVCs/ IVCs are connected with distant spiral arms (Davies, 1972) seems more plausible than the explanation suggested above.

With the techniques now available, the only method of making a reliable distance determination for an HVC/IVC is to show that a star with approximately the same galactic coordinates is associated with it. Then a distance determination for the star will give an approximate distance for the HVC/IVC. Three of the HVC/IVCs, listed

Table 9.5.1

Intermediate and High Velocity Clouds in the Area Surveyed by Kepner (1970)

l	b	V	N_{II}	l	b	V	N_{II}	l	b	V	N_{II}
48.60	11.46	-97	13.1	48.66	11.33	-75	5.8	50.19	10.48	-96	8.4
50.43	14.77	-75	5.5	50.72	9.40	-95	8.4	50.74	9.38	-79	8.7
51.43	10.26	-95	13.8	51.53	10.45	-73	11.6	51.97	16.37	-53	4.7
52.45	10.49	-94	6.2	52.84	14.44	-53	4.7	52.84	9.67	-73	5.5
52.93	16.76	-74	1.8	53.05	6.98	-72	9.5	53.12	16.34	-53	3.3
53.51	8.30	-93	8.4	53.57	8.18	-114	5.5	53.73	14.97	-52	3.3
53.85	17.25	-74	4.4	53.96	7.40	-72	11.6	54.41	8.76	-72	10.9
54.63	8.49	-114	8.4	55.29	11.60	-93	8.0	55.32	11.52	-72	12.4
55.39	9.58	-93	4.7	55.68	18.28	-94	2.9	55.74	18.13	-73	7.3
55.96	7.91	-113	8.7	56.18	12.10	-72	19.7	56.27	11.90	-51	8.7
56.48	8.41	-113	5.5	56.61	18.77	-73	4.0	56.87	10.64	-90	6.2
57.19	12.34	-93	3.3	57.20	12.31	-71	8.7	57.85	8.65	-134	4.0
58.07	17.98	-51	5.5	58.62	9.36	-92	10.9	58.91	11.09	-92	2.5
59.68	9.50	-91	5.5	59.70	11.79	-71	6.1	59.72	11.75	-134	8.4
59.78	14.04	-92	3.3	60.83	11.77	-70	8.7	61.16	13.50	-92	5.5
61.44	8.24	-133	8.4	61.75	12.21	-92	3.3	61.78	14.60	-113	6.9
61.89	14.37	-92	5.5	61.95	11.78	-70	5.8	62.18	13.73	-113	4.7
62.39	15.77	-113	8.1	62.45	10.75	-91	2.5	62.60	15.30	-92	3.8
63.59	15.60	-130	10.9	63.70	15.35	-92	7.3	64.26	11.67	-91	4.7
64.50	13.56	-134	8.3	64.76	15.51	-113	6.2	64.82	15.38	-92	11.3
65.31	11.83	-91	7.3	65.32	16.83	-93	8.4	65.36	16.74	-114	6.2
66.01	15.22	-92	8.0	66.42	14.29	-71	4.4	66.51	11.70	-92	5.5
66.82	15.94	-114	4.7	66.83	15.92	-72	4.7	67.97	16.02	-114	2.9
68.23	17.96	-94	4.4	68.91	13.91	-156	3.3	69.20	18.35	-105	8.0
69.41	12.83	-114	2.9	70.15	18.80	-99	6.6	70.16	13.51	-93	4.4
70.48	19.05	-95	4.7	71.05	14.02	-82	7.3	71.23	13.64	-103	6.2
71.67	8.27	-72	3.3	71.94	7.90	-114	5.8	72.03	11.98	-102	4.0
72.08	14.24	-99	8.0	72.17	19.40	-99	6.9	72.43	8.99	-72	5.5
72.45	14.38	-94	6.6	72.60	18.30	-120	5.8	72.68	10.70	-101	4.0

l	b	V	N_H	l	b	V	N_H	l	b	V	N_H
72.75	8.39	-114	6.9	73.14	19.82	-106	4.4	73.36	13.93	-145	4.7
73.40	13.84	-187	5.5	73.48	9.17	-101	4.7	73.52	13.60	-103	7.6
74.08	12.42	-102	5.8	74.10	10.07	-99	10.2	74.37	14.19	-99	5.5
74.39	11.80	-186	5.5	74.46	10.30	-94	9.1	75.86	13.42	-103	5.8
76.95	13.53	-98	3.3	79.48	17.99	-76	5.5	79.86	19.90	-65	4.7
80.14	12.36	-41	5.8	80.33	11.41	-119	6.9	81.31	11.74	-124	5.5
82.30	19.40	-43	3.6	82.58	11.54	-118	4.7	83.08	12.74	-61	6.9
83.39	19.50	-95	4.7	83.63	16.25	-63	3.6	84.45	14.97	-62	4.7
84.68	11.97	-118	3.3	85.10	13.29	-62	3.3	85.34	12.68	-125	4.7
85.51	10.53	-97	4.4	85.91	18.86	-44	8.0	86.02	11.66	-61	8.0
86.20	18.14	-64	5.8	86.76	12.41	-54	6.9	87.85	12.56	-62	8.0
88.20	14.02	-126	4.7	88.28	18.60	-149	5.8	88.82	15.04	-41	6.6
88.86	12.85	-84	5.8	89.02	14.65	-126	6.6	89.09	10.54	-82	7.3
89.14	14.43	-147	3.6	89.16	12.34	-62	6.9	89.33	18.79	-149	2.5
89.71	13.41	-83	3.6	90.24	10.62	-104	5.5	90.28	12.45	-40	12.7
91.10	13.06	-41	12.4	91.68	12.13	-41	10.2	92.55	16.80	-42	5.5
92.59	12.59	-40	16.4	94.60	11.43	-41	36.4	94.92	12.76	-41	11.3
104.30	8.50	-118	35.0	105.00	17.00	-48	36.0	105.00	19.00	-129	6.0
107.00	19.00	-50	37.0	107.50	8.30	-136	9.0	113.00	12.00	-50	86.0
113.70	12.30	-51	90.0	115.00	15.00	-123	17.0	118.00	12.50	-141	10.0
118.00	10.00	-132	14.0	119.30	14.20	-59	47.0	119.50	10.50	-160	2.0
121.00	16.00	-116	12.0	122.00	11.30	-57	51.0	124.00	16.00	-120	11.0
125.00	16.00	-70	26.0	125.00	11.00	-74	30.0	125.00	18.00	-118	16.0
157.26	9.29	-85	8.4	157.33	9.40	-106	4.7	157.92	10.29	-85	3.6
161.18	7.91	-148	5.5	161.30	8.87	-127	7.7	164.17	12.99	-105	6.6
164.24	18.04	-62	4.4	164.38	18.36	-41	7.3	165.96	16.76	-83	5.8
165.98	16.80	-104	6.6	167.21	14.52	-41	17.5	168.10	16.39	-41	11.6
168.18	16.67	-62	6.9	169.88	8.65	-106	7.3	170.08	15.84	-41	9.5
170.28	7.31	-127	6.6	170.62	7.91	-105	3.3	170.64	17.14	-41	16.0
171.55	14.11	-41	11.3	171.65	9.77	-105	6.9	172.46	9.13	-109	12.4
176.15	19.69	-168	5.8	181.29	8.56	-88	9.0	195.40	12.46	-84	5.5
195.64	12.53	-91	11.3	195.90	12.34	-88	9.5	205.70	19.44	-217	2.5

Notes to Table (9.5.1):

l & b are the galactic coordinates of the HVC/IVC in degrees

V is the 21cm. radial velocity of the HVC/IVC in km/s

N_H is the observed HI column density for the HVC/IVC in atoms $cm.^{-2} \times 10^{19}$.

A Histogram Showing the Distribution of HVCs/IVCs as a Function of Galactic Longitude

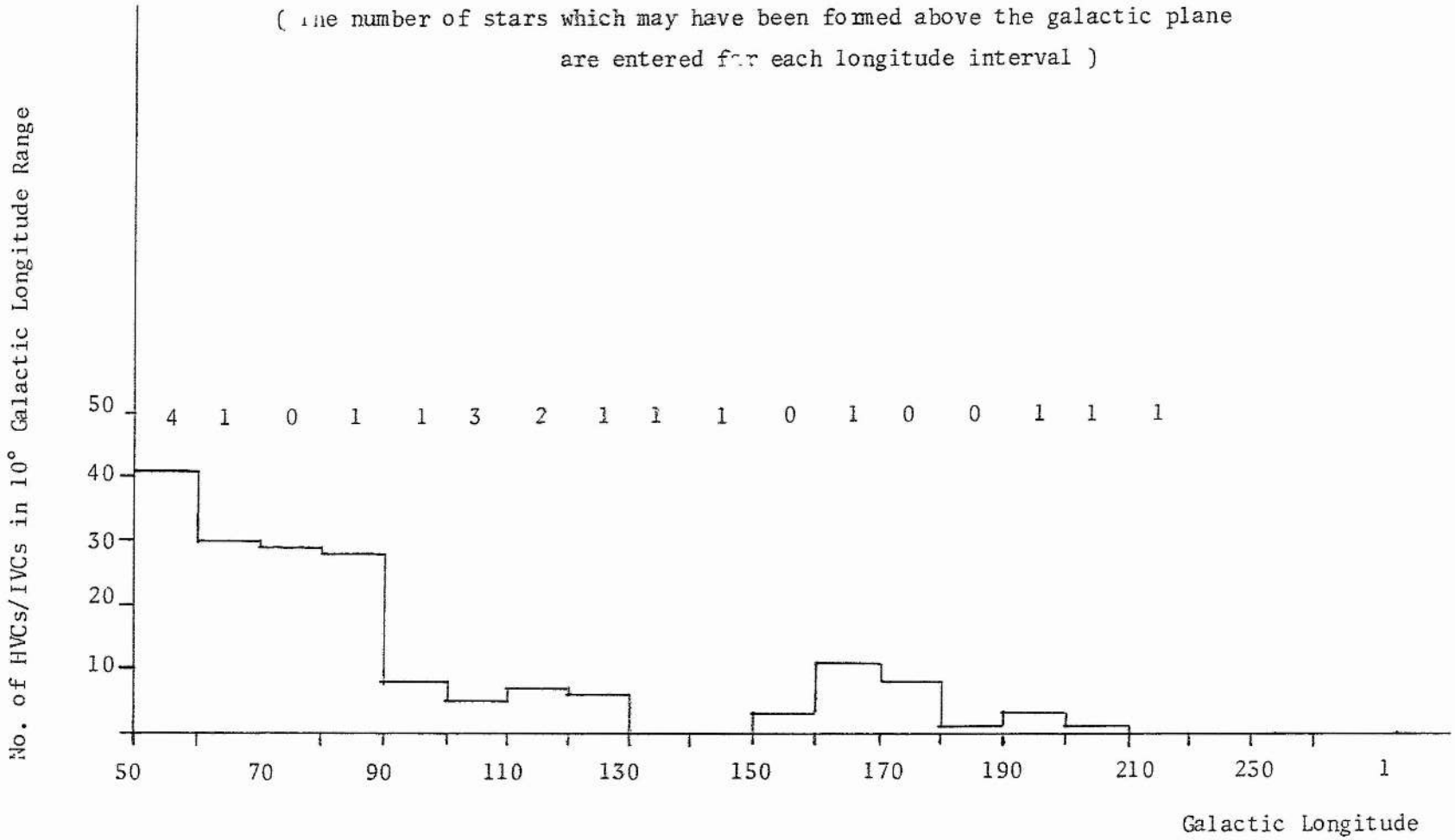

Fig 9.5.1

in Table (9.5.1), appear to have programme stars which lie within 20% of the mean angular diameter from the centre of the cloud. These are listed in Table (9.5.2).

The velocity of the interstellar CaII in the direction of HD 186618 is -5km/sec whereas the radial velocity of the HVC is -119km/sec. Thus if the HVC contains CaII gas, it almost certainly lies beyond HD 186618, which places it at a distance of at least (2.64 $\pm$ 0.12)kpc. No interstellar CaII(K) line has been reported in the spectrum of HD 189775, and so comments cannot be made on the distance of the IVC in this direction.

The interstellar CaII(K) velocity observed in the direction of HD 223959 is -55km/sec (§7.2). Unfortunately this is based on two 1'O.H.P. plates and the standard error is consequently very high at $\pm$ 53km/sec (§5.6). When this is corrected for the solar motion it becomes -47km/sec (§9.1), which agrees remarkably well with the radial velocity of the IVC in this direction, which is -59km/sec (Hulbosch, 1975).

If this CaII(K) velocity is more or less correct, then it would appear that the IVC in the direction of HD 223959 is certainly no more distant than the star itself, and is within 700pc (§7.2). Another case of an IVC which may be within 2kpc of the Sun is the IVC called R1 by Rickard (1971). This is discussed by Hulbosch (1975) who suggests that it lies between 400 and 1700 pc.

Another approach to this problem, suggested by Kiang (1976) is to see if the observed interstellar reddening, for the star, corresponds with the observed neutral hydrogen column density. According to Heiles (1975), the neutral hydrogen column density in the direction of HD 223959 is 24.1×10^{20} toms cm^{-2} for the IVC. For HD 223959, $E_{B-V} = 0.33$, which gives a neutral hydrogen column density of 12.7×10^{20} atoms cm^{-2} when substituted into equation (8.4.4).

It has been suggested (§8.4) that the constant term in equation (8.4.1) represents the mean of the contributions to the observed neutral hydrogen column densities, in the directions of the programme stars, as a result of HI beyond the stars. If this is the case, then the figure obtained from Heiles (1975) must be corrected. This results

TABLE 9.5.2

Programme Stars which may be Associated with HVCs/IVCs

Star	l_{Star}	b_{Star}	l_{Cloud}	b_{Cloud}	Mean Diam. of Cloud
HD 186618	80.48	11.49	80.33	11.41	1°.3
HD 189775	86.04	11.54	86.02	11.66	3°.5
HD 223959	119.51	14.09	119.30	14.20	2°.1

in an HI column density in the direction of HD 223959 of 14.5×10^{20} atoms cm^{-2}.

If HVCs/IVCs originate in the galactic halo as a result of the infall of extragalactic matter, as suggested by Hulbosch (1975), their gas to dust ratio may be different from that observed in ordinary galactic gas. This possibility has already been considered (§8.4). Nonetheless, if the IVC is between the observer and HD 223959, a contribution to the reddening in the star would be expected as a result. In this case the column density of ordinary gas in the direction of HD 223959 would be 9.8×10^{20} atoms cm^{-2}.

In view of the errors involved and the uncertainties in equation (8.4.4), no definite conclusion concerning the location of the IVC, in the direction of HD 223959, can be made. However, if the IVC were beyond the star, then the interstellar reddening should suggest an HI column density of 9.8×10^{20} atoms cm^{-2}. The fact that it suggests 12.7×10^{20}, indicates that at least part of the IVC may be between the observer and the star.

Thus it would appear that some of the IVCs may be local objects, although this cannot be stated conclusively as further observations are needed (§10.2). If a relation between HVCs and IVCs exists, as tentatively proposed by Hulbosch (1975), then some of the HVCs may be local objects as well. This would not preclude the possibility that distant IVCs/HVCs exist and form extensions to the spiral arms as proposed by Kepner (1970), Davies (1972) and Verschuur (1973a).

It has already been established that $\sim$ 50% of the intermediate galactic latitude programme stars, considered in this analysis, were probably formed at considerable distances from the galactic plane (§9.4). This departs from the currently held view that Extreme Population I objects are formed in the spiral arms, close to the galactic plane, where the highest gas densities are to be expected. Consequently, it is necessary to consider the formation of these stars.

As it seems possible that some IVCs, and possibly HVCs as well, are comparatively close objects, the possibility of a connection

between these stars and HVCs/IVCs is worthy of consideration. The first point to notice is that there is no comparison between the radial velocities of these stars and those of the HVCs/IVCs. It is hardly possible, therefore, that HVCs/IVCs, as they are observed at present, could at any time in the past have given rise to these stars. However, if HVCs/IVCs originate as the result of the infall of extragalactic matter, then as they approach the galactic plane, they would presumably begin to accrete matter. As a result of momentum conservation, the velocity would begin to fall. Thus an HVC would become an IVC and ultimately an LVC (low velocity cloud).

This view would be consistent with the evidence put forward by Hulsbosch (1975), suggesting that IVCs may closer than HVCs. LVCs are difficult to detect on account of the large amount of local neutral hydrogen with these radial velocities. The HVCs/IVCs would presumably be attracted to the spiral arms as a result of the increased gravitational attraction, and this might, to some extent, account for the spiral features observed at intermediate galactic latitudes. On entering a spiral arm, the HVCs/IVCs could cause an increase in gas pressure in the galactic plane, resulting in the expulsion of gas and stars. This may also give rise to the observed intermediate galactic latitude spiral features.

An HVC losing speed and accreting matter may undergo gravitational collapse and ultimately give rise to a star. These would be expected to have a non-zero velocity towards the galactic plane. Evidence in support of the view that stars can be formed at considerable distances from the galcatic plane has been obtained by Grasdalen et al. (1973), and from the H_2CO observations made by Sume et al. (1975).

Their observations of the dust cloud L 1251 suggest that its distance is 0.5kpc (Table 8.1.2), and so its distance from the galactic plane is 149pc. A T Tauri star appears to be associated with this dust cloud. Whether a dust cloud such as L 1251 could ever have been an HVC is still a matter for speculation, and further observations are needed.

Any connection between HVCs/IVCs and stars formed away from the galactic plane, would imply some correlation between the distribution at varying galactic longitudes. This is demonstrated in Fig (9.5.1), where there is some evidence of a correlation if the incompleteness of the samples are taken into account. More complete samples are needed before any definite conclusions can be drawn.

Chapter Ten

The Achievements of this Survey and Suggestions for Future Work.

10.1 A Summary of the Principal Results of the Present Survey

10.2 Suggested Observations to Develop an Understanding of Intermediate Latitude Galactic Structure.

10.1 A Discussion of the Results Obtained in the Present Survey

Early type OB stars appear to exist in considerable numbers at large distances from the galactic plane. The Local and Perseus Arms appear to extend to distances of 0.5 and 1kpc respectively. Furthermore, the density wave theory successfully explains the observed stellar radial velocities at distances of up to 1kpc from the galactic plane, although the theory was developed assuming an infintesimally thin galactic disk.

These results are consistent with 21cm observations, and their interpretation, made by Kepner (1970), Davies (1972) and Verschuur (1973a). Extensions of the spiral arms, in the direction of the galactic centre, to distances of 1 to 2kpc on either side of the galactic plane have been reported by Kilkenny et al.(1975). Similar extensions of the spiral arms in the anticentre region would therefore be expected. The interpretation of observed HVCs as intermediate galactic latitude extensions to distant spiral arms, could not be confirmed. This was because it did not prove possible to observe OB stars at the distances originally hoped for on account of the surprisingly high interstellar reddening, which was comparable to that observed in the galactic plane.

Additional evidence for this surprisingly high interstellar reddening on the northern side of the galactic plane ($b \geqslant 6°$), is to be found by comparing the number of OB stars found on each side of the galactic plane. For instance in the HD Catalogue there are 776 O-B5 stars listed for which $b > 6°$ and 1898 O-B5 stars for which $b \leqslant -6°$. The Sun is 8 ± 12 pc north of the galactic plane (Allen, 1973 Page 283) and thus the apparent asymmetry is almost certainly significant, in that it appears to be too large to be explained by any error in locating the Sun in the galactic plane.

The infall of extragalactic matter has been suggested by Hulsbosch (1975) as a possible explanation of high velocity clouds. It has been suggested (§9.5) that HVCs will be retarded as they

approach the galactic plane, begin to accrete matter and possibly give rise to star formation. This would account for the existence of young early type stars whose distances from and velocity components normal to the galactic plane are incompatible with their evolutionary lifetimes, if the star had been formed in the galactic plane and ejected from it.

Such an infall of extragalactic matter will sweep extragalactic dust into the northern galactic hemisphere. This will tend to become trapped by gas near the galactic plane. Stars formed from HVCs on the other hand could pass straight through the galactic plane. This would explain the observed distribution of OB stars and also the surprisingly high interstellar reddening observed in the region surveyed.

An additional explanation to the fact that the observed OB stars are surprisingly close is due to the fact that the sun is located on the inside edge of the Local Arm. Thus any attempt to observe stars in the anticentre region means that observations have to be made through dust in the Local Arm.

If the suggested infall of extragalactic matter does occur then it should be reflected in the observed distribution of galactic neutral hydrogen. More neutral hydrogen in the northern than in the southern galactic hemisphere is to be expected. Unfortunately the surveys in the southern galactic hemisphere are incomplete. The survey by Weaver & Williams (1974b) does indicate that in the region $0° < l < 180°$ there is more neutral hydrogen in the area of $b > 0°$. However, for $180° < l < 250°$ there is more neutral hydrogen in the southern galactic hemisphere. Since there are only a few stars in this latter region, it is possible that the depletion in the northern galactic hemisphere, of stars and dust, is the result of a gravitational interaction with the Magellanic Clouds.

The association Cepheus OB2 is not only the region in which the programme stars appear to be most densely concentrated, but also the region in which the Intermediate and Local Arms may merge (§8.2). The whole association appears to have a velocity component towards the North Galactic Pole of 19 ± 5km/sec, which is the mean W component

of all the programme stars in the association, weighted by their standard deviation, using the method prescribed by Barford (1967, page 62).

The Intermediate Arm may have merged with the Local Arm some 10^7 years ago. The resulting shock in the interstellar medium could have given rise to star formation. The increase in gas pressure could have given rise to the expulsion of stars and gas from the galactic plane.

10.2 Suggested Observations to Develop an Understanding of Intermediate Latitude Galactic Structure.

Many more faint OB stars have to be considered if the observations and conclusions of Kepner (1970), Davies (1972) and Verschuur (1973a) are to be verified. In fact the sample of OB stars must be as complete as possible. Therefore an extensive search for faint OB stars should be carried out at all galactic longitudes and latitudes for which $|b|>6°$. The method of obtaining transmission grating spectra described by Graham & Miller (1974) might prove useful.

This would serve to eliminate some of the white dwarfs and subluminous stars, although a number would probably be indistinguishable from normal OB stars. On completing a survey of this sort, photometric and spectroscopic observations will have to be obtained for these stars. At the same time care would have to be taken to ensure that the observations of the known intermediate and high latitude OB stars are complete. The region $200° < l < 228°$ is a region in which it may be possible to observe stars associated with the outer spiral arms of the Galaxy without having to observe exceedingly faint stars, because of the small interstellar absorption (§8.1).

Rubin et al. (1974) have published a list of faint blue stars in this region. Some of these may prove to be luminous stars in the Arm V and W, discussed by Davies (1972). Proper motions for some of these stars have been published by Cudworth (1975).

As a preliminary to more extensive observations all programme stars should be observed on the ubvy system (Strömgren, 1963). This is an improvement on the UBV system in that the narrower bands give a better resolution. Consequently the index

$$c_1 = (u - v) - (v - b)$$

gives a measure of the "Balmer-jump" which is adequate for distinguishing white dwarfs, subdwarfs and horizontal branch stars from normal OB stars in many cases (Graham, 1970, Kilkenny & Hill, 1975b).

Having eliminated most of the subluminous stars, Hβ photometry and spectroscopy can be carried out. An image tube spectrograph can be used to obtain spectra of faint stars in a relatively short time. These are quite satisfactory as a final check for subluminous stars, and for radial velocity and MK spectral type determinations. However, for spectrophotometry, a high quality photographic or electronographic spectrogram is desirable. For the brighter stars, high dispersion Coudé spectra would show the velocity structure of interstellar lines. This could then be analysed in a similar way to a 21cm profile to determine spiral structure.

A recent comparison of interstellar CaII, NaI and KI absorption lines in stellar spectra, by Hobbs (1974), suggests that the strength of the CaIIK line may be unreliable as an indicator of the column density of interstellar gas between the observer and a star. This is thought to be due to a large depletion factor for the CaII, as compared with the NaI and KI gases. Consequently, it would be prudent to discontinue using the CaIIK line. The NaI and KI lines would provide useful alternatives. Nachman & Hobbs (1973) suggest that optical depth integrals be used to evaluate column densities. This is better than using equivalent widths because no assumptions about the nature of the absorbers are required. A comparison of HI with NaI and KI column densities would be worthwhile. This is because a different composition of the interstellar gas, as well as a different gas to dust ratio for the interstellar medium, might be expected at high galactic latitudes if there is an infall of extragalactic matter, as suggested by Hulsbosch (1975). Accurate neutral hydrogen column densities cannot be obtained by making 21cm. observations in the directions of OB stars, because of the relatively large solid angles in which the observations are made. However, measuring the optical depth integral of the interstellar Lyman-α

line in the ultraviolet spectra of OB stars will give a relaible HI column density.

Braunsfurth & Rohlfs (1973) have derived an expression for the fractional abundance of molecular hydrogen. They have shown that if this fractional abundance is not universally observed, then the only alternative is a varying composition of the interstellar medium. For this reason molecular hydrogen column densities should be observed for all programme stars. The technique for doing this is given by Spitzer Jr. et al. (1974) and references cited therein.

Very much more accurate proper motions are needed for a detailed study of galactic structure, high velocity stars, dynamical lifetimes and the force law normal to the galactic plane. In fact the techniques for accurate proper motion determination have recently become available. Muanwong (1975) has developed the plate overlap method for measuring proper motions and an accuracy of ± 0.0008"/annum can be obtained using this method. It is very important that this method be applied to determine accurate proper motions for intermediate and high latitude early type stars.

Improved proper motions and radial velocities can be used to derive better estimates for the galactocentric distance and solar motion components, as discussed by Balona & Feast (1974). The reductions would then be carried out using these improved results. Alternative fits to the Schmidt Rotation Curve should be tried. Among these are the polynomial representations derived by Balona & Feast (1974) and Burton (1971).

A study of HII regions and dust clouds can also yield valuable information concerning galactic structure, for reasons already discussed (§8.1 & §8.2). Radial velocities of optical HII regions can be determined using the Hα emission line. For distant HII regions this may not be visible, and in these cases it may be possible to observe a radio recombination line, in order to measure the radial velocity. There appear to be comparatively few HII regions

at intermediate galactic latitudes and an extensive search is needed. Similarly more OH and formaldehyde observations of dust clouds are needed to obtain complete kinematic data.

A survey of subluminous halo stars is currently underway at the St. Andrews University Observatory. It is hoped that a detailed kinematic study of these stars will yield a more precise expression for the force law normal to the galactic plane, and establish any variations in this force law that may occur from place to place in the galactic disk. The results of this work could then be applied to normal OB stars and used to derive more precise dynamical lifetimes.

Adopting a stellar chemical composition that is appropriate to its MK spectral type, the evolutionary lifetime of each star could be calculated explicitly, using the method of Haselgrove & Hoyle (1956). Comparing this with a more precise dynamical lifetime will give an accurate determination of the point of origin of each star, assuming no perturbations from nearby stars.

Although 21cm observations in the direction of each star will not yield reliable neutral hydrogen column densities, it is still useful to make these observations. This is because the neutral hydrogen profiles reflect streaming motions of the HI gas, and following the method of Burton (1972), it is possible to deduce information about the spatial and velocity distributions of neutral hydrogen. Neutral hydrogen 21cm. observations have been made in the directions of most of the programme stars listed in Table (7.2.1) by Prof. Th. Schmidt-Kaler and Dr. D. Kilkenny using the Bonn Radio Telescope. The data are currently being reduced. Correspondingly, it would be useful to follow up optical observations of any additional programme stars with similar 21cm observations.

Future developments in the theory of galactic structure will probably take the form of producing a revised density wave theory, which will account for the extensions of the spiral arms in the direction normal to the galactic plane. It is hoped that the observations reported here will contribute to the eventual development of such a theory.

REFERENCES

Abt, H.A. & Biggs, E.S.,
1972, " Bibliography of Stellar Radial Velocities ", Kitt Peak National Observatory.

Abt, H.A. & Golson, J.C.,
1962, Ap.J. 136, 363

Abt, H.A., Levy, S.G. & Gandet, T.L.,
1972, A.J. 77, 138

Abt, H.A. & Osmer, P.S.,
1965, Ap.J. 141, 949

Abt, H.A. & Smith, G.H.,
1969, P.A.S.P. 81, 332

Allen, C.W., 1973, " Astrophysical Quantities ", 3rd Edition, Athlone.

Alter, G., Balazs, B. & Ruprecht, J.,
1970, " Catalogue of Star Clusters and Associations ", 2nd Edition, Budapest, Akademiai Kiado.

Andrews, P.J., 1968, Mem. R.A.S. 72(2), 35

Argelander, F.W.A.,
1859 - 1862, Bonner Sternwerzeichniss, Sec 1 - 3, Astron. Beob. Sternwarte Konigl. Rhein. Friedrich - Wilhelms - Univ. Bonn, 3, 4, 5.

Aźusienis, A. & Straiźys, V.,
1969, Astr. Obs. Buil., Vilnius 24, 33

Balona, L. & Crampton, D.
1974, M.N.R.A.S. 166(1), 203

Balona, L.A. & Feast, M.W.,
1974, M.N.R.A.S. 167, 621

Barbaro, G., Dallaporta, N. & Fabris, G.,
1969, Astrophys. Space Sci. 3, 123

Barford, N.C., 1967, " Experimental Measurements:Precision, Error and Truth ", Addison - Wesley Publishing Company, Inc.

Beals, C.S. & Oke, J.B.,
1953, M.N.R.A.S. 113, 530

Blaauw, A., 1952, B.A.N. 11, 459
1963, " Basic Astronomical Data ", Stars and Stellar Systems, University of Chicago Press, 3, 401

Blaauw, A., Gum, C.S., Pawsey, J.L. & Westerhout, G.,
1959, I.A.U. Information Bulletin No. 1

Blanco, V.M., Demers, S., Douglass, G.G. & Fitzgerald, M.P.
1968, Publ. U.S. Nav. Obs. 2nd Series, 21

Boulon, J., 1957, J. Observateurs, Marseille, 40, 107
1963, J. Observateurs, Marseille, 46, 187

Braunsfurth, E. & Rohlfs, K.
1973, I.A.U. Symposium 52, 231

Burton, W.B., 1971, Astron. & Astrophys. 10, 76
1972, Astron. & Astrophys. 19, 51
1974, " Galactic and Extra Galactic Radio Astronomy ", Ed. G.L. Verschuur and K.I. Kellermann, Springer - Verlag, Page 82

Burton, W.B. & Bania, T.M.,
1974, Astron. & Astrophys. 33, 425

Burton, W.B. & Verschuur, G.L.,
1973, Astron. & Astrophys. Suppl. 12, 145

Cannon, A.J., 1924 - 1936, Ann. Harv. Coll. Obs. 100, 1

Cannon, A.J. & Pickering, E.C.,
1918 - 1924, Ann. Harv. Coll. Obs. 91 - 99, 1

Chuadze, A.D., 1973, Abastumansk. astrofiz. Obs. Gora Kanobili Bjull. 44, 105

Cohen, J.G., 1974, Ap.J. 194, 37

Courtes, G., Cruvellier, P. & Georgelin, Y.,
1966, J. Observateurs, Marseille, 49, 329

Cousins, A.W.J., Eggen, O.J. & Stoy, R.H.,
1961, R. Obs. Bull. No. 25

Cousins, A.W.J. & Stoy, R.H.
1963, R. Obs. Bull. No. 64

Crampton, D. & Fisher, W.A.,
1974, Publ. Dom. Astrophys. Obs., 14(12), 283
Crampton, D. & Georgelin, Y.M.,
1975, Astron. & Astrophys. 40, 317
Crampton, D., Leir, A. & Younger, F.,
1973, Publ. Dom. Astrophys. Obs., 14(8), 51
Crawford, D.L., 1958, Ap.J. 128, 185
1960, Ap.J. 132, 66
1973, I.A.U. Symposium 54, 93
Crawford, D.L., Barnes, J.V. & Golson, J.C.,
1971, A.J. 76, 1058
Crawford, D.L., Barnes, J.V., Golson, J.C. & Hube, D.P.,
1973, A.J. 78, 738
Crawford, D.L. & Mander, J.,
1966, A.J. 71, 114
Cudworth, K.M., 1975, A.J. 80, 826
Curtiss, R.H., 1904, Ap.J. 20, 149
Davies, R.D., 1972, M.N.R.A.S. 160, 381
Dewitt, J.H. & Seyfert, C.K.,
1950, P.A.S.P. 62, 241
Dickel, H.R., Wendker, H. & Bieritz, J.H.,
1969, Astron. & Astrophys. 1, 270
Dieter, N.H., 1972, Astron. & Astrophys. Suppl. 5, 21
1973, Ap.J. 183, 449
Drilling, J.S., 1975, A.J. 80, 128
Edlen, M.B., 1955, Trans. I.A.U. 9, 220
Efroymson, M.A., 1965, " Mathematical Methods for Digital Computers ", Ed. A. Ralston & H.S. Wiff, John Wiley & Sons Inc., Page 191
Emerson, D.T. 1974, M.N.R.A.S. 169, 607
Evans, R.D. 1955, " The Atomic Nucleus ", Mc. Graw Hill, New York
Ewen, H.I. & Purcell, E.M.,
1951, Nature 168, 356
Feast, M.W., 1972, Vistas in Astronomy, 13, 207
Feast, M.W. & Shuttleworth, M.,
1965, M.N.R.A.S. 130, 245

Feast, M.W., Thackeray, A.D. & Wesselink, A.J.,
1957, Mem.R.A.S. 68, 1
Feinstein, A., 1974, M.N.R.A.S. 169, 171
Fernie, J.D., 1965, A.J. 70, 575
Filin, A.Ia., 1957, Soviet Astr. 1, 517
Fitzgerald, M.P., 1968, A.J. 73, 983
Fitzgerald, P., 1964, Publ. David Dunlap Obs. 2, 417
Georgelin, Y.M., Georgelin, Y.P. & Roux, S.,
1973, Astron & Astrophys. 25, 337
Graham, J.A., 1967, M.N.R.A.S. 135, 377
1970, P.A.S.P. 82, 1305
Graham, J.A. & Miller, E.W.,
1974, P.A.S.P. 86, 829
Grasdalen, G.L., Kuhi, L.V. & Harlan, E.A.
1973, P.A.S.P. 85, 193
Greaves, W.M.H., Davidson, C. & Martin, E.
1929, M.N.R.A.S. 90, 11
Greenstein, J.L., 1971, I.A.U. Symposium 42, 46
Greenstein, J.L. & Sargent, A.I.,
1974, Ap.J. Suppl. 28, 157
Guetter, H.H., 1974, P.A.S.P. 86, 795
Gutierrez - Moreno, A. & Moreno, H.,
1970, Astron. & Astrophys. 7, 35
1972, Astron. & Astrophys. 17, 41
Hardie, R.H., 1962, " Astrophysical Techniques ", Stars and Stellar Systems, University of Chicago Press, 2, 178
Harding, G.A. & Candy, M.P.,
1971, R. Obs. Bull. No. 164
Hardorp, J., Rohlfs, K., Slettebak, A. & Stock, J.,
1959, " Luminous Stars in the Northern Milky Way " 1,
(Hamburg - Bergedorf: Hamburger Sternwarte
& Warner and Swasey Observatory)

Hardorp, J., Theile, I. & Voigt, H.H.,
1964, " Luminous Stars in the Northern Milky Way " 3,
(Hamburg - Bergedorf: Hamburger Sternwarte
& Warner and Swasey Observatory)
1965, " Luminous Stars in the Northern Milky Way " 5,
(Hamburg - Bergedorf: Hamburger Sternwarte
& Warner and Swasey Observatory)

Hartmann, J.H., 1899, Ap.J. 10, 321
1901, Astr. Nachr. 155, 81

Häselgrove, C.B. & Hoyle, F.,
1956, M.N.R.A.S. 116, 515

Haug, U., 1970a, Astron. & Astrophys. 9, 453
1970b, Astron. & Astrophys. Suppl. 1, 35

Haug, U. & Kohoutek, L.,
1971, Astron. & Astrophys. 13, 71

Heiles, C., 1975, Astron. & Astrophys. Suppl. 20, 37

Heiles, C. & Habing, H.J.,
1974, Astron. & Astrophys. Suppl. 14, 1

Herr, R.B., 1969, A.J. 74, 200

Hertzsprung, E., 1922, Ap.J. 55, 370

Hilditch, R.W., 1974, Private Communication

Hill, P.W., 1968, Observatory 88, 163
1969, Mon. Not. astr. Soc. Sth. Afr. 27, 45
1971, Mem.R.A.S. 75, 1
1973, Private Communication
1974, Private Communication

Hill, P.W. & Hill, S.R.,
1966, M.N.R.A.S. 133, 205

Hiltner, W.A., 1955, Ap.J. Suppl. 2, 389

Hiltner, W.A. & Johnson, H.L.,
1956, Ap.J. 124, 367

Hobbs, L.M., 1974, Ap.J. 191, 381

Hube, D.P., 1970, Mem.R.A.S. 72, 233

Hulsbosch, A.N.M. 1975, Astron. & Astrophys. 40, 1

Iben, I., 1972, I.A.U. Colloquium 17, XI - 1

Isserstedt, J., 1968, Veröff. Astr. Inst. Ruhr - Univ. Bochum 1, 1

Isserstedt, J. & Schmidt-Kaler, Th.,
1970, Astron. & Astrophys. 7, 481

Jaschek, C., Conde, H. & de Sierra, A.C.,
1964, " Catalogue of Stellar Spectra Classified on the Morgan-Keenan System ", La Plata

Jeffers, H.M., van den Bos, W.H. & Greeby, F.M.,
1963, Publ. Lick. Obs. 21, " Index Catalogue of Visual Double Stars ".

Johnson, H.L., 1963, " Basic Astronomical Data " , Stars and Stellar Systems, University of Chicago Press, 3, 216

Johnson, H.L., Hoag, A.A., Iriarte, B., Mitchell, R.I. & Hallam, K.L.,
1961, Lowell Obs. Bull. 5(8), 133

Johnson, H.L., Mitchell, R.I., Iriarte, B. & Wisniewski, W.Z.,
1966, Commun. Lunar Planet. Lab. 63, 99

Johnson, H.L. & Morgan, W.W.,
1953, Ap.J. 117, 313
1955, Ap.J. 122, 142

Kahn, F.D., 1974, Astron. & Astrophys. 37, 149

Keeler, J.E., 1894, Publ. Lick. Obs. 3, 195

Kelly, B.D. & Kilkenny, D.,
1973, Observatory 93, 145

Kennedy, P.M. & Buscombe, W.,
1974, " MK Spectral Classifications Published since Jaschek's La Plata Catalogue ", Evanston

Kerr, F.J. & Knapp, G.R.,
1974, I.A.U. Symposium 60, 179

Kepner, M., 1970, Astron. & Astrophys. 5, 444

Kiang, T., 1976, Private Communication

Kiefer, L. & Baker, R.H.,
1941, Ap.J. 94, 482

Kienle, H., 1969, " Structure and Evolution of the Galaxy ", Ed. L.N. Mavridis, D. Reidel Publ. Co., Page 1

Kilkenny, D., 1973, Ph.D. Thesis, University of St. Andrews.
1974, Observatory 94, 4
1975, A.J. 80, 134

Kilkenny, D. & Hill, P.W.,
1975a, M.N.R.A.S. 172, 649
1975b, M.N.R.A.S. 173, 625

Kilkenny, D., Hill, P.W. & Schmidt-Kaler, Th.,
1975, M.N.R.A.S. 171, 353

King, I., 1952, A.J. 57, 253

Klinkmann, W., 1973, Ph.D. Thesis, Ruhr - Universitat, Bochum.

Kodaira, K., 1971, P.A.S.J. 23, 159

Kukarkin, B.V., Kholopov, P.N., Efremov, Yu.N., Kukarkina, N.P., Kurochkin, N.E., Medvedeva, G.I., Perova, N.B., Fedorovich, V.P. & Frolov, M.S., 1969,1970, " General Catalogue of Variable Stars ", Sternberg State Astronomical Institute of the Moscow State University, 3rd Edition.
1971, " First Supplement of the General Catalogue of Variable Stars ", Sternberg State Astronomical Institute of the Moscow State University.

Kwee, K.K., Muller, C.A. & Westerhout, G.
1954, B.A.N. 12, 211

Lanczos, C., 1957, " Applied Analysis ", Publ. Pitman, Bath. Page 426.

Lang, K.R., 1974, " Astrophysical Formulae ", Springer-Verlag, Berlin, Heidelberg, New York.

Lilley, A.E., 1955, Ap.J. 121, 559

Lin, C.C., Yuan, C. & Shu, F.H.,
1969, Ap.J. 155, 721

Lindblad, B., 1922, Ap.J. 55, 85
1926, Uppsala Astr. Obs. Medd. No.3

Lindblad, P.O., 1966, B.A.N. Suppl. 1, 77

Lloyd-Evans, T., 1973, Private Communication

Lynds, B.T., 1962, Ap.J. Suppl. 7, 1

Mathewson, D.M., Cleary, M.N. & Murray, J.D.,
1974, Ap.J. 190, 291

Maury, A.C. & Pickering, E.C.,
1897, Ann. Harv. Coll. Obs. 28, 1

Maxwell, J.C., 1868, Phil. Trans. 158, 532

Merrill, P.W., 1931, Ap.J., 188

Meng, S.Y. & Kraus, J.D.,
1970, A.J. 75, 535

Minn, Y.K. & Greenberg, J.M.,
1973a, Astron. & Astrophys. 22, 13
1973b, Astron. & Astrophys. 24, 393

Moffat, A.F.J., Schmidt-Kaler, Th. & Vogt, N.,
1973, I.A.U. Symposium 54, 114

Moll, W.J.H., 1921, Proc. Phys. Soc. 33, 207

Morgan, W.W., Code, A.D. & Whitford, A.E.,
1955, Ap.J. Suppl. 2, 41

Morgan, W.W. & Keenan, P.C.,
1973, A. Rev. Astr. Astrophys. 11, 29

Morgan, W.W., Keenan, P.C. & Kellman, E.,
1943, " An Atlas of Stellar Spectra", University
of Chicago Press.

Morgan, W.W., Sharpless, S. & Osterbrock, D.,
1952, A.J. 57, 3

Morgan, W.W., Whitford, A.E. & Code, A.D.,
1953, Ap.J. 118, 318

Muanwong, K. 1975, Ph.D. Thesis, University of Sussex.

Nachman, P. & Hobbs, L.M.,
1973, Ap.J. 182, 481

Nandy, K. & Schmidt, E.G.,
1975, Ap.J. 198, 119

Nassau, J.J & Stephenson, C.B.,
1963, " Luminous Stars in the Northern Milky Way " 4,
(Hamburg - Bergedorf: Hamburger Sternwarte
& Warner and Swasey Observatory)

Nassau, J.J., Stephenson, C.B. & Mac Connell, D.J.,
1965, " Luminous Stars in the Northern Milky Way " 6,
(Hamburg - Bergedorf: Hamburger Sternwarte
& Warner and Swasey Observatory)

Neckel, Th., 1967, Landessternw, Heidelberg-Konigstuhl,
Veröff. 19, 1

Oort, J.H., 1927, B.A.N. 3, 275
1928, B.A.N. 4, 269
1960, B.A.N. 15, 45

Pearce, J.A., 1932, Trans. I.A.U. 4, 187
1955, Trans. I.A.U. 9, 441

Petrie, R.M., 1953a, Publ. Dom. Astrophys. Obs. 9, 251
1953b, Publ. Dom. Astrophys. Obs. 9, 297
1960, Ann. Astrophys. 23(5), 744
1962, " Astronomical Techniques ", Stars and Stellar
Systems, University of Chicago Press, 2, 63
1963, " Basic Astronomical Data ", stars and Stellar
Systems, University of Chicago Press, 3, 64
1965, Publ. Dom. Astrophys. Obs. 12, 317

Petrie, R.M. & Lee, E.K.,
1966, Publ. Dom. Astrophys. Obs. 12, 435

Petrie, R.M. & Pearce, J.A.,
1962, Publ. Dom. Astrophys. Obs. 12, 1

Pickering, E.C., 1899, Am. J. Sci. 39, 46

Pickering, E.C. & Fleming, W.P.,
1897, Ann. Harv. Coll. Obs. 26, 1

Planck, M., 1901, Ann. Physik 4, 553

Plaskett, J.S., 1913, Ap.J. 37, 373
1924, Publ. Dom. Astrophys. Obs. 2, 287

Plaskett, J.S. & Pearce, J.A.,
1931, Publ. Dom. Astrophys. Obs. 5, 1

Pogson, N., 1856, M.N.R.A.S. 17, 12

Poveda, A., Ruiz, J. & Allen, C.,
1967, Bol. Obs. Tonantzintla Tacubaya 4, 86

Reddish, V.C., 1967, M.N.R.A.S. 135, 251

Rickard, J.J., 1971, Astron & Astrophys. 11, 270

Rohlfs, K., 1967, Z. Astrophys. 66, 225

Rubin, V.C., Westpfahl Jr., D. & Tuve, M.,
1974, A.J. 79, 1406

Rutherfurd, L.M., 1863, Sill. Amer. J. 35, 71

Ryter, C., Cesarsky, C.J. & Audouze, J.,
1975, Ap.J. 198, 103

Sampson, R.A., 1922, M.N.R.A.S. 83, 174
1925, M.N.R.A.S. 85, 212
1930, M.N.R.A.S. 90, 636

Sanford, R.F., 1949, Ap.J. 110, 117

Savage, B.D. & Jenkins, E.B.,
1972, Ap.J. 172, 481

Schlesinger, F., 1899, Ap.J. 10, 1

Schmidt, K.-H., 1975, Astrophys. Space Sci. 34, 23

Schmidt, M., 1956, B.A.N. 13, 11
1965, " Galactic Structure ", Stars and Stellar Systems, University of Chicago Press, 5, 513

Schmidt-Kaler, Th.,
1965a, Landolt-Börnstein, ed. K.H. Hellwege, Springer - Verlag, Berlin, Heidelberg, New York, New Ser. Group VI 1, 284
1965b, Landolt-Börnstein, ed. K.H. Hellwege, Springer - Verlag, Berlin, Heidelberg, New York, New Ser. Group VI 1, 307
1965c, Landolt-Börnstein, ed. K.H. Hellwege, Springer - Verlag, Berlin, Heidelberg, New York, Ne Ser. Group VI 1, 299

Schmidt-Kaler, Th.,
1967, I.A.U. Symposium No. 31, 161
1971, " Structure and Evolution of the Galaxy ", Ed. L.N. Mavridis, D. Reidel Publ. Co., Page 85

Schoenberg, E., 1929, Hdb. d. Astrophys. (Berlin: Julius Springer), 2, 268

Schulte, D.H. & Crawford, D.L.,
1961, Kitt Peak Contributions, No. 10

Seares, F.H. & Joyner, M.C.,
1944, Ap.J. 100, 264
1945, Ap.J. 101, 15

Secchi, P.A., 1868, " Spettri Prismatici delle Stelle Fisse ", Memoira, Roma.

Serkowski, K., 1963, A.J. 138, 1035

Shapley, H., 1918, Proc. Nat. Acad. Sci. 4, 224

Sharpless, S., 1959, Ap.J. Suppl. 4, 257

Sherwood, W.A., 1974, Publ. R. Obs. Edinburgh, 9, 85
1975, Astrophys. Space Sci. 34(1), 1

Simonson III, S.C.,
1968, Ap.J. 154, 923
1975, Ap.J. 201, L103

Sinnerstad, U., Arkling, J., Alm, S.H. & Brattlund, P.,
1968, Ark. Astr. 5(5), 105

Sivan, J.P., 1974, Astron. & Astrophys. Suppl. 16, 163

Slettebak, A. & Stock, J.,
1957, Z. Astrophys. 42, 67

Smith, L.F., 1968, M.N.R.A.S. 141, 317

Smithsonian Astrophysical Observatory Star Catalogue,
1966, U.S. Government.

Sokolnikoff, I.S. & Redheffer, R.M.,
1966, " Mathematics of Physics and Engineering ", Mc. Graw Hill, New York.

Spitzer Jr., L., Cochran, W.D. & Hirshfeld, A.,
1974, Ap.J. Suppl. 28, 373

Stephens, C.L. & van Breda, I.G.,
1972, Proceedings of the ESO/CERN Conference on Auxiliary Instrumentation for Large Telescopes, Page 499.

Stibbs, D.W.N., 1975, Private Communication

Stock, J., 1969, Vistas in Astronomy 11, 127

Stock, J., Nassau, J.J. & Stephenson, C.B.,
1960, " Luminous Stars in the Northern Milky Way " 2, (Hamburg - Bergedorf: Hamburger Sternwarte & Warner and Swasey Observatory)

Strömgren, B., 1948, Ap.J. 108, 242
1951, A.J. 56, 142
1952, A.J. 57, 200
1956a, Vistas in Astronomy 2, 1336
1956b, " Third Berkeley Symposium on Mathematical Statistics and Probability ", ed. Neyman, 3, 49
1963, Q. J. R. Astr. Soc. 4, 8

Sulentic, J.W. & Tifft, W.G.,
1970, " The Revised New General Catalogue of Nonstellar Astronomical Objects ", The University of Arizona Press, Tucson, Arizona.

Sume, A., Downes, D. & Wilson, T.L.,
1975, Astron. & Astrophys. 39, 435

Trumpler, R.J., 1930a, Lick Obs. Bull. 14, 154
1930b, P.A.S.P. 42, 214
1930c, P.A.S.P. 42, 267

Trumpler, R.J. & Weaver, H.F.,
1953, " Statistical Astronomy ", University of California Press.

Uranova, T.A., 1975, Soviet Astr. 18, 746

van Breda, I.G., 1972, P.A.S.P. 84, 212

van Breda, I.G., Hill, P.W., Campbell, R.J., Lynas-Gray, A.E., Carr, D.M., 1974, Proceedings of the First CAMAC Conference, Luxemburg.

van de Hulst, H.C., 1954, Ned. Tijschr. v Natuurkunde 11, 201

van de Hulst, H.C., Muller, C.A. & Oort, J.H., 1954, B.A.N. 12, 117

Verschuur, G.L., 1973a, Astron. & Astrophys. 22, 139

1973b, Astron. & Astrophys. 27, 407

Vogel, H.C., 1900, Ap.J. 11, 393

Wackerling, L.R., 1970, Mem.R.A.S. 73, 153

Walborn, N.R., 1972, A.J. 77(9), 750

Weaver, H., 1971, I.A.U. Symposium 38, 126

1974, Highlights of Astronomy 3, 423

Weaver, H. & Williams, D.R.W., 1973, Astron. & Astrophys. Suppl. 8, 1

1974a, Astron. & Astrophys. Suppl. 17, 1

1974b, Astron. & Astrophys. Suppl. 17, 251

Weaver, H.A., 1946, Popular Astron. 54, 211

Wesselink, A.J., 1941, Leid. Ann. 17, No. 3

Wesselius, P.R. & Sancisi, R., 1971, Astron. & Astrophys. 11, 246

Wiemar, W., 1974, Veröff. Astr. Inst. Univ. Bonn, Nr. 88

Wilsing, J. & Scheiner, J., 1909, Publ. Astrophys. Obs. Potsdam. 19, 1

Wilsing, J., Scheiner, J. & Munch, W. 1919, Publ. Astrophys. Obs. Potsdam. 24, 1

Wilson, R.E., 1963, Carnegie Institution of Washington, Publication 601

Wright, K.O., 1962, " Astronomical Techniques ", Stars and Stellar Systems, University of Chicago Press, 2, 83

Zinn, R.J., 1970, Ap.J. 162, 909

Zu[illegible] R.S., 1933, Lick Obs. Bull. 16, 119